

# Nonlinear Mathematical Models: Theory and Methods



By

Muhammad Aqib Abbasi

Department of Mathematics

Quaid-i-Azam University,  
Islamabad, Pakistan

2024

# Nonlinear Mathematical Models: Theory and Methods



By

Muhammad Aqib Abbasi

Supervised By

Dr. Maria Samreen

Department of Mathematics

Quaid-i-Azam University,  
Islamabad, Pakistan

2024

# Nonlinear Mathematical Models: Theory and Methods



By

Muhammad Aqib Abbasi

A DISSERTATION SUBMITTED IN THE PARTIAL FULFILLMENT  
OF THE REQUIREMENTS FOR THE DEGREE OF THE  
DOCTOR OF PHILOSOPHY  
IN  
MATHEMATICS

Supervised By

Dr. Maria Samreen

Department of Mathematics

Quaid-i-Azam University,  
Islamabad, Pakistan

2024



*In the name of Allah, the Most Beneficent, the Most Merciful.*



# Author's Declaration

I, Muhammad Aqib Abbasi, declare that my PhD thesis titled "**Nonlinear Mathematical Models: Theory and Methods**" is my work and has not been submitted previously by me for taking any degree from the Quaid-i-Azam University Islamabad, Pakistan, or anywhere else in the country/world.

If my statement is found incorrect at any time, even after I graduate, the university has the right to withdraw my Ph.D. degree.



Name of student: **Muhammad Aqib Abbasi**

Date: **20-Nov-2024**

# Plagiarism Undertaking

I solemnly declare that the research work presented in the thesis titled “**Nonlinear Mathematical Models: Theory and Methods**” is solely my research work with no significant contribution from any other person. Small contribution/help, wherever taken, has been duly acknowledged, and I have written this complete thesis.

I understand the HEC and **Quaid-i-Azam University** Islamabad’s zero-tolerance policy towards plagiarism. Therefore, as the Author of the above-titled thesis, I declare that no portion of my thesis has been plagiarized and that any material used as a reference is appropriately referred/cited.

I understand that if I am found guilty of any formal plagiarism in the above-titled thesis, even after my PhD degree, HEC and the University have the right to publish my name on the HEC/University Website, where students who submit plagiarized thesis are placed.

Student/Author Signature: \_\_\_\_\_



Name **Muhammad Aqib Abbasi**

## Certificate of Approval

This is to certify that the research work presented in this thesis entitled **Nonlinear Mathematical Models: Theory and Methods** was conducted by Mr. **Muhammad Aqib Abbasi** under the kind supervision of **Dr. Maria Samreen**. No part of this thesis has been submitted anywhere else for any other degree. This thesis is submitted to the Department of Mathematics, Quaid-i-Azam University, Islamabad, in partial fulfillment of the requirements for the degree of Doctor of Philosophy in the field of Mathematics from the Department of Mathematics, Quaid-i-Azam University, Islamabad, Pakistan.

**Student Name: Muhammad Aqib Abbasi**

Signature: 

### **External committee:**

#### **a) External Examiner 1:**

Name: **Dr. Quanita Kiran**

Signature: 

Designation: Professor

Office Address: National University of

Science and Technology, Islamabad, Pakistan.

#### **b) External Examiner 2:**

Name: **Dr. Mujeeb Ur Rehman**

Signature: 

Designation: Professor

Office Address: School of Natural

Sciences (SNS), National University of

Science and Technology, Islamabad, Pakistan.

#### **c) Internal Examiner:**

Name: **Dr. Maria Samreen**

Signature: 

Designation: Associate Professor

Office Address: Department of Mathematics,

Quaid-i-Azam University, Islamabad.

### **Supervisor Name:**

**Dr. Maria Samreen**

Signature: 

### **Name of Dean/ HOD**

**Prof. Dr. Asif Ali**

Signature: 

(Acting Chairman)

**Nonlinear Mathematical Models:**

**Theory and Methods**

**By**

**Muhammad Aqib Abbasi**

**CERTIFICATE**

A DISSERTATION SUBMITTED IN THE PARTIAL FULFILLMENT OF THE  
REQUIREMENTS FOR THE DEGREE OF THE  
**DOCTOR OF PHILOSOPHY IN MATHEMATICS**

**We accept this dissertation as conforming to the required standard**

1.



Prof. Dr. Asif Ali  
(Acting Chairman)

2.



Dr. Maria Samreen  
(Supervisor)

3.



Dr. Quanita Kiran  
(External Examiner)  
National University of Science and  
Technology (NUST),  
Islamabad, Pakistan

4.



Dr. Mujeeb Ur Rehman  
(External Examiner)  
School of Natural Sciences (SNS),  
National University of Sciences and Technology,  
Islamabad, Pakistan

**Department of Mathematics**

**Quaid-i-Azam University**

**Islamabad, Pakistan**

**2024**

# Acknowledgments

All praise is for Allah alone, the Lord of the universe. I am thankful to Almighty Allah, who gave me knowledge, strength, and wisdom and helped me complete this journey. Indeed, success is achieved only with the help of Allah. Thanks to the Holy Lord, who kept my parents safe and to whose prayers I am here today.

My heartfelt thanks go to my supervisor, Dr. Maria Samreen, for her unwavering guidance, support, and mentorship throughout this research journey. I also wanted to express my deep appreciation for Dr. Qamar Din. Your extensive knowledge and technical assistance have been vital in facilitating the necessary discussions and analyzing the results. Thank you so much. I also want to thank Dr. Muhammad Salman Khan for his help in this journey. This study would not have been possible without your continuous support and technical assistance. Your guidance has helped me achieve my research objectives and shaped my academic and scientific perspective. I am honoured to have the opportunity to work alongside such knowledgeable and experienced researchers. The knowledge and skills I have gained from this collaboration will undoubtedly contribute to my future academic and professional pursuits. Thank you for your unwavering commitment and dedication to this research endeavor.

I am immensely grateful to my family, friends, and colleagues for their unwavering support and encouragement throughout my journey. Their understanding and mounting have been instrumental in helping me navigate through the ups and downs of my journey. Last, I express my heartfelt gratitude towards my institution, which has been pivotal in making my research successful. Their support has allowed me to pursue my academic and scientific goals with purpose and conviction.

# Dedication

With great honor and utmost gratitude, I dedicate my PhD thesis to my loving family, with a special mention to my father and mother. Throughout my academic journey, my father has been my guiding light; he has mentored me and provided me with the necessary guidance to achieve my goals. On the other hand, my mother has been my unwavering source of love, understanding, and support. Her constant encouragement and sacrifices have laid the foundation for my success, and I am forever indebted to her. My parent's unwavering belief in me has been the cornerstone of my academic pursuits, inspiring me to push beyond my limits and reach for the stars. Their steadfast dedication to my dreams has been a driving force in my life, and I can confidently say that I would not be where I am today without their constant presence. Therefore, I dedicate my Ph.D. work to my family, especially my father and mother. Thank you for being my pillars of strength and my sources of inspiration. I hope to make both of you proud and that this achievement will make all your sacrifices and efforts worthwhile.

# Preface

Understanding the process that controls the connections between species and the transmission of diseases is a critical task in a complex network of natural and social systems. This thesis presents significant results related to these complex systems to better understand their dynamics, emphasizing the dynamics of infectious diseases and the connections between prey and predator.

The motivation behind our study is the fundamental need to understand the complex dynamics that determine the growth and decrease in populations and the sensitive equilibrium of the system. Prey-predator interactions, with complex mathematical models control, provide insight into the complex balance of life in the natural environment. Our goal is to provide practical outcomes with broad implications for animal conservation and management while extending the boundaries of ecological knowledge by exploring the theoretical foundations of dynamical systems.

In addition, the epidemic models help to strengthen international health systems as a response to the ongoing threat of infectious diseases. These models offer an opportunity to investigate the critical points that may cause epidemics or the emergence of stable, controlled states through the complex combination of parameters and variables they possess. Our goal is to contribute to managing and maintaining viral diseases by providing knowledge and methods that go beyond theoretical research and into the real world. This will ultimately assist societies throughout the world.

This thesis employs computational simulations, mathematical exploration, and practical applications. Our motivation arises from the conviction that extensive investigation into the dynamics of dynamic systems may contribute to more sensible approaches to preserving biodiversity, appropriate ecosystem management, and maintaining the stability of the global community.

Let us give an overview of the topics that each chapter covers.

**Chapter 1. Introduction and preliminaries.** The main focus of this chapter is to provide readers with the fundamental concepts of dynamical systems used in this thesis. This chapter will present the basic definitions, the conditions for fixed point stability, bifurcation analysis, chaos control, and the related literature.

**Chapter 2. Fixed points stability, bifurcation analysis, and chaos control of a Lotka-Volterra model with two predators and their prey.** The study of the population dynamics of a three-species Lotka-Volterra model is crucial in gaining a deeper

understanding of the delicate balance between prey and predator populations. Therefore, in this chapter, we discussed the stability of fixed points and the occurrence of Hopf bifurcation in a three-dimensional predator-prey model. Using bifurcation theory, our study provides a comprehensive analysis of the conditions for the existence of Hopf bifurcation. This is validated through detailed numerical simulations and visual representations demonstrating the potential for chaos in these systems. To mitigate the instability, we employ a hybrid control strategy that ensures the stability of the controlled model even in the presence of Hopf bifurcation. This chapter is significant in advancing the field of ecology but also has far-reaching practical implications for wildlife management and conservation efforts. Our results provide a deeper understanding of the complex dynamics of prey-predator interactions and have the potential to inform sustainable management practices and ensure the survival of these species.

**Chapter 3. Fixed points stability, periodic behavior, bifurcation analysis, and chaos control of a prey-predator model incorporating the Allee effect and fear effect.** In this chapter, we analyze the dynamics of a two-dimensional prey-predator model that incorporates the Allee and fear effects. We conduct stability analysis of the fixed points in discrete and continuous forms and focus on the periodic behavior of the discrete-time model.

In addition, we discussed the bifurcation behavior of discrete and continuous models using bifurcation theory and presented numerical examples to validate our theoretical findings. We also identified the direction of bifurcation using attractive bifurcation plots and employed a simple control technique to avoid bifurcation.

This chapter contributes to a better understanding of the prey-predator system and has implications for other complex systems in various fields, including population dynamics, physical models, epidemiology, and economics. Overall, this chapter reveals additional illumination on the prey-predator model's dynamics and increases our understanding of its dynamic behavior.

**Chapter 4. Fixed points stability, multi-parameter bifurcation analysis, and chaos control of a prey-predator model incorporating the Allee effect and fear effect.** This chapter presents the dynamic analysis of the prey-predator model by adding the fear and Allee effects. We also present the stability, bifurcation analysis, and chaos control of the model. From the numerical examples, we conclude that the crowding effect should be minimized to maintain the stability of the model. Also, in the interior fixed point, when fear and Allee effects are taken as bifurcation parameters, backward bifurcations occur, which shows that in the presence of the crowding effect, the increase of the fear effect stabilizes the model.



Similarly, the more significant Allee effect stabilizes the model. While the decrease of these two effects causes an increase in growth rate, which causes bifurcation in the system due to overcrowding, the addition of the Allee effect and the fear effect should be, to a certain extent, so that the excess of both impacts controls the crowding development. A simple control method is employed to prevent bifurcation. This chapter improves our comprehension of the prey-predator system while potentially having implications for other complex systems in various fields, including population dynamics, epidemiology, and economics.

**Chapter 5. Fixed points stability, bifurcation analysis, and chaos control of an epidemic model with vaccination and vital dynamics.** The spread of infectious diseases remains a significant threat to global health and stability. A crucial aspect of controlling and mitigating the impact of these diseases is a detailed understanding of their dynamics. This chapter thoroughly examines a discrete-time epidemic model's stability and bifurcation characteristics, considering vaccination and vital dynamics. We may better understand the system's behavior presented in this chapter with mathematical techniques from nonlinear dynamics. From studying the stability of fixed points, we can learn much about how the system responds to parameter changes and the circumstances needed for profound disease control. Additionally, investigating bifurcation occurrences provides a more detailed relationship between small parameter changes and qualitative changes in system behavior. The complex interactions between various parameters and their effects on the system's dynamics are mainly illustrated in the study of one-parametric bifurcation and co-dimension two-parameter bifurcation. This chapter also shows how crucial chaos control is in modeling epidemics. Managing the chaos in the system is an essential tool for preventing the spread of infectious diseases and ensuring long-term disease control.

All the chapters contain theorems related to a qualitative analysis of different models, for which we have provided proofs. The bibliography section gives all of the references used in this study.

# Contents

<b>1</b>	<b>Introduction and preliminaries</b>	<b>1</b>
1.1	Origin and evolution of prey-predator models . . . . .	1
1.2	Types of mathematical models . . . . .	2
1.3	Discretization techniques . . . . .	2
1.4	Stability of the fixed points . . . . .	3
1.4.1	Local stability . . . . .	3
1.4.2	Global stability . . . . .	5
1.5	Bifurcation analysis . . . . .	5
1.5.1	Hopf bifurcation criteria for continuous-time systems in terms of eigenvalues . . . . .	6
1.5.2	Neimark-Sacker bifurcation criteria for discrete-time systems in terms of eigenvalues . . . . .	7
1.5.3	Neimark-Sacker bifurcation criteria for discrete-time systems with- out finding the eigenvalues . . . . .	7
1.6	Chaos control . . . . .	8
<b>2</b>	<b>Fixed points stability, bifurcation analysis, and chaos control of a Lotka- Volterra model with two predators and their prey</b>	<b>10</b>
2.1	Introduction . . . . .	10
2.2	Positivity and uniform boundedness of the solutions . . . . .	14
2.3	Stability of the fixed points . . . . .	15
2.4	Bifurcation analysis . . . . .	22
2.4.1	Hopf bifurcation . . . . .	23
2.5	Numerical simulations . . . . .	24
2.6	Chaos control . . . . .	38
2.7	Conclusion . . . . .	41
<b>3</b>	<b>Fixed points stability, periodic behavior, bifurcation analysis, and chaos control of a prey-predator model incorporating the Allee effect and fear</b>	

<b>effect</b>	<b>43</b>
3.1 Introduction . . . . .	43
3.2 Positivity and uniform boundedness of the solutions . . . . .	47
3.3 Stability of the fixed points . . . . .	49
3.4 Periodicity . . . . .	53
3.5 Bifurcation analysis . . . . .	60
3.5.1 Hopf bifurcation . . . . .	69
3.6 Numerical simulations . . . . .	73
3.6.1 Bi-parameter plots . . . . .	81
3.7 Chaos control . . . . .	83
3.8 Conclusion . . . . .	84
<b>4 Fixed points stability, multi-parameter bifurcation analysis, and chaos control of a prey-predator model incorporating the Allee effect and fear effect</b>	<b>86</b>
4.1 Introduction . . . . .	86
4.2 Positivity and uniform boundedness of the solutions . . . . .	90
4.3 Stability of the fixed points . . . . .	92
4.4 Bifurcation analysis . . . . .	96
4.4.1 Hopf bifurcation . . . . .	104
4.5 Numerical simulations . . . . .	108
4.6 Chaos control . . . . .	121
4.7 Conclusion . . . . .	124
<b>5 Fixed points stability, bifurcation analysis, and chaos control of an epidemic model with vaccination and vital dynamics</b>	<b>127</b>
5.1 Introduction . . . . .	127
5.2 Stability of the fixed points . . . . .	131
5.2.1 Global stability of the positive fixed point . . . . .	135
5.3 Bifurcation analysis . . . . .	142
5.3.1 Period-doubling bifurcation . . . . .	143
5.3.2 Neimark-Sacker bifurcation . . . . .	148
5.3.3 Codimension-two bifurcation analysis . . . . .	150
5.4 Numerical simulations . . . . .	152
5.5 Chaos control . . . . .	158
5.6 Conclusion . . . . .	159

# Chapter 1

## Introduction and preliminaries

This chapter is related to a brief introduction to mathematical models and their mathematical framework for modelling in discrete and continuous cases. Moreover, the preliminary results related to stability analysis, bifurcation, and chaos control are discussed and used in the upcoming chapters.

### 1.1 Origin and evolution of prey-predator models

The interactions between the two species and the resulting impacts on one another make up the prey-predator relationship. Prey-predator is the alliance between the two living organisms living in an ecosystem. The Lotka-Volterra model is a classic and well-established framework for understanding prey-predator dynamics in ecology. Alfred Lotka [1] and Vito Volterra [2] were the two scientists who initially created this model, with Lotka developing it in 1925 and Volterra in 1927. They formulated the interaction between the prey-predator species' growth through differential equations. This set of differential equations represents the growth of prey species and predators' impact on them.

Scientists and ecologists have refined and improved the Lotka-Volterra model. The model has been enhanced with more realistic features, including spatial dynamics, the impact of other species, and environmental variation. Gradually, the dimension and non-linearity of the simple Lotka-Volterra model increase with time. Additional factors, like functional responses [3], the Allee effect ([4], [5], and [6]), a fear effect [7], prey refuges [8], and time delay [9], began to be included in the model to judge the population dynamics through different environmental factors.

Many scientists have discussed the ecological competition system of differential equations developed from the Lotka-Volterra type ([10] and [11]). Many added a third species to the prey-predator model to show the competition between two predators ([12] and [13]),

computing that only one prey or predator may catch up as a victim to another omnivore type. Investigating an increased number of predator and prey species, scientists have refined and extended the Lotka-Volterra model. Much work has been done on prey-predator models, and many show different behaviors in different prey-predator models. Some find a constant solution and offer local and global stability. Many show bifurcation behavior, the existence and uniqueness of positive stable solutions, and countless other results have been discussed. In this thesis, we discuss some of these results concerning prey-predator models.

## 1.2 Types of mathematical models

In this subsection, we will discuss the only two types of mathematical models based on the nature of the time involved in them. Continuous-time models represent the phenomenon's evolution over a continuous interval of time. Differential equations describe these models. Discrete-time models represent the phenomenon's evolution over a discrete interval of time. The difference equations describe these models.

## 1.3 Discretization techniques

Discrete-time models can also be independently formulated, similar to continuous-time models. However, researchers also discretize continuous-time models into discrete forms using various techniques. We will use only two methods in the following thesis chapters and describe them in detail here.

- Euler's Method ([14]):

Consider an  $n$ -dimensional continuous-time dynamical system of the following form:

$$\frac{d\xi}{dt} = \Phi(\xi, t), \quad (1.3.1)$$

where  $\xi = [\xi_1, \xi_2, \dots, \xi_n]^T$  is a vector representing the state variables. To discretize the continuous domain, divide the time interval into equal steps of length  $\Delta t$ , i.e.,  $t_0, t_1, t_2, \dots, t_n$ . Let the solution be constant over each interval, then  $\xi(t) \approx \xi_k$ , where  $\xi_k$  is the constant vector within the  $k$ th interval. Now we can write

$$\frac{d\xi}{dt} \approx \frac{\xi_{k+1} - \xi_k}{\Delta t}.$$

Now, (1.3.1) becomes:

$$\xi_{k+1} = \xi_k + \Delta t (\Phi(\xi_k, t_k)).$$

- Piece-wise constant argument ([15]):

Consider an n-dimensional continuous-time dynamical system of the following form:

$$\frac{d\xi}{dt} = \xi\Phi(\xi, t), \quad (1.3.2)$$

where  $\xi = [\xi_1, \xi_2, \dots, \xi_n]^T$  is a vector representing the state variables. Assume that the average rate of change in all the above differential equations changes over regular time intervals. Then we can write:

$$\frac{1}{\xi(t)} \frac{d\xi(t)}{dt} = \Phi(\xi, t), \quad (1.3.3)$$

where  $t$  represents the integer fragment of  $t$  and  $t \in (0, \infty)$ . Moreover, integrating (1.3.3) on an interval  $[k, k+1)$  for  $k = 0, 1, 2, \dots$ , we get the resulting scheme:

$$\xi(t) = \xi_k \exp[\{\Phi(\xi, t)\}(t - k)]. \quad (1.3.4)$$

Taking  $t \rightarrow k+1$ , we obtain the discretized form, which is as follows:

$$\xi_{k+1} = \xi_k \exp[\{\Phi(\xi, t_k)\}]. \quad (1.3.5)$$

## 1.4 Stability of the fixed points

The dynamic system's stability is the concept that determines the system's behavior over time. These concepts apply to both discrete and continuous-time models (see [16] for more details). Before describing the types of stability, we define the fixed point as:

**Definition 1.** [16] A point  $\lambda \in \Lambda$  is called a fixed-point of the mapping  $\xi : \Lambda \rightarrow \Lambda$  if  $\xi(\lambda) = \lambda$ .

Now, we discuss the stability of the model in terms of two types:

### 1.4.1 Local stability

The dynamic system's local stability is its behavior around a specific fixed point. A system is locally stable if it returns to that fixed point when perturbed slightly from it over time. The local stability can be analyzed using linearization techniques around the fixed point. It can be interpreted as the eigenvalues of the system's Jacobian matrix calculated at the selected point. The following theorems are used to discuss the local stability of the fixed point.

**Theorem 1.4.1.** [16] Let the following smooth map represent a discrete-time dynamical

system  $\Gamma$ :

$$\xi \mapsto \Gamma(\xi), \xi \in \mathbb{R}^n.$$

Let  $\xi_0$  be the fixed point of  $\Gamma$ , and  $\mathcal{A}$  be the Jacobian matrix of  $\Gamma$  calculated at the fixed point  $\xi_0$ . The  $\xi_0$  is said to be stable if all the multipliers (eigenvalues)  $\eta_1, \eta_2, \dots, \eta_n$  of  $\mathcal{A}$  satisfy  $|\eta| < 1$ .

**Theorem 1.4.2.** [16] Let the following smooth map represent a continuous-time dynamical system  $\Gamma$ :

$$\dot{\xi} = \Gamma(\xi), \xi \in \mathbb{R}^n.$$

Let  $\xi_0$  be the fixed point of  $\Gamma$ , and  $\mathcal{A}$  be the Jacobian matrix of  $\Gamma$  calculated at the fixed point  $\xi_0$ . The  $\xi_0$  is said to be stable if all the multipliers (eigenvalues)  $\eta_1, \eta_2, \dots, \eta_n$  of  $\mathcal{A}$  satisfy  $\text{Re}(\eta) < 0$ .

The above theorems provide the necessary criteria for determining the system's stability in terms of the multiplier. The system's stability can also be calculated based on its characteristic functions. Therefore, utilizing the characteristic function of the Jacobian matrix of the system, which is evaluated at the fixed point, we can calculate the stability of two- and three-dimensional discrete-time models using the subsequent results:

**Theorem 1.4.3.** [16] Consider the following characteristic function of a two-dimensional discrete-time system calculated at the fixed point  $(\hat{\xi}_1, \hat{\xi}_2)$ :

$$\lambda^2 - \Theta_a \lambda + \Theta_b = 0,$$

where  $\Theta_a$  and  $\Theta_b$  are real numbers. Then the fixed point  $(\hat{\xi}_1, \hat{\xi}_2)$  of a two-dimensional discrete-time system is a:

- source (unstable) iff  $|\Theta_b| > 1$ , and  $|\Theta_a| < |1 + \Theta_b|$ ,
- saddle point iff  $(\Theta_a)^2 > 4(\Theta_b)$ , and  $|\Theta_a| > |1 + \Theta_b|$ ,
- Non-hyperbolic point iff  $|\Theta_a| = |1 + \Theta_b|$ , or  $\Theta_b = 1$ , and  $\Theta_a \leq 2$ .
- If the above third condition does not hold, then  $(\hat{\xi}_1, \hat{\xi}_2)$  is a sink (stable) iff  $|\Theta_a| < 1 + \Theta_b < 2$ .

**Theorem 1.4.4.** [17] Consider the following characteristic function of a three-dimensional discrete-time system calculated at the fixed point  $(\hat{\xi}_1, \hat{\xi}_2, \hat{\xi}_3)$ :

$$\lambda^3 + \Theta_a \lambda^2 + \Theta_b \lambda + \Theta_c = 0,$$

where  $\Theta_a, \Theta_b$  and  $\Theta_c$  are real numbers. Then, the following are the necessary and sufficient conditions for all of the roots of the equations mentioned above to lie in an open

disc:

$$|\Theta_a + \Theta_c| < 1 + \Theta_b, |\Theta_a - 3\Theta_c| < 3 - \Theta_b, \text{ and } \Theta_c^2 + \Theta_b - \Theta_c\Theta_a < 1.$$

### 1.4.2 Global stability

A dynamic system is said to be globally stable if it is locally stable for all initial conditions and within its state space. Global stability is a stronger condition than local stability. It ensures the regular behavior of the entire system. Let  $I$  be an interval of real numbers and for some initial values  $\xi_0, \xi_1, \dots \in I$  if we have the following difference equations:

$$\xi_{n+1} = f(\xi_n, \xi_{n-1}), n = 0, 1, \dots \quad (1.4.1)$$

Then the following definitions are used to judge the global stability of the equation (1.4.1).

**Definition 2.** Let  $\xi^*$  be the fixed point of the equation (1.4.1). Then  $\xi^*$  is called a global attractor if for every  $\xi_0, \xi_1, \dots, \xi_n \in I$  we have

$$\lim_{n \rightarrow \infty} \xi_n = \xi^*.$$

**Definition 3.** If the fixed point  $\xi^*$  of (1.4.1) is locally stable and a global attractor, it is called global asymptotically stable.

## 1.5 Bifurcation analysis

Bifurcations happen when a slight variation in a parameter causes the system to go from one stable state to another. These changes can be utilized to identify significant thresholds above which the system cannot return to its initial form. Bifurcations can also show how environmental changes, such as shifts in the prey or predator populations, might impact the system's dynamics in the context of a prey-predator model.

Many types of bifurcations exist in dynamic systems, but in this thesis, we discuss the Hopf, Neimark-Sacker, and period-doubling bifurcations. The Neimark-Sacker bifurcation is similar to the Hopf bifurcation. In the Hopf bifurcation, the system induces limit cycles, while in the Neimark-Sacker bifurcation, a stable periodic orbit appears instead of the limit cycle. A slight modification in a parametric factor during period-doubling bifurcation leads the system to adopt a new behavior with twice the period of the initial system. Mathematically, we have the following criteria for these types of bifurcations:

**Definition 4.** [16] In the two-dimensional continuous-time dynamical system, the bifurcation corresponding to the occurrence of the multipliers  $\eta_{1,2} = i\mu_0, \mu_0 > 0$  is called a Hopf bifurcation.



**Definition 5.** [16] *In the two-dimensional discrete-time dynamical system, the bifurcation corresponds to the occurrence of the multipliers  $\eta_{1,2} = a \pm bi$  with  $|\eta_1| = |\eta_2| = 1$  is called a Neimark-Sacker bifurcation.*

**Definition 6.** [16] *In two-dimensional discrete-time dynamical systems, the bifurcation is associated with the occurrence of the multipliers  $\eta_1 = -1$  and  $\eta_2 < 1$  is called the period-doubling bifurcation.*

The system's bifurcation over the fixed point  $(\xi^*, \Theta^*)$  can also be analyzed regarding characteristic polynomials. For this, we have the following results: First, we have criteria for Hopf bifurcation without calculating eigenvalues. For this, we have the following theorems (see [18]).

### 1.5.1 Hopf bifurcation criteria for continuous-time systems in terms of eigenvalues

First, we will examine the eigenvalue criteria related to the Hopf bifurcation using the following theorem:

**Theorem 1.5.1.** [19] *Let us have the following  $n$ -dimensional autonomous system of differential equations:*

$$\frac{d\xi}{dt} = \Gamma(\xi, \Theta), \quad (1.5.1)$$

where  $\xi \in \mathbb{R}^n$ , and  $\Gamma \in C^\infty$ . Suppose that  $(\xi^*, \Theta^*)$  is the fixed point for the system, and  $P(\mu, \Theta)$  is the characteristic polynomial of the variational matrix of that system given as follows:

$$P[\mu, \Theta] = \zeta_n[\Theta] \mu^n + \zeta_{n-1}[\Theta] \mu^{n-1} + \cdots + \zeta_1[\Theta] \mu + \zeta_0[\Theta]. \quad (1.5.2)$$

Then, the system undergoes Hopf bifurcation about  $(\xi^*, \Theta^*)$  if the underlying axioms are satisfied:

$$\begin{aligned} (I) : & \zeta_0[\Theta^*] > 0, D_1[\Theta^*] > 0, \dots, D_{n-2}[\Theta^*] > 0, D_{n-1}[\Theta^*] = 0, \\ (II) : & \frac{dD_{n-1}[\Theta^*]}{d\Theta} \neq 0. \end{aligned} \quad (1.5.3)$$

where

$$D_n[\Theta] = \det \begin{pmatrix} \zeta_1[\Theta] & \cdots & 0 \\ \vdots & \cdots & \vdots \\ \zeta_{2n-1}[\Theta] & \cdots & \zeta_n[\Theta] \end{pmatrix}. \quad (1.5.4)$$

**Lemma 1.5.2.** *The conditions (1.5.3) can be reduces for  $n = 3$  in the following form:*

$$\begin{aligned} (I) : & \zeta_0[\Theta^*] > 0, D_1[\Theta^*] > 0, D_2[\Theta^*] = \zeta_1[\Theta^*]\zeta_2[\Theta^*] - \zeta_0[\Theta^*] = 0, \\ (II) : & \frac{dD_2[\Theta^*]}{d\Theta} \neq 0. \end{aligned} \tag{1.5.5}$$

The following results can be used to determine a more detailed view of the Neimark-Sacker bifurcation in higher-dimensional discrete-time models.

### 1.5.2 Neimark-Sacker bifurcation criteria for discrete-time systems in terms of eigenvalues

Now, we discuss the eigenvalue criteria for finding the Neimark-Sacker bifurcation, which can be seen from the following lemma.

**Lemma 1.5.3.** *[19] Let  $\xi_{j+1} = \Gamma_\eta(\xi_j)$  be a  $\kappa$  - dimensional system with bifurcation parameter  $\eta \in \mathbb{R}$ . Let  $V(\xi^*) = (\beta_{mn})_{\kappa \times \kappa}$  be the variational matrix evaluated at fixed point  $\xi^*$ . Then the characteristic function of  $V(\xi^*)$  is:*

$$\mathbf{C}_\eta(\delta) = \delta^\kappa + \beta_1\delta^{\kappa-1} + \cdots + \beta_{\kappa-1}\delta + \beta_\kappa. \tag{1.5.6}$$

**C1:** *Eigenvalues assignment. The characteristic function (1.5.6) has two complex conjugate eigenvalues  $\xi_1(\eta)$  and  $\bar{\xi}_1(\eta)$  with  $|\xi_1(\eta)| = 1$  at  $\xi = \xi_0$  and the others  $\xi_j(\eta), j = 3, \dots, n$ , with  $\xi_j(\eta_0) < 1$ .*

**C2:** *Transversality condition  $\frac{d|\xi_1(\eta_0)|}{d\xi} \neq 0$ .*

**C3:** *Non-resonance condition  $\xi_1^m(\eta_0) \neq 1$  or resonance condition  $\xi_1^m(\eta_0) = 1, m = 3, 4, 5, \dots$ . Then a Neimark-Sacker bifurcation occurs at  $\xi = \xi_0$ .*

### 1.5.3 Neimark-Sacker bifurcation criteria for discrete-time systems without finding the eigenvalues

Without eigenvalue criteria, we can also determine the existence of a Neimark-Sacker bifurcation, for which we can use the following criteria:

**Lemma 1.5.4.** *[19] Let  $\xi_{j+1} = \Gamma_\eta(\xi_j)$  be a  $\kappa$  - dimensional system with bifurcation parameter  $\eta \in \mathbb{R}$ . Let  $V(\xi^*) = (\beta_{mn})_{\kappa \times \kappa}$  be the variational matrix evaluated at fixed point  $\xi^*$ . Then the characteristic function of  $V(\xi^*)$  is:*

$$\mathbf{C}_\eta(\delta) = \delta^\kappa + \beta_1\delta^{\kappa-1} + \cdots + \beta_{\kappa-1}\delta + \beta_\kappa.$$

Here, all  $\beta_\kappa$  depend on both bifurcation parameter  $\eta$  and any controlled parameters  $\zeta$ . Let

$\Theta_i^\pm(\eta, \zeta) = |(\mathbb{A}_1 \pm \mathbb{A}_2)|, i = 1, 2, 3, \dots, \kappa$  be the sequence of determinants with

$$\mathbb{A}_1 = \begin{bmatrix} 1 & \beta_1 & \beta_2 & \dots & \beta_{i-1} \\ 0 & 1 & \beta_1 & \dots & \beta_{i-2} \\ 0 & 0 & 1 & \dots & \beta_{i-3} \\ \dots & \dots & \dots & \dots & \dots \\ 0 & 0 & 0 & \dots & 1 \end{bmatrix}, \text{ and } \mathbb{A}_2 = \begin{bmatrix} \beta_{\kappa-i+1} & \beta_{\kappa-i+2} & \dots & \beta_\kappa \\ \beta_{\kappa-i+2} & \beta_{\kappa-i+3} & \dots & 0 \\ \dots & \dots & \dots & \dots \\ \beta_{\kappa-1} & \beta_\kappa & \dots & 0 \\ \beta_\kappa & 0 & \dots & 0 \end{bmatrix}. \quad (1.5.7)$$

If all of the following apply, the Neimark-Sacker bifurcation occurs at  $\eta_0$ :

**C1 Eigenvalue conditions:**  $\Theta_{\kappa-1}^-(\eta_0, \zeta) = 0, \Theta_{\kappa-1}^+(\eta_0, \zeta) > 0, \mathbf{C}_{\eta_0} > 0, (-1)^\kappa \mathbf{C}_{\eta_0} > 0, \Theta_i^\pm(\eta_0, \zeta) > 0, i = \kappa - 3, \kappa - 5, \dots, 1$  ( or 2), when  $\kappa$  is even or odd, respectively.

**C2 Transversality condition:**  $\left[ \frac{d(\Theta_{\kappa-1}^-(\eta, \zeta))}{dh} \right]_{\eta=\eta_0} \neq 0.$

**C3 Resonance condition**  $\cos(\frac{2\pi}{m}) = \psi$ , or **non-resonance condition:**  $\cos(\frac{2\pi}{m}) \neq \psi$ , where  $m = 3, 4, 5, \dots$ , and  $\psi = -1 + 0.5\mathbf{C}_{\eta_0}(1) \frac{\Theta_{\kappa-3}^-(\eta_0, \zeta)}{\Theta_{\kappa-2}^+(\eta_0, \zeta)}.$

## 1.6 Chaos control

The concept behind chaos control is suppressing or eliminating any chaotic effects while maintaining the system's desired functionality. Several chaos control techniques have been developed to stabilize chaotic systems. These techniques help manage population dynamics and other complex systems where chaos can result in unpredictable behavior. This section highlights why chaos control techniques are preferable to included management methods and why using them in our predator-prey environment is crucial. These techniques can significantly influence conservation and population management by maintaining system stability and preventing bifurcation.

The main goal of controlling chaotic dynamics in biological systems is to prevent the overuse of resources or the extinction of entire species. In prey-predator models, this can be achieved by maintaining population stability at a sustainable level. Additionally, the controlled system can investigate the effects of different control strategies on the dynamics of prey-predator relationships. For example, by varying the value of the control parameter, we can assess the efficiency of various management strategies, such as eliminating predators or increasing the prey's resources.

Different control techniques are used to delay or eliminate the chaotic dynamics of any population model. A detailed comparison of the more common of these methods is given

in reference [20]. Recently, some used methods can be seen in the articles ([21], [22], [23], and [24]). In this thesis, we used a simple hybrid control feedback technique. This control strategy stabilizes the system and avoids bifurcation by combining parameter perturbation and feedback control.

# Chapter 2

## Fixed points stability, bifurcation analysis, and chaos control of a Lotka-Volterra model with two predators and their prey

### 2.1 Introduction

This chapter has been published, and its publication view can be accessed from reference [19]. We began with the literature review, which is as follows: The Lotka-Volterra model, created by Lotka [1] and Volterra [2], was the first and most basic representation of prey-predator interactions. Scientists have made many changes to this model and created many prey-predator models. These models were later innovated and changed into two categories. Continuous-time models began to be used to study changes in the populations of all continuously breeding species. In contrast, discrete-time models began to be used to study changes in the population of all species whose breeds are seasonal. These modified models are very significant for analyzing population changes in ecology. Some scientists looked at the dynamics of prey-predator populations in ecology and assisted in developing continuous-time models for huge populations ([25], [26], [27], [28], [29], [30], [31], [32], [33], [34], and [35]). Hadziabdic *et al.* [36] observed the dynamics in the community of the prey-predator model and developed the extinction conditions of one predator and the coexistence of predators. In addition, some researchers described the stability and diffusion pattern of some prey-predator models ([17], [37], [38], and [39]). A large number of scientists have shown that discrete-time models are more efficient for studying small-size population species and give efficient results than continuous-time models ([40], [41], [42],

[43], [44], [45], [46], [47], [48], [49], and [50]). Furthermore, using discrete-time models is more appropriate for non-overlapping generation, and these models describe the dynamic behavior of non-overlapping generation more efficiently. Cushing *et al.* [51] showed that dynamically, a discrete Leslie-Gower system and the well-known Lotka-Volterra differential system have the same behavior. Din [52] formulated the parametric criteria for the stability of the Leslie-Gower type prey-predator system and controlled the chaos in the system. Recently, Din ([53], [21], [22], [23], [24], [54], and [55]) worked on many discrete-time models and described the parametric conditions for the stability of these models. He traced various types of bifurcation occurring in these models theoretically, graphically, and numerically and controlled them with different chaos control strategies. Abbasi and Din [20] studied the effects of crowding in a discrete prey-predator model and analyzed the stability and bifurcation of this model. In addition, they compared different chaos control strategies and controlled the chaos in the model with the approach that yielded the best results. Some researchers have also studied the dynamical behavior of various continuous-time prey-predator models by converting them into discrete-time models in different ways. Dhar *et al.* [56] converted a continuous-time prey-predator model using Euler's method to its discrete form and discussed the effect of crowding on it. For a class of the Lotka-Volterra model, Mickens [57] implemented a non-standard difference technique. Tassaddiq *et al.* [58] implemented a piecewise constant argument to discretization a prey-predator model. They discussed its stability and bifurcation analysis. Some scientists have introduced different functional responses in prey-predator models and analyzed the dynamical behavior of these models, such as Holling-type functional responses, Beddington-DeAngelis functional responses, and square root functional responses ([3], [59], [60], [61], and [62]). The implementation of these functional responses highly affects the dynamical behavior of prey-predator interaction (Geo *et al.* [63]). Sun *et al.* [64] modified a discrete-time model and calculated the interval of existence, persistence, and global stability of the modified model. They also investigated the emerging chaos in the model and controlled the chaotic behavior by introducing immigration parameters. The bifurcation and chaotic behavior of discrete-time prey-predator models have recently been the subject of multiple papers ([65], [66], [67], [68], [69], [70], [71], and [72]). Different control strategies are implemented by ([52], [53], [21], [22], [23], [24], [54], [55], and [20]) to control the emerging chaos in various discrete-time models. For interested readers, here we have some recent work related to this study ([76], [77], [78], [79], [80], [81], and [82]). Motivated by the literature review, in this chapter, applying bifurcation theory, we investigate the stability of fixed points and the bifurcation of a three-dimensional prey-predator model. Next, taking into account the three-dimensional Lotka-Volterra prey-predator system, we have the following system (Hadziabdic *et al.* [36]):

$$\begin{cases} \dot{x}(t) = \alpha x(t) - \beta x^2(t) - \gamma x(t)y(t) - \delta x(t)z(t), \\ \dot{y}(t) = -\eta y(t) + \xi x(t)y(t), \\ \dot{z}(t) = -\theta z(t) - \zeta z(t)x(t) + \omega x(t)z(t) + \kappa y(t)z(t). \end{cases} \quad (2.1.1)$$

This system of a differential equation modeling the population dynamics of a predator  $y(t)$ , a scavenger  $z(t)$ , and the prey  $x(t)$ , where:  $\alpha$  represents the growth rate of  $x(t)$ ,  $\beta$  denotes to the carrying capacity of  $x(t)$ , and  $\gamma$  is the change rate of  $x(t)$  due to the presence of  $y(t)$ .  $\delta$  is the change rate of  $x(t)$  due to the presence of  $z(t)$ .  $\eta$  is the natural death rate of  $y(t)$ , and  $\xi$  is the change rate of  $y(t)$  due to the presence of  $x(t)$ .  $\theta$  is the natural death rate of  $z(t)$ ;  $\zeta$  is related to carrying capacity of  $z(t)$ .  $\omega$  is the change rate of  $z(t)$  due to the presence of  $x(t)$ , and  $\kappa$  is the change rate of  $z(t)$  due to the presence of  $y(t)$ . To reduce the number of parameters, we use the following scaling (see [83], [84], [85]):

$$x = \tilde{x}\hat{x}, y = \tilde{y}\hat{y}, z = \tilde{z}\hat{z}, \text{ and } t = \tilde{t}\hat{t},$$

where,  $\tilde{x}$ ,  $\tilde{y}$ ,  $\tilde{z}$ , and  $\tilde{t}$  are constants, to be chosen, and  $\hat{x}$ ,  $\hat{y}$ ,  $\hat{z}$ , and  $\hat{t}$  are the variables. Subbing these into the system (2.1.1), our ODEs lead to:

$$\frac{d(\tilde{x}\hat{x})}{d(\tilde{t}\hat{t})} = \alpha(\tilde{x}\hat{x}) - \beta(\tilde{x}\hat{x})^2 - \gamma(\tilde{x}\hat{x})(\tilde{y}\hat{y}) - \delta(\tilde{x}\hat{x})(\tilde{z}\hat{z}),$$

$$\frac{d\hat{x}}{d\hat{t}} = \alpha\tilde{t}\hat{x} - \beta\tilde{t}\hat{x}^2 - \gamma\tilde{t}\hat{x}\hat{y} - \delta\tilde{t}\hat{x}\hat{z}.$$

Now, take  $\tilde{t} = \frac{1}{\alpha}$ ,  $\tilde{x} = \frac{\alpha}{\xi}$ ,  $\tilde{y} = \frac{\alpha}{\gamma}$ , and  $\tilde{z} = \frac{\alpha}{\delta}$ . We have:

$$\frac{d\hat{x}}{d\hat{t}} = \hat{x} - \frac{\beta}{\xi}\hat{x}^2 - \hat{x}\hat{y} - \hat{x}\hat{z}.$$

Using the shift  $\frac{\beta}{\xi} = r$  and replacing  $\hat{x}$  by  $x$ ,  $\hat{t}$  by  $t$ , we get

$$\frac{dx}{dt} = x - rx^2 - xy - xz.$$

Similarly, for  $y$  and  $z$ , one can use the scaling  $x = \tilde{x}\hat{x}, y = \tilde{y}\hat{y}, z = \tilde{z}\hat{z}, t = \tilde{t}\hat{t}$ , shifting  $\tilde{t} = \frac{1}{\alpha}$ ,  $\tilde{x} = \frac{\alpha}{\xi}$ ,  $\tilde{y} = \frac{\alpha}{\gamma}$ ,  $\tilde{z} = \frac{\alpha}{\delta}$ ,  $\frac{\eta}{\alpha} = b$ ,  $\frac{\gamma}{\alpha} = c$ ,  $\frac{\zeta}{\xi} = d$ ,  $\frac{\omega}{\xi} = e$ ,  $\frac{\kappa}{\gamma} = f$ , and replacing  $\tilde{t}$  by  $t$ ,  $\tilde{x}$  by

$x$ ,  $\tilde{y}$  by  $y$ , and  $\tilde{z}$  by  $z$  to get the following system of equations:

$$\begin{cases} \dot{x}(t) = x(t) - rx^2(t) - x(t)y(t) - x(t)z(t), \\ \dot{y}(t) = -by(t) + x(t)y(t), \\ \dot{z}(t) = -cz(t) - dz(t)x(t) + ex(t)z(t) + fy(t)z(t). \end{cases} \quad (2.1.2)$$

The prey-predator model (2.1.2) demonstrates the interaction between a predator  $y(t)$ , a prey  $x(t)$ , and a scavenger population  $z(t)$ . The study of a system's behavior can be performed using either discrete or continuous models. The choice of the type of model used depends on the system being studied and the questions being asked. In the case of the Lotka-Volterra model with two predators and their prey, a discrete form of the model was used in addition to the continuous form to highlight the differences in the system's dynamics under both approaches. The discrete form of the model allows for the explicit investigation of population changes over discrete time steps.

In contrast, the continuous form represents the system's dynamics. Using discrete and continuous models allows for a deeper understanding of the system's behavior, including the stability of the fixed points, bifurcations, and the potential for chaos. In particular, the model's discrete form can help identify any discontinuities in the system's behavior, which may not be apparent in the continuous form. This information can then inform control strategies for the system, as the discrete form provides a clearer picture of the potential for rapid population changes. Therefore, the use of discrete and continuous models in studying the Lotka-Volterra model with two predators and their prey provides a complete understanding of the system's behavior and contributes to advancing knowledge in ecology and chaos control. We are also converting this model to discrete form for better qualitative analysis, including stability, bifurcation, and chaos control. Using piece-wise constant arguments, the system (2.1.2) can be converted into discrete form, which is given below:

$$\begin{cases} x_{n+1} = x_n e^{(1-rx_n-y_n-z_n)}, \\ y_{n+1} = y_n e^{(-b+x_n)}, \\ z_{n+1} = z_n e^{(-c-dx_n+ex_n+fy_n)}. \end{cases} \quad (2.1.3)$$

Investigating stability, bifurcation, and chaos in this model can provide valuable insights into the factors that shape these complex relationships. These findings can then be utilized to develop effective control strategies, helping to stabilize the system and preserve the delicate balance of the natural world. Our essential contribution is using numerical and analytical methods to perform a comprehensive system analysis in discrete and continuous form, which has yet to be done previously. Our study reveals multiple stable



fixed points, bifurcations, and chaotic behavior in the system, which can be controlled through appropriate control strategies. The rest of the chapter's details are as follows: In Section 2, we discussed the positivity of the solution. The existence and parametric conditions for the stability of the fixed points are calculated in Section 3. Section 4 is about boundedness and the existence of the positive fixed points of the discretized model (2.1.3). Local stability of fixed points of the system (2.1.3) is investigated in Section 5. In Section 6, we use the bifurcation theory for the systems (2.1.2) and (2.1.3) to derive the parametric conditions of bifurcation. The emerging chaos in the model (2.1.3) is controlled in Section 7. Numerical examples and graphical plots are given in Section 8. Finally, we conclude our investigations in Section 9.

## 2.2 Positivity and uniform boundedness of the solutions

From system (2.1.2), we have

$$\begin{cases} \dot{x} = x - rx^2 - xy - xz, \\ \dot{y} = -by + xy, \\ \dot{z} = -cz - dzx + exz + fyz. \end{cases} \quad (2.2.1)$$

Let  $(x(0), y(0), z(0)) > 0$ , then from the first equation of system (2.2.1) we have

$$x(t) = x(0)\exp\left[\int_0^t (1 - rx - y - z)\right] > 0.$$

Similarly, from the second and third equation of the system (2.2.1), one can write

$$\begin{aligned} y(t) &= y(0)\exp\left[\int_0^t (-b + x)\right] > 0, \text{ and} \\ z(t) &= z(0)\exp\left[\int_0^t (-c - dx + ex + fy)\right] > 0. \end{aligned}$$

Since the initial population  $(x(0), y(0), z(0))$  of the system is positive, we have  $x(t) > 0$ ,  $y(t) > 0$  and  $z(t) > 0 \forall t > 0$ . Assuming that the predator and scavenger populations have only prey to eat and no alternative food sources, then the predator, prey, and scavenger populations will be bounded. This is because the predator and scavenger populations depend on the prey population for survival. If there are more predators, there will be fewer prey, leading to fewer scavengers. Similarly, if the scavenger population increases, it will compete with the predator population for the prey, and this competition will lead

to a decrease in the total population of predators and scavengers. The prey population, in turn, depends on environmental factors such as food availability, temperature, and disease. If the prey population decreases too much, the predator and scavenger populations will also decrease because there will not be enough prey to support them. This creates a feedback loop where changes in one population affect the other populations, and ultimately, the total population is bounded by the environment's carrying capacity, which is the maximum number of individuals that the environment can support. Therefore, in a system where predator, prey, and scavenger populations have only prey to eat, the total population will be bounded, and the populations will oscillate over time in response to changes in environmental conditions and the dynamics of predator-prey-scavenger interactions. Therefore, if the predator and prey populations have only prey for food, then it is enough to show that the boundedness of the prey population is the boundedness of the total population. The following Lemmas shows the boundedness of the prey population.

**Lemma 2.2.1.** (see, [74]) Suppose that  $s_t$  satisfies  $s_0 > 0$  and  $s_{t+1} \leq s_t e^{[\tilde{\gamma}^*(1-\tilde{\delta}^*s_t)]}$  for  $t \in [0, \infty]$ , where  $\tilde{\delta}^* > 0$  is a constant. Then  $\lim_{t \rightarrow \infty} \sup s_t \leq \frac{1}{\tilde{\gamma}^* \tilde{\delta}^*} e^{(\tilde{\gamma}^*-1)}$ .

**Lemma 2.2.2.** Assuming that  $x_n$  satisfies  $x_0 > 0$ , then the prey population of the system (2.1.3) is uniformly bounded.

*Proof.* Assume that  $x_n$  is the positive solution of the prey population of the system (2.1.3) and  $x_0 > 0$ . Then, from the first equation of the model (2.1.3), we have:

$$x_{n+1} \leq x_n e^{[1-rx_n]}, \quad (2.2.2)$$

for all  $n = 0, 1, 2, \dots$ .

Using Lemma 4.2.3 we obtain,

$$\lim_{n \rightarrow \infty} \sup x_n \leq \frac{1}{r} := M_1.$$

Hence the proof is completed. □

## 2.3 Stability of the fixed points

This section begins by outlining the presence of fixed points in the system (2.1.2) and (2.1.3). The fixed points of the systems (2.1.2) and (2.1.3) can be found by solving the

equations in the following system:

$$\begin{cases} 0 = x - rx^2 - xy - xz, \\ 0 = -by + xy, \\ 0 = -cz - dzx + exz + fyz. \end{cases} \quad (2.3.1)$$

Solving (2.3.1), we get the following equilibria:

$E_0 = (0, 0, 0)$  : extinction of all populations.

$E_1 = \left(\frac{1}{r}, 0, 0\right)$  : existence of only  $x$  population.

$E_2 = (b, 1 - br, 0)$  : existence of  $x$  and  $y$  populations.

$E_3 = \left(-\frac{c}{d-e}, 0, \frac{cr+d-e}{d-e}\right)$  : existence of  $x$  and  $z$  populations.

$E_* = \left(b, \frac{bd-be+c}{f}, \frac{be-bd-bfr-c+f}{f}\right)$  : coexistence of all populations.

The fixed point  $E_2$  will be positive when  $br < 1$ ,  $E_3$  will be positive when  $e > d$ , and  $e - d - cr > 0$ . The interior fixed point  $E_*$  is positive iff the following conditions hold:

$$c + bd > be \text{ and } be + f > c + bd + bfr.$$

Now, we discuss the local stability of fixed points of the system (2.1.2). The variational matrices about the fixed points are given below:

$$V(E_0) = \begin{pmatrix} 1 & 0 & 0 \\ 0 & -b & 0 \\ 0 & 0 & -c \end{pmatrix}, V(E_1) = \begin{pmatrix} -1 & -\frac{1}{r} & -\frac{1}{r} \\ 0 & \frac{1}{r} - b & 0 \\ 0 & 0 & -\frac{d-e+cr}{r} \end{pmatrix},$$

$$V(E_2) = \begin{pmatrix} -br & -b & -b \\ 1 - br & 0 & 0 \\ 0 & 0 & -c + f - b(d - e + fr) \end{pmatrix}, \text{ and}$$

$$V(E_3) = \begin{pmatrix} \frac{cr}{d-e} & \frac{c}{d-e} & \frac{c}{d-e} \\ 0 & \frac{c}{e-d} - b & 0 \\ -d + e - cr & \frac{crf}{d-e} + f & 0 \end{pmatrix}.$$

The eigenvalues of  $V(E_0)$  are  $\{1, -b, -c\}$ , thus  $E_0$  is unstable. The eigenvalues of  $V(E_1)$  are  $\{-1, -\frac{br-1}{r}, -\frac{cr+d-e}{r}\}$ , which shows that  $E_1$  is sink when  $br > 1$  and  $cr + d > e$ . Similarly,  $\lambda_1 = -c + f - b(d - e + fr)$ ,  $\lambda_2 = \frac{1}{2} \left(-br - \sqrt{b} \sqrt{-4 + 4br + br^2}\right)$ , and

$\lambda_3 = \frac{1}{2} \left( -br + \sqrt{b} \sqrt{-4 + 4br + br^2} \right)$  are the eigenvalues of  $V(E_2)$ . The fixed point

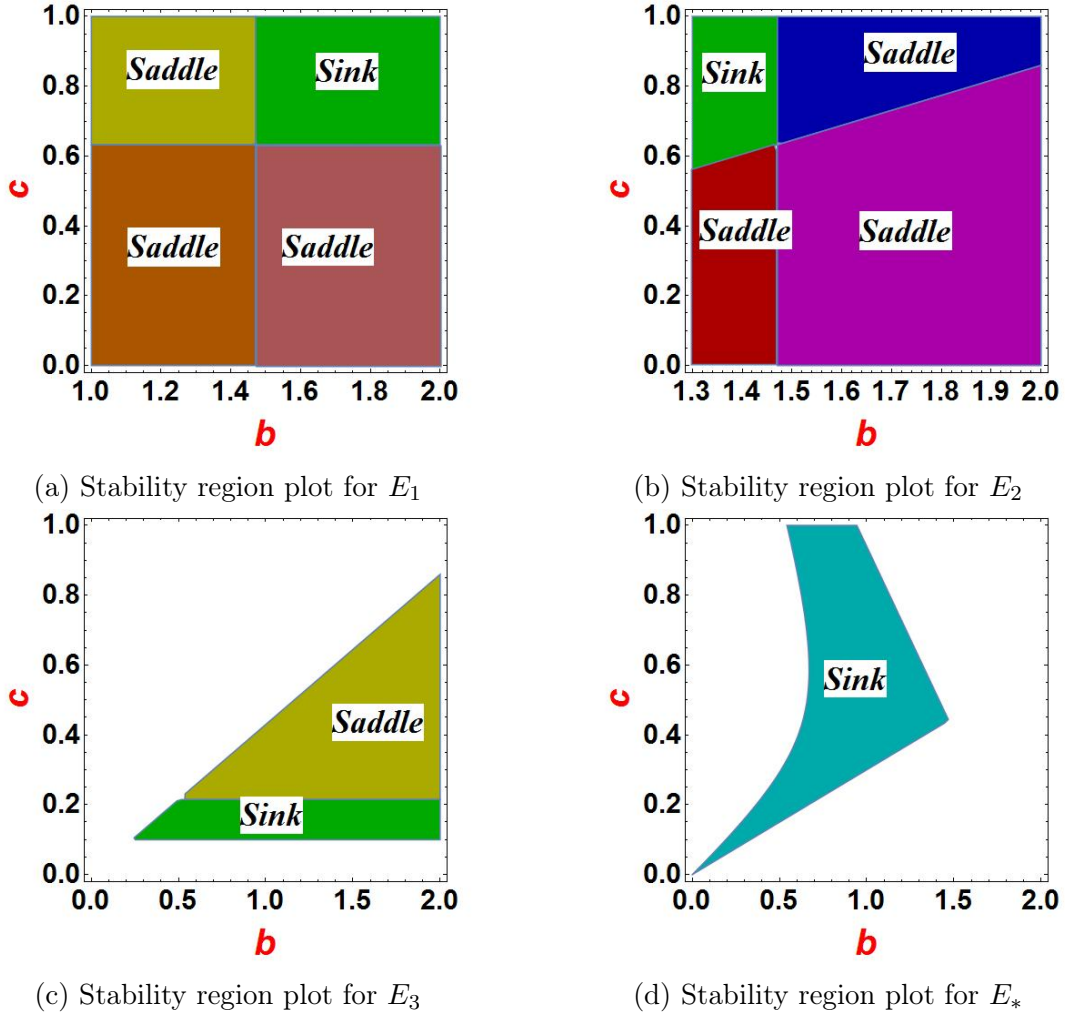


Figure 2.1: Topological classification of fixed points

$E_2$  is sink when  $Re(\lambda_1) < 0$ ,  $Re(\lambda_2) < 0$ , and  $Re(\lambda_3) < 0$ . The eigenvalues of the variational matrix  $V(E_3)$  are  $\lambda_1 = \frac{-bd+be-c}{d-e}$ ,  $\lambda_2 = \frac{cr-\sqrt{-4c^2dr+4c^2er+c^2r^2-4cd^2+8cde-4ce^2}}{2(d-e)}$ , and  $\lambda_3 = \frac{cr+\sqrt{-4c^2dr+4c^2er+c^2r^2-4cd^2+8cde-4ce^2}}{2(d-e)}$ . The fixed point  $E_3$  is sink when  $Re(\lambda_1) < 0$ ,  $Re(\lambda_2) < 0$ , and  $Re(\lambda_3) < 0$ . Assume

$$c + bd > be \text{ and } be + f > c + bd + bfr.$$

holds, then the variational matrix about the unique positive fixed point is given by:

$$V(E_*) = \begin{pmatrix} -br & -b & -b \\ \frac{c+bd-be}{f} & 0 & 0 \\ \frac{(d-e)(c-f+b(d-e+fr))}{f} & -c+f-b(d-e+fr) & 0 \end{pmatrix}. \quad (2.3.2)$$

The characteristic polynomial of (2.3.2) is given by:

$$P_{E_*}(\lambda) = \lambda^3 + (br)\lambda^2 + \left( \frac{b((b(d-e+fr+1)-f)(d-e) + (d+1-e)c)}{f} \right) \lambda - \frac{(b(d-e)+c)(b)(b(d-e+fr)+c-f)}{f}. \quad (2.3.3)$$

The fixed point  $E_*$  is stable according to the Routh-Hurwitz criterion [73] if the conditions hold:

$$\begin{aligned} &e < d, b^2(d-e)(d-e+fr+1) + bc(1+d-e) > fb(d-e), f(b^2(d-e) + bc) > \\ &((d-e)b^2 + bc)((d-e+fr)b + c), \text{ and} \\ &bf\left(c(b(d(r+2)-e(r+2)+fr+r)-f) + b(d-e)(b((1+r)d + (1+r)(fr-e) + r) - f(1+r)) + c^2\right) > 0. \end{aligned}$$

Now, we determined the parametric conditions for the local stability of each fixed point in the system (2.1.3) and presented their regional stability. We use eigenvalue criteria to discuss the stability of the fixed points. All the fixed points are stable when the absolute values of the eigenvalues are less than one and unstable when the absolute values of the eigenvalues are greater than one. Furthermore, the sink, source, saddle, and nonexistence region plots for every fixed point are also depicted. The variational matrix of structure (2.1.3) calculated at  $E_0(0, 0, 0)$  is given by:

$$V(0, 0, 0) = \begin{pmatrix} \mathbf{e} & 0 & 0 \\ 0 & \mathbf{e}^{-b} & 0 \\ 0 & 0 & \mathbf{e}^{-c} \end{pmatrix}. \quad (2.3.4)$$

The eigenvalues of (2.3.4) are  $\mu_1(E_0) = \mathbf{e}$ ,  $\mu_2(E_0) = \mathbf{e}^{-b}$ , and  $\mu_3(E_0) = \mathbf{e}^{-c}$ . Thus,  $E_0(0, 0, 0)$  is a saddle point. The variational matrix of system (2.1.3) evaluated at  $E_1(\frac{1}{r}, 0, 0)$  is given by:

$$V\left(\frac{1}{r}, 0, 0\right) = \begin{pmatrix} 0 & -\frac{1}{r} & -\frac{1}{r} \\ 0 & e^{\frac{1}{r}-b} & 0 \\ 0 & 0 & e^{-\frac{d-e+cr}{r}} \end{pmatrix}. \quad (2.3.5)$$

The eigenvalues of (2.3.5) are  $\mu_1(E_1) = 0$ ,  $\mu_2(E_1) = e^{\frac{1}{r}-b}$ , and  $\mu_3(E_1) = e^{-c-\frac{d}{r}+\frac{e}{r}}$ . Hence,  $E_1(\frac{1}{r}, 0, 0)$  is sink when  $1 < br$ ,  $cr + d > e$  and saddle point if  $1 > br$ ,  $cr + d < e$ . The region plot for the existence of the sink is given in Figure 2.2. The variational matrix of

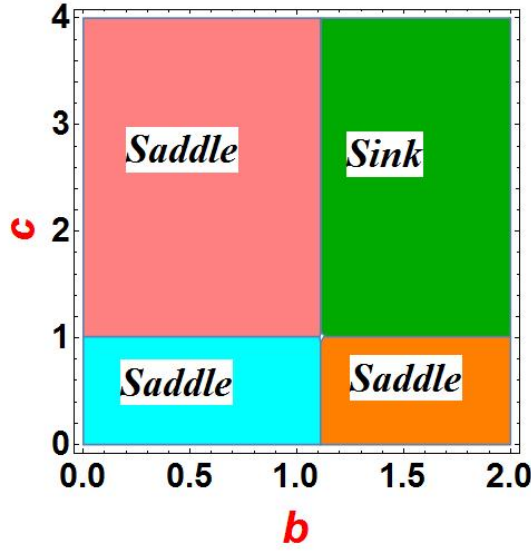


Figure 2.2: Topological classification of  $E_1$

system (2.1.3) evaluated at  $E_2(b, 1 - br, 0)$  is given by:

$$V(b, 1 - br, 0) = \begin{pmatrix} 1 - br & -b & -b \\ 1 - br & 1 & 0 \\ 0 & 0 & e^{-c+f-b(d-e+fr)} \end{pmatrix}. \quad (2.3.6)$$

The eigenvalues of (2.3.6) are:

$$\begin{aligned} \mu_1(E_2) &= \frac{1}{2} \left( -br - \sqrt{b} \sqrt{br(r+4) - 4} + 2 \right), \\ \mu_2(E_2) &= \frac{1}{2} \left( -br + \sqrt{b} \sqrt{br(r+4) - 4} + 2 \right), \text{ and} \\ \mu_3(E_2) &= e^{-b(d-e+fr)-c+f}. \end{aligned}$$

The fixed point  $E_2(b, 1 - b^2, 0)$  is stable when  $|\mu_1(E_2)| < 1$ ,  $|\mu_2(E_2)| < 1$  and  $|\mu_3(E_2)| < 1$ . The topological classification is given in Figure 2.3.

The variational matrix of structure (2.1.3) calculated at  $E_3\left(-\frac{c}{d-e}, 0, -\frac{-cr-d+e}{d-e}\right)$  is given by:

$$V\left(-\frac{c}{d-e}, 0, -\frac{-cr-d+e}{d-e}\right) = \begin{pmatrix} \frac{cr}{d-e} + 1 & \frac{c}{d-e} & \frac{c}{d-e} \\ 0 & e^{\frac{c}{e-d}-b} & 0 \\ e-d-cr & \frac{crf}{d-e} + f & 1 \end{pmatrix}. \quad (2.3.7)$$

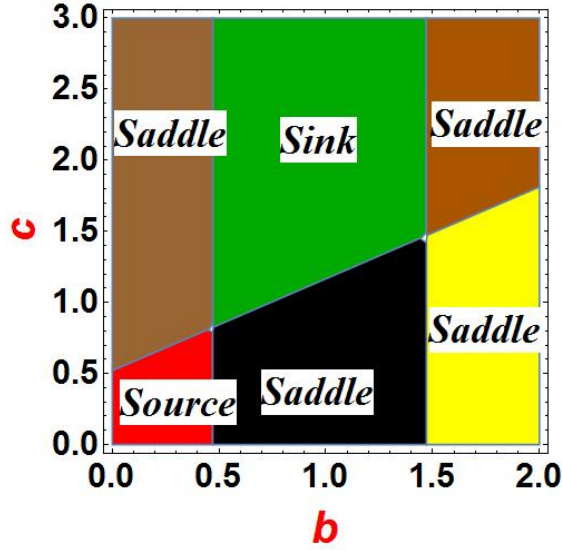


Figure 2.3: Topological classification of  $E_2$

The eigenvalues of (2.3.7) are:

$$\mu_1(E_3) = \frac{-e^{-b} \sqrt{e^{2b}(-c)(4cr(d-e) - cr^2 + 4(d-e)^2)} + cr + 2d - 2e}{2(d-e)},$$

$$\mu_2(E_3) = \frac{e^{-b} \sqrt{e^{2b}(-c)(4cr(d-e) - cr^2 + 4(d-e)^2)} + cr + 2d - 2e}{2(d-e)}, \text{ and}$$

$$\mu_3(E_3) = e^{\frac{c}{e-d}-b}.$$

Thus, the boundary point  $E_3 \left( -\frac{c}{d-e}, 0, -\frac{-cr-d+e}{d-e} \right)$  of system (2.1.3) is stable when  $|\mu_1(E_3)| < 1$ ,  $|\mu_2(E_3)| < 1$ , and  $|\mu_3(E_3)| < 1$ . The topological classifications are given in Figure 2.4. The variational matrix of (2.1.3) at  $\left( b, -\frac{bd+be-c}{f}, -\frac{bd-be+bfr+c-f}{f} \right)$  is given by:

$$V(E^*) = \begin{pmatrix} 1-br & -b & -b \\ \frac{c+bd-be}{f} & 1 & 0 \\ \frac{(d-e)(c-f+b(d-e+fr))}{f} & f-c-b(d+bf-e) & 1 \end{pmatrix}. \quad (2.3.8)$$

The characteristic function of (2.3.8) is given by:

$$P(\mu) = \mu^3 + \zeta_1 \mu^2 + \zeta_2 \mu + \zeta_3,$$

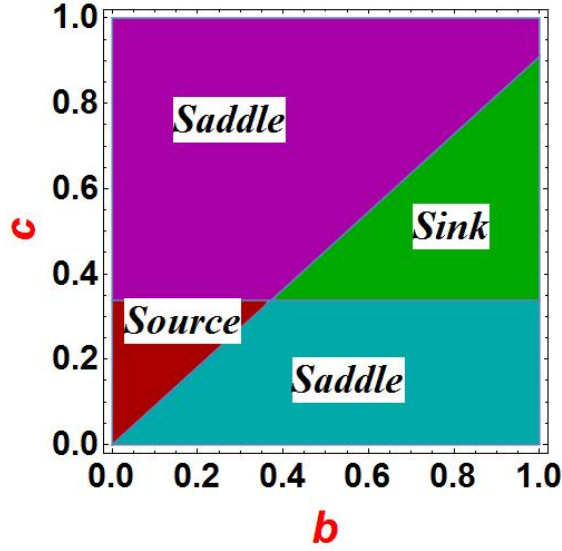


Figure 2.4: Topological classification of  $E_3$

where

$$\begin{aligned}
\zeta_1 &= br - 3, \\
\zeta_2 &= \frac{b((d-e)(b)(1+d-e+fr) + (d-e+1)c + f(-d+e-2r))}{f} + 3, \\
\zeta_3 &= -\frac{b(bd-be+c)(b^2f+bd-be+c-f)}{f} - \frac{b^2d}{f} + \frac{b^2e}{f} - \frac{bc}{f} + br - 1 \\
&\quad - \frac{(d-e)(b)(bd+c-be+bfr-f)}{f}.
\end{aligned} \tag{2.3.9}$$

We have the following theorem for the local stability of  $E^* = \left(b, -\frac{bd+be-c}{f}, -\frac{bd-be+bfr+c-f}{f}\right)$  using Routh-Hurwitz criteria.

**Theorem 2.3.1.** *The fixed point  $E^* = \left(b, -\frac{bd+be-c}{f}, -\frac{bd-be+bfr+c-f}{f}\right)$  of the system (2.1.3) is locally asymptotically stable if the underlying axioms are satisfied:*

$$\begin{aligned}
|\zeta_1 + \zeta_3| &< 1 + \zeta_2, \\
|\zeta_1 - 3\zeta_3| &< 3 - \zeta_2, \\
\zeta_3^2 + \zeta_2 - \zeta_3\zeta_1 &< 1.
\end{aligned} \tag{2.3.10}$$

The topological classifications are given in Figure 2.5. Now, we deal with the existence and uniqueness of the positive fixed point of the system (2.1.3). In this regard, we have the following lemma:

**Lemma 2.3.2.** *If  $c + bd > be$  and  $be + f > c + bd + bfr$  then there exists the unique positive fixed point  $\left(b, \frac{bd-be+c}{f}, \frac{be-bd-bfr-c+f}{f}\right)$  of the system (2.1.3).*



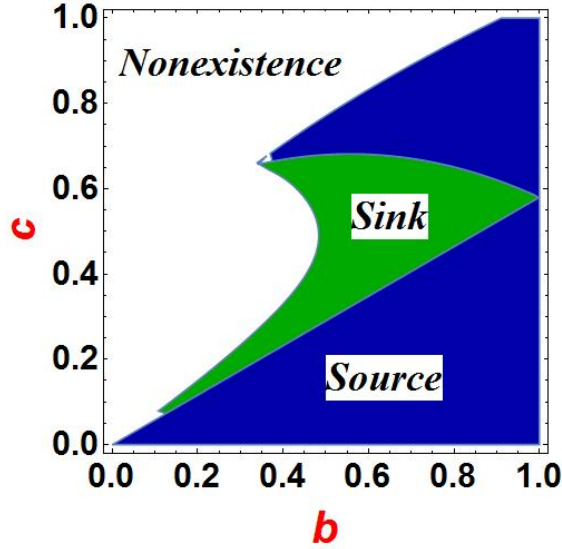


Figure 2.5: Topological classifications of  $E^*$

*Proof.* By solving the following set of equations, one can determine the fixed points of the system (2.1.3).

$$\begin{aligned} x &= x\mathbf{e}^{(1-rx-y-z)}, \\ y &= y\mathbf{e}^{(-b+x)}, \\ z &= z\mathbf{e}^{(-c-dx+ex+fy)}. \end{aligned}$$

If we ignore the trivial and the boundary fixed points, we have left

$$\begin{aligned} 0 &= 1 - rx - y - z, \\ 0 &= -b + x, \\ 0 &= -c - dx + ex + fy. \end{aligned}$$

The second equation of the system mentioned above yields  $x = b$ . By putting  $x = b$  in the last equation of the system, as mentioned above, we get  $y = \frac{c+bd-be}{f}$ . Finally, by putting the values of  $x$  and  $y$  in the above system's first equation, we get  $z = \frac{be-bd-bfr-c+f}{f}$ . Thus,  $(x^*, y^*, z^*) = \left(b, \frac{bd-be+c}{f}, \frac{be-bd-bfr-c+f}{f}\right)$  be the only positive fixed point of the system (2.1.3). Hence, the proof is completed.  $\square$

## 2.4 Bifurcation analysis

The Hopf bifurcation of the system (2.1.2) and Neimark-Sacker bifurcation of the system (2.1.3) at the fixed point  $\left(b, -\frac{bd+be-c}{f}, -\frac{bd-be+bfr+c-f}{f}\right)$ , is covered in this section. Us-

ing bifurcation theory, we calculate the parametric conditions for the existence of both bifurcations in terms of eigenvalues without finding eigenvalues. We also observed that closed invariant circles were produced due to both bifurcations.

### 2.4.1 Hopf bifurcation

In this section, we discuss the bifurcation over the positive fixed point of the system (2.1.2). For this, we use the criteria of Hopf bifurcation without calculating the eigenvalues given in Section 1.5 of Chapter 1. Consider system (2.1.2) with characteristic function (2.3.3), choose  $c$  as a bifurcation parameter, and then the following lemmas show the existence of Hopf bifurcation at  $E^*$ .

**Lemma 2.4.1.** *Assume that  $c + bd > be$  and  $be + f > c + bd + bfr$ , then the unique positive fixed point  $\left(b, -\frac{bd+be-c}{f}, -\frac{bd-be+bfr+c-f}{f}\right)$  undergoes Hopf bifurcation when we choose  $c$  as a bifurcation parameter. The bifurcation parameter  $c$  varies in the limited neighborhood of*

$$c^* = \frac{1}{2} \left( -\sqrt{-2b(b^2 - 1)fr(d - e - 1) + b^2r^2(d - e + 1)^2 + (b^2 - 1)^2f^2} - b(bf + d(r + 2) - e(r + 2) + r) + f \right),$$

or

$$c^* = \frac{1}{2} \left( \sqrt{-2b(b^2 - 1)fr(d - e - 1) + b^2r^2(d - e + 1)^2 + (b^2 - 1)^2f^2} - b(bf + d(r + 2) - e(r + 2) + r) + f \right),$$

and if the following conditions hold:

$$\begin{aligned} \zeta_0[\Theta^*] &= \frac{b(b(d - e) + c)(f - (d + fr - e)b - c)}{f} > 0, \text{ iff } e < d, \text{ and } f > c + (d + fr - e)b, \\ D_1[\Theta^*] &= \frac{b((d - e)(b(d - e + fr + 1) - f) + c(d - e + 1))}{f} > 0, \text{ iff } e < d, \text{ and} \\ &\quad (d - e)(d)(b(d + fr + 1 - e)) > (d - e)df. \\ D_2[\Theta^*] &= \left[ \frac{b((b^2 - 1)f(d - e) + (d - e + 1)(c + (d - e)b))}{f} \right] [br] \\ &\quad + \left( \frac{((d - e)b + c)(b)(b(bf - e + d) - f + c)}{f} \right) = 0, \text{ iff} \\ c &= \frac{1}{2} \left( -\sqrt{-2b(b^2 - 1)fr(d - e - 1) + b^2r^2(d - e + 1)^2 + (b^2 - 1)^2f^2} \right. \end{aligned} \tag{2.4.1}$$

$$-b(fb + d(2 + r) + r - e(r + 2)) + f). \quad (2.4.2)$$

Using the theory in Section 1.5 of Chapter 1, we have derived the following conditions for the existence of Neimark-Sacker bifurcation in System 2.1.3.

**Theorem 2.4.2.** *The fixed point  $\left(b, -\frac{bd+be-c}{f}, -\frac{bd-be+bfr+c-f}{f}\right)$  of structure (2.1.3) go through Neimark-Sacker bifurcation if the following conditions hold:*

$$\begin{aligned} \zeta_1 - \zeta_2 + \zeta_3(\zeta_1 - \zeta_3) &= 0, \\ 1 + \zeta_2 - \zeta_3(\zeta_1 + \zeta_2) &> 0, \\ 1 + \zeta_1 + \zeta_2 + \zeta_3 &> 0, \\ 1 - \zeta_1 + \zeta_2 - \zeta_3 &> 0, \end{aligned}$$

where  $\zeta_1, \zeta_2$  and  $\zeta_3$  are given in (2.3.9).

## 2.5 Numerical simulations

In the section on simulation, we aim to demonstrate the validity of the mathematical analysis performed in the previous sections through numerical simulations of the Lotka-Volterra model with two predators and their prey. The simulation examples will be conducted in discrete and continuous forms to highlight the differences in the dynamics and stability of the model under different conditions. The simulation examples will include cases where the system converges to a stable equilibrium, where the system exhibits periodic behavior, and where the system exhibits chaotic behavior. For each simulation example, we will discuss the results obtained, including the time evolution of the population sizes of the predators and prey and the phase portraits of the system. The simulation results will validate the theoretical analysis performed in the previous sections and provide further insight into the dynamics and stability of the Lotka-Volterra model with two predators and their prey. The simulation examples will demonstrate the importance of considering both discrete and continuous forms of the model in understanding the system's behavior and the role of chaos in the dynamics of predator-prey interactions. In addition, we have also discussed the effectiveness of the control scheme in maintaining stability in the system, even in the presence of bifurcations and chaos. The numerical examples demonstrate the control scheme's success in regulating the population sizes of the predators and prey and maintaining stability in the system.

Moreover, the numerical examples also highlight the importance of carefully considering the control parameters, as small changes in the control parameters can lead to significant

changes in the system's dynamics. The numerical examples demonstrate the robustness of the control scheme in the presence of different initial conditions and changes in the control parameters. Therefore, the numerical examples provide strong evidence for the validity of the previous sections' theoretical results and demonstrate the control scheme's effectiveness in maintaining stability in the Lotka-Volterra model with two predators and their prey. These numerical examples are crucial in understanding the system's behavior and provide valuable insight into the role of chaos and bifurcations in prey-predator interactions.

**Example 1.** *If the numerical values of parameters are selected as:  $d = 0.01, e = 2.8, f = 3.24, b = 0.5, r = 0.5, c \in (3, 3.6)$  with initial population  $(0.2897, 0.3975, 0.3241)$ .*

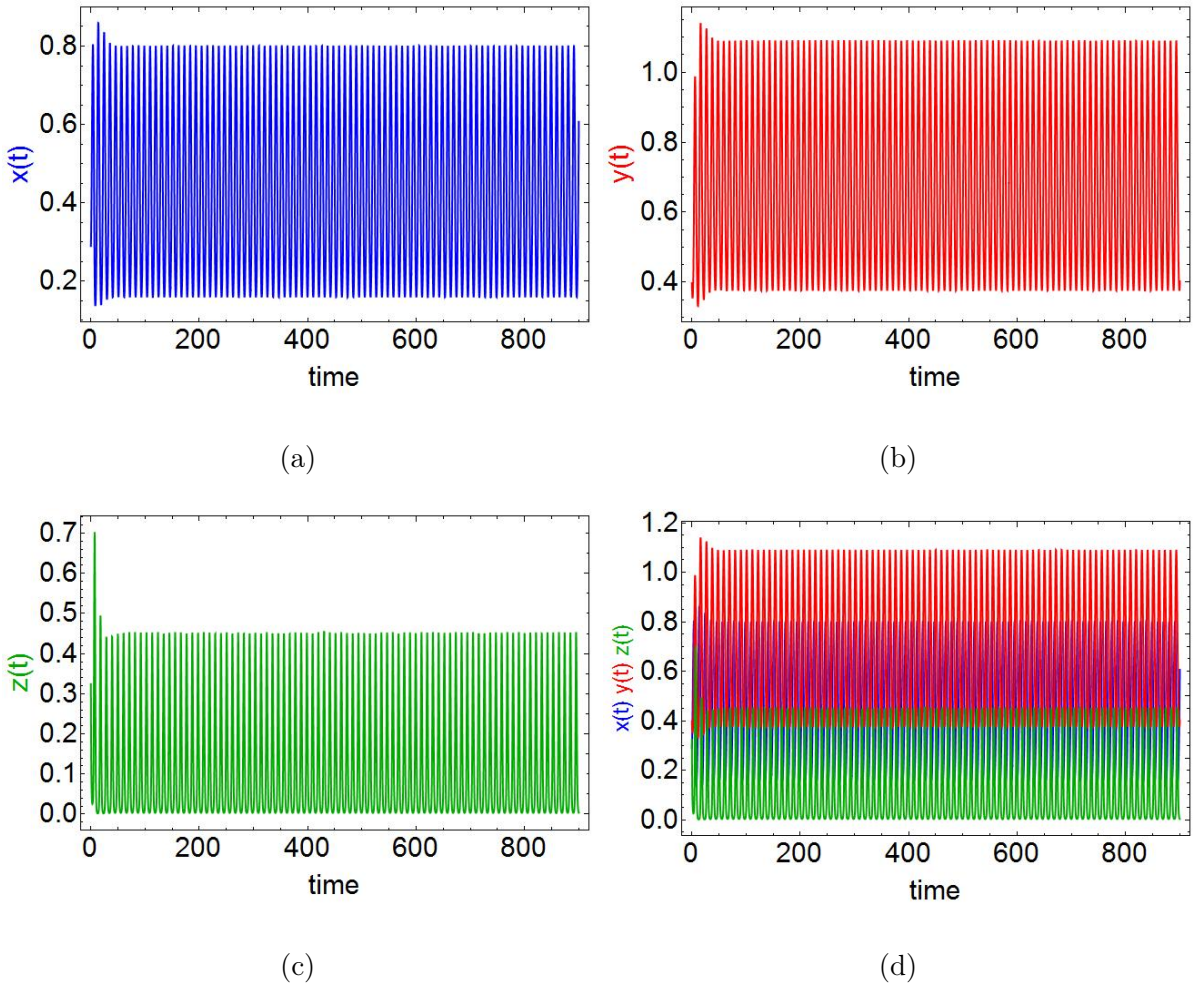


Figure 2.6: Time series plots for above parametric values.

Then in model (5.1.2), the backward Hopf bifurcation arises for  $E^* = (0.5, 0.633082, 0.116918)$  when we choose  $c$  as a bifurcation parameter. It was observed that the bifurcation arises at  $c = 3.4461849455248306$ . For these selected parametric values  $d = 0.01, e = 2.8, f =$

3.24,  $b = 0.5$ , and with the chaotic parameter  $c = 3.4461849455248306$ , we have:

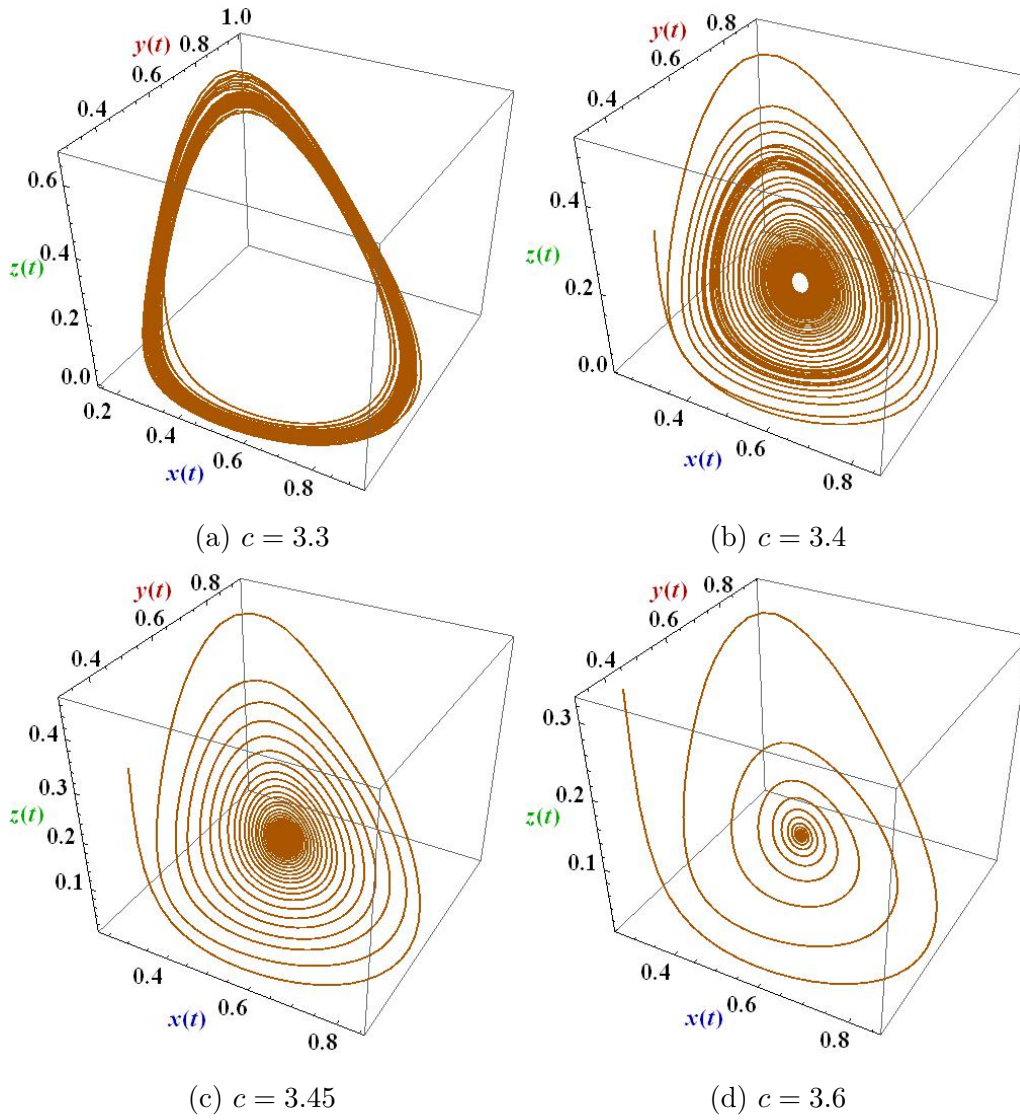


Figure 2.7: Phase plots for different values of  $c$ .

$$V(E^*) = \begin{pmatrix} 0 & 0 & 0 \\ 0.633082 & 0. & 0 \\ 0.326202 & 0.378815 & 0. \end{pmatrix}. \quad (2.5.1)$$

The characteristic function of (2.5.1) is:

$$C(\mu) = \mu^3 + 0.25\mu^2 + 0.479642\mu + 0.11991. \quad (2.5.2)$$

Thus, from (2.5.2), we have conditions:



$$\begin{aligned}
(I) : \zeta_0[\Theta^*] &= 0.11991 > 0, D_1[\Theta^*] = \zeta_1[\Theta^*] = 0.479642 > 0, \\
D_2[\Theta^*] &= \zeta_1[\Theta^*]\zeta_2[\Theta^*] - \zeta_0[\Theta^*] = 0, \\
(II) : \frac{dD_2[\Theta^*]}{d\Theta} &= -0.32714 \neq 0.
\end{aligned}$$

Thus, all the conditions of Hopf bifurcation are satisfied. Therefore, in the system (5.1.2),

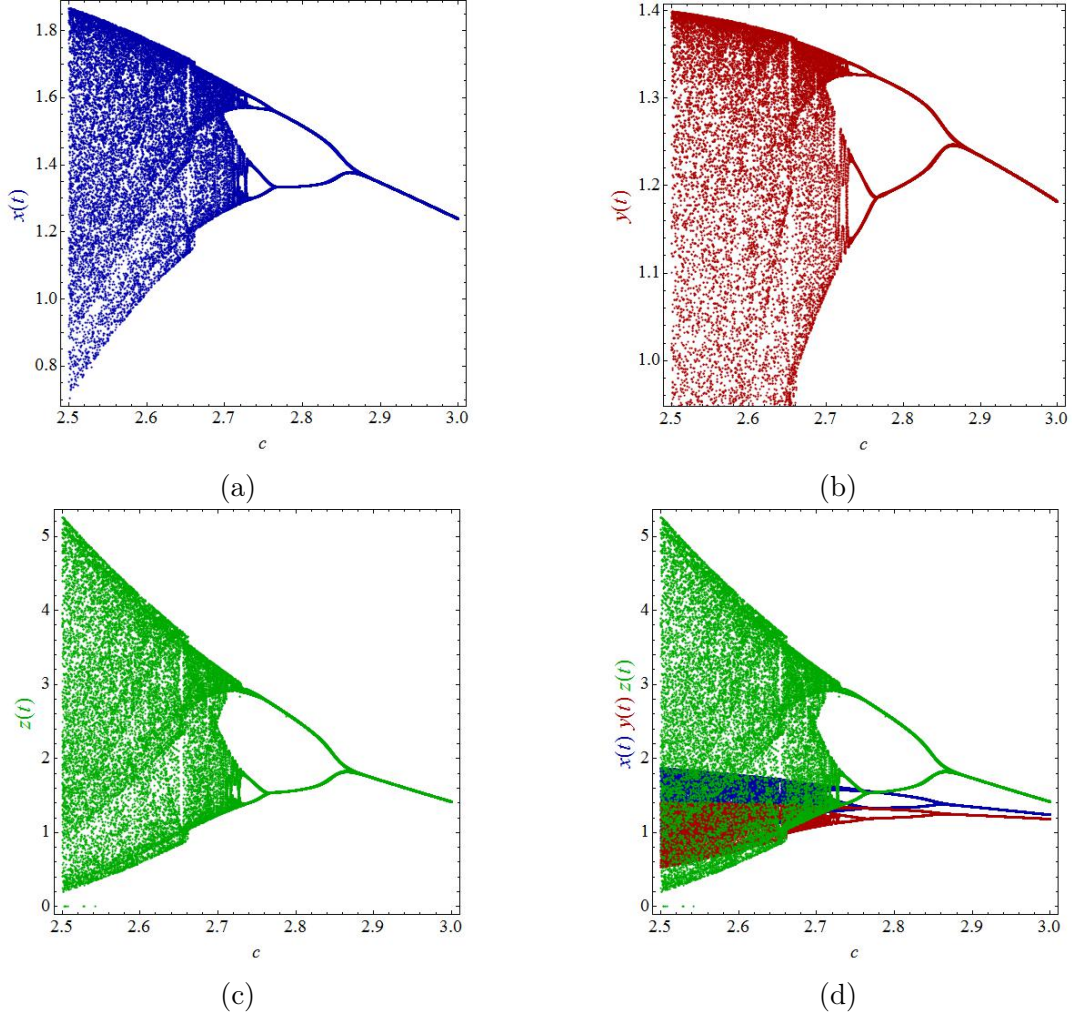


Figure 2.8: Flip bifurcation plots

the backward Hopf bifurcation emerges for these fixed parametric values. The chaotic plots for  $d = 0.01, e = 2.8, f = 3.24, b = 0.5, r = 0.5, c = 3.4461849455248306$ ,  $time \in [0, 600]$  and with initial conditions  $(0.5, 0.633082, 0.116918)$  are shown in Figure 2.6. Furthermore, the phase plots for different values of chaotic parameter  $c$  are given in Figure 2.7. These plots confirm the dynamical complexity and existence of Hopf bifurcation in the model (5.1.2). From the phase plots, it can be noticed that the closed invariant curves are formed due to Hopf bifurcation. Thus, for the parametric values  $d = 0.01, e = 3.8, f =$

2.4,  $b = 0.54$ ,  $r = 0.45$ ,  $c = 2.562730676041003$ ,  $time \in [0, 600]$  the system (5.1.2) has limit cycles around the unstable fixed point  $E^*$ . When the value of the bifurcation parameter decreases from  $c = 3$ , we numerically find that the limit cycle splits into period orbits. Thus, backward flip bifurcation emerges, and the chaotic region increases when the value of  $c$  further decreases. Figure 2.8 shows the backward flip bifurcation diagrams.

**Example 2.** Let we have:  $d = 0.01$ ,  $e = 3.8$ ,  $f = 3.5$ ,  $b = 0.45$ ,  $r = 0.45$ ,  $c \in (2.3, 4)$  and initial population  $(0.5, 1.4, 0.9)$ . Then in model (5.1.2), the Hopf bifurcation arises for  $E^* = (0.45, 0.244923, 0.552577)$ , when we choose  $c$  as a bifurcation parameter. It is observed that the chaotic region begins from  $c = 2.5627306760410034$ . For the parametric values  $d = 0.01$ ,  $e = 3.8$ ,  $f = 3.5$ ,  $b = 0.45$ ,  $r = 0.45$ ,  $c = 2.5627306760410034$  we have:

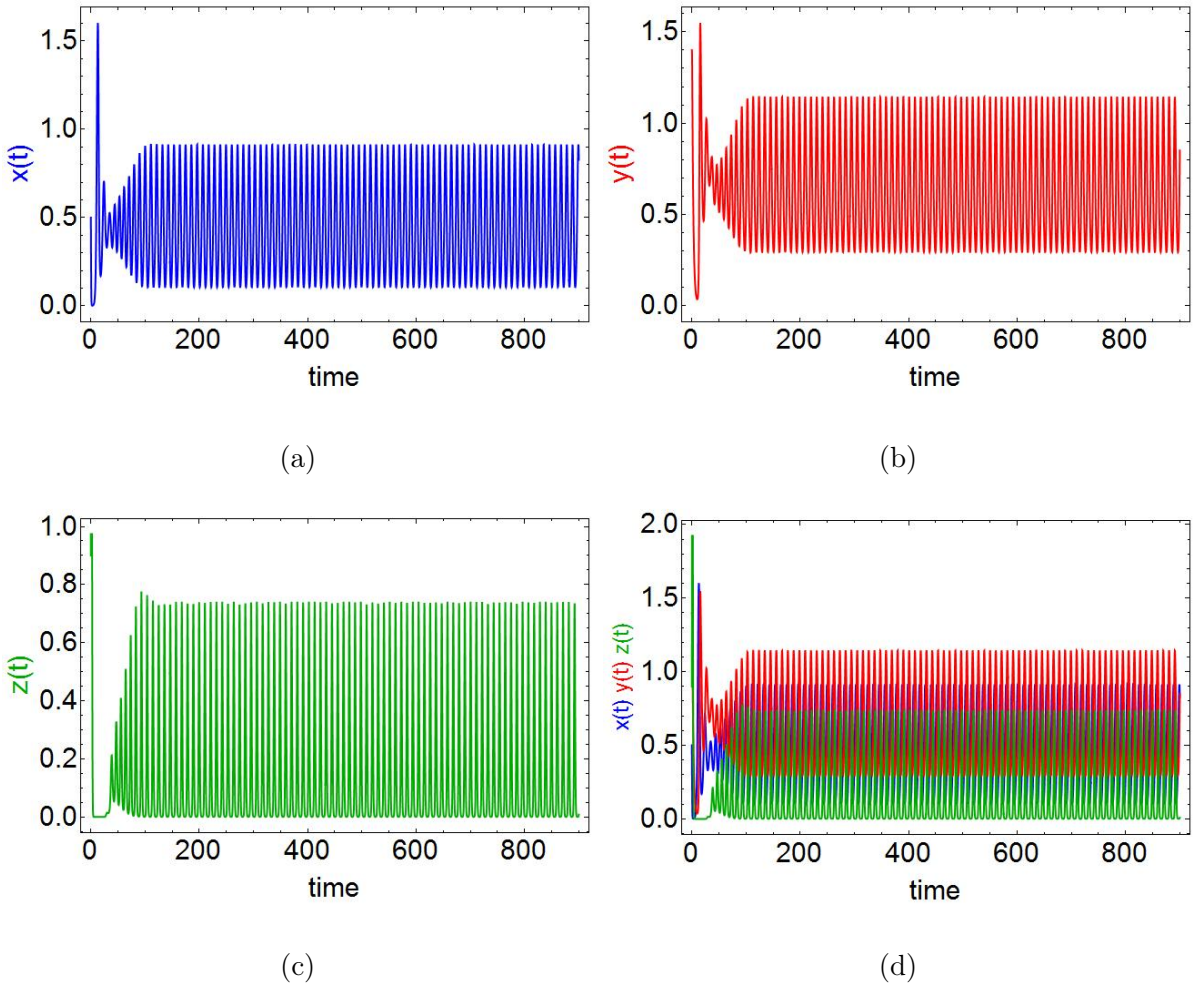


Figure 2.9: Time series plots for  $d = 0.01$ ,  $e = 3.8$ ,  $f = 3.5$ ,  $b = 0.45$ ,  $r = 0.45$ ,  $c \in (2.3, 4)$  and initial population  $(0.5, 1.4, 0.9)$ .

$$V(E^*) = \begin{pmatrix} 0 & 0 & 0 \\ 0.244923 & 0. & 0 \\ 2.09427 & 1.93402 & 2.220446049250313 \times 10^{-16} \end{pmatrix}. \quad (2.5.3)$$

The characteristic function of (2.5.3) is:

$$C(\mu) = \mu^3 + 0.2025\mu^2 + 1.05264\mu + 0.213159. \quad (2.5.4)$$

Thus, from (2.5.4), we have the following conditions:

$$\begin{aligned} (I) : \zeta_0[\Theta^*] &= 0.213159 > 0, D_1[\Theta^*] = \zeta_1[\Theta^*] = 1.05264 > 0, \\ D_2[\Theta^*] &= \zeta_1[\Theta^*]\zeta_2[\Theta^*] - \zeta_0[\Theta^*] = 0, \\ (II) : \frac{dD_2[\Theta^*]}{d\Theta} &= 0.0658046 \neq 0. \end{aligned}$$

Hence, we have seen that the chaos arises in (5.1.2). Moreover, all the conditions of Lemma 2.4.1 are satisfied. Therefore, model (5.1.2) experiences Hopf bifurcation for selected parametric values. Furthermore, bifurcation plots for the above preferred parametric values are depicted in figure 2.9. These plots show that the bifurcation continues in the model (5.1.2) for a long time.

We have explored the system's dynamics over an infinite time interval with the continuous time model. However, it is often necessary to simulate the system over a finite time interval with discrete time steps. This is where the numerical simulation of the discrete-time model comes in. First, we will show the system's stability (2.1.3).

**Example 3.** For the parametric values  $b = 0.7, r = 0.7, c = 2.73, d = 1, e = 2.8, f = 3.2$  and initial population  $(x_0, y_0, z_0) = (0.4443, 0.4975, 0.1)$  the positive fixed point  $(0.7, 0.459375, 0.050625)$  of (2.1.3) is locally asymptotically stable. The variational matrix and characteristic function at  $(0.7, 0.459375, 0.050625)$  is:

$$V(0.7, 0.4625, 0.0475) = \begin{pmatrix} 0 & 0 & 0 \\ 0.4625 & 1. & 0 \\ 0.0855 & 0.152 & 1. \end{pmatrix}.$$

$$C(\mu) = \mu^3 - 0.66\mu - 0.25\mu + 0.828,$$

where  $\zeta_1 = -0.66, \zeta_2 = -0.25$ , and  $\zeta_3 = 0.828$ . Furthermore, from (2.3.10), we have the



following inequalities:

$$\begin{aligned} |\zeta_1 + \zeta_3| &= 0.168 < 1 + \zeta_2 = 0.75, \\ |\zeta_1 - 3\zeta_3| &= 3.144 < 3 - \zeta_2 = 3.25, \\ \zeta_3^2 + \zeta_2 - \zeta_3\zeta_1 &= 0.982064 < 1. \end{aligned}$$

Therefore, all the stability conditions are satisfied, and we have the stability plots in Figure 2.10.

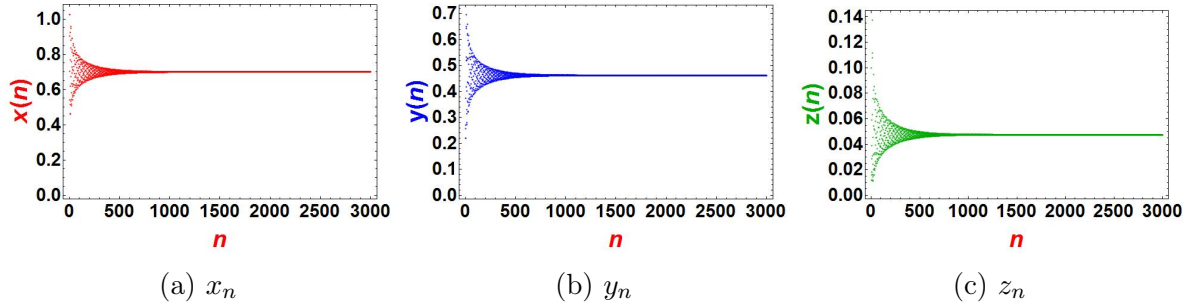


Figure 2.10: Stability diagrams.

**Example 4.** Let us have the initial population  $(x_0, y_0, z_0) = (0.4443, 0.4975, 0.1)$  and parametric values:  $b = 0.7, r = 0.7, d = 1, e = 2.8, f = 3.2, c \in [2.5, 2.8]$ . Then the positive fixed point of (2.1.3) experiences Hopf bifurcation when we choose  $c$  as a bifurcation parameter. It is visible that the bifurcation emerges at  $c = 2.7294647587715626$ . Thus,  $[2.7294647587715626, 2.8]$  is the bifurcation region. The variational matrix for the above parametric values is given by:

$$V(0.7, 0.459208, 0.0507923) = \begin{pmatrix} 0 & 0 & 0 \\ 0.459208 & 1. & 0 \\ 0.0914261 & 0.162535 & 1. \end{pmatrix}, \quad (2.5.5)$$

The characteristic function of (2.5.5) is

$$C(\mu) = \mu^3 - 2.51\mu^2 + 2.40544\mu - 0.843197,$$

The eigenvalues of  $C(\mu)$  are  $\mu_{1,2} = 0.833401 \pm 0.552668i$  and  $\mu_3 = 0.843197$ , with  $|\mu_{1,2}| = 1$ . Moreover, all the conditions of Lemma 1.5.3 and Lemma 1.5.4 are satisfied. The bifurcation plots are given in Figure 2.11, and their phase plots are given in Figure 2.12.

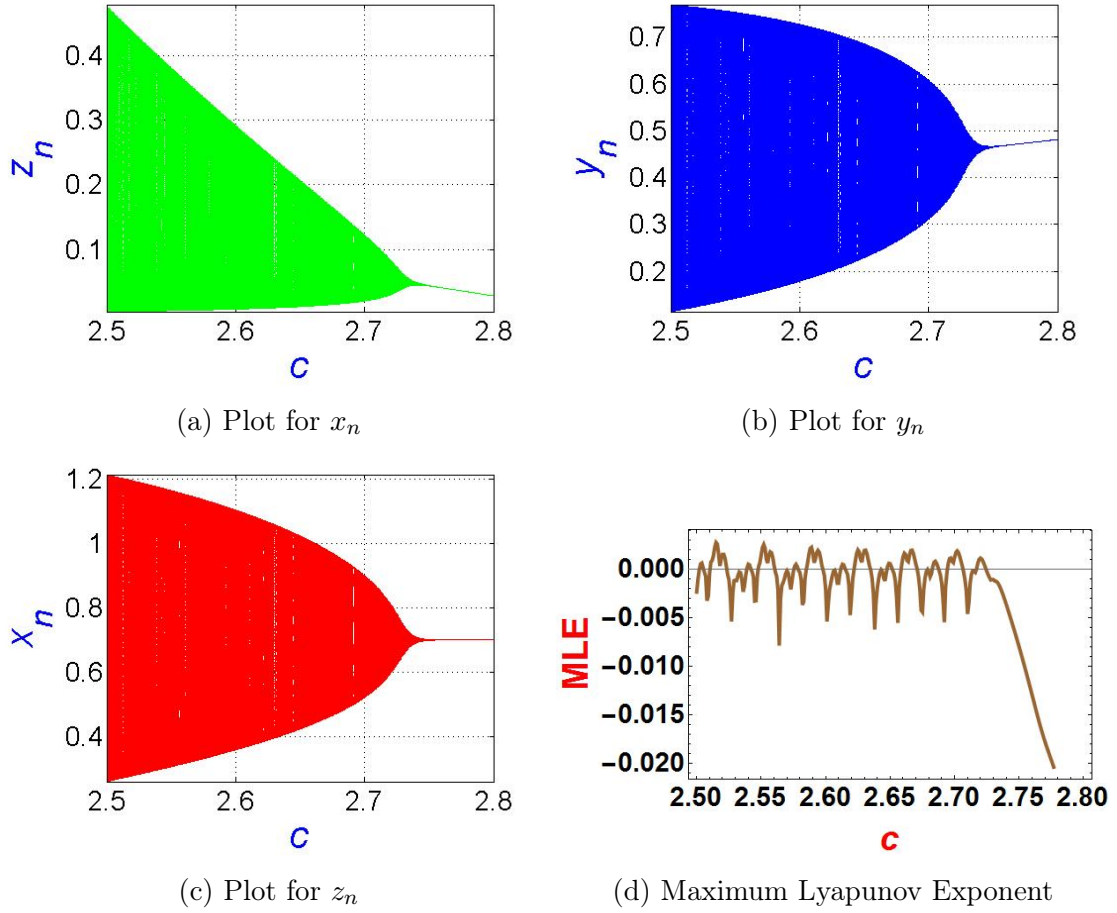


Figure 2.11: Chaotic plots and MLE of system (2.1.3)

$$\begin{aligned}
\zeta_1 - \zeta_2 + \zeta_3(\zeta_1 - \zeta_3) &= 0, \\
1 + \zeta_2 - \zeta_3(\zeta_1 + \zeta_2) &= 0.578036 > 0, \\
1 + \zeta_1 + \zeta_2 + \zeta_3 &= 0.0522462 > 0, \\
1 - \zeta_1 + \zeta_2 - \zeta_3 &= 6.75864 > 0.
\end{aligned}$$

For the above parametric values and for  $\rho_1 = 0.9$ , the controlled system (2.6.1) is:

$$\begin{cases} x_{n+1} = 0.9x_n e^{[1-0.7x_n-y_n-z_n]} + 0.1x_n, \\ y_{n+1} = 0.9y_n e^{[-0.7+x_n]} + 0.1y_n, \\ z_{n+1} = 0.9z_n e^{[-2.72946+1.8x_n+3.2y_n]} + 0.1z_n. \end{cases} \quad (2.5.6)$$

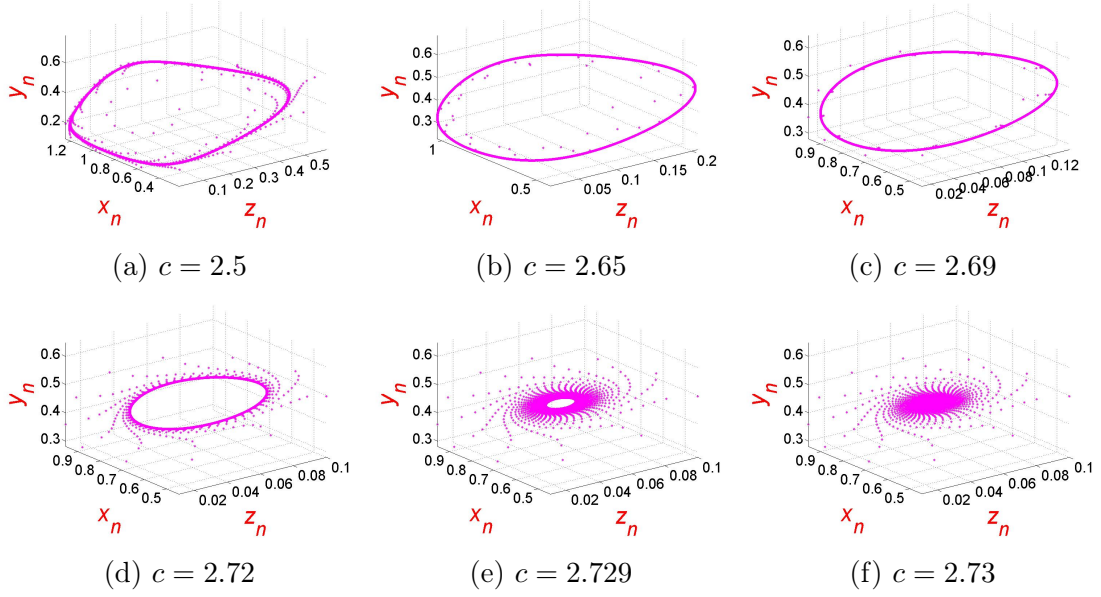


Figure 2.12: Phase portraits of the system (4) for different values of  $c$ .

The Jacobian matrix of (2.5.6) at  $\left(b, \frac{bd-be+c}{f}, \frac{be-bd-bfr-c+f}{f}\right)$  is:

$$J(0.7, 0.459208, 0.0507923) = \begin{pmatrix} 0 & 0 & 0 \\ 0.413287 & 1. & 0 \\ 0.0822835 & 0.146282 & 1. \end{pmatrix},$$

with characteristic polynomial:

$$C(\mu) = \mu^3 - 2.559\mu^2 + 2.43021\mu - 0.833122,$$

Furthermore, we have the following conditions:

$$\begin{aligned} |\bar{\zeta}_1 + \bar{\zeta}_3| &= 3.39212 < 1 + \bar{\zeta}_2 = 3.43021, \\ |\bar{\zeta}_1 - 3\bar{\zeta}_3| &= 0.0596343 < 3 - \bar{\zeta}_2 = 0.569791, \\ \bar{\zeta}_3^2 + \bar{\zeta}_2 - \bar{\zeta}_3 \times \bar{\zeta}_1 &= 0.992343 < 1. \end{aligned}$$

It shows that the control model is stable.

**Example 5.** If we choose  $b = 0.7, r = 0.7, c = 2.9, d = 1.6, e = 1.9$ , and  $f \in [5.45, 5.95]$  with initial conditions  $(x_0, y_0, z_0) = (0.1443, 0.1648, 0.1364)$ . Then positive fixed point  $\left(b, -\frac{bd+be-c}{f}, -\frac{bd-be+bfr+c-f}{f}\right)$  experiences Hopf bifurcation when we choose  $f$  as a bifurcation parameter. It can be seen that Hopf bifurcation emerges at  $f = 5.61706994636882$ . The variational matrix and the characteristics polynomial for the above parametric values are given below:

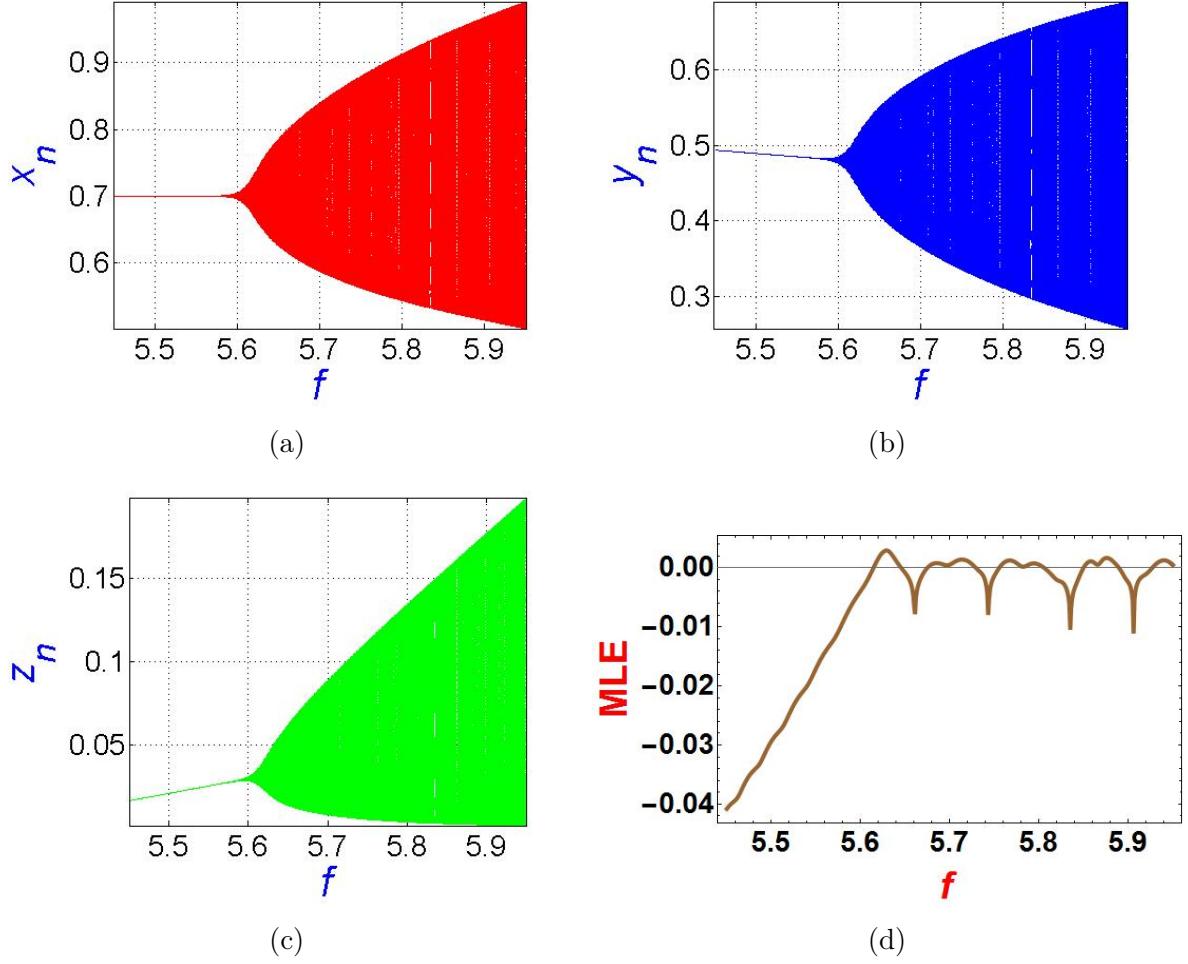


Figure 2.13: Bifurcation diagrams and MLE for system (2.1.3).

$$V(0.7, 0.478897, 0.0311026) = \begin{pmatrix} 0 & 0 & 0 \\ 0.478897 & 1. & 0 \\ 0.00933079 & 0.174706 & 1. \end{pmatrix},$$

$$C(\mu) = \mu^3 - 2.5100000000000002\mu^2 + 2.3617597091695623\mu - 0.7931934486925974.$$

The eigenvalues are  $\mu_{1,2} = 0.858403 \pm 0.512975i$  and  $\mu_3 = 0.793193$  with  $|\mu_{1,2}| = 1$ . Figures 2.13 and Figure 2.14 show the chaotic and phase plots. Moreover, we have the following conditions:

$$\begin{aligned} \zeta_1 - \zeta_2 + \zeta_3(\zeta_1 - \zeta_3) &= 0, \\ 1 + \zeta_2 - \zeta_3(\zeta_1 + \zeta_2) &= 0.741688 > 0, \\ 1 + \zeta_1 + \zeta_2 + \zeta_3 &= 0.0585663 > 0, \\ 1 - \zeta_1 + \zeta_2 - \zeta_3 &= 6.66495 > 0. \end{aligned}$$

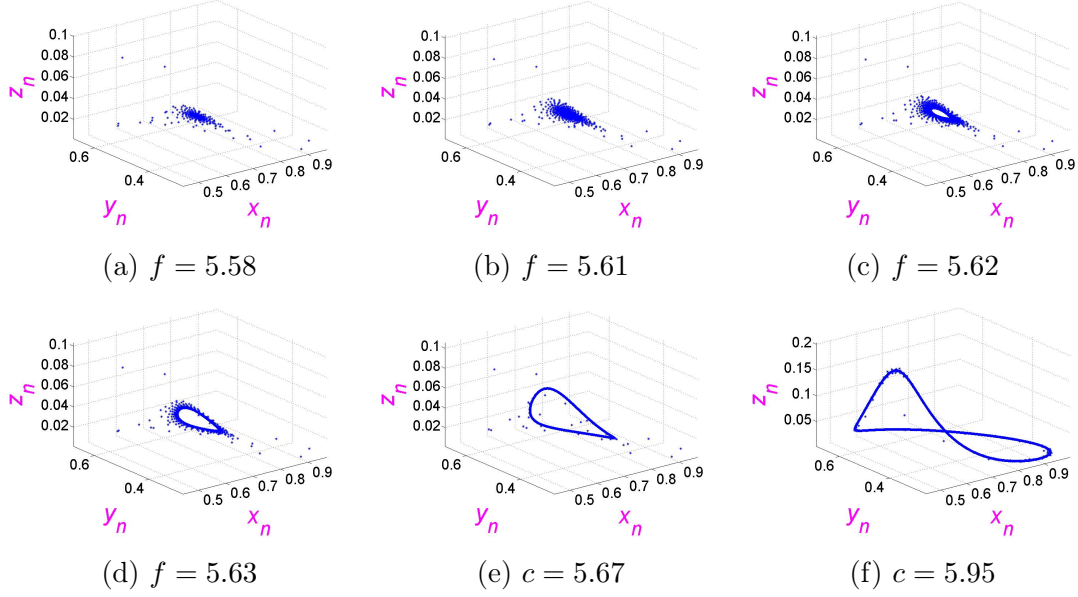


Figure 2.14: Phase portraits of system (2.1.3) for different values of  $f$ .

The controlled system for the above parametric values with  $\rho_1 = 0.9$  is:

$$\begin{cases} x_{n+1} = 0.9x_n e^{[1-0.7x_n-y_n-z_n]} + 0.1x_n, \\ y_{n+1} = 0.9y_n e^{[-0.7+x_n]} + 0.1y_n, \\ z_{n+1} = 0.9z_n e^{[-2.9+0.3x_n+5.61707y_n]} + 0.1z_n. \end{cases} \quad (2.5.7)$$

The Jacobian matrix of (2.5.7) at  $\left(b, -\frac{bd+be-c}{f}, -\frac{bd-be+bfr+c-f}{f}\right)$  is:

$$J(0.7, 0.478897, 0.0311026) = \begin{pmatrix} 0 & 0 & 0 \\ 0.431008 & 1. & 0 \\ 0.00839771 & 0.157235 & 1. \end{pmatrix},$$

with characteristic function:

$$C(\mu) = \mu^3 - 2.559\mu^2 + 2.3948253644273465\mu - 0.7931305605396384.$$

Furthermore, we have the following conditions:

$$\begin{aligned} |\bar{\zeta}_1 + \bar{\zeta}_3| &= 3.35213 < 1 + \bar{\zeta}_2 = 3.39483, \\ |\bar{\zeta}_1 - 3\bar{\zeta}_3| &= 0.179608 < 3 - \bar{\zeta}_2 = 0.605175, \\ \bar{\zeta}_3^2 + \bar{\zeta}_2 - \bar{\zeta}_3 \times \bar{\zeta}_1 &= 0.99426 < 1. \end{aligned}$$

Therefore, our controlled system is stable for the above-chosen parametric values.

**Example 6.** If we take the numerical values of the parameters as  $b = 0.78, r = 0.78, d = 1.4, e = 2.6, f = 3.3$ , and  $c \in [1.35, 1.85]$  with an initial population  $(x_0, y_0, z_0) = (0.9, 0.2, 0.1)$ . Then  $\left(b, -\frac{bd+be-c}{f}, -\frac{bd-be+bfr+c-f}{f}\right)$  experiences Hopf bifurcation for the rate of change of  $x$  due to the presence of  $y$ , i.e., for parameter  $c$ . At  $c = 1.3916714099570726$ , the forward Hopf bifurcation emerges. Furthermore, we have the following chaotic plots (figure 2.15): The variational matrix for the above-chosen parametric values is:

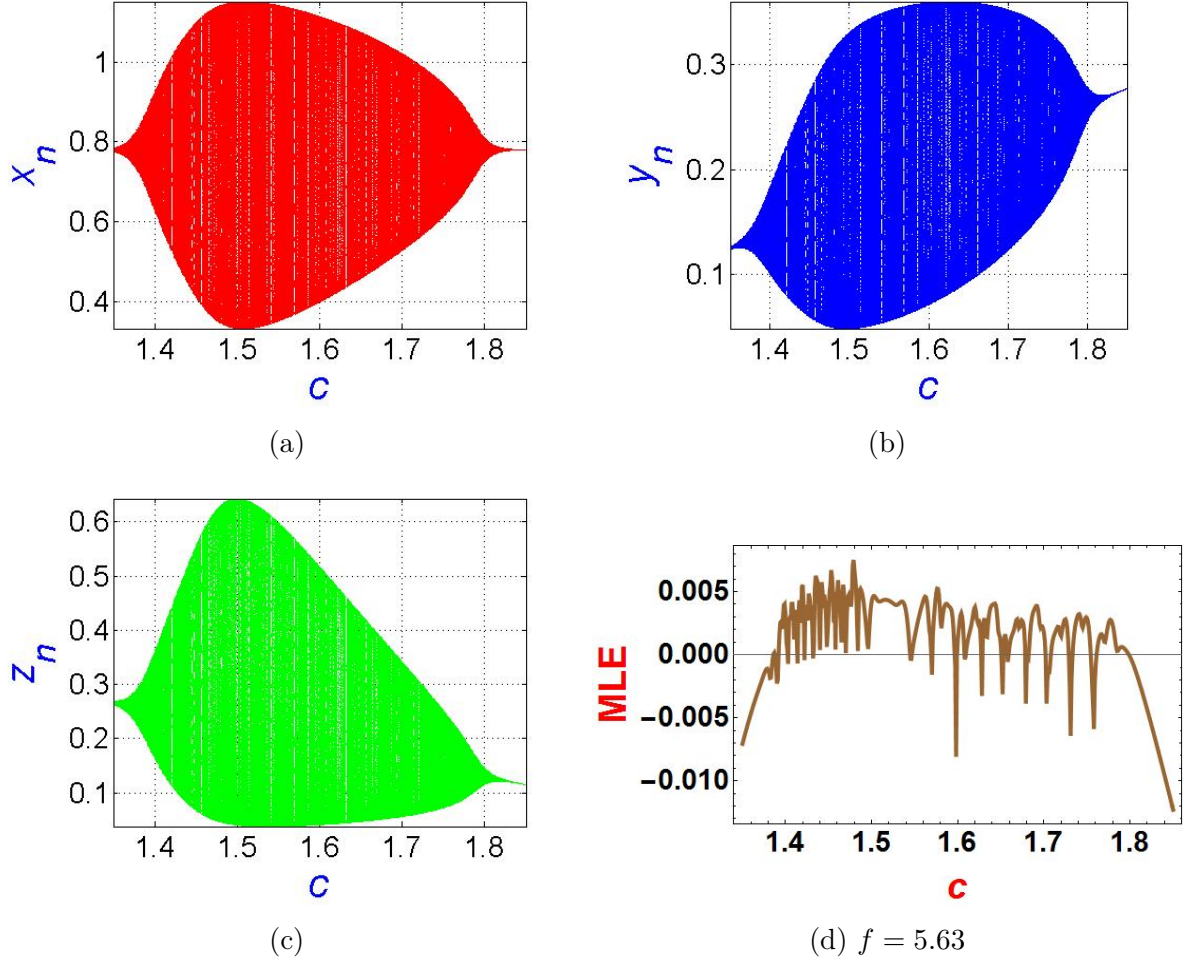


Figure 2.15: Bifurcation diagrams and MLE of system (2.1.3).

$$V(0.78, 0.138082, 0.253518) = \begin{pmatrix} 0 & 0 & 0 \\ 0.138082 & 1. & 0 \\ 0.304221 & 0.836609 & 1. \end{pmatrix}. \quad (2.5.8)$$

The characteristic function of (2.5.8) is:

$$P(\mu) = \mu^3 - 2.3916\mu^2 + 2.12819676971112\mu - 0.6464905514294517.$$



The eigenvalues are  $\mu_{1,2} = 0.872555 \pm 0.488516i$  with  $|\mu_{1,2}| = 1$  and  $\mu_3 = 0.646491 < 1$ . Moreover, we have the following conditions:

$$\begin{aligned}\zeta_1 - \zeta_2 + \zeta_3(\zeta_1 - \zeta_3) &= 0, \\ 1 + \zeta_2 - \zeta_3(\zeta_1 + \zeta_2) &= 1.1641 > 0, \\ 1 + \zeta_1 + \zeta_2 + \zeta_3 &= 0.0901062 > 0, \\ 1 - \zeta_1 + \zeta_2 - \zeta_3 &= 6.16629 > 0.\end{aligned}$$

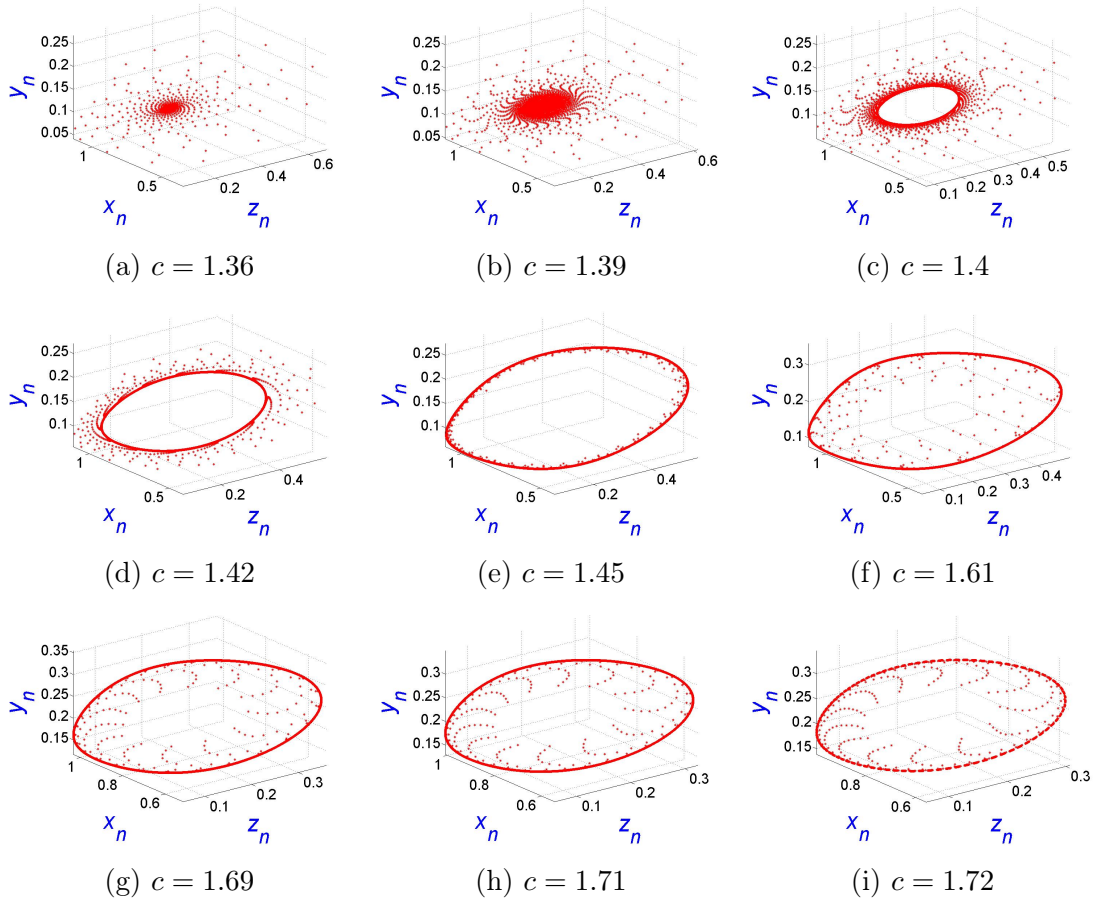


Figure 2.16: Phase plots of forward Hopf bifurcation for different values of  $c$

The backward Hopf bifurcation also emerges at  $c = 1.7933390793266026$  for the exact numerical values of the parameter. Moreover, we have

$$V(0.78, 0.2598, 0.1318) = \begin{pmatrix} 0 & 0 & 0 \\ 0.2598 & 1. & 0 \\ 0.15816 & 0.434941 & 1. \end{pmatrix}. \quad (2.5.9)$$

The characteristic function of (2.5.9) is:

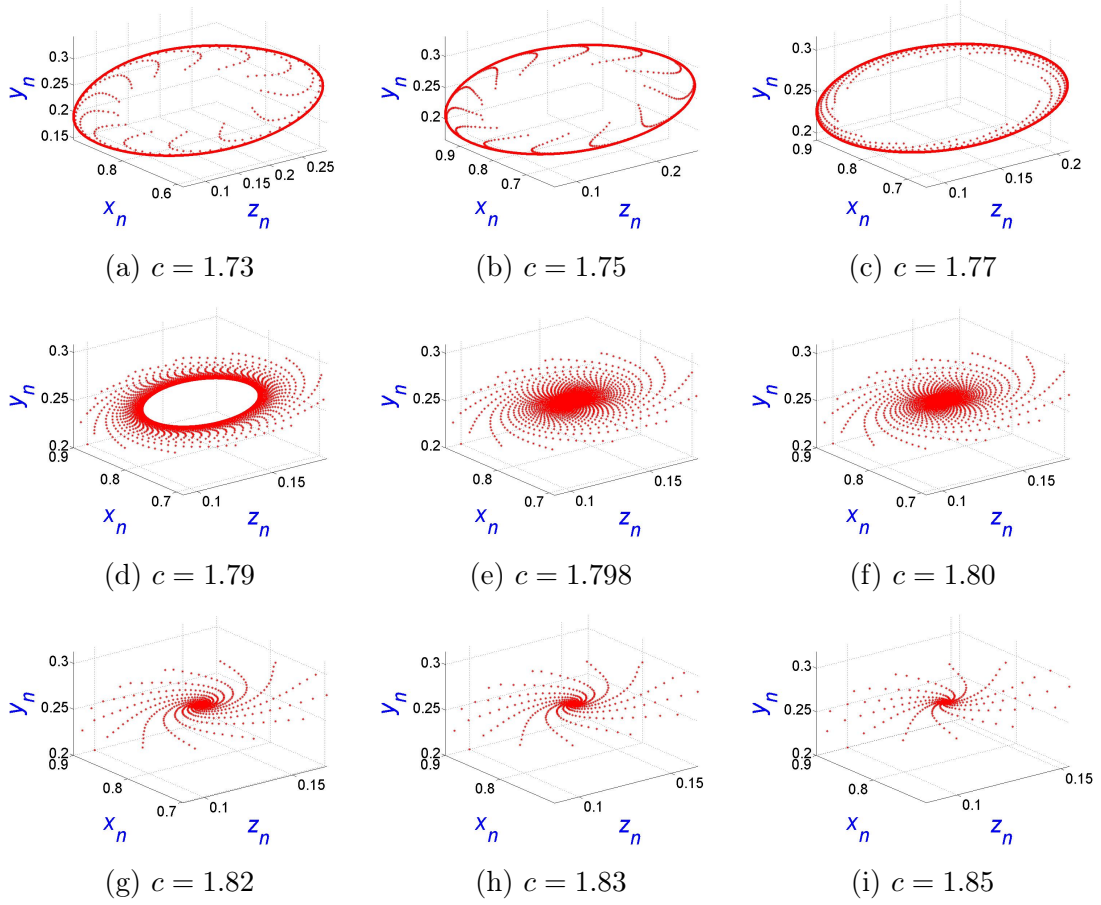


Figure 2.17: Phase plots of backward Hopf bifurcation for different values of  $c$

$$P(\mu) = \mu^3 - 2.3916\mu^2 + 2.109208843522742\mu - 0.6294707702429106.$$

We have the roots of the above characteristic function  $P(\mu)$ :

$$\mu_{1,2} = 0.881065 \pm 0.472996i \text{ with } |\mu_{1,2}| = 1, \text{ and } \mu_3 = 0.629471 < 1.$$

Moreover, we have the following conditions:

$$\begin{aligned} \zeta_1 - \zeta_2 + \zeta_3(\zeta_1 - \zeta_3) &= 0, \\ 1 + \zeta_2 - \zeta_3(\zeta_1 + \zeta_2) &= 1.20753 > 0, \\ 1 + \zeta_1 + \zeta_2 + \zeta_3 &= 0.0881381 > 0, \\ 1 - \zeta_1 + \zeta_2 - \zeta_3 &= 6.13028 > 0. \end{aligned}$$

For the above parametric values and for  $\rho_1 = 0.9$ , the controlled system (2.6.1) is:



$$\begin{cases} x_{n+1} = 0.9x_n e^{[1-0.7x_n-y_n-z_n]} + 0.1x_n, \\ y_{n+1} = 0.9y_n e^{[-0.7+x_n]} + 0.1y_n, \\ z_{n+1} = 0.9z_n e^{[-2.72946+1.8x_n+3.2y_n]} + 0.1z_n. \end{cases} \quad (2.5.10)$$

The Jacobian matrix of (2.5.10) at  $\left(b, -\frac{bd+be-c}{f}, -\frac{bd-be+bfr+c-f}{f}\right)$  is:

$$J(0.7, 0.459208, 0.0507923) = \begin{pmatrix} 0 & 0 & 0 \\ 0.23382 & 1. & 0 \\ 0.142344 & 0.391447 & 1. \end{pmatrix},$$

with characteristic function:

$$C(\mu) = \mu^3 - 2.45244\mu^2 + 2.168947163253421\mu - 0.6522545078324241.$$

Furthermore, we have the following conditions:

$$\begin{aligned} |\bar{\zeta}_1 + \bar{\zeta}_3| &= 3.10469 < 1 + \bar{\zeta}_2 = 3.16895, \\ |\bar{\zeta}_1 - 3\bar{\zeta}_3| &= 0.495676 < 3 - \bar{\zeta}_2 = 0.831053, \\ \bar{\zeta}_3^2 + \bar{\zeta}_2 - \bar{\zeta}_3 \times \bar{\zeta}_1 &= 0.9999999999999998 < 1. \end{aligned}$$

Hence, the controlled system is stable for above selected parametric values.

## 2.6 Chaos control

In this section, we control the bifurcation that arises in the system (2.1.3). To prevent the chaos in the model (2.1.3), we apply a hybrid control feedback methodology proposed by Luo *et al.*[75]. The Lotka-Volterra model used in the model (2.1.3) represents a prey-predator system where the predator population affects the prey population and vice versa. In some cases, this system can exhibit chaotic behavior, making it difficult to predict the population dynamics. The hybrid control feedback methodology used in this study aims to eliminate the chaos in the system by introducing an external control input. The control input used in the study combines linear and nonlinear feedback controls. The linear feedback control reduces the magnitude of the state variables when they exceed a certain threshold.

In contrast, the nonlinear feedback control works by adding a nonlinear function of the state variables to the control input. This combination of control inputs helps to suppress

the chaos in the system while maintaining the stability of the fixed points. In biological terms, the hybrid control feedback methodology can be seen as controlling the prey-predator system by introducing an external control input. This control input could represent the introduction of a new predator population, a new prey population, or any other external factor that affects the prey-predator system. In physical terms, the hybrid control feedback methodology can be seen as controlling the prey-predator system by introducing an external physical force, such as a predator's hunting behavior or a prey's migration patterns. In instrumental terms, the hybrid control feedback methodology can be seen as a means of controlling the prey-predator system through the use of instruments such as sensors, cameras, or other monitoring devices that can detect changes in the prey-predator system and provide an external control input to suppress the chaos. If the model experiences Hopf bifurcation at a fixed point,  $\left(b, -\frac{-bd+be-c}{f}, -\frac{bd-be+bfr+c-f}{f}\right)$ , which is unstable, then our control system under hybrid methodology is as follows:

$$\begin{cases} x_{n+1} = \rho_1 x_n \mathbf{e}^{[1-rx_n-y_n-z_n]} + (1 - \rho_1)x_n, \\ y_{n+1} = \rho_1 y_n \mathbf{e}^{[-b+x_n]} + (1 - \rho_1)y_n, \\ z_{n+1} = \rho_1 z_n \mathbf{e}^{[-c-dx_n+ex_n+fy_n]} + (1 - \rho_1)z_n, \end{cases} \quad (2.6.1)$$

where  $\rho_1 \in (0, 1)$  is a controlled parameter. The values of  $\rho_1$  represent the strength of the feedback signal applied to the system to control the chaos. Therefore, different values of  $\rho_1$  would represent different control or management action levels to regulate the prey-predator interactions and reduce chaos in the system. Taking the appropriate control parameter value  $\rho_1$ , we can delay or eliminate the chaos from the model (2.1.3). Values close to 0 would indicate a weak level of management action; values close to 1 would indicate a strong level of management action; and values between 0 and 1 would indicate a moderate level of management action. The variational matrix of the controlled model (2.6.1) calculated at  $\left(b, -\frac{-bd+be-c}{f}, -\frac{bd-be+bfr+c-f}{f}\right)$  is given by:

$$V_C(E^*) = \begin{pmatrix} 1 - br\rho_1 & -b\rho_1 & -b\rho_1 \\ \frac{(c+b(d-e))\rho_1}{f} & 1 & 0 \\ \frac{(d-e)(c-f+b(d-e+fr))\rho_1}{f} & -(c-f+b(d-e+fr))\rho_1 & 1 \end{pmatrix}. \quad (2.6.2)$$

The characteristic function of (5.2.7) is given by:

$$P_C(\mu) = \mu^3 + \bar{\zeta}_1\mu^2 + \bar{\zeta}_2\mu + \bar{\zeta}_3, \quad (2.6.3)$$

where

$$\begin{aligned}
\bar{\zeta}_1 &= b\rho_1 r - 3, \\
\bar{\zeta}_2 &= \frac{b\rho_1^2(bd - be + c)}{f} + \frac{b\rho_1^2(d - e)(bd - be + bfr + c - f)}{f} - 2b\rho_1 r + 3, \\
\bar{\zeta}_3 &= -\frac{b\rho_1^2(bd - be + c)}{f} - \frac{b\rho_1^3(bd - be + c)(bd - be + bfr + c - f)}{f} + b\rho_1 r - 1 \\
&\quad - \frac{b\rho_1^2(d - e)(bd - be + bfr + c - f)}{f}.
\end{aligned} \tag{2.6.4}$$

The fixed point  $\left(b, -\frac{bd+be-c}{f}, -\frac{bd-be+bfr+c-f}{f}\right)$  of the controlled structure (2.6.1) is lo-

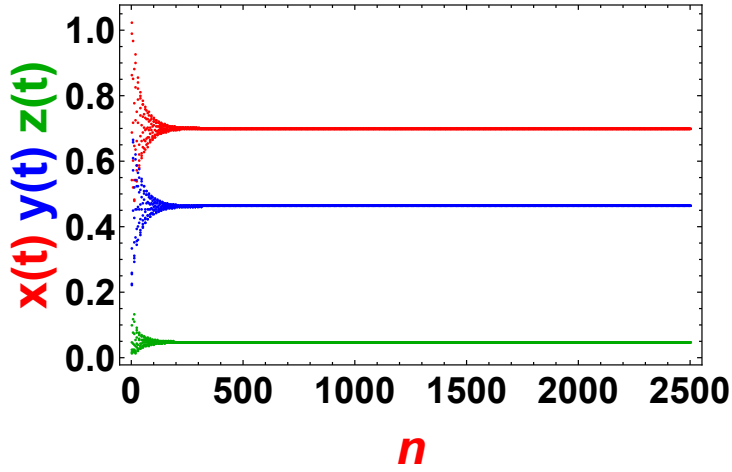


Figure 2.18: Stability of the controlled system (2.6.1).

cally asymptotically stable if the subsequent conditions are satisfied:

$$\begin{aligned}
|\bar{\zeta}_1 + \bar{\zeta}_3| &< 1 + \bar{\zeta}_2, \\
|\bar{\zeta}_1 - 3\bar{\zeta}_3| &< 3 - \bar{\zeta}_2, \\
\bar{\zeta}_3^2 + \bar{\zeta}_2 - \bar{\zeta}_3 \times \bar{\zeta}_1 &< 1.
\end{aligned}$$

In our case, we can use the following biological, physical, ecological, and instrumental control parameters to control the chaos in the system (2.1.3): Several control inputs can be implemented to regulate the prey-predator system and prevent the emergence of chaos. The first is a biological control input, such as introducing a new predator or prey population better adapted to the environment or restoring a degraded habitat. The second is a physical control input, such as submitting a physical barrier to limit the movement of the predator population or creating a new habitat. The third is an instrumental control input, such as using predator population control methods, such as hunting or trapping, or ecological monitoring and surveillance methods to monitor the prey-predator system.

In all of these cases, the control inputs regulate the prey-predator system and prevent the emergence of chaos by reducing the impact of the predator population on the prey population and promoting the adaptation of the prey population to the environment.

## 2.7 Conclusion

In this chapter, we analyze the Lotka-Volterra model dynamically. We calculate five fixed points,  $E_0(0, 0, 0)$ , the extinction of all populations,  $E_1 = (\frac{1}{r}, 0, 0)$  existence of prey population,  $E_2(b, 1 - br, 0)$  existence of prey and predator population,  $E_3 = (-\frac{c}{d-e}, 0, -\frac{-cr-d+e}{d-e})$  the coexistence of prey and scavenger populations in the absence of the predator population,  $E_* = (b, -\frac{bd+be-c}{f}, -\frac{bd-be+bfr+c-f}{f})$  coexistence of prey, predators, and scavenger populations. Biologically, these fixed points are reasonable because the prey population can exist without predator and scavengers, as prey food does not depend on predator and scavengers  $E_1$ , the predator and prey can coexist without a scavenger  $E_2$ , and the prey and the scavenger can coexist in the absence of the predator  $E_3$ . However, the predator and scavenger cannot coexist without the prey because the predator and scavenger will have no food source and die off  $E_0$ . We investigated the stability of these fixed points of the model in both discrete and continuous forms and derived the parametric criteria for the stability of fixed points. We noticed that the model experiences Hopf bifurcation in the continuous form when we choose  $c$  as a bifurcation parameter. From the time-series plots in figure 2.9, we see that bifurcation has been increasing for a very long time, making it difficult for us to estimate the consistency of this model. So, we decided to convert this model to a discrete form to control bifurcation and stabilization. Due to the excellent numerical results and lots of chaos control strategies, we converted the model to discrete form using a piece-wise constant argument. We have seen that the discrete model is also undergoing bifurcation on the same parameter. We have noticed that the systems in both cases, continuous form (5.1.2) and discrete form (2.1.3), experience Hopf bifurcation for the same parameter  $c$ . In addition, we observed that the system (2.1.3) also experiences Hopf bifurcation for the parameter  $f$ . Bifurcation diagrams are plotted for both systems (5.1.2) and (2.1.3). We also plotted MLE to confirm the chaotic region. The bifurcation in the parameters  $c$  and  $f$  indicates that the predator and prey population change rate should be monitored carefully. A rapid decline in the prey population can result in a corresponding decline in the predator population, as the predators will have a reduced food source and may struggle to find enough to eat. On the other hand, a rapid increase in the prey population can lead to an initial increase in the predator population as the predators have more food available. However, suppose the prey population continues to increase faster than the predator population can adapt. In that case, it can lead to a decline in the predator population as the predators become overwhelmed and unable to

keep up with the abundance of food. Additionally, numerical examples are provided to support our theoretical findings. We use the hybrid control feedback technique to control the disorder in the change rate of prey and predator populations. Numerically, we see that the bifurcation is controlled through this technique, and the controlled system is stable for parametric values, through which system (2.1.3) experiences bifurcation. In this way, we controlled the bifurcation in the system and proved that the controlled system (2.6.1) is stable. In short, this research represents a major step in understanding prey-predator interactions. The study's analysis of the fixed point stability, bifurcation, and chaos control of a Lotka-Volterra model provides a comprehensive examination of the complex dynamics between two predators and their prey. The results emphasize the significance of parameters  $c$  and  $f$  in shaping the behavior of prey-predator interactions, and the emergence of bifurcation in these parameters highlights the intricate dynamics of these systems. When enough prey is available, the scavengers may compete with the predators for food, potentially reducing the amount of prey available for the predators to hunt. This can lead to a decline in the predator population and an increase in the scavenger population, causing a shift in the balance of the ecosystem. Additionally, an overpopulation of scavengers can consume too much of the remains of hunted prey, leaving less food for the predators. This could result in a decline in the predator population, which can have cascading effects throughout the ecosystem. Therefore, the study highlights the importance of considering multiple predators when studying prey-predator interactions, as multiple predators can lead to chaos in the system. However, the study also suggests that chaos control techniques may be valuable for managing these interactions. A promising avenue for future research would be to investigate the co-dimensional two-bifurcation of the same model under different functional responses. This would provide a deeper understanding of the complex interplay between predator and prey populations and the potential for chaos control techniques to manage prey-predator interactions. By expanding our knowledge in this area, we can better understand and manage the delicate balance between predator and prey populations and their impact on ecosystems.

# Chapter 3

## Fixed points stability, periodic behavior, bifurcation analysis, and chaos control of a prey-predator model incorporating the Allee effect and fear effect

### 3.1 Introduction

This chapter has been published. The publishing view of this chapter is available at reference [86]. The interaction between predators and prey has long stimulated the interest of ecologists. Understanding these interactions involves using the Lotka-Volterra model, a well-known model. Ecologists can better understand how these complicated interactions operate in the ecosystem by including the Allee and fear effects in their analyses of the relationship between predators and prey using the Lotka-Volterra model. According to recent studies, the Allee effect and the fear effect, among other factors, have been discovered to influence population dynamics significantly. The phenomenon where prey shows increased attention and lower activity when predators are around is known as the fear effect, first postulated by Lima and Dill [87]. Acting this way may result in fewer prey-predator contacts and fewer predator attacks. Contrarily, the Allee effect, which was initially put up by Allee *et al.* [4], suggests that there is a population density below which a species cannot survive because of diminished reproductive success or higher mortality. In his study of population changes, Allee discovered a phenomenon known as the Allee effect, which happens when population density is too low and the birth rate

falls. In contrast, the death rate rises [88]. Recent investigations have demonstrated the significance of including these additional parameters in prey-predator models. By adding these extra factors, prey-predator models may be able to estimate population dynamics more accurately and realistically. However, research into how these components impact the model's stability is underway. In this research, we will study how the fear and Allee effects affect the dynamics of a prey-predator system. We will use a mathematical approach to examine the stability and bifurcation of the model and discuss some interesting results. We have the following recent studies from the literature related to these effects:

Recently, Wang *et al.* [104] examined the Allee and fear effects on a prey-predator model, added the delay to the model, and observed the dynamical effects of the model. Umrao and Srivastava [105] examined the dynamic attributes of a predator-prey model in their study while accounting for the Allee and fear effects. They also looked at the influence of mild and strong Allee effects on the interaction between cooperative hunting among predators and fear among prey species. They concluded that the system exhibits a wider variety of predator-prey behavioral patterns than in earlier studies. The Allee effect, a fear effect, and prey refuge were investigated by Huang *et. al* [89] using a prey-predator model. By boosting the Allee effect, or prey refuge, they demonstrated the complexity of the model. Additionally, they showed that the Allee effect, or fear effect, does not alter prey density but may decrease predator population at positive fixed points. According to the qualitative analysis in [106], the Allee and Fear effects significantly identify how the model behaves dynamically. Lai *et. al* [90] investigate the fear and the additive Allee effect to examine how a prey-predator model behaves dynamically. They observed that the density of predatory species decreased with increasing fear effect strength by considering the influence of fear on the prey species. However, fear has a minimal effect on the final prey density. Chen *et. al* [107] analyzed the impact of the Allee effect on the prey-predator model and other food resources for the predators. Xie [91] investigated the influence of Allee and the fear effect using a Holling type II functional response in a prey-predator environment. Not only is a Hopf bifurcation observed in the system, but the author also determined what is necessary for fixed points to be stable. By eliminating periodic solutions, the fear effect was also found to increase the stability of the positive fixed point of the system, and the Allee effect also had a major impact on the persistence of the predator species. When the fear effect, mild Allee effect, and delay were present, Li *et. al* [92] explored the dynamical analysis of a prey-predator model. They demonstrated how the model bifurcates and determines the stability conditions. They add the gestation delay to the model to make it more realistic. According to their research, the Allee effect and the delay undermine the model; however, the fear effect may promote peaceful living together. The Allee effect can happen when there

are not enough individuals to mate due to inbreeding, social preferences for mating, low mating success rates, and less inbreeding over time. The impact of the Allee effect on the dynamics of prey-predator systems has recently attracted more attention from scientists. Through a comparison of the logistic prey growth term's dynamical properties in the ratio-dependent prey-predator model with and without the Allee effect, the authors in [34] demonstrated that the Allee effect may be used to eliminate the oscillation caused by species densities. The reasons for various bifurcation behaviors were also predicted and quantitatively confirmed using parametric illustrations and phase graphs. The researchers from [93] explored the same discrete time model. They proved how modifying the integral step size might result in period doubling and an invariant circle to create chaotic orbits. [94] introduces ratio-dependent interaction terms into the Leslie-type model. They use state-impulsive feedback control to control the chaos. They also establish the prerequisites for a first-order periodic solution's existence, singularity, and long-term stability. The authors of reference [95] showed how a predator-prey model with fear and the Allee effect could create a repeating pattern of population growth and decline. They supported their theoretical conclusions by demonstrating through numerical evidence that the system shows saddle-node bifurcation. In [96], the authors investigated the complex dynamics of a ratio-dependent Allee and fear-affected Leslie-Gower prey-predator model. The Allee effect and the fear effect, which can have considerable effects on the growth of populations, are considered in the model. Here, we go through the mathematical model and the underlying assumptions in extensive detail. From [97], we have the following model:

$$\begin{cases} \frac{dx}{dt} = \gamma x \left(1 - \frac{x}{\kappa}\right) - \frac{\mu xy}{x+\omega} - \zeta x, \\ \frac{dy}{dt} = \frac{\mu \beta xy}{x+\omega} - \theta y - \delta y^2. \end{cases} \quad (3.1.1)$$

First, we will include the fear effect in the model (3.1.1). To better replicate the behavior of animals in nature, the fear effect, sometimes referred to as predator avoidance behavior, is added to prey-predator models. In natural environments, prey animals frequently engage in actions like escaping or hiding to avoid predators. Such activities may significantly change the dynamics of both prey and predator populations. Researchers can better comprehend how these behaviors affect people of various species and how they interact by considering the impact of fear in a prey-predator system. To introduce the fear effect, we have to add the term  $\frac{1}{1+Fy}$  in the model (3.1.1), which represents the fear effect with parameter  $F$  as a level of fear. Thus, by adding the fear effect, the model (3.1.1) becomes:

$$\begin{cases} \frac{dx}{dt} = \frac{\gamma x}{1+Fy} \left(1 - \frac{x}{\kappa}\right) - \frac{\mu xy}{x+\omega} - \zeta x, \\ \frac{dy}{dt} = \frac{\mu \beta xy}{x+\omega} - \theta y - \delta y^2. \end{cases} \quad (3.1.2)$$



The Allee effect will now be incorporated into the model (3.1.2). In population ecology, this phenomenon, known as the Allee effect, is where the population density decreases, and there is a corresponding slowdown in the population growth rate. In other words, certain species only survive when a specific minimum number of individuals comprise their population. The consequences for preserving ecosystems are significant. If a population falls below a critical threshold, the struggle for recovery or survival intensifies. Challenges emerge in the quest for mates, protection against predators, and various other factors. As far as conservation is concerned, it is crucial to understand and address the Allee effect. Maintaining a population above a certain threshold is vital for successful reproduction and long-term viability. Doing so can significantly improve the overall health and sustainability of the ecosystem. Conservation techniques to achieve this goal include habitat protection and well-planned reintroduction efforts. By implementing these strategies, we can overcome the Allee effect's obstacles and protect the biological landscape's resilience and balance. Let  $\mathcal{U}(\Lambda, x)$  be the fertility of a species with  $x$  adults in an isolated patch to introduce the Allee effect. Population density raises fertility, the description of which is:

$$\mathcal{U}(\Lambda, x) = \frac{\gamma x}{x + \Lambda}, \quad (3.1.3)$$

where  $\gamma$  denotes the inherent growth rates of the prey population and the prey population density at time  $t$  is denoted by  $x$ ,  $\Lambda > 0$  represents the level of Allee, which can determine how much of an impact Allee has on the prey.  $\mathcal{U}(\Lambda, x)$  satisfied  $\lim_{\Lambda \rightarrow +\infty} \mathcal{U}(\Lambda, x) = 0$ ,  $\lim_{x \rightarrow 0} \mathcal{U}(\Lambda, x) = 0$ ,  $\lim_{\Lambda \rightarrow 0} \mathcal{U}(\Lambda, x) = \gamma$ ,  $\lim_{x \rightarrow +\infty} \mathcal{U}(\Lambda, x) = \gamma$ ,  $\frac{\partial \mathcal{U}(\Lambda, x)}{\partial \Lambda} < 0$ . More details regarding the Allee effect can be seen in [99]. Thus, the model (3.1.2) with the Allee effect becomes:

$$\begin{cases} \frac{dx}{dt} = \frac{\gamma x}{1+Fy} \left(1 - \frac{x}{\mathcal{K}}\right) \frac{x}{x+\Lambda} - \frac{\mu xy}{x+\omega} - \zeta x, \\ \frac{dy}{dt} = \frac{\mu \beta xy}{x+\omega} - \theta y - \delta y^2. \end{cases} \quad (3.1.4)$$

Thus, our desired model is a system (3.1.4). Here,  $x$  and  $y$  represent the numbers of prey and predator. In ecological terms,  $\gamma$  indicates the intrinsic growth rates of the prey population. The ecological limitation at which a habitat can support a certain species is known as carrying capacity  $\mathcal{K}$ . The parameter  $\omega$  is the half-saturation constant. The efficacy of the predator's quest for food is indicated in this context by the symbol  $\mu$ . The mortality rates of the prey and predator populations are  $\zeta$  and  $\theta$ , respectively.  $\beta$  represents the biomass conversion, and  $\delta$  indicates the intra-specific competition. The fear effect in the model (3.1.4) can be analyzed from Figure 3.1.

The discretization of the continuous-time model is essential from a biological point of view, as it enables the simulation of predator-prey dynamics over discrete time scales. This, in turn, allows for easier comparison with actual population data and more effective

incorporation of time-sensitive ecological components. Consequently, we transformed the preceding system (3.1.4) into discrete form using an approach based on piece-wise constant arguments. Although there is some information loss associated with every transformation, the piece-wise constant technique was chosen as it can capture the critical elements of the continuous model and is computationally feasible. The driving force behind the discrete form of the continuous-time model's conversion was the better alignment of the simulation with the ecological dynamics seen in actual population data. As predator-prey interactions over discrete-time scales are frequently observed in environmental investigations, the discrete-time representation allows a more accurate picture of these interactions. For this, we transform the preceding system (3.1.4) into discrete form as follows:

$$\begin{cases} x_{n+1} = x_n \exp \left[ \frac{\gamma}{1+F y_n} \left( 1 - \frac{x_n}{\mathcal{K}} \right) \frac{x_n}{x_n+\Lambda} - \frac{\mu y_n}{x_n+\omega} - \zeta \right], \\ y_{n+1} = y_n \exp \left[ \frac{\mu \beta x_n}{x_n+\omega} - \theta - \delta y_n \right]. \end{cases} \quad (3.1.5)$$

Here, we assume that all biological parameters are positive and that predator and prey populations must remain non-negative. This restriction will be imposed on the initial conditions and the simulation discussion. The prey population grows logistically, experiencing an exponential increase proportionate to its current size before declining when it approaches the ecosystem's carrying capacity  $\mathcal{K}$ .

Let's first analyze the critical findings concerning the fixed points of the systems (3.1.4) and (3.1.5).

## 3.2 Positivity and uniform boundedness of the solutions

**Theorem 3.2.1.** *There is a single solution for the model (3.1.4) if  $(x(0), y(0)) > 0$  and is positive  $\forall t \geq 0$ .*

*Proof.* The model (3.1.4) has a unique solution in  $[0, \mathbb{I})$  where  $0 < \mathbb{I} < \infty$  because the right-hand side is continuous and locally Lipschitzian in  $\mathbb{R}_+^2$ .

$$\begin{cases} x(t) = x(0) \exp \left[ \int_0^t \left\{ \frac{\gamma}{1+F y(\xi)} \left( 1 - \frac{x(\xi)}{\mathcal{K}} \right) \frac{x(\xi)}{x(\xi)+\Lambda} - \frac{\mu y(\xi)}{x(\xi)+\omega} - \zeta \right\} d\xi \right] > 0, \\ y(t) = y(0) \exp \left[ \int_0^t \left\{ \frac{\mu \beta x(\xi)}{x(\xi)+\omega} - \theta - \delta y(\xi) \right\} d\xi \right] > 0. \end{cases} \quad (3.2.1)$$

□

**Theorem 3.2.2.** *The total population of the model (3.1.4) is uniformly bounded in  $\mathbb{R}$ .*

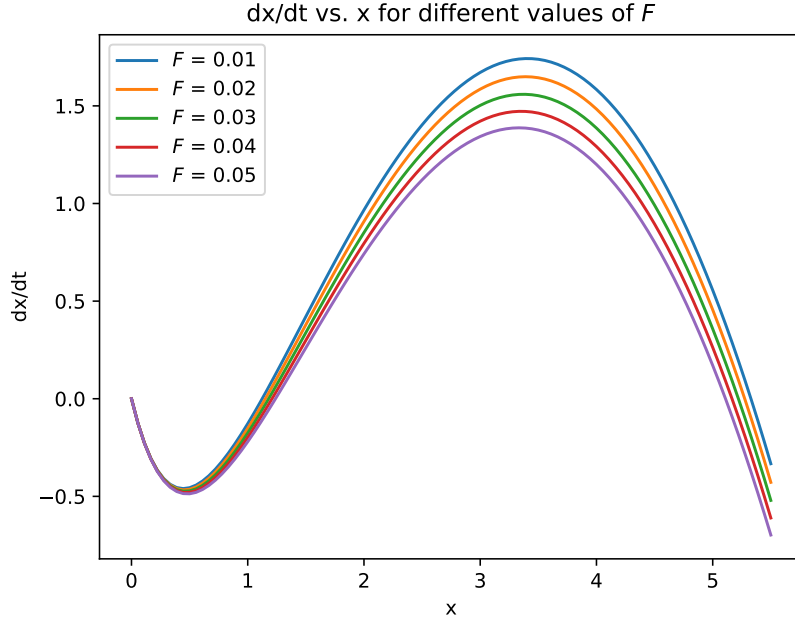


Figure 3.1: Behavior of Fear effect for  $\gamma = 4.6, \mathcal{K} = 8.2, \Lambda = 1.4, \mu = 1.1, \omega = 1.1, \zeta = 1.0$ , and  $y = 1.5$

*Proof.* From the first differential equation of (3.1.4), we have:

$$\begin{aligned} \frac{dx}{dt} &\leq \gamma x \left(1 - \frac{x}{\mathcal{K}}\right), \\ \implies \lim_{t \rightarrow \infty} \sup x(t) &\leq \mathcal{K}. \end{aligned}$$

From the second differential equation of (3.1.4), we have:

$$\begin{aligned} \frac{dy}{dt} &\leq \mu \beta y \left(1 - \frac{\delta}{\mu \beta} y\right), \\ \implies \lim_{t \rightarrow \infty} \sup y(t) &\leq \frac{\mu \beta}{\delta}. \end{aligned}$$

Hence,  $(x(t), y(t)) \in [0, \mathcal{K}] \times [0, \frac{\mu \beta}{\delta}]$ . Hence, the proof is completed.  $\square$

Now, we will show that every solution of the system (3.1.5) is bounded.

**Lemma 3.2.3.** ([74]) Suppose that  $\mathcal{S}_t$  satisfies  $\mathcal{S}_0 > 0$  and  $\mathcal{S}_{t+1} \leq \mathcal{S}_t \exp[m(1 - n\mathcal{S}_t)]$  for  $t \in [0, \infty]$ , where  $n > 0$  is a constant. Then  $\lim_{t \rightarrow \infty} \sup \mathcal{S}_t \leq \frac{1}{mn} \exp(m - 1)$ .

**Lemma 3.2.4.** In the system (3.1.5), each positive solution  $(x_n, y_n)$  is bounded uniformly.

*Proof.* Assume the positive solution  $(x_n, y_n)$  of (3.1.5) with the starting population  $(x_0, y_0)$

$> 0$ . Then we have:

$$x_{n+1} \leq x_n \exp \left[ \gamma \left( 1 - \frac{x_n}{\mathcal{K}} \right) \right], \quad (3.2.2)$$

for all  $n = 0, 1, 2, \dots$ . From Lemma 3.2.3, we have

$$\lim_{n \rightarrow \infty} \sup x_n \leq \frac{\mathcal{K}}{\gamma} \exp(\gamma - 1) := \Omega_1.$$

Similarly, we have

$$\begin{aligned} y_{n+1} &\leq y_n \exp [\mu\beta - \delta y_n] \\ &= y_n \exp \left[ (\mu\beta) \left( 1 - \frac{\delta}{\mu\beta} y_n \right) \right]. \end{aligned} \quad (3.2.3)$$

From Lemma 3.2.3, we have

$$\lim_{n \rightarrow \infty} \sup y_n \leq \frac{1}{\delta} \exp(\mu\beta - 1) := \Omega_2.$$

Thus, it shows that  $\lim_{n \rightarrow \infty} \sup (x_n, y_n) \leq \Omega$ , where  $\Omega = \max[\Omega_1, \Omega_2]$ . Hence, the proof is completed.  $\square$

### 3.3 Stability of the fixed points

Solving the following equations will lead to the fixed points  $(\hat{x}, \hat{y})$  of the model (3.1.4):

$$\begin{cases} 0 = \frac{\gamma\hat{x}}{1+F\hat{y}} \left( 1 - \frac{\hat{x}}{\mathcal{K}} \right) \frac{\hat{x}}{\hat{x}+\Lambda} - \frac{\mu\hat{x}\hat{y}}{\hat{x}+\omega} - \zeta\hat{x}, \\ 0 = \frac{\mu\beta\hat{x}\hat{y}}{\hat{x}+\omega} - \theta\hat{y} - \delta\hat{y}^2. \end{cases}$$

The fixed points that result from these equations are as follows:

$$\mathcal{E}_0 = (0, 0), \mathcal{E}_1 = \left( \frac{-\sqrt{(\zeta\kappa - \gamma\kappa)^2 - 4\gamma\zeta\kappa\Lambda} + \gamma\kappa - \zeta\kappa}{2\gamma}, 0 \right), \mathcal{E}_2 = \left( 0, -\frac{\theta}{\delta} \right), \text{ and } \mathcal{E}_* = (\hat{x}, \hat{y}).$$

The fixed points of system (3.1.5) will also be the same. Here we will discuss only those fixed points that are non-negative. The boundary fixed point  $\mathcal{E}_1$  will be positive when  $(\zeta\kappa - \gamma\kappa)^2 \geq 4\gamma\zeta\kappa\Lambda$ , and  $\sqrt{(\zeta\kappa - \gamma\kappa)^2 - 4\gamma\zeta\kappa\Lambda} + \zeta\kappa < \gamma\kappa$ . The positivity and uniqueness of the interior fixed point can be seen from Theorem 3.2.1 and the following isocline graph 3.2.

**Lemma 3.3.1.** *For system (3.1.4), the fixed point  $\mathcal{E}_0 = (0, 0)$  is stable.*

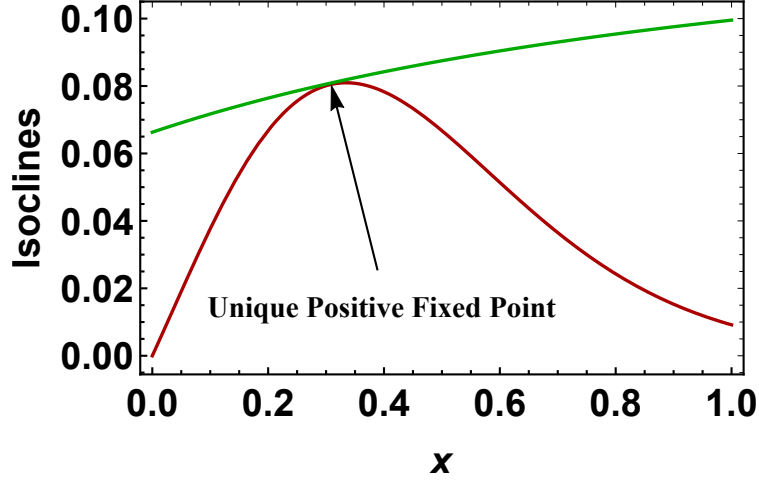


Figure 3.2: Uniqueness of positive fixed point  $\mathcal{E}_* = (\hat{x}, \hat{y})$ .

*Proof.* First, we find the variational matrix of model (3.1.4) at  $\mathcal{E}_0 = (0, 0)$  which is as follows:

$$\mathbb{N}_{\mathcal{E}_0}(0, 0) = \begin{pmatrix} -\zeta & 0 \\ 0 & -\theta \end{pmatrix}. \quad (3.3.1)$$

The latent roots of (3.3.1) are:  $\Pi_{\{1,2\}}(\mathcal{E}_0) = \{-\zeta, -\theta\}$ . Thus, the fixed point  $\mathcal{E}_0 = (0, 0)$  is stable for system (3.1.4).  $\square$

**Lemma 3.3.2.** *For system (3.1.5), the fixed point  $\mathcal{E}_0 = (0, 0)$  is stable.*

*Proof.* The variational matrix  $\mathbb{M}_{\mathcal{E}_0}$  of system (3.1.5) at  $\mathcal{E}_0 = (0, 0)$  is given below:

$$\mathbb{M}_{\mathcal{E}_0}(0, 0) = \begin{pmatrix} e^{-\zeta} & 0 \\ 0 & e^{-\theta} \end{pmatrix}. \quad (3.3.2)$$

The latent roots of (3.3.2) are:  $\Pi_{\{1,2\}}^*(\mathcal{E}_0) = \{e^{-\zeta}, e^{-\theta}\}$ , with  $|\Pi_{\{1,2\}}^*| < 1$ . Hence  $\mathcal{E}_0 = (0, 0)$  is stable for system (3.1.5).  $\square$

For system (3.1.4), we have calculated the following variational matrix at the boundary fixed point:  $\mathcal{E}_1 = \left( \frac{-\sqrt{(\zeta\kappa - \gamma\kappa)^2 - 4\gamma\zeta\kappa\Lambda} + \gamma\kappa - \zeta\kappa}{2\gamma}, 0 \right)$ :

$$\mathbb{N}_{\mathcal{E}_1} \left( \frac{-\sqrt{(\zeta\kappa - \gamma\kappa)^2 - 4\gamma\zeta\kappa\Lambda} + \gamma\kappa - \zeta\kappa}{2\gamma}, 0 \right) = \begin{pmatrix} \Theta_{11} & \Theta_{12} \\ 0 & \Theta_{22} \end{pmatrix}, \quad (3.3.3)$$

where,

$$\begin{aligned}\Theta_{11} &= \frac{\gamma\sqrt{\kappa(\kappa(\gamma-\zeta)^2-4\gamma\zeta\Lambda)} + \zeta\sqrt{\kappa(\kappa(\gamma-\zeta)^2-4\gamma\zeta\Lambda)} + \kappa(-(\gamma-\zeta)^2) + 4\gamma\zeta\Lambda}{2\gamma(\kappa+\Lambda)}, \\ \Theta_{12} &= \frac{\left(-\sqrt{\kappa(\kappa(\gamma-\zeta)^2-4\gamma\zeta\Lambda)} + \gamma\kappa - \zeta\kappa\right) \left(\frac{2\gamma\mu}{\sqrt{\kappa(\kappa(\gamma-\zeta)^2-4\gamma\zeta\Lambda)} - \gamma(\kappa+2\omega) + \zeta\kappa} - \zeta F\right)}{2\gamma}, \\ \Theta_{22} &= \frac{\beta\mu \left(\sqrt{\kappa(\kappa(\gamma-\zeta)^2-4\gamma\zeta\Lambda)} - \gamma\kappa + \zeta\kappa\right)}{\sqrt{\kappa(\kappa(\gamma-\zeta)^2-4\gamma\zeta\Lambda)} - \gamma(\kappa+2\omega) + \zeta\kappa} - \theta.\end{aligned}$$

The latent roots of (3.3.3) are:

$$\begin{aligned}\Pi_1(\mathcal{E}_1) &= \frac{\gamma\sqrt{\kappa(\kappa(\gamma-\zeta)^2-4\gamma\zeta\Lambda)} + \zeta\sqrt{\kappa(\kappa(\gamma-\zeta)^2-4\gamma\zeta\Lambda)} + \kappa(-(\gamma-\zeta)^2) + 4\gamma\zeta\Lambda}{2\gamma(\kappa+\Lambda)}, \\ \Pi_2(\mathcal{E}_1) &= \frac{-(\theta - \beta\mu) \left(\sqrt{\kappa(\kappa(\gamma-\zeta)^2-4\gamma\zeta\Lambda)} + \zeta\kappa\right) - \beta\gamma\kappa\mu + \gamma\theta(\kappa+2\omega)}{\sqrt{\kappa(\kappa(\gamma-\zeta)^2-4\gamma\zeta\Lambda)} - \gamma(\kappa+2\omega) + \zeta\kappa}.\end{aligned}$$

Therefore the fixed point  $\mathcal{E}_1 = \left(\frac{-\sqrt{(\zeta\kappa-\gamma\kappa)^2-4\gamma\zeta\kappa\Lambda}+\gamma\kappa-\zeta\kappa}{2\gamma}, 0\right)$  is stable when  $\Pi_{1,2}(\mathcal{E}_1) < 0$  and unstable otherwise. Now, the variational matrix of system (3.1.5) calculated at the fixed point  $\mathcal{E}_1(\bar{x}, 0) = \left(\frac{-\sqrt{(\zeta\kappa-\gamma\kappa)^2-4\gamma\zeta\kappa\Lambda}+\gamma\kappa-\zeta\kappa}{2\gamma}, 0\right)$  is given below:

$$\mathbb{M}_{\mathcal{E}_1}(\bar{x}, 0) = \begin{pmatrix} \Phi_{11} & \Phi_{12} \\ 0 & \Phi_{22} \end{pmatrix}, \quad (3.3.4)$$

where,

$$\begin{aligned}\Phi_{11} &= \frac{(\bar{x}(\bar{x}(-\gamma\bar{x} - 2\gamma\Lambda + \kappa) + (\gamma+2)\kappa\Lambda) + \kappa\Lambda^2) e^{\frac{\gamma\bar{x}(\kappa-\bar{x})}{\kappa(\bar{x}+\Lambda)} - \zeta}}{\kappa(\bar{x}+\Lambda)^2}, \\ \Phi_{12} &= \bar{x} e^{\frac{\gamma\bar{x}(1-\frac{\bar{x}}{\kappa})}{\bar{x}+\Lambda} - \zeta} \left( \frac{\gamma F \bar{x}(\bar{x} - \kappa)}{\kappa(\bar{x} + \Lambda)} - \frac{\mu}{\bar{x} + \omega} \right), \text{ and} \\ \Phi_{22} &= e^{\frac{\beta\mu\bar{x}}{\bar{x}+\omega} - \theta}.\end{aligned}$$

The latent roots of (3.3.4) are:

$$\Pi_{\{1,2\}}^*(\mathcal{E}_1) = \left\{ e^{\frac{\beta\mu\bar{x}}{\bar{x}+\omega} - \theta}, \frac{(\bar{x}(\bar{x}(-\gamma\bar{x} - 2\gamma\Lambda + \kappa) + (\gamma+2)\kappa\Lambda) + \kappa\Lambda^2) e^{\frac{\gamma\bar{x}(\kappa-\bar{x})}{\kappa(\bar{x}+\Lambda)} - \zeta}}{\kappa(\bar{x} + \Lambda)^2} \right\}.$$

Therefore for the system (3.1.5) the fixed point  $\mathcal{E}_1(\hat{x}, 0) = \left( \frac{-\sqrt{(\zeta\kappa - \gamma\kappa)^2 - 4\gamma\zeta\kappa\Lambda} + \gamma\kappa - \zeta\kappa}{2\gamma}, 0 \right)$  is stable when  $|\Pi_{\{1,2\}}^*(\mathcal{E}_1)| < 1$ . To discuss the dynamics of the interior fixed point  $(\hat{x}, \hat{y})$  for system (3.1.4), we have computed the variational matrix as follows:

$$\mathbb{N}_{\mathcal{E}_*}(\hat{x}, \hat{y}) = \begin{pmatrix} -\zeta - \frac{\mu\omega\hat{y}}{(\omega + \hat{x})^2} + \frac{\gamma\hat{x}(2\kappa\Lambda + \hat{x}(\kappa - 3\Lambda - 2\hat{x}))}{(\Lambda + \hat{x})^2(F\hat{y}\kappa + \kappa)} & \hat{x} \left( \frac{\gamma F \hat{x}(\hat{x} - \kappa)}{\kappa(\Lambda + \hat{x})(F\hat{y} + 1)^2} - \frac{\mu}{\omega + \hat{x}} \right) \\ \frac{\beta\mu\omega\hat{y}}{(\omega + \hat{x})^2} & -\theta - 2\delta\hat{y} + \frac{\beta\mu\hat{x}}{\omega + \hat{x}} \end{pmatrix}. \quad (3.3.5)$$

**Theorem 3.3.3.** *For system (3.1.4), the interior fixed point  $\mathcal{E}_* = (\hat{x}, \hat{y})$  is locally asymptotically stable if the eigenvalues of the variational matrix (3.3.5) are less than zero.*

The variational matrix of the system (3.1.5) at the interior fixed point  $(\hat{x}, \hat{y})$  can be computed as follows:

$$\mathbb{M}_{\mathcal{E}_*}(\hat{x}, \hat{y}) = \begin{pmatrix} \hat{x} \left( \frac{\gamma(\kappa\Lambda - \hat{x}(2\Lambda + \hat{x}))}{(\Lambda + \hat{x})^2(F\hat{y}\kappa + \kappa)} + \frac{\mu\hat{y}}{(\omega + \hat{x})^2} \right) + 1 & \hat{x} \left( \frac{\gamma F \hat{x}(\hat{x} - \kappa)}{\kappa(\Lambda + \hat{x})(F\hat{y} + 1)^2} - \frac{\mu}{\omega + \hat{x}} \right) \\ \frac{\beta\mu\omega\hat{y}}{(\omega + \hat{x})^2} & 1 - \delta\hat{y} \end{pmatrix}. \quad (3.3.6)$$

The characteristic function of (3.3.6) is:

$$\Gamma(\mu) = \mu^2 - (\Gamma_{Tr})\mu + \Gamma_{Det},$$

where,

$$\Gamma_{Tr} = \frac{\gamma\hat{x}(\kappa\Lambda - \hat{x}(2\Lambda + \hat{x}))}{(\Lambda + \hat{x})^2(\kappa + \kappa\hat{y}F)} + \hat{y} \left( \frac{\mu\hat{x}}{(\hat{x} + \omega)^2} - \delta \right) + 2, \quad (3.3.7)$$

$$\begin{aligned} \Gamma_{Det} &= \left[ \hat{x} \left( \frac{\gamma(\kappa\Lambda - \hat{x}(2\Lambda + \hat{x}))}{(\Lambda + \hat{x})^2(F\hat{y}\kappa + \kappa)} + \frac{\mu\hat{y}}{(\omega + \hat{x})^2} \right) + 1 \right] [1 - \delta\hat{y}] \\ &- \hat{x} \left[ \frac{\beta\mu\omega\hat{y}}{(\omega + \hat{x})^2} \right] \left[ \frac{\gamma F \hat{x}(\hat{x} - \kappa)}{\kappa(\Lambda + \hat{x})(F\hat{y} + 1)^2} - \frac{\mu}{\omega + \hat{x}} \right]. \end{aligned} \quad (3.3.8)$$

Using stability criteria of discrete-time systems, we can write the following theorem for the stability analysis of the interior fixed point  $(\hat{x}, \hat{y})$  for system (3.1.5).

**Theorem 3.3.4.** *For system (3.1.5), the interior fixed point  $(\hat{x}, \hat{y})$  is a*

- $\mathcal{C}_1$  : *Source iff  $|\Gamma_{Det}| > 1$ , and  $|\Gamma_{Tr}| < |1 + \Gamma_{Det}|$ ,*
- $\mathcal{C}_2$  : *Saddle point iff  $(\Gamma_{Tr})^2 > 4(\Gamma_{Det})$ , and  $|\Gamma_{Tr}| > |1 + \Gamma_{Det}|$ ,*
- $\mathcal{C}_3$  : *Non-hyperbolic point iff  $|\Gamma_{Tr}| = |1 + \Gamma_{Det}|$ , or  $\Gamma_{Det} = 1$ , and  $\Gamma_{Tr} \leq 2$ .*
- $\mathcal{C}_4$  : *If condition  $\mathcal{C}_3$  does not hold then  $(\hat{x}, \hat{y})$  is a sink iff  $|\Gamma_{Tr}| < 1 + |\Gamma_{Det}| < 2$ .*

We will discuss our main finding on the periodic behavior of the system (3.1.5) in the following section. We will use mathematical concepts to demonstrate that there is periodic behavior in the model.

### 3.4 Periodicity

In this section, we will determine the conditions under which the parameters in the system (3.1.5) display periodic behavior with a typical integer period in terms of the time variables. In a prey-predator system, the periodic nature of the system is essential. It helps improve our understanding of the seasonal fluctuations in population cycles encountered by hunters (predators) and their prey. This will help us understand the seasonal behavior of the populations. Understanding these cycles enables us to predict when there will be an increase or decrease in the number of prey and predators. This is incredibly helpful for controlling nature and maintaining the health of our environment. As a result, by examining these recurring patterns, we may contribute to preserving nature and influencing decisions that will benefit the environment and future generations. Let the set of all integers be denoted by  $\mathbb{Z}$ , non-negative integers by  $\mathbb{Z}^+$ , non-negative real numbers by  $\mathbb{R}^+$ , and the two-dimensional Euclidean vector space by  $\mathbb{R}^2$ . Here, in the next part of this section, for our convenience, the notations below will be used:

$$\mathcal{I}_\Omega = \{0, 1, 2, \dots, \Omega - 1\}, \tilde{p} = \frac{1}{\Omega} \sum_{m=0}^{\Omega-1} p(m), p^u = \max_{m \in \mathcal{I}_\Omega} p(m), p^l = \min_{m \in \mathcal{I}_\Omega} p(m),$$

where for  $m \in \mathbb{N}$ ,  $\{p(m)\}$  is a sequence of real numbers with periodic  $\Omega$ . We assume that all of the parameters  $(\gamma, F, \kappa, \Lambda, \mu, \omega, \zeta, \beta, \theta, \delta) : \mathbb{N} \rightarrow \mathbb{R}^+$  in system (3.1.5) are  $\Omega$ -periodic. In this situation, the fixed positive integer  $\Omega$  stands for the chosen common period for the parameter in equation (3.1.5). The exponential formulation of the equations included in the system (3.1.5) assures that the upcoming trajectory  $(x(m), y(m))$  constantly remains within the positive quadrant of the plane during the process of evolution assuming the initial conditions  $(x(0), y(0)) > (0, 0)$  ([110]). We will concentrate on populations  $(x(m), y(m))$  where both  $x(0)$  and  $y(0)$  are greater than zero, taking into



account biological considerations. Assume that  $\mathcal{X}$  and  $\mathcal{Y}$  are normed vector spaces, that  $\mathcal{L} : \text{Dom}\mathcal{L} \subset \mathcal{X} \rightarrow \mathcal{Y}$  is a linear mapping, and that  $\mathcal{N} : \mathcal{X} \rightarrow \mathcal{Y}$  is a continuous mapping. The mapping indicated by  $\mathcal{L}$  will be referred to as Fredholm mapping with an index of zero if  $\dim \text{Ker}\mathcal{L} = \text{codim}\text{Im}\mathcal{L} < +\infty$  and  $\text{Im}\mathcal{L}$  is closed in  $\mathcal{Y}$ . In the event where  $\mathcal{L}$  is a Fredholm mapping with an index of zero, and continuous projections are possible,

$$\mathcal{P} : \mathcal{X} \rightarrow \mathcal{X} \text{ and } \mathcal{Q} : \mathcal{Y} \rightarrow \mathcal{Y},$$

such that  $\text{Im}\mathcal{P} = \text{Ker}\mathcal{L}, \text{Im}\mathcal{L} = \text{Ker}\mathcal{Q} = \text{Im}(\mathcal{I} - \mathcal{Q})$ , it follows that  $\mathcal{L}|_{\text{Dom}\mathcal{L} \cap \text{Ker}\mathcal{P}} : (\mathcal{I} - \mathcal{P})\mathcal{X} \rightarrow \text{Im}\mathcal{L}$  is invertible. We use  $\mathcal{K}_{\mathcal{P}}$  to represent the map's inverse. If  $\mathcal{U}$  is an open bounded subset of  $\mathcal{X}$ , the mapping  $\mathcal{N}$  will be called  $\mathcal{L}$ -compact on  $\overline{\mathcal{U}}$  if  $\mathcal{Q}\mathcal{N}(\overline{\mathcal{U}})$  is bounded and  $\mathcal{K}_{\mathcal{P}}(\mathcal{I} - \mathcal{Q})\mathcal{N} : \overline{\mathcal{U}} \rightarrow \mathcal{X}$  is compact. Given that  $\text{Im}\mathcal{Q}$  is isomorphic to  $\text{Ker}\mathcal{L}$ , there is an isomorphism denoted as  $\mathcal{J} : \text{Im}\mathcal{Q} \rightarrow \text{Ker}\mathcal{L}$ .

**Lemma 3.4.1.** (*Continuation Theorem [108]*) *Let us have a Fredholm mapping  $\mathcal{L}$  of zero index and  $\mathcal{N}$  be  $\mathcal{L}$ -compact on  $\overline{\mathcal{U}}$ . Suppose the following conditions are true:*

- *Every solution of the equation  $\mathcal{L}x = \Lambda\mathcal{N}x$  with each  $0 < \Lambda < 1$  is such that  $x \in \partial\mathcal{U}$ .*
- *For each  $x \in \partial\mathcal{U} \cap \text{Ker}\mathcal{L}$ ,  $\mathcal{Q}\mathcal{N}x \neq 0$  and the Brouwer degree  $\deg\{\mathcal{J}\mathcal{Q}\mathcal{N}, \mathcal{U} \cap \text{Ker}\mathcal{L}, 0\} \neq 0$ .*

*Then, there exists at least one solution of the operator equation  $\mathcal{L}x = \mathcal{N}x$  in  $\text{Dom}\mathcal{L} \cap \overline{\mathcal{U}}$ .*

**Lemma 3.4.2.** (*[109]*) *Consider an  $\Omega$ -periodic function  $p : \mathbb{Z} \rightarrow \mathbb{R}$ , i.e.,  $p(m + \Omega) = p(m)$ . Then for any fixed  $m_1, m_2 \in \mathcal{I}_{\Omega}$ , and any  $m \in \mathbb{N}$ , one has*

$$p(m) \leq p(m_1) + \sum_{k=0}^{\Omega-1} |p(k+1) - p(k)|, p(k) \geq p(m_2) - \sum_{k=0}^{\Omega-1} |p(k+1) - p(k)|.$$

*Let us define*

$$q_2 = \{v = v(m) : v(m) \in \mathbb{R}^2, m \in \mathbb{N}\}.$$

*For  $b = (b_1, b_2)^T \in \mathbb{R}^2$ , define  $|b| = \max\{b_1, b_2\}$ . Let  $q^{\Omega} \subset q_2$  represent the subspace of all  $\Omega$ -periodic sequences provided with the usual supremum norm  $\|\cdot\|$ , i.e.,*

$$|v| = \max_{m \in \mathcal{I}_{\Omega}} |v_1(m)| + \max_{m \in \mathcal{I}_{\Omega}} |v_2(m)|, \text{ for any } v = \{v(m) : m \in \mathbb{N}\} \in q^{\Omega}.$$

*It is simple to demonstrate that  $q^{\Omega}$  is a finite-dimensional Banach space. Let*

$$q_0^{\Omega} = \left\{ v = \{v(m)\} \in q^{\Omega} : \sum_{m=0}^{\Omega-1} v(m) = 0, m \in \mathbb{N} \right\},$$

$$q_c^\Omega = \{v = \{v(m)\} \in q^\Omega : v(m) = J \in \mathbb{R}^2, m \in \mathbb{N}\};$$

then it follows that  $q_0^\Omega$  and  $q_c^\Omega$  are both closed linear sub spaces of  $q^\Omega$  and  $q^\Omega = q_0^\Omega \oplus q_c^\Omega$ ,  $\dim q_c^\Omega = 2$ . We are now prepared to present and prove the significant findings of this study.

**Theorem 3.4.3.** *If  $\left(-\frac{e^{\bar{u}}\bar{\gamma}(2e^{\bar{u}}\bar{\Lambda}-\bar{\kappa}\bar{\Lambda}+e^{2\bar{u}})}{(\bar{\Lambda}+e^{\bar{u}})^2(e^{\bar{v}}\bar{F}\bar{\kappa}+\bar{\kappa})}\right)(-e^{\bar{v}}\bar{\delta}) < \left(\frac{e^{\bar{u}+\bar{v}}\bar{\gamma}(e^{\bar{u}}-\bar{\kappa})\bar{F}}{\bar{\kappa}(\bar{\Lambda}+e^{\bar{u}})(e^{\bar{v}}\bar{F}+1)^2}\right)\left(\frac{e^{\bar{u}}\bar{\beta}\bar{\mu}\bar{\omega}}{(\bar{\omega}+e^{\bar{u}})^2}\right)$ ,  $\bar{\theta}\Omega > \bar{\mu}\beta, C > \bar{\mu}\beta - \bar{\theta}\Omega$ , and  $\bar{\theta}\Omega > \bar{\mu}\bar{\beta}e^{\bar{\Theta}_1}$ . The system represented by equation (3.1.5) possesses at least one positive solution for the period  $\Omega$ .*

*Proof.* Suppose  $x(m) = e^{\{u(m)\}}, y(m) = e^{\{v(m)\}}$ , so that the conversion of system (3.1.5) is:

$$\begin{cases} u_{m+1} - u_m = -\xi(m) + \frac{\gamma(m)}{1+F(m)e^{v(m)}} \left(1 - \frac{e^{u(m)}}{\mathcal{K}(m)}\right) \left(\frac{e^{u(m)}}{e^{u(m)}+\Lambda(m)}\right) - \frac{\mu(m)e^{v(m)}}{e^{u(m)}+\omega(m)}, \\ v_{m+1} - v_m = -\theta(m) - \delta(m)e^{v(m)} + \frac{\mu(m)\beta(m)e^{u(m)}}{e^{u(m)}+\omega(m)}. \end{cases} \quad (3.4.1)$$

Let,  $\mathcal{X} = q^\Omega = \mathcal{Y}$ , and

$$\mathcal{L}y(m) = y(m+1) - y(m) = \begin{bmatrix} u(m+1) - u(m) \\ v(m+1) - v(m) \end{bmatrix},$$

where

$$\mathcal{N}y(m) = \begin{bmatrix} -\xi(m) + \frac{\gamma(m)}{1+F(m)e^{v(m)}} \left(1 - \frac{e^{u(m)}}{\mathcal{K}(m)}\right) \left(\frac{e^{u(m)}}{e^{u(m)}+\Lambda(m)}\right) - \frac{\mu(m)e^{v(m)}}{e^{u(m)}+\omega(m)} \\ -\theta(m) - \delta(m)e^{v(m)} + \frac{\mu(m)\beta(m)e^{u(m)}}{e^{u(m)}+\omega(m)} \end{bmatrix},$$

$\forall y \in \mathcal{X}$  and  $m \in \mathbb{N}$ . It can be easily seen that  $\mathcal{L}$  is a bounded linear operator and

$$\text{Ker } \mathcal{L} = q_c^\Omega, \text{Im } \mathcal{L} = q_0^\Omega,$$

and

$$\dim \text{Ker } \mathcal{L} = 2 = \text{codim Im } \mathcal{L}.$$

Given that  $\text{Im } \mathcal{L}$  is closed in  $\mathcal{Y}$ , we may infer that  $\mathcal{L}$  meets the criteria for a Fredholm mapping with zero index. Define

$$\mathcal{P}_u = \frac{1}{\Omega} \sum_{n=0}^{\Omega-1} y(n), y \in \mathcal{X}, \mathcal{Q}_z = \frac{1}{\Omega} \sum_{n=0}^{\Omega-1} z(n), z \in \mathcal{Y}.$$

It can be easily seen that  $\mathcal{P}$  and  $\mathcal{Q}$  are continuous projectors with the properties  $\text{Im } \mathcal{P} = \text{Ker } \mathcal{L}$  and  $\text{Im } \mathcal{L} = \text{Ker } \mathcal{Q} = \text{Im}(\mathcal{I} - \mathcal{Q})$ .

It is also important to remember that there is a generalized inverse operator (to  $\mathcal{L}$ )

$\mathcal{K}_{\mathcal{P}} : Im\mathcal{L} \rightarrow Ker\mathcal{P} \cap Dom\mathcal{L}$  exists and is provided by

$$\mathcal{K}_{\mathcal{P}}(z) = \sum_{n=0}^{\Omega-1} z(n) - \frac{1}{\Omega} \sum_{n=0}^{\Omega-1} z(n).$$

Clearly,  $\mathcal{K}_{\mathcal{P}}(\mathcal{I} - \mathcal{Q})\mathcal{N}$  and  $\mathcal{Q}\mathcal{N}$  are continuous. The Arzela-Ascoli theorem makes it simple to demonstrate that for an open bounded set  $\mathcal{U} \subset \mathcal{X}$ ,  $\overline{\mathcal{K}_{\mathcal{P}}(\mathcal{I} - \mathcal{Q})\mathcal{N}(\mathcal{U})}$  is compact. Furthermore,  $\mathcal{Q}\mathcal{N}(\mathcal{U})$  is bounded. Thus,  $\mathcal{N}$  is  $\mathcal{L}$ -compact on  $\mathcal{U}$  with any open bounded subset  $\mathcal{U} \subset \mathcal{X}$ . We need an open bounded set  $\mathcal{U}$  to apply the continuation theorem. The system that corresponds to the operator equation  $\mathcal{L}y = \lambda\mathcal{N}\mathcal{Y}$ ,  $\lambda \in (0, 1)$  is as follows:

$$\begin{bmatrix} u(m+1) - u(m) \\ v(m+1) - v(m) \end{bmatrix} = \lambda \begin{bmatrix} -\xi(m) + \frac{\gamma(m)}{1+F(m)e^{v(m)}} \left(1 - \frac{e^{u(m)}}{\mathcal{K}(m)}\right) \left(\frac{e^{u(m)}}{e^{u(m)}+\Lambda(m)}\right) - \frac{\mu(m)e^{v(m)}}{e^{u(m)}+\omega(m)} \\ -\theta(m) - \delta(m)e^{v(m)} + \frac{\mu(m)\beta(m)e^{u(m)}}{e^{u(m)}+\omega(m)} \end{bmatrix}. \quad (3.4.2)$$

Now, consider an arbitrary solution  $(u(m), v(m))^T \in \mathcal{X}$  of the system (3.4.2) for a certain  $\lambda \in (0, 1)$ . Applying  $\sum_{m=0}^{\Omega-1}$  on both sides of system (3.4.2) we get:

$$\begin{bmatrix} 0 \\ 0 \end{bmatrix} = \begin{bmatrix} \sum_{m=0}^{\Omega-1} \{u(m+1) - u(m)\} \\ \sum_{m=0}^{\Omega-1} \{v(m+1) - v(m)\} \end{bmatrix} = \lambda \begin{bmatrix} \sum_{m=0}^{\Omega-1} \left\{ -\xi(m) + \frac{\gamma(m)}{1+F(m)e^{v(m)}} \left(1 - \frac{e^{u(m)}}{\mathcal{K}(m)}\right) \left(\frac{e^{u(m)}}{e^{u(m)}+\Lambda(m)}\right) - \frac{\mu(m)e^{v(m)}}{e^{u(m)}+\omega(m)} \right\} \\ \sum_{m=0}^{\Omega-1} \left\{ -\theta(m) - \delta(m)e^{v(m)} + \frac{\mu(m)\beta(m)e^{u(m)}}{e^{u(m)}+\omega(m)} \right\} \end{bmatrix}. \quad (3.4.3)$$

Based on the system mentioned above, we can express the following from its right-hand side:

$$\begin{bmatrix} \bar{\xi}\Omega \\ \bar{\theta}\Omega \end{bmatrix} = \begin{bmatrix} \sum_{m=0}^{\Omega-1} \left\{ \frac{\gamma(m)}{1+F(m)e^{v(m)}} \left(1 - \frac{e^{u(m)}}{\mathcal{K}(m)}\right) \left(\frac{e^{u(m)}}{e^{u(m)}+\Lambda(m)}\right) - \frac{\mu(m)e^{v(m)}}{e^{u(m)}+\omega(m)} \right\} \\ \sum_{m=0}^{\Omega-1} \left\{ -\delta(m)e^{v(m)} + \frac{\mu(m)\beta(m)e^{u(m)}}{e^{u(m)}+\omega(m)} \right\} \end{bmatrix}. \quad (3.4.4)$$

From systems (3.4.2) and (3.4.4), we can obtain:

$$\begin{bmatrix} \sum_{m=0}^{\Omega-1} |u(m+1) - u(m)| \\ \sum_{m=0}^{\Omega-1} |v(m+1) - v(m)| \end{bmatrix} \leq \lambda \begin{bmatrix} \sum_{m=0}^{\Omega-1} \left\{ \xi(m) + \frac{\gamma(m)}{1+F(m)e^{v(m)}} \left(1 - \frac{e^{u(m)}}{\mathcal{K}(m)}\right) \left(\frac{e^{u(m)}}{e^{u(m)}+\Lambda(m)}\right) - \frac{\mu(m)e^{v(m)}}{e^{u(m)}+\omega(m)} \right\} \\ \sum_{m=0}^{\Omega-1} \left\{ \theta(m) - \delta(m)e^{v(m)} + \frac{\mu(m)\beta(m)e^{u(m)}}{e^{u(m)}+\omega(m)} \right\} \end{bmatrix}$$

$$= \begin{bmatrix} 2\lambda\bar{\xi}\Omega \\ 2\lambda\bar{\theta}\Omega \end{bmatrix} < \begin{bmatrix} 2\bar{\xi}\Omega \\ 2\bar{\theta}\Omega \end{bmatrix}. \quad (3.4.5)$$

Since  $(u(m), v(m))^T \in \mathcal{X}$ , there exist  $a_i, b_i \in \mathcal{I}_\Omega$  such that

$$\begin{cases} u(a_1) = \min_{m \in \mathcal{I}_\Omega} u(m), u(b_1) = \max_{m \in \mathcal{I}_\Omega} u(m) \\ v(a_2) = \min_{m \in \mathcal{I}_\Omega} v(m), v(b_2) = \max_{m \in \mathcal{I}_\Omega} v(m) \end{cases} \quad (3.4.6)$$

From (3.4.6) and (3.4.4), we have:

$$\begin{aligned} \bar{\xi}\Omega &\leq \sum_{m=0}^{\Omega-1} \left\{ \frac{\gamma(m)}{1 + F(m)e^{v(m)}} \left( 1 - \frac{e^{u(m)}}{\mathcal{K}(m)} \right) \left( \frac{e^{u(m)}}{e^{u(m)} + \Lambda(m)} \right) \right\} \\ &\leq \sum_{m=0}^{\Omega-1} \gamma(m)e^{u(m)} \\ &\leq \sum_{m=0}^{\Omega-1} \gamma(m)e^{u(b_1)} \\ &= \bar{\gamma}e^{u(b_1)} \\ u(b_1) &\geq \ln\left(\frac{\bar{\xi}\Omega}{\bar{\gamma}}\right) = \Theta_1. \end{aligned}$$

Using Lemma 3.4.2 and (3.4.5), we have:

$$u(m) \geq u(b_1) - \sum_{m=0}^{\Omega-1} |u(m+1) - u(m)| \geq \Theta_1 - 2\bar{\xi}\Omega = \mathcal{H}_1. \quad (3.4.7)$$

Again, from (3.4.6) and (3.4.4), we have:

$$\begin{aligned} \bar{\theta}\Omega &\leq \sum_{m=0}^{\Omega-1} \{\mu(m)\beta(m) - \delta(m)e^{v(m)}\} \leq \sum_{m=0}^{\Omega-1} \{\mu(m)\beta(m) + \delta(m)e^{v(b_2)}\} \\ e^{v(b_2)} &\geq \frac{\bar{\theta}\Omega - \bar{\mu}\bar{\beta}}{\bar{\delta}} \\ v(b_2) &\geq \ln \left| \frac{\bar{\theta}\Omega - \bar{\mu}\bar{\beta}}{\bar{\delta}} \right| = \Theta_2. \end{aligned}$$

From Lemma 3.4.2 and (3.4.5), we can write:

$$v(m) \geq v(b_2) - \sum_{m=0}^{\Omega-1} |v(m+1) - v(m)| \geq \Theta_2 - 2\bar{\theta}\Omega = \mathcal{H}_2. \quad (3.4.8)$$

Now, again, from (3.4.6) and (3.4.4), we have:

$$\begin{aligned}
\bar{\xi}\Omega &\geq \sum_{m=0}^{\Omega-1} \left\{ -\mu(m) - \gamma(m) \left( 1 - \frac{e^{u(a_1)}}{\mathcal{K}(m)} \right) \right\} \\
&= \sum_{m=0}^{\Omega-1} \left\{ -\mu(m) - \gamma(m) + \frac{\gamma(m)e^{u(a_1)}}{\mathcal{K}(m)} \right\} \\
&\geq \left\{ -\bar{\mu} - \bar{\gamma} + \frac{\bar{\gamma}e^{u(a_1)}}{\bar{\mathcal{K}}} \right\} \\
u(a_1) &\leq \ln \left| \frac{(\bar{\xi}\Omega + \bar{\mu} + \bar{\gamma}) \bar{\mathcal{K}}}{\bar{\gamma}} \right| = \Theta_3.
\end{aligned}$$

Again, using Lemma 3.4.2 and (3.4.5), we have:

$$u(m) \leq u(a_1) + \sum_{m=0}^{\Omega-1} |u(m+1) - u(m)| \leq \Theta_3 + 2\bar{\xi}\Omega = \mathcal{H}_3. \quad (3.4.9)$$

Now, again, from (3.4.6) and (3.4.4), we have:

$$\bar{\theta}\Omega \leq \sum_{m=0}^{\Omega-1} \{ \mu(m)\beta(m) - \delta(m)e^{v(m)} \} \leq \sum_{m=0}^{\Omega-1} \{ \mu(m)\beta(m) - \delta(m)e^{v(a_2)} \}$$

$$\begin{aligned}
e^{v(a_2)} &\leq \frac{C + \bar{\mu}\bar{\beta} - \bar{\theta}\Omega}{\bar{\delta}} \\
v(a_2) &\leq \ln \left| \frac{C + \bar{\mu}\bar{\beta} - \bar{\theta}\Omega}{\bar{\delta}} \right| = \Theta_4,
\end{aligned}$$

where  $C$  denotes any positive constant such that  $C > \bar{\mu}\bar{\beta} - \bar{\theta}\Omega$ . Again, using Lemma 3.4.2 and (3.4.5), we have:

$$v(m) \leq v(a_2) + \sum_{m=0}^{\Omega-1} |v(m+1) - v(m)| \leq \Theta_4 + 2\bar{\theta}\Omega = \mathcal{H}_4. \quad (3.4.10)$$

Now, from (3.4.7), (3.4.8), (3.4.9), and (3.4.10), it can be written as:

$$\max_{m \in I_\Omega} |u(m)| \leq \max \{ |\mathcal{H}_1|, |\mathcal{H}_3| \} := \mathcal{O}_1$$

and

$$\max_{m \in I_\Omega} |v(m)| \leq \max \{ |\mathcal{H}_2|, |\mathcal{H}_4| \} := \mathcal{O}_2.$$

$\mathcal{O}_1$  and  $\mathcal{O}_1$  are clearly independent of  $\lambda$ . Consider the equation  $\mathcal{O} = \mathcal{O}_1 + \mathcal{O}_2 + \mathcal{O}_3$ , where

$\mathcal{O}_3 > 0$  is believed to be sufficiently large such that  $\mathcal{O}_3 > |\Theta_1| + |\Theta_2| + |\Theta_3| + |\Theta_4|$ . Let's now examine the subsequent system of equations:

$$\begin{cases} -\bar{\xi} + \frac{1}{\Omega} \sum_{m=0}^{\Omega-1} \left( \frac{\gamma(m)}{1+F(m)e^v} \left( 1 - \frac{e^u}{\bar{\kappa}} \right) \left( \frac{e^u}{e^u + \Lambda(m)} \right) \right) - \frac{1}{\Omega} \sum_{m=0}^{\Omega-1} \left( \frac{\epsilon\mu(m)e^v}{e^u + \omega(m)} \right) = 0, \\ -\bar{\theta} - \frac{1}{\Omega} \sum_{m=0}^{\Omega-1} (\delta(m)e^v) + \frac{1}{\Omega} \sum_{m=0}^{\Omega-1} \left( \frac{\mu(m)\beta(m)e^u}{e^u + \omega(m)} \right) = 0, \end{cases} \quad (3.4.11)$$

where  $(u, v) \in \mathbb{R}^2$  and the parameter  $\epsilon \in [0, 1]$ . The system below is comparable to the one above:

$$\begin{cases} -\bar{\xi} + \frac{\bar{\gamma}}{1+\bar{F}e^v} \left( 1 - \frac{e^u}{\bar{\kappa}} \right) \left( \frac{e^u}{e^u + \bar{\Lambda}} \right) - \frac{1}{\Omega} \sum_{m=0}^{\Omega-1} \left( \frac{\epsilon\mu(m)e^v}{e^u + \omega(m)} \right) = 0, \\ -\bar{\theta} - \bar{\delta}e^v + \frac{1}{\Omega} \sum_{m=0}^{\Omega-1} \left( \frac{\mu(m)\beta(m)e^u}{e^u + \omega(m)} \right) = 0. \end{cases} \quad (3.4.12)$$

It is demonstrated that any  $(\bar{u}, \bar{v})$  in the system (3.4.12) satisfies

$$\Theta_1 \leq \bar{u} \leq \Theta_3, \Theta_2 \leq \bar{v} \leq \Theta_4. \quad (3.4.13)$$

Let

$$\Pi = \{(u, v)^T \in \mathcal{X} : \|(u, v)\| < \mathcal{O}\},$$

then  $\Pi$  is an open, bounded set in  $\mathcal{X}$  and satisfies the first condition of Lemma 3.4.1. When  $(u, v) \in \partial\Pi \cap \text{Ker}\mathcal{L}$ ,  $(u, v)$  is a constant vector in  $\mathbb{R}^2$  with  $\|(u, v)\| = |u| + |v| = \mathcal{O}$ . Then

$$\mathcal{QN} \begin{bmatrix} u \\ v \end{bmatrix} = \begin{bmatrix} -\bar{\xi} + \frac{\bar{\gamma}}{1+\bar{F}e^v} \left( 1 - \frac{e^u}{\bar{\kappa}} \right) \left( \frac{e^u}{e^u + \bar{\Lambda}} \right) - \frac{1}{\Omega} \sum_{m=0}^{\Omega-1} \left( \frac{\epsilon\mu(m)e^v}{e^u + \omega(m)} \right) \\ -\bar{\theta} - \bar{\delta}e^v + \frac{1}{\Omega} \sum_{m=0}^{\Omega-1} \left( \frac{\mu(m)\beta(m)e^u}{e^u + \omega(m)} \right) \end{bmatrix} \neq \begin{bmatrix} 0 \\ 0 \end{bmatrix}. \quad (3.4.14)$$

Thus, for all  $(u, v)^T \in \partial\Pi \cap \text{Ker}\mathcal{L}$ ,  $\mathcal{QN} \neq 0$ . Hence, the second part of Lemma 3.4.1 is satisfied. Consider the homotopy that is being used to determine the Brouwer degree

$$\mathcal{A}_\epsilon((u, v)^T) = \epsilon\mathcal{QN}((u, v)^T) + (1 - \epsilon)\mathcal{G}((u, v)^T), \epsilon \in [0, 1],$$

where

$$\mathcal{G}((u, v)^T) = \begin{bmatrix} -\bar{\xi} + \left( 1 - \frac{e^u}{\bar{\kappa}} \right) \left( \frac{e^u}{e^u + \bar{\Lambda}} \right) \\ \bar{\theta} + \bar{\delta}e^v - \frac{1}{\Omega} \sum_{m=0}^{\Omega-1} \left( \frac{\mu(m)\beta(m)e^u}{e^u + \omega(m)} \right) \end{bmatrix}. \quad (3.4.15)$$

From (3.4.13), we can write  $0 \notin \mathcal{A}_\epsilon(\partial\Pi \cap \text{Ker}\mathcal{L}), \epsilon \in [0, 1]$ , and it is easy to verify that  $\mathcal{G}((u, v)^T) = 0$  has a unique solution in  $\mathbb{R}^2$ . According to the invariance property of homotopy

$$\begin{aligned} \deg(\mathcal{J}\mathcal{Q}\mathcal{N}, \Pi \cap \text{Ker}\mathcal{L}, 0) &= \deg(\mathcal{Q}\mathcal{N}, \Pi \cap \text{Ker}\mathcal{L}, 0) \\ &= \deg(\mathcal{G}, \Pi \cap \text{Ker}\mathcal{L}, 0) \\ &= \sum_{x \in \mathcal{G}^{-1}(0)} \text{sig}\mathcal{J}_\mathcal{G}(x) \neq 0, \end{aligned}$$

where  $\deg(., ., .)$  is the Brouwer degree,  $\mathcal{J} = I_d$  since  $\text{Im}\mathcal{Q} = \text{Ker}\mathcal{L}$  and the Jacobian of  $\mathcal{G}$  is

$$\mathcal{J}_\mathcal{G}(x) = \det \begin{pmatrix} -\frac{e^u(-K\Lambda + 2\Lambda e^u + e^{2u})}{K(\Lambda + e^u)^2} & 0 \\ -\frac{\beta\mu e^u\omega}{(e^u + \omega)^2} & \delta e^v \end{pmatrix} < 0, \quad (3.4.16)$$

where  $K\Lambda < 2\Lambda e^u + e^{2u}$ . Thus, if  $\Pi$  satisfies all the conditions of Lemma 3.4.1, then it follows that  $\mathcal{L}x = \mathcal{N}x$  has at least one  $\Omega$  periodic solution in  $\text{Dom}\mathcal{L} \cap \bar{\Pi}$ , say  $(\bar{u}(m), \bar{v}(m))^T$ . Let  $\bar{x}(m) = \exp\bar{u}(m)$  and  $\bar{y}(m) = \exp\bar{v}(m)$ , then  $(\bar{u}(m), \bar{v}(m))^T$  is an  $\Omega$  periodic solution of system (4.1.5) with strictly positive components. Hence, the proof is completed.  $\square$

### 3.5 Bifurcation analysis

This section will focus on the theoretical analysis of all the bifurcations present in the models (3.1.4) and (3.1.5). Bifurcations happen when a slight variation in a parameter causes the system to go from one stable state to another. These changes can be utilized to identify significant thresholds above which the system cannot go back to its initial form. Bifurcations can show how environmental changes, such as shifts in the prey or predator populations, might impact the system's dynamics in the context of a prey-predator model. We found that the Hopf bifurcation induces limit cycles in both systems. It has been observed that Hopf bifurcation results in adjacent invariant circles. As an alternative, it is possible to find certain isolated orbits with periodic behavior and trajectories that closely encircle the consistent circle [98]. The bifurcation may be supercritical if a stable closed invariant curve exists or sub-critical if not. A slight modification in a parametric factor during flip bifurcation leads the system to adopt a new behavior with twice the period of the initial system. We have only noticed the flip bifurcation in the system (3.1.5). For interested readers to study further results on Hopf and flip bifurcations, relevant papers include those by [52], [100], [101], [102], and [103]. We have the following criteria for

these two types of bifurcations: The variational matrix of (3.1.5) at  $(\hat{x}, \hat{y})$  is:

$$\Delta(\hat{x}, \hat{y}) = \begin{pmatrix} \hat{x} \left( \frac{\gamma(\kappa\Lambda - \hat{x}(2\Lambda + \hat{x}))}{(\Lambda + \hat{x})^2(F\hat{y}\kappa + \kappa)} + \frac{\mu\hat{y}}{(\omega + \hat{x})^2} \right) + 1 & \hat{x} \left( \frac{\gamma F \hat{x}(\hat{x} - \kappa)}{\kappa(\Lambda + \hat{x})(F\hat{y} + 1)^2} - \frac{\mu}{\omega + \hat{x}} \right) \\ \frac{\beta\mu\omega\hat{y}}{(\omega + \hat{x})^2} & 1 - \delta\hat{y} \end{pmatrix}.$$

The characteristic function is:

$$\Pi(\xi) = \xi^2 - (\Pi_{Tr})\xi + \Pi_{Det}, \quad (3.5.1)$$

where,

$$\Pi_{Tr} = \frac{\gamma\hat{x}(\kappa\Lambda - \hat{x}(2\Lambda + \hat{x}))}{(\Lambda + \hat{x})^2(\kappa + \kappa\hat{y}F)} + \hat{y} \left( \frac{\mu\hat{x}}{(\hat{x} + \omega)^2} - \delta \right) + 2, \quad (3.5.2)$$

$$\begin{aligned} \Pi_{Det} &= \left( \hat{x} \left( \frac{\gamma(\kappa\Lambda - \hat{x}(2\Lambda + \hat{x}))}{(\Lambda + \hat{x})^2(F\hat{y}\kappa + \kappa)} + \frac{\mu\hat{y}}{(\omega + \hat{x})^2} \right) + 1 \right) (1 - \delta\hat{y}) \\ &- \hat{x} \left( \frac{\gamma F \hat{x}(\hat{x} - \kappa)}{\kappa(\Lambda + \hat{x})(F\hat{y} + 1)^2} - \frac{\mu}{\omega + \hat{x}} \right) \left( \frac{\beta\mu\omega\hat{y}}{(\omega + \hat{x})^2} \right). \end{aligned} \quad (3.5.3)$$

Let  $(\Pi_{Tr})^2 > 4\Pi_{Det}$ , and  $(\Pi_{Tr}) + \Pi_{Det} = -1$ , then it follows that:

$$\gamma = \frac{(\Lambda + \hat{x})^2 \left( \hat{y} \left( 2\delta - \frac{\mu\hat{x}(\omega(\beta\mu+2)+2\hat{x})}{(\hat{x}+\omega)^3} \right) + \frac{\delta\mu\hat{x}\hat{y}^2}{(\hat{x}+\omega)^2} - 4 \right)}{\hat{x} \left( \frac{\beta\mu\hat{x}\omega\hat{y}F(\kappa-\hat{x})(\Lambda+\hat{x})}{\kappa(\hat{x}+\omega)^2(\hat{y}F+1)^2} + \frac{(1-\delta\hat{y})(\kappa\Lambda-\hat{x}(2\Lambda+\hat{x}))}{\kappa+\kappa\hat{y}F} + \frac{\kappa\Lambda-\hat{x}(2\Lambda+\hat{x})}{\kappa+\kappa\hat{y}F} \right)}. \quad (3.5.4)$$

For the above value of  $\gamma$ , the latent roots of (3.5.1) are  $\xi_1 = -1$  and  $\xi_2 \neq 1$ . Consider the following selection by setting  $\gamma$  to the aforementioned value:

$$F_{B1} = \{(\gamma, F, \kappa, \Lambda, \mu, \omega, \zeta, \beta, \theta, \delta) \in \mathbb{R}_+^{10} : (\Pi_{Tr})^2 > 4\Pi_{Det}, (\Pi_{Tr}) + \Pi_{Det} = -1, \text{ and } |\xi_2| \neq 1\}.$$

The flip bifurcation happens in the system (3.1.5) at  $(\hat{x}, \hat{y})$  when the parameters vary in the small neighborhood of set  $F_{B1}$ . Now consider the arbitrary parameters  $(\gamma = \gamma_1, F, \kappa, \Lambda, \mu, \omega, \zeta, \beta, \theta, \delta) \in F_{B1}$ , then the system (3.1.5) is given as:

$$\begin{cases} x_{n+1} \rightarrow x_n \exp \left[ \frac{\gamma_1}{1+F y_n} \left( 1 - \frac{x_n}{\kappa} \right) \frac{x_n}{x_n + \Lambda} - \frac{\mu y_n}{x + \omega} - \zeta \right], \\ y_{n+1} \rightarrow y_n \exp \left[ \frac{\mu \beta x_n}{x_n + \omega} - \theta - \delta y_n \right]. \end{cases} \quad (3.5.5)$$



Consider the perturbation of (3.5.5) as below:

$$\begin{cases} x_{n+1} \rightarrow x_n \exp \left[ \frac{\gamma_1 + \tilde{\gamma}}{1 + F y_n} \left( 1 - \frac{x_n}{\mathcal{K}} \right) \frac{x_n}{x_n + \Lambda} - \frac{\mu y_n}{x + \omega} - \zeta \right], \\ y_{n+1} \rightarrow y_n \exp \left[ \frac{\mu \beta x_n}{x_n + \omega} - \theta - \delta y_n \right]. \end{cases} \quad (3.5.6)$$

Let  $\Phi = x - \bar{x}$  and  $\Psi = y - \bar{y}$ . We can obtain the following system by transforming the origin of the positive fixed point of equation (3.5.6):

$$\begin{cases} \Phi \rightarrow \Theta_{11}\Phi + \Theta_{12}\Psi + \Theta_{13}\Phi^2 + \Theta_{14}\Phi\Psi + \Theta_{15}\Psi^2 + \Theta_{16}\Phi^3 + \Theta_{17}\Phi^2\Psi + \Theta_{18}\Phi\Psi^2 \\ + \Theta_{19}\Psi^3 + \Omega_{11}\tilde{\gamma}\Phi + \Omega_{12}\tilde{\gamma}\Psi + \Omega_{13}\tilde{\gamma}^2 + \Omega_{14}\Phi\Psi\tilde{\gamma} + \Omega_{15}\Phi^2\tilde{\gamma} + \Omega_{16}\Psi^2\tilde{\gamma} + \Omega_{17}\Phi\tilde{\gamma}^2 \\ + \Omega_{18}\Psi\tilde{\gamma}^2 + \Omega_{19}\tilde{\gamma}^3 + O(\Phi, \Psi, \tilde{\gamma})^4, \\ \Psi \rightarrow \Theta_{21}\Phi + \Theta_{22}\Psi + \Theta_{23}\Phi^2 + \Theta_{24}\Phi\Psi + \Theta_{25}\Psi^2 + \Theta_{26}\Phi^3 + \Theta_{27}\Phi^2\Psi + \Theta_{28}\Phi\Psi^2 \\ + \Theta_{29}\Psi^3 + O(\Phi, \Psi)^4, \end{cases} \quad (3.5.7)$$

where,

$$\begin{aligned} \Theta_{11} &= 1 + \left[ -\frac{\tilde{\gamma}\hat{x}}{(\mathcal{S})(F\hat{x}+1)\mathcal{K}} + \frac{\tilde{\gamma}}{(\mathcal{S})(F\hat{y}+1)} \right. \\ &\quad \left. - \left[ \frac{\tilde{\gamma}\hat{x}}{(\mathcal{Z})^2(F\hat{x}+1)} \right] [\mathcal{W}] + \frac{\mu\hat{y}}{(\Delta)^2} \right] \hat{x} [\mathcal{W}], \\ \Theta_{12} &= \hat{x} \left[ -\frac{\mu}{\Delta} - [\mathcal{W}] \frac{\tilde{\gamma}\hat{x}F}{(\mathcal{S})(F\hat{y}+1)^2} \right], \\ \Theta_{13} &= -\frac{\tilde{\gamma}x}{(\mathcal{S})(Fy+1)\mathcal{K}} + \frac{\tilde{\gamma}}{(\mathcal{S})(Fy+1)} [\mathcal{W}] - \frac{\tilde{\gamma}x}{(\mathcal{S})^2(Fy+1)} [\mathcal{W}] \\ &\quad + \frac{\mu\hat{y}}{(\Delta)^2} + \frac{1}{2}\hat{x} \left[ -2\frac{\tilde{\gamma}}{(F\hat{y}+1)\mathcal{K}(\mathcal{S})} + 2\frac{\tilde{\gamma}\hat{x}}{\mathcal{K}(F\hat{y}+1)(\mathcal{S})^2} \right. \\ &\quad \left. - 2[\mathcal{W}] \frac{\tilde{\gamma}}{(Fy+1)(\mathcal{S})^2} + 2[\mathcal{W}] \frac{\tilde{\gamma}\hat{x}}{(F\hat{y}+1)(\mathcal{S})^3} - 2\frac{\mu\hat{y}}{(\Delta)^3} \right] \\ &\quad + \frac{1}{2}\hat{x} \left[ -\frac{\tilde{\gamma}\hat{x}}{(\mathcal{S})(F\hat{y}+1)\mathcal{K}} + [\mathcal{W}] \frac{\tilde{\gamma}}{(F\hat{y}+1)(\mathcal{S})} - \frac{\tilde{\gamma}\hat{x}}{(F\hat{y}+1)(\mathcal{S})^2} \right. \\ &\quad \left. [\mathcal{W}] + \frac{\mu\hat{y}}{(\Delta)^2} \right]^2, \\ \Theta_{14} &= -\frac{\tilde{\gamma}\hat{x}F}{(\mathcal{S})(F\hat{y}+1)^2} [\mathcal{W}] - \frac{\mu}{\Delta} + \hat{x} \left[ \frac{\tilde{\gamma}\hat{x}F}{(F\hat{y}+1)^2\mathcal{K}(\mathcal{S})} \right. \\ &\quad \left. - [\mathcal{W}] \frac{\tilde{\gamma}F}{(\mathcal{S})(F\hat{y}+1)^2} + [\mathcal{W}] \frac{\tilde{\gamma}\hat{x}F}{(\mathcal{S})^2(F\hat{y}+1)^2} + \frac{\mu}{(\Delta)^2} \right] \end{aligned}$$

$$\begin{aligned}
& + \hat{x} \left[ -\frac{\tilde{\gamma} \hat{x}}{(1+F\hat{y})\mathcal{K}(\mathcal{S})} + \frac{\tilde{\gamma}}{(1+F\hat{y})(\mathcal{S})} [\mathcal{W}] - \frac{\tilde{\gamma} \hat{x}}{(1+F\hat{y})(\mathcal{S})^2} \right. \\
& \quad \left. [\mathcal{W}] + \frac{\mu \hat{y}}{(\Delta)^2} \right] \left[ -\frac{\tilde{\gamma} \hat{x} F}{(F\hat{y}+1)^2(\mathcal{S})} [\mathcal{W}] - \frac{\mu}{\Delta} \right], \\
\Theta_{15} &= [\mathcal{W}] \frac{\hat{x}^2 \tilde{\gamma} F^2}{(1+F\hat{y})^3(\mathcal{S})} + \frac{1}{2} \hat{x} \left[ -\frac{\tilde{\gamma} \hat{x} F}{(F\hat{y}+1)^2(\mathcal{S})} [\mathcal{W}] - \frac{\mu}{\Delta} \right]^2, \\
\Theta_{16} &= [\mathcal{W}] \frac{\hat{x}^2 \tilde{\gamma} F^2}{(F\hat{y}+1)^3(\mathcal{S})} + \frac{1}{2} \hat{x} \left[ -[\mathcal{W}] \frac{\tilde{\gamma} \hat{x} F}{(1+F\hat{y})^2(\mathcal{S})} - \frac{\mu}{\Delta} \right]^2, \\
\Theta_{17} &= [\mathcal{W}] \frac{\hat{x}^2 \tilde{\gamma} F^2}{(F\hat{y}+1)^3(\mathcal{S})} + \frac{1}{2} \hat{x} \left[ -[\mathcal{W}] \frac{\tilde{\gamma} \hat{x} F}{(F\hat{y}+1)^2(\mathcal{S})} - \frac{\mu}{\Delta} \right]^2 \\
& \quad \left[ \frac{\tilde{\gamma} \hat{x} F}{(F\hat{y}+1)^2 \mathcal{K}(\mathcal{S})} - [\mathcal{W}] \frac{\tilde{\gamma} F}{(F\hat{y}+1)^2(\mathcal{S})} + \frac{\tilde{\gamma} \hat{x} F}{(F\hat{y}+1)^2(\mathcal{S})^2} \right. \\
& \quad \left. [\mathcal{W}] + \frac{\mu}{(\Delta)^2} \right] + \left[ -\frac{\tilde{\gamma} \hat{x}}{\mathcal{K}(\mathcal{S})(1+F\hat{y})} + [\mathcal{W}] \frac{\tilde{\gamma}}{(\mathcal{S})(1+F\hat{y})} \right. \\
& \quad \left. - [\mathcal{W}] \frac{\tilde{\gamma} \hat{x}}{(F\hat{y}+1)(\mathcal{S})^2} + \frac{\mu \hat{y}}{(\Delta)^2} \right] \left[ -\frac{\tilde{\gamma} \hat{x} F}{(F\hat{y}+1)^2(\mathcal{S})} [\mathcal{W}] - \frac{\mu}{\Delta} \right] \\
& \quad + \frac{1}{2} \hat{x} \left[ 2 \frac{\tilde{\gamma} F}{(F\hat{y}+1)^2 \mathcal{K}(\mathcal{S})} - 2 \frac{\tilde{\gamma} \hat{x} F}{(F\hat{y}+1)^2 \mathcal{K}(\mathcal{S})^2} + 2 \frac{\tilde{\gamma} F}{(F\hat{y}+1)^2(\mathcal{S})^2} \right. \\
& \quad \left. [\mathcal{W}] - 2 [\mathcal{W}] \frac{\tilde{\gamma} \hat{x} F}{(F\hat{y}+1)^2(\mathcal{S})^3} - 2 \frac{\mu}{(\Delta)^3} \right] \\
& \quad + \frac{1}{2} \hat{x} \left[ -2 \frac{\tilde{\gamma}}{\mathcal{K}(F\hat{y}+1)(\mathcal{S})} + 2 \frac{\tilde{\gamma} \hat{x}}{(F\hat{y}+1) \mathcal{K}(\mathcal{S})^2} - 2 \frac{\tilde{\gamma}}{(F\hat{y}+1)(\mathcal{S})^2} [\mathcal{W}] \right. \\
& \quad \left. + 2 [\mathcal{W}] \frac{\tilde{\gamma} \hat{x}}{(F\hat{y}+1)(\mathcal{S})^3} - 2 \frac{\mu \hat{y}}{(\Delta)^3} \right] \left[ -[\mathcal{W}] \frac{\tilde{\gamma} \hat{x} F}{(F\hat{y}+1)^2(\mathcal{S})} - \frac{\mu}{\Delta} \right] \\
& \quad + \hat{x} \left[ -\frac{\tilde{\gamma} \hat{x}}{\mathcal{K}(F\hat{y}+1)(\mathcal{S})} + [\mathcal{W}] \frac{\tilde{\gamma}}{(F\hat{y}+1)(\mathcal{S})} - [\mathcal{W}] \frac{\tilde{\gamma} \hat{x}}{(F\hat{y}+1)(\mathcal{S})^2} \right. \\
& \quad \left. + \frac{\mu \hat{y}}{(\Delta)^2} \right] \left[ \frac{\tilde{\gamma} \hat{x} F}{(F\hat{y}+1)^2 \mathcal{K}(\mathcal{S})} - [\mathcal{W}] \frac{\tilde{\gamma} F}{(F\hat{y}+1)^2(\mathcal{S})} + \frac{\tilde{\gamma} \hat{x} F}{(F\hat{y}+1)^2(\mathcal{S})^2} \right. \\
& \quad \left. [\mathcal{W}] + \frac{\mu}{(\Delta)^2} \right] + \frac{1}{2} \hat{x} \left[ -\frac{\tilde{\gamma} \hat{x}}{\mathcal{K}(F\hat{y}+1)(\mathcal{S})} + [\mathcal{W}] \frac{\tilde{\gamma}}{(F\hat{y}+1)(\mathcal{S})} \right. \\
& \quad \left. - [\mathcal{W}] \frac{\tilde{\gamma} \hat{x}}{(F\hat{y}+1)(\mathcal{S})^2} + \frac{\mu \hat{y}}{(\Delta)^2} \right]^2 \left[ -[\mathcal{W}] \frac{\tilde{\gamma} \hat{x} F}{(F\hat{y}+1)^2(\mathcal{S})} - \frac{\mu}{\Delta} \right], \\
\Theta_{18} &= [\mathcal{W}] \frac{\tilde{\gamma} \hat{x} F^2}{(F\hat{y}+1)^3(\mathcal{S})} + \frac{1}{2} \left[ -[\mathcal{W}] \frac{\tilde{\gamma} \hat{x} F}{(F\hat{y}+1)^2(\mathcal{Z})} - \frac{\mu}{\Delta} \right]^2 \\
& \quad + \frac{1}{2} \hat{x} \left[ -2 \frac{\tilde{\gamma} \hat{x} F^2}{(F\hat{y}+1)^3 \mathcal{K}(\mathcal{S})} + 2 [\mathcal{W}] \frac{\tilde{\gamma} F^2}{(F\hat{y}+1)^3(\mathcal{S})} \right. \\
& \quad \left. - 2 [\mathcal{W}] \frac{\tilde{\gamma} \hat{x} F^2}{(F\hat{y}+1)^3(\mathcal{S})^2} \right] + \hat{x} \left[ \frac{\tilde{\gamma} \hat{x} F}{(F\hat{y}+1)^2 \mathcal{K}(\mathcal{S})} - \frac{\tilde{\gamma} F}{(F\hat{y}+1)^2(\mathcal{S})} \right.
\end{aligned}$$

$$\begin{aligned}
& [\mathcal{W}] + [\mathcal{W}] \frac{\tilde{\gamma} \hat{x} F}{(F \hat{y} + 1)^2 (\mathcal{S})^2} + \frac{\mu}{(\Delta)^2} \Big[ - \frac{\tilde{\gamma} \hat{x} F}{(F \hat{y} + 1)^2 (\mathcal{S})} \\
& [\mathcal{W}] - \frac{\mu}{\Delta} \Big] + \frac{\hat{x}^2 \tilde{\gamma} F^2}{(F \hat{y} + 1)^3 (\mathcal{S})} \Big[ - \frac{\tilde{\gamma} \hat{x}}{\mathcal{K} (F \hat{y} + 1) (\mathcal{S})} \\
& + \frac{\tilde{\gamma}}{(F \hat{y} + 1) (\mathcal{S})} [\mathcal{W}] - [\mathcal{W}] \frac{\tilde{\gamma} \hat{x}}{(F \hat{y} + 1) (\mathcal{S})^2} + \frac{\mu \hat{y}}{(\Delta)^2} \Big] [\mathcal{W}] \\
& + \frac{1}{2} \hat{x} \Big[ - \frac{\tilde{\gamma} \hat{x}}{\mathcal{K} (\mathcal{S}) (1 + F \hat{y})} + \frac{\tilde{\gamma}}{(\mathcal{S}) (1 + F \hat{y})} [\mathcal{W}] \\
& [\mathcal{W}] - \frac{\tilde{\gamma} \hat{x}}{(1 + F \hat{y}) (\mathcal{S})^2} + \frac{\mu \hat{y}}{(\Delta)^2} \Big] \Big[ - \frac{\tilde{\gamma} \hat{x} F}{(F \hat{y} + 1)^2 (\mathcal{S})} \\
& [\mathcal{W}] - \frac{\mu}{\Delta} \Big]^2, \\
\Theta_{19} &= - [\mathcal{W}] \frac{\hat{x}^2 \tilde{\gamma} F^3}{(F \hat{y} + 1)^4 (\mathcal{S})} + [\mathcal{W}] \frac{\hat{x}^2 \tilde{\gamma} F^2}{(F \hat{y} + 1)^3 (\mathcal{S})} \\
& \Big[ - [\mathcal{W}] \frac{\tilde{\gamma} \hat{x} F}{(F \hat{y} + 1)^2 (\mathcal{S})} - \frac{\mu}{\Delta} \Big] + \frac{1}{6} \hat{x} \Big[ - [\mathcal{W}] \frac{\tilde{\gamma} \hat{x} F}{(F \hat{y} + 1)^2 (\mathcal{S})} \\
& - \frac{\mu}{\Delta} \Big]^3, \\
\Omega_{11} &= - [\mathcal{W}] \frac{\hat{x}^2 \tilde{\gamma} F^3}{(F \hat{y} + 1)^4 (\mathcal{S})} + [\mathcal{W}] \frac{\hat{x}^2 \tilde{\gamma} F^2}{(F \hat{y} + 1)^3 (\mathcal{S})} \Big[ - \frac{\tilde{\gamma} \hat{x} F}{(F \hat{y} + 1)^2 (\mathcal{S})} \\
& [\mathcal{W}] - \frac{\mu}{\Delta} \Big] + \frac{1}{6} \frac{\hat{x}^2}{(1 + F \hat{y}) (\mathcal{S})} \Big[ - [\mathcal{W}] \frac{\tilde{\gamma} \hat{x} F}{(1 + F \hat{y})^2 (\mathcal{S})} - \frac{\mu}{\Delta} \Big]^3 \\
& [\mathcal{W}] + \hat{x} \Big[ - \frac{\hat{x}}{\mathcal{K} (\mathcal{S}) (1 + F \hat{y})} + \frac{1}{(\mathcal{S}) (1 + F \hat{y})} [\mathcal{W}] - \frac{\hat{x}}{(1 + F \hat{y}) (\mathcal{S})^2} \\
& [\mathcal{W}] \Big] + \frac{\hat{x}^2}{(1 + F \hat{y}) (\mathcal{S})} \Big[ - \frac{\tilde{\gamma} \hat{x}}{\mathcal{K} (1 + F \hat{y}) (\mathcal{S})} + [\mathcal{W}] \frac{\tilde{\gamma}}{(1 + F \hat{y}) (\mathcal{S})} \\
& - [\mathcal{W}] \frac{\tilde{\gamma} \hat{x}}{(1 + F \hat{y}) (\mathcal{S})^2} + \frac{\mu \hat{y}}{(\Delta)^2} \Big] [\mathcal{W}], \\
\Omega_{12} &= - [\mathcal{W}] \frac{\hat{x}^2 F}{(1 + F \hat{y})^2 (\mathcal{S})} + \frac{\hat{x}^2}{(1 + F \hat{y}) (\mathcal{S})} \Big[ - \frac{\tilde{\gamma} \hat{x} F}{(1 + F \hat{y})^2 (\mathcal{S})} \\
& [\mathcal{W}] - \frac{\mu}{\Delta} \Big] [\mathcal{W}], \\
\Omega_{13} &= \frac{1}{2} [\mathcal{W}]^2 \frac{\hat{x}^3}{(1 + F \hat{y})^2 (\mathcal{S})^2}, \\
\Omega_{14} &= [\mathcal{W}] \frac{\hat{x} F}{(F \hat{y} + 1)^2 (\mathcal{K})} + \frac{\hat{x}}{(F \hat{y} + 1) (\mathcal{K})} \Big[ - [\mathcal{W}] \frac{\tilde{\gamma} \hat{x} F}{(F \hat{y} + 1)^2 (\mathcal{K})} \\
& - \frac{\mu}{\Delta} \Big] [\mathcal{W}] + \hat{x} \Big[ \frac{\hat{x} F}{(F \hat{y} + 1)^2 \mathcal{K} (\mathcal{S})} - [\mathcal{W}] \frac{F}{(F \hat{y} + 1)^2 (\mathcal{S})} \\
& + [\mathcal{W}] \frac{\hat{x} F}{(F \hat{y} + 1)^2 (\mathcal{S})^2} \Big] + \frac{\hat{x}^2}{(F \hat{y} + 1) (\mathcal{S})} \Big[ \frac{\tilde{\gamma} \hat{x} F}{(F \hat{y} + 1)^2 \mathcal{K} (\mathcal{S})}
\end{aligned}$$

$$\begin{aligned}
& - [\mathcal{W}] \frac{\tilde{\gamma} F}{(F \hat{y} + 1)^2 (\mathcal{S})} + [\mathcal{W}] \frac{\tilde{\gamma} \hat{x} F}{(F \hat{y} + 1)^2 (\mathcal{S})^2} + \frac{\mu}{(\Delta)^2} \Big] [\mathcal{W}] \\
& + \hat{x} \Big[ - \frac{\hat{x}}{\mathcal{K} (\mathcal{S}) (1 + F \hat{y})} + \frac{1}{(\mathcal{S}) (1 + F \hat{y})} [\mathcal{W}] - \frac{\hat{x}}{(1 + F \hat{y}) (\mathcal{S})^2} \\
& [\mathcal{W}] \Big[ - [\mathcal{W}] \frac{\tilde{\gamma} \hat{x} F}{(1 + F \hat{y})^2 (\mathcal{S})} - \frac{\mu}{\Delta} \Big] - \frac{\hat{x}^2 F}{(\mathcal{S}) (1 + F \hat{y})^2} \\
& \Big[ - \frac{\tilde{\gamma} \hat{x}}{\mathcal{K} (1 + F \hat{y}) (\mathcal{K})} + \frac{\tilde{\gamma}}{(1 + F \hat{y}) (\mathcal{K})} [\mathcal{W}] - [\mathcal{W}] \frac{\tilde{\gamma} \hat{x}}{(1 + F \hat{y}) (\mathcal{K})^2} \\
& + \frac{\mu \hat{y}}{(\Delta)^2} \Big] [\mathcal{W}] + \frac{\hat{x}^2}{(1 + F \hat{y}) (\mathcal{K})} \Big[ - \frac{\tilde{\gamma} \hat{x}}{\mathcal{K} (1 + F \hat{y}) (\mathcal{K})} + \frac{\tilde{\gamma}}{(1 + F \hat{y}) (\mathcal{K})} \\
& [\mathcal{W}] - [\mathcal{W}] \frac{\tilde{\gamma} \hat{x}}{(1 + F \hat{y}) (\mathcal{K})^2} + \frac{\mu \hat{y}}{(\Delta)^2} \Big] \Big[ - \frac{\tilde{\gamma} \hat{x} F}{(1 + F \hat{y})^2 (\mathcal{K})} \\
& [\mathcal{W}] - \frac{\mu}{\Delta} \Big] [\mathcal{W}], \\
\Omega_{15} & = - \frac{\hat{x}}{\mathcal{K} (F \hat{y} + 1) (\mathcal{K})} + [\mathcal{W}] \frac{1}{(F \hat{y} + 1) (\mathcal{K})} - [\mathcal{W}] \frac{\hat{x}}{(F \hat{y} + 1) (\mathcal{K})^2} \\
& + \frac{\hat{x}}{(F \hat{y} + 1) (\mathcal{K})} \Big[ - \frac{\tilde{\gamma} \hat{x}}{\mathcal{K} (F \hat{y} + 1) (\mathcal{K})} + [\mathcal{W}] \frac{\tilde{\gamma}}{(F \hat{y} + 1) (\mathcal{K})} \\
& - [\mathcal{W}] \frac{\tilde{\gamma} \hat{x}}{(F \hat{y} + 1) (\mathcal{K})^2} + \frac{\mu \hat{y}}{(\Delta)^2} \Big] [\mathcal{W}] + \frac{1}{2} \hat{x} \Big[ - 2 \frac{1}{\mathcal{K} (F \hat{y} + 1) (\mathcal{K})} \\
& + 2 \frac{\hat{x}}{(F \hat{y} + 1) \mathcal{K} (\mathcal{K})^2} - 2 [\mathcal{W}] \frac{1}{(F \hat{y} + 1) (\mathcal{K})^2} + 2 \frac{\hat{x}}{(F \hat{y} + 1) (\mathcal{K})^3} \\
& [\mathcal{W}] \Big] + \frac{1}{2} \frac{\hat{x}^2}{(F \hat{y} + 1) (\mathcal{K})} \Big[ - 2 \frac{\tilde{\gamma}}{\mathcal{K} (F \hat{y} + 1) (\mathcal{K})} + 2 \frac{\tilde{\gamma} \hat{x}}{(F \hat{y} + 1) \mathcal{K} (\mathcal{K})^2} \\
& - 2 \frac{\tilde{\gamma}}{(F \hat{y} + 1) (\mathcal{K})^2} [\mathcal{W}] + 2 [\mathcal{W}] \frac{\tilde{\gamma} \hat{x}}{(F \hat{y} + 1) (\mathcal{K})^3} - 2 \frac{\mu \hat{y}}{(\Delta)^3} \Big] [\mathcal{W}] \\
& + \hat{x} \Big[ - \frac{\tilde{\gamma} \hat{x}}{\mathcal{K} (1 + F \hat{y}) (\mathcal{K})} + \frac{\tilde{\gamma}}{(1 + F \hat{y}) (\mathcal{K})} [\mathcal{W}] - \frac{\tilde{\gamma} \hat{x}}{(1 + F \hat{y}) (\mathcal{K})^2} [\mathcal{W}] \\
& + \frac{\mu \hat{y}}{(\Delta)^2} \Big] \Big[ - \frac{\hat{x}}{\mathcal{K} (F \hat{y} + 1) (\mathcal{K})} + \frac{1}{(F \hat{y} + 1) (\mathcal{K})} [\mathcal{W}] - \frac{\hat{x}}{(F \hat{y} + 1) (\mathcal{K})^2} \\
& [\mathcal{W}] \Big] + \frac{1}{2} \frac{\hat{x}^2}{(F \hat{y} + 1) (\mathcal{K})} \Big[ - \frac{\tilde{\gamma} \hat{x}}{\mathcal{K} (F \hat{y} + 1) (\mathcal{K})} + \frac{\tilde{\gamma}}{(F \hat{y} + 1) (\mathcal{K})} \\
& [\mathcal{W}] - \frac{\tilde{\gamma} \hat{x}}{(F \hat{y} + 1) (\mathcal{K})^2} [\mathcal{W}] + \frac{\mu \hat{y}}{(\Delta)^2} \Big]^2 [\mathcal{W}], \\
\Omega_{16} & = [\mathcal{W}] \frac{\hat{x}^2 F^2}{(F \hat{y} + 1)^3 (\mathcal{K})} + \frac{\tilde{\gamma} \hat{x}^3 F^2}{(F \hat{y} + 1)^4 (\mathcal{K})^2} [\mathcal{W}]^2 - \frac{\hat{x}^2 F}{(F \hat{y} + 1)^2 (\mathcal{K})} \\
& \Big[ - \frac{\tilde{\gamma} \hat{x} F}{(1 + F \hat{y})^2 (\mathcal{K})} [\mathcal{W}] - \frac{\mu}{\Delta} \Big] [\mathcal{W}] + \frac{1}{2} \frac{\hat{x}^2}{(1 + F \hat{y}) (\mathcal{K})} \\
& \Big[ - \frac{\tilde{\gamma} \hat{x} F}{(F \hat{y} + 1)^2 (\mathcal{K})} [\mathcal{W}] - \frac{\mu}{\Delta} \Big]^2 [\mathcal{W}],
\end{aligned}$$

$$\begin{aligned}
\Omega_{17} &= \frac{1}{2} \frac{\hat{x}^2}{(F\hat{y}+1)^2(\mathcal{K})^2} [\mathcal{W}]^2 + \frac{\hat{x}^2}{(F\hat{y}+1)(\mathcal{K})} \left[ -\frac{\hat{x}}{\mathcal{K}(F\hat{y}+1)(\mathcal{K})} \right. \\
&\quad \left. + [\mathcal{W}] \frac{1}{(F\hat{y}+1)(\mathcal{K})} - \frac{\hat{x}}{(F\hat{y}+1)(\mathcal{K})^2} [\mathcal{W}] \right] [\mathcal{W}] \\
&\quad + \frac{1}{2} \frac{\hat{x}^3}{(F\hat{y}+1)^2(\mathcal{K})^2} \left[ -\frac{\tilde{\gamma}\hat{x}}{\mathcal{K}(F\hat{y}+1)(\mathcal{K})} + \frac{\tilde{\gamma}}{(F\hat{y}+1)(\mathcal{K})} [\mathcal{W}] \right. \\
&\quad \left. - \frac{\tilde{\gamma}\hat{x}}{(F\hat{y}+1)(\mathcal{K})^2} [\mathcal{W}] + \frac{\mu\hat{y}}{(\Delta)^2} \right] [\mathcal{W}]^2, \\
\Omega_{18} &= -\frac{\hat{x}^3 F}{(1+F\hat{y})^3(\mathcal{K})^2} [\mathcal{W}]^2 + \frac{1}{2} \frac{\hat{x}^3}{(1+F\hat{y})^2(\mathcal{K})^2} \left[ -\frac{\tilde{\gamma}\hat{x}F}{(1+F\hat{y})^2(\mathcal{K})} \right. \\
&\quad \left. [\mathcal{W}] - \frac{\mu}{\Delta} \right] [\mathcal{W}]^2, \\
\Omega_{19} &= \frac{1}{6} \frac{x^4}{(Fy+1)^3(\Delta)^3} [\mathcal{W}]^3, \\
\Theta_{21} &= y \left[ \frac{\mu\beta(\Delta) - \mu\beta\hat{x}}{(\Delta)^2} \right], \Theta_{22} = -\delta\hat{y} + 1 \\
\Theta_{23} &= \frac{1}{2} \hat{y} \left[ -2 \left( \frac{\mu\beta(\Delta) - \mu\beta\hat{x}}{(\Delta)^3} \right) \right] + \frac{1}{2} \hat{y} \left[ \frac{\mu\beta(\Delta) - \mu\beta\hat{x}}{(\Delta)^2} \right]^2, \\
\Theta_{24} &= \frac{1}{2} \hat{y} \left[ -2 \left( \frac{\mu\beta(\Delta) - \mu\beta\hat{x}}{(\Delta)^3} \right) \right] + \frac{1}{2} \hat{y} \left[ \frac{\mu\beta(\Delta) - \mu\beta\hat{x}}{(\Delta)^2} \right]^3 \\
&\quad - \hat{y} \left[ \frac{\mu\beta(\Delta) - \mu\beta\hat{x}}{(\Delta)^2} \right] \delta, \Theta_{25} = -\delta + \frac{1}{2} \hat{y} \delta^2, \\
\Theta_{26} &= \frac{1}{6} \hat{y} \left[ 6 \left( \frac{\mu\beta(\Delta) - \mu\beta\hat{x}}{(\Delta)^4} \right) \right] + \frac{1}{2} y \left[ -2 \left( \frac{\mu\beta(\Delta) - \mu\beta\hat{x}}{(\Delta)^3} \right) \right] \\
&\quad \left[ \frac{\mu\beta(\Delta) - \mu\beta\hat{x}}{(\Delta)^2} \right] + \frac{1}{6} \hat{y} \left[ \frac{\mu\beta(\Delta) - \mu\beta\hat{x}}{(\Delta)^2} \right]^3, \\
\Theta_{27} &= -\left[ \frac{\mu\beta(\Delta) - \mu\beta\hat{x}}{(\Delta)^3} \right] - \frac{1}{2} \hat{y} \left[ -2 \left( \frac{\mu\beta(\Delta) - \mu\beta\hat{x}}{(\Delta)^2} \right) \right] \delta \\
&\quad + \frac{1}{2} \left[ \frac{\mu\beta(\Delta) - \mu\beta\hat{x}}{(\Delta)^2} \right]^2 - \frac{1}{2} \hat{y} \left[ \frac{\mu\beta(\Delta) - \mu\beta\hat{x}}{(\Delta)^2} \right]^2, \\
\Theta_{28} &= -\left[ \frac{\mu\beta(\Delta) - \mu\beta\hat{x}}{(\Delta)^2} \right] \delta + \frac{1}{2} \hat{y} \left[ \frac{\mu\beta(\Delta) - \mu\beta\hat{x}}{(\Delta)^2} \right] \delta^2, \text{ and} \\
\Theta_{29} &= \frac{1}{2} \delta^2 - \frac{1}{6} y \delta^3, \text{ with } \mathcal{W} = \left[ \frac{-\hat{x} + \mathcal{K}}{\mathcal{K}} \right], \hat{x} + \omega = \Delta, \text{ and } \mathcal{S} = \hat{x} + \Lambda.
\end{aligned}$$

If  $\mathcal{S} = \begin{pmatrix} \Theta_{12} & \Theta_{12} \\ -1 - \Theta_{11} & \xi_2 - \Theta_{11} \end{pmatrix}$  be a non-singular matrix, then consider the following translation:

$$\begin{pmatrix} \Phi \\ \Psi \end{pmatrix} = \mathcal{S} \begin{pmatrix} \tilde{x} \\ \tilde{y} \end{pmatrix}. \quad (3.5.8)$$

Taking  $\mathcal{S}^{-1}$  on both sides of (3.5.8) we get

$$\begin{pmatrix} \tilde{x} \\ \tilde{y} \end{pmatrix} \rightarrow \begin{pmatrix} -1 & 0 \\ 0 & \xi_2 \end{pmatrix} \begin{pmatrix} \tilde{x} \\ \tilde{y} \end{pmatrix} + \begin{pmatrix} f(\Phi, \Psi, \tilde{\gamma}) \\ g(\Phi, \Psi, \tilde{\gamma}) \end{pmatrix}, \quad (3.5.9)$$

$$\begin{aligned} f(\Phi, \Psi, \tilde{\gamma}) &= -\frac{(-\xi_2 + \Theta_{11})\Omega_{19}\tilde{\gamma}^3}{\Theta_{12}(\mathcal{T})} - \frac{(-\xi_2 + \Theta_{11})\Omega_{17}\tilde{\gamma}^2\Phi}{\Theta_{12}(\mathcal{T})} - \frac{(-\xi_2 + \Theta_{11})\Omega_{18}\tilde{\gamma}^2\Psi}{\Theta_{12}(\mathcal{T})} \\ &- \frac{(-\xi_2 + \Theta_{11})\Omega_{13}\tilde{\gamma}^2}{\Theta_{12}(\mathcal{T})} - \frac{(-\xi_2 + \Theta_{11})\Omega_{15}\tilde{\gamma}\Phi^2}{\Theta_{12}(\mathcal{T})} - \frac{(-\xi_2 + \Theta_{11})\Omega_{14}\tilde{\gamma}\Phi\Psi}{\Theta_{12}(\mathcal{T})} \\ &- \frac{(-\xi_2 + \Theta_{11})\Omega_{11}\Phi\tilde{\gamma}}{\Theta_{12}(\mathcal{T})} - \frac{(-\xi_2 + \Theta_{11})\Omega_{16}\tilde{\gamma}\Psi^2}{\Theta_{12}(\mathcal{T})} - \frac{(-\xi_2 + \Theta_{11})\Omega_{12}\Psi\tilde{\gamma}}{\Theta_{12}(\mathcal{T})} \\ &+ \left( -\frac{(-\xi_2 + \Theta_{11})\Theta_{16}}{\Theta_{12}(\mathcal{T})} - \frac{\Theta_{26}}{\mathcal{T}} \right) \Phi^3 + \left( -\frac{(-\xi_2 + \Theta_{11})\Theta_{17}}{\Theta_{12}(\mathcal{T})} - \frac{\Theta_{27}}{\mathcal{T}} \right) \Psi\Phi^2 \\ &+ \left( -\frac{(-\xi_2 + \Theta_{11})\Theta_{13}}{\Theta_{12}(\mathcal{T})} - \frac{\Theta_{23}}{\mathcal{T}} \right) \Phi^2 + \left( -\frac{(-\xi_2 + \Theta_{11})\Theta_{18}}{\Theta_{12}(\mathcal{T})} - \frac{\Theta_{28}}{\mathcal{T}} \right) \Psi^2\Phi \\ &+ \left( -\frac{(-\xi_2 + \Theta_{11})\Theta_{14}}{\Theta_{12}(\mathcal{T})} - \frac{\Theta_{24}}{\mathcal{T}} \right) \Psi\Phi + \left( -\frac{(-\xi_2 + \Theta_{11})\Theta_{19}}{\Theta_{12}(\mathcal{T})} - \frac{\Theta_{29}}{\mathcal{T}} \right) \Psi^3 \\ &+ \left( -\frac{(-\xi_2 + \Theta_{11})\Theta_{15}}{\Theta_{12}(\mathcal{T})} - \frac{\Theta_{25}}{\mathcal{T}} \right) \Psi^2, \\ g(\Phi, \Psi, \tilde{\gamma}) &= \frac{(1 + \Theta_{11})\Omega_{19}\tilde{\gamma}^3}{\Theta_{12}(\mathcal{T})} + \frac{(1 + \Theta_{11})\Omega_{17}\tilde{\gamma}^2\Phi}{\Theta_{12}(\mathcal{T})} + \frac{(1 + \Theta_{11})\Omega_{18}\tilde{\gamma}^2\Psi}{\Theta_{12}(\mathcal{T})} \\ &+ \frac{(1 + \Theta_{11})\Omega_{13}\tilde{\gamma}^2}{\Theta_{12}(\mathcal{T})} + \frac{(1 + \Theta_{11})\Omega_{15}\tilde{\gamma}\Phi^2}{\Theta_{12}(\mathcal{T})} + \frac{(1 + \Theta_{11})\Omega_{14}\tilde{\gamma}\Phi\Psi}{\Theta_{12}(\mathcal{T})} \\ &+ \frac{(1 + \Theta_{11})\Omega_{11}\Phi\tilde{\gamma}}{\Theta_{12}(\mathcal{T})} + \frac{(1 + \Theta_{11})\Omega_{16}\tilde{\gamma}\Psi^2}{\Theta_{12}(\mathcal{T})} + \frac{(1 + \Theta_{11})\Omega_{12}\Psi\tilde{\gamma}}{\Theta_{12}(\mathcal{T})} + \left( \frac{(1 + \Theta_{11})\Theta_{16}}{\Theta_{12}(\mathcal{T})} \right. \\ &+ \left. \frac{\Theta_{26}}{\mathcal{T}} \right) \Phi^3 + \left( \frac{(1 + \Theta_{11})\Theta_{17}}{\Theta_{12}(\mathcal{T})} + \frac{\Theta_{27}}{\mathcal{T}} \right) \Psi\Phi^2 + \left( \frac{(1 + \Theta_{11})\Theta_{13}}{\Theta_{12}(\mathcal{T})} + \frac{\Theta_{23}}{\mathcal{T}} \right) \Phi^2 \\ &+ \left( \frac{(1 + \Theta_{11})\Theta_{18}}{\Theta_{12}(\mathcal{T})} + \frac{\Theta_{28}}{\mathcal{T}} \right) \Psi^2\Phi + \left( \frac{(1 + \Theta_{11})\Theta_{14}}{\Theta_{12}(\mathcal{T})} + \frac{\Theta_{24}}{\mathcal{T}} \right) \Psi\Phi \\ &+ \left( \frac{(1 + \Theta_{11})\Theta_{19}}{\Theta_{12}(\mathcal{T})} + \frac{\Theta_{29}}{\mathcal{T}} \right) \Psi^3 + \left( \frac{(1 + \Theta_{11})\Theta_{15}}{\Theta_{12}(\mathcal{T})} + \frac{\Theta_{25}}{\mathcal{T}} \right) \Psi^2, \text{ where } \mathcal{T} = \xi_2 + 1. \end{aligned}$$

If we consider  $W^c(0,0,0)$  to be the center manifold of (3.5.9) computed at  $(0,0)$  in a restricted neighborhood of  $\tilde{\gamma} = 0$ , we can approximate  $W^c(0,0,0)$  as follows:

$$W^c(0,0,0) = \{(\tilde{x}, \tilde{y}, \tilde{\gamma}) \in R^3 : \tilde{y} = \varrho_1\tilde{x}^2 + \varrho_2\tilde{x}\tilde{\gamma} + \varrho_3\tilde{\gamma}^2 + O((|\tilde{x}| + |\tilde{\gamma}|)^3)\},$$

where,

$$\begin{aligned}\varrho_1 &= -\frac{\Theta_{15}(\Theta_{11}+1)^3 - \Theta_{12}(\Theta_{14} - \Theta_{25})(\Theta_{11}+1)^2 + \Theta_{12}^2(\Theta_{13} - \Theta_{24})(\Theta_{11}+1) + \Theta_{12}^3\Theta_{23}}{\Theta_{12}(\xi_2^2 - 1)}, \\ \varrho_2 &= -\frac{(1 + \Theta_{11})(\Omega_{11}\Theta_{12} - \Omega_{12}\Theta_{11} - \Omega_{12})}{\Theta_{12}(\xi_2^2 - 1)} \\ \varrho_3 &= \frac{(1 + \Theta_{11})\Omega_{13}}{\Theta_{12}(\xi_2 + 1)(-\xi_2 + 1)}.\end{aligned}$$

Consequently, the map that is only applicable to the center manifold  $W^c(0, 0, 0)$  is provided by:

$$F : \tilde{x} \rightarrow -\tilde{x} + \chi_1\tilde{x}^2 + \chi_2\tilde{x}\tilde{\gamma} + \chi_3\tilde{x}^2\tilde{\gamma} + \chi_4\tilde{x}\tilde{\gamma}^2 + \chi_5\tilde{x}^3 + O((|\tilde{x}|, |\tilde{\gamma}|)^4),$$

where,

$$\begin{aligned}\chi_1 &= \left[ -\frac{(-\xi_2 + \Theta_{11})\Theta_{13}}{\Theta_{12}(\mathcal{T})} - \frac{\Theta_{23}}{\mathcal{T}} \right] \Theta_{12}^2 + \left[ -\frac{(-\xi_2 + \Theta_{11})\Theta_{14}}{\Theta_{12}(\mathcal{T})} - \frac{\Theta_{24}}{\mathcal{T}} \right] \times \\ &\quad (-1 - \Theta_{11})\Theta_{12} + \left[ -\frac{(-\xi_2 + \Theta_{11})\Theta_{15}}{\Theta_{12}(\mathcal{T})} - \frac{\Theta_{25}}{\mathcal{T}} \right] (-1 - \Theta_{11})^2, \\ \chi_2 &= -\frac{(-\xi_2 + \Theta_{11})\Omega_{11}}{\mathcal{T}} - \frac{(-\xi_2 + \Theta_{11})\Omega_{12}(-1 - \Theta_{11})}{\Theta_{12}(\mathcal{T})}, \\ \chi_3 &= -\frac{(-\xi_2 + \Theta_{11})\Theta_{12}\Omega_{15}}{\mathcal{T}} - \frac{(-\xi_2 + \Theta_{11})\Omega_{14}(-1 - \Theta_{11})}{\mathcal{T}} - \frac{(-\xi_2 + \Theta_{11})\Omega_{11}\varrho_1}{\mathcal{T}} \\ &\quad - \frac{(-\xi_2 + \Theta_{11})\Omega_{16}(-1 - \Theta_{11})^2}{\Theta_{12}(\mathcal{T})} - \frac{(-\xi_2 + \Theta_{11})\Omega_{12}(\xi_2 - \Theta_{11})\varrho_1}{\Theta_{12}(\mathcal{T})} \\ &\quad + 2 \left( -\frac{(-\xi_2 + \Theta_{11})\Theta_{13}}{\Theta_{12}(\mathcal{T})} - \frac{\Theta_{23}}{\mathcal{T}} \right) \Theta_{12}^2\varrho_2 + \left( -\frac{(-\xi_2 + \Theta_{11})\Theta_{14}}{\Theta_{12}(\mathcal{T})} - \frac{\Theta_{24}}{\mathcal{T}} \right) \times \\ &\quad (-1 - \Theta_{11})\Theta_{12}\varrho_2 + \left( -\frac{(-\xi_2 + \Theta_{11})\Theta_{14}}{\Theta_{12}(\mathcal{T})} - \frac{\Theta_{24}}{\mathcal{T}} \right) (\xi_2 - \Theta_{11})\varrho_2\Theta_{12} + \\ &\quad 2 \left( -\frac{(-\xi_2 + \Theta_{11})\Theta_{15}}{\Theta_{12}(\mathcal{T})} - \frac{\Theta_{25}}{\mathcal{T}} \right) (-1 - \Theta_{11})(\xi_2 - \Theta_{11})\varrho_2, \\ \chi_4 &= -\frac{(-\xi_2 + \Theta_{11})\Omega_{17}}{\mathcal{T}} - \frac{(-\xi_2 + \Theta_{11})\Omega_{18}(-1 - \Theta_{11})}{\Theta_{12}(\mathcal{T})} - \frac{(-\xi_2 + \Theta_{11})\Omega_{11}\varrho_2}{\mathcal{T}} \\ &\quad - \frac{(-\xi_2 + \Theta_{11})\Omega_{12}(\xi_2 - \Theta_{11})\varrho_2}{\Theta_{12}(\mathcal{T})} + 2 \left( -\frac{(-\xi_2 + \Theta_{11})\Theta_{13}}{\Theta_{12}(\mathcal{T})} - \frac{\Theta_{23}}{\mathcal{T}} \right) \Theta_{12}^2\varrho_3 \\ &\quad + \left( -\frac{(-\xi_2 + \Theta_{11})\Theta_{14}}{\Theta_{12}(\mathcal{T})} - \frac{\Theta_{24}}{\mathcal{T}} \right) (-1 - \Theta_{11})\Theta_{12}\varrho_3\end{aligned}$$

$$\begin{aligned}
& + \left( -\frac{(-\xi_2 + \Theta_{11})\Theta_{14}}{\Theta_{12}(\mathcal{T})} - \frac{\Theta_{24}}{\mathcal{T}} \right) (\xi_2 - \Theta_{11}) \varrho_3 \Theta_{12} \\
& + 2 \left( -\frac{(-\xi_2 + \Theta_{11})\Theta_{15}}{\Theta_{12}(\mathcal{T})} - \frac{\Theta_{25}}{\mathcal{T}} \right) (-1 - \Theta_{11}) (\xi_2 - \Theta_{11}) \varrho_3, \\
\chi_5 & = -\frac{(-\xi_2 + \Theta_{11})\Omega_{19}}{\Theta_{12}(\mathcal{T})} - \frac{(-\xi_2 + \Theta_{11})\Omega_{11}\varrho_3}{\mathcal{T}} - \frac{(-\xi_2 + \Theta_{11})\Omega_{12}(\xi_2 - \Theta_{11})\varrho_3}{\Theta_{12}(\mathcal{T})}, \\
& \text{where } \mathcal{T} = \xi_2 + 1.
\end{aligned}$$

Now, we define the following two discriminatory quantities:

$$\begin{aligned}
\Phi_1 & = \left( \frac{\partial^2 F}{\partial \tilde{x} \partial \bar{\alpha}} + \frac{1}{2} \frac{\partial F}{\partial \bar{\alpha}} \frac{\partial^2 F}{\partial \tilde{x}^2} \right)_{(0,0)} = \chi_2, \\
\Phi_2 & = \left( \frac{1}{6} \frac{\partial^3 F}{\partial \tilde{x}^3} + \left( \frac{1}{2} \frac{\partial^2 F}{\partial \tilde{x}^2} \right)^2 \right)_{(0,0)} = \chi_5 + \chi_1^2.
\end{aligned}$$

Based on the details above, the subsequent theorem results:

**Theorem 3.5.1.** *If the parameter in the neighborhood of  $\bar{\alpha}$  varies and  $\Phi_2 \neq 0$ , the model (3.1.5) undergoes flip bifurcation at the specific fixed point  $(\hat{x}, \hat{y})$ . Moreover, the period-two orbits that divide from  $(\hat{x}, \hat{y})$  are stable if  $\Phi_2 > 0$ , but they become unstable if  $\Phi_2 < 0$ .*

### 3.5.1 Hopf bifurcation

First, we will study the Hopf bifurcation in the continuous-time system (3.1.4). The presence of center points in the corresponding linear system is a requirement for the Hopf bifurcation of a two-dimensional continuous-time nonlinear system. The latent roots of the fixed point of a two-dimensional model are:

$$\Phi_{1,2} = \frac{1}{2} \left[ \mathbb{A} \pm \sqrt{\mathbb{A} - 4\mathbb{B}} \right].$$

When  $\mathbb{A} = 0$  and  $\mathbb{B} > 0$ , the latent roots  $\Phi_{1,2} = \sqrt{-4\mathbb{B}}$  are pure imaginary numbers, and the fixed point is the center point. At  $(\hat{x}, \hat{y})$  the Jacobian matrix of the system (3.1.4) is obtained by

$$\mathbb{M}_C(\hat{x}, \hat{y}) = \begin{pmatrix} -\zeta - \frac{\mu\omega\hat{y}}{(\omega+\hat{x})^2} + \frac{\gamma\hat{x}(2\kappa\Lambda+\hat{x}(\kappa-3\Lambda-2\hat{x}))}{(\Lambda+\hat{x})^2(F\hat{y}\kappa+\kappa)} & \hat{x} \left( \frac{\gamma F \hat{x}(\hat{x}-\kappa)}{\kappa(\Lambda+\hat{x})(F\hat{y}+1)^2} - \frac{\mu}{\omega+\hat{x}} \right) \\ \frac{\beta\mu\omega\hat{y}}{(\omega+\hat{x})^2} & -\theta - 2\delta\hat{y} + \frac{\beta\mu\hat{x}}{\omega+\hat{x}} \end{pmatrix}.$$

The characteristic function is:

$$\Omega(\Phi) = \Phi^2 - \mathbb{A}\Phi + \mathbb{B}, \quad (3.5.10)$$



where,

$$\mathbb{A} = -\zeta - \theta + \frac{\beta\mu\hat{x}}{\hat{x} + \omega} + \frac{\gamma\hat{x}(2\kappa\Lambda + \hat{x}(\kappa - 3\Lambda - 2\hat{x}))}{(\Lambda + \hat{x})^2(\kappa + \kappa\hat{y}F)} - \frac{\mu\omega\hat{y}}{(\hat{x} + \omega)^2} - 2\delta\hat{y}, \quad (3.5.11)$$

$$\begin{aligned} \mathbb{B} &= \left( -\zeta - \frac{\mu\omega\hat{y}}{(\omega + \hat{x})^2} + \frac{\gamma\hat{x}(2\kappa\Lambda + \hat{x}(\kappa - 3\Lambda - 2\hat{x}))}{(\Lambda + \hat{x})^2(F\hat{y}\kappa + \kappa)} \right) \left( -\theta - 2\delta\hat{y} + \frac{\beta\mu\hat{x}}{\omega + \hat{x}} \right) \\ &- \left( \frac{\beta\mu\omega\hat{y}}{(\omega + \hat{x})^2} \right) \left( \hat{x} \left( \frac{\gamma F \hat{x} (\hat{x} - \kappa)}{\kappa(\Lambda + \hat{x})(F\hat{y} + 1)^2} - \frac{\mu}{\omega + \hat{x}} \right) \right). \end{aligned} \quad (3.5.12)$$

We shall now explain the Hopf bifurcation of system (3.1.4) at five distinct parameters, i.e., at  $\beta, \mu, \omega, \delta$ , and  $\theta$ . Therefore, to discuss the Hopf bifurcation of the system (3.1.4) we have the following theorem:

**Theorem 3.5.2.** *The positive fixed point  $(\hat{x}, \hat{y})$  of (3.1.4) undergoes Hopf bifurcation when*

$$\begin{aligned} 0 &< \left( -\zeta - \frac{\mu\omega\hat{y}}{(\omega + \hat{x})^2} + \frac{\gamma\hat{x}(2\kappa\Lambda + \hat{x}(\kappa - 3\Lambda - 2\hat{x}))}{(\Lambda + \hat{x})^2(F\hat{y}\kappa + \kappa)} \right) \left( -\theta - 2\delta\hat{y} + \frac{\beta\mu\hat{x}}{\omega + \hat{x}} \right) \\ &- \left( \hat{x} \left( \frac{\gamma F \hat{x} (\hat{x} - \kappa)}{\kappa(\Lambda + \hat{x})(F\hat{y} + 1)^2} - \frac{\mu}{\omega + \hat{x}} \right) \right) \left( \frac{\beta\mu\omega\hat{y}}{(\omega + \hat{x})^2} \right), \text{ and} \\ 0 &= -\zeta - \theta + \frac{\beta\mu\hat{x}}{\hat{x} + \omega} + \frac{\gamma\hat{x}(2\kappa\Lambda + \hat{x}(\kappa - 3\Lambda - 2\hat{x}))}{(\Lambda + \hat{x})^2(\kappa + \kappa\hat{y}F)} - \frac{\mu\omega\hat{y}}{(\hat{x} + \omega)^2} - 2\delta\hat{y}. \end{aligned}$$

From the second condition of the above theorem, one can derive the following values of parameters for which the system (3.1.4) undergoes Hopf bifurcation:

$$\begin{aligned} \beta &= \frac{(\hat{x} + \omega) \left( \zeta + \theta + \frac{\gamma\hat{x}(\hat{x}(-\kappa + 3\Lambda + 2\hat{x}) - 2\kappa\Lambda)}{(\Lambda + \hat{x})^2(\kappa + \kappa\hat{y}F)} + \hat{y} \left( 2\delta + \frac{\mu\omega}{(\hat{x} + \omega)^2} \right) \right)}{\mu\hat{x}}, \\ \mu &= \frac{(\hat{x} + \omega)^2 \left( \zeta + \theta + \frac{\gamma\hat{x}(\hat{x}(-\kappa + 3\Lambda + 2\hat{x}) - 2\kappa\Lambda)}{(\Lambda + \hat{x})^2(\kappa + \kappa\hat{y}F)} + 2\delta\hat{y} \right)}{\beta\hat{x}(\hat{x} + \omega) - \omega\hat{y}}, \\ \delta &= -\frac{\zeta + \theta - \frac{\beta\mu\hat{x}}{\hat{x} + \omega} - \frac{\gamma\hat{x}(2\kappa\Lambda + \hat{x}(\kappa - 3\Lambda - 2\hat{x}))}{(\Lambda + \hat{x})^2(\kappa + \kappa\hat{y}F)} + \frac{\mu\omega\hat{y}}{(\hat{x} + \omega)^2}}{2\hat{y}}, \\ \theta &= -\zeta + \frac{\beta\mu\hat{x}}{\hat{x} + \omega} + \frac{\gamma\hat{x}(2\kappa\Lambda + \hat{x}(\kappa - 3\Lambda - 2\hat{x}))}{(\Lambda + \hat{x})^2(\kappa + \kappa\hat{y}F)} - \frac{\mu\omega\hat{y}}{(\hat{x} + \omega)^2} - 2\delta\hat{y}. \end{aligned}$$

Similarly, the bifurcation value of any other parameter can also be calculated. The Neimark-Sacker bifurcation of the system (3.1.5) at the particular positive fixed point  $(\hat{x}, \hat{y})$  is now investigated using the bifurcation theory and a bifurcation parameter  $\gamma$ . We have determined the necessary conditions under which the system described in equation (3.1.5) will possess a fixed point that is non-hyperbolic and has two complex conjugate eigenvalues with a modulus of one. Assume that  $\Psi_{NS} = \{(\gamma = \gamma_2, F, \kappa, \Lambda, \mu, \omega, \zeta, \beta, \theta, \delta) :$

$(\Pi_{Tr})^2 - 4\Pi_{Det} < 0$  and  $\Pi_{Det} = 1$  of equation (3.5.1) }. The positive fixed point of the system (3.1.5) experiences the Neimark-Sacker bifurcation when the parameters vary in the small range around  $\Psi_{NS}$ . In this case, we investigate the system (3.1.5) with these parameters, which are defined by the following map:

$$\begin{cases} x_{n+1} \rightarrow x_n \exp \left[ \frac{\gamma_2}{1+F y_n} \left( 1 - \frac{x_n}{\mathcal{K}} \right) \frac{x_n}{x_n + \Lambda} - \frac{\mu y_n}{x + \omega} - \zeta \right], \\ y_{n+1} \rightarrow y_n \exp \left[ \frac{\mu \beta x_n}{x_n + \omega} - \theta - \delta y_n \right]. \end{cases} \quad (3.5.13)$$

The following map can be used to represent a map perturbation (3.5.13) when  $\bar{\gamma}$  is used as the bifurcation parameter:

$$\begin{cases} x_{n+1} \rightarrow x_n \exp \left[ \frac{\gamma_2 + \bar{\gamma}}{1+F y_n} \left( 1 - \frac{x_n}{\mathcal{K}} \right) \frac{x_n}{x_n + \Lambda} - \frac{\mu y_n}{x + \omega} - \zeta \right], \\ y_{n+1} \rightarrow y_n \exp \left[ \frac{\mu \beta x_n}{x_n + \omega} - \theta - \delta y_n \right]. \end{cases} \quad (3.5.14)$$

where  $|\bar{\gamma}| \ll 1$  is taken as a small perturbation parameter. The characteristic function  $\Pi(\xi)$  of (3.5.14) at  $(\hat{x}, \hat{y})$  with  $\Pi(\xi) = 0$  has two roots that are complex conjugates and their modulus is equal to one when

$$\frac{1}{\kappa \hat{y} (\Lambda + \hat{x})^2 (\hat{y} F + 1)^2 (\delta \omega^3 + \hat{x} (\omega (3\delta \omega - \mu (\beta \mu + 1)) + \hat{x} (3\delta \omega - \mu + \delta \hat{x}) + \delta \mu \hat{y} (\hat{x} + \omega)))} \left\{ \hat{x} (\hat{x} + \omega) \left( - (\hat{x} + \omega)^2 \left( - \kappa \Lambda + 2\Lambda \hat{x} + \hat{x}^2 \right) + \hat{y} \left( \kappa \Lambda \omega^2 (F - \delta) + \hat{x} \left( \Lambda \omega (\kappa F (\beta \mu + 2) + 2\delta (\omega - \kappa) - 2\omega F) + \hat{x} \left( \kappa F (\beta \mu \omega + \Lambda) - \omega F (\Lambda (\beta \mu + 4) + \omega) - \delta \kappa \Lambda + \delta \omega (4\Lambda + \omega) + \hat{x} \left( - F (\beta \mu \omega + 2\Lambda + 2\omega) + 2\delta (\Lambda + \omega) + \hat{x} (\delta - F) \right) \right) \right) \right) + \delta \hat{y}^2 F (\hat{x} + \omega)^2 \left( - \kappa \Lambda + 2\Lambda \hat{x} + \hat{x}^2 \right) \right\} = \gamma_2.$$

Taking  $u = x - \hat{x}$  and  $v = y - \hat{y}$ , where  $(\hat{x}, \hat{y})$  is the unique positive fixed point of the system (3.5.14), or equivalently positive fixed point of (3.1.5). Transforming the fixed point  $(\hat{x}, \hat{y})$  to the origin  $(0, 0)$ , we get the underlying map:

$$\begin{cases} \Phi \rightarrow \varrho_{11} \Phi + \Theta_{12} \Psi + \Theta_{13} \Phi^2 + \Theta_{14} \Phi \Psi + \Theta_{15} \Psi^2 + \Theta_{16} \Phi^3 + \Theta_{17} \Phi^2 \Psi + \Theta_{18} \Phi \Psi^2 \\ + \Theta_{19} \Psi^3 + O(|\Phi|, |\Psi|)^4, \\ \Psi \rightarrow \Theta_{21} \Phi + \Theta_{22} \Psi + \Theta_{23} \Phi^2 + \Theta_{24} \Phi \Psi + \Theta_{25} \Psi^2 + \Theta_{26} \Phi^3 + \Theta_{27} \Phi^2 \Psi + \Theta_{28} \Phi \Psi^2 \\ + O(|\Phi|, |\Psi|)^4. \end{cases} \quad (3.5.15)$$

and the coefficients  $\Theta_{14}, \Theta_{15}, \Theta_{16}, \Theta_{17}, \Theta_{23}, \Theta_{24}, \Theta_{25}, \Theta_{26}, \Theta_{27}, \Theta_{28}$ , and  $\Theta_{29}$  are given above can be calculated by replacing  $\gamma_1$  by  $\gamma_2 + \bar{\gamma}$ . The characteristic function of (3.5.14) at the

fixed point  $(0, 0)$  can be expressed as follows:

$$\Pi(\xi) = \xi^2 - (\Pi_{Tr}(\gamma))\xi + \Pi_{Det}(\gamma), \quad (3.5.16)$$

where,

$$\begin{aligned} \Pi_{Tr}(\tilde{\gamma}) &= \hat{x} \left( \frac{(\tilde{\gamma} + \gamma_2)(\kappa\Lambda - \hat{x}(2\Lambda + \hat{x}))}{(\Lambda + \hat{x})^2(\kappa + \kappa\hat{y}F)} + \frac{\mu\hat{y}}{(\hat{x} + \omega)^2} \right) - \delta\hat{y} + 2, \text{ and} \\ \Pi_{Det}(\tilde{\gamma}) &= \left[ \hat{x} \left( \frac{(\tilde{\gamma} + \gamma_2)(\kappa\Lambda - \hat{x}(2\Lambda + \hat{x}))}{(\Lambda + \hat{x})^2(\kappa + \kappa\hat{y}F)} + \frac{\mu\hat{y}}{(\hat{x} + \omega)^2} \right) + 1 \right] [1 - \delta\hat{y}] - \\ &\quad \left[ \frac{\beta\mu\omega\hat{y}}{(\hat{x} + \omega)^2} \right] \left[ \hat{x} \left( \frac{(\tilde{\gamma} + \gamma_2)\hat{x}F(\hat{x} - \kappa)}{\kappa(\Lambda + \hat{x})(\hat{y}F + 1)^2} - \frac{\mu}{\hat{x} + \omega} \right) \right]. \end{aligned}$$

As  $(\gamma, F, \kappa, \Lambda, \mu, \omega, \zeta, \beta, \theta, \delta) \in \Psi_{NS}$ , the roots of (3.5.16) are conjugate complex numbers  $\xi_1, \xi_2$  with  $|\xi_1| = |\xi_2| = 1$ . Thus, it is obvious that  $\xi_1$  and  $\xi_2 = \frac{\Pi_{Tr}}{2} \pm \frac{\iota}{2}\sqrt{4\Pi_{Det} - \Pi_{Tr}^2}$ . We have  $|\xi_1| = |\xi_2| = \sqrt{\Pi_{Det}}$ , with  $\left(\frac{d|\xi_{1,2}|}{d\tilde{\gamma}}\right)_{\tilde{\gamma}=0} \neq 0$ . Moreover, we assume that  $\Pi_{Tr}(0) = 2 - \delta\hat{y} + \hat{x} \left( \frac{(\tilde{\gamma} + \gamma_2)(\kappa\Lambda - \hat{x}(2\Lambda + \hat{x}))}{(\Lambda + \hat{x})^2(\kappa + \kappa\hat{y}F)} + \frac{\mu\hat{y}}{(\hat{x} + \omega)^2} \right) \neq 0, -1$ . Further,  $(\gamma, F, \kappa, \Lambda, \mu, \omega, \zeta, \beta, \theta, \delta) \in \Psi_{NS}$  implies that  $-2 < \Pi_{Tr}(0) < 2$ . Thus,  $\Pi_{Tr}(0) \neq \pm 2, 0, -1$  gives  $\xi_1^r, \xi_2^r \neq 1$  for all  $r = 1, 2, 3, 4$  at  $\tilde{\gamma} = 0$ . Therefore, when  $\tilde{\gamma} = 0$  and the following criteria are met, the roots of (3.5.16) do not occur at the point where the unit circle and coordinate axes intersect. Now transforming the fixed point  $(\hat{x}, \hat{y})$  of (3.5.14) to the origin, we get the normal form of (3.5.14) as:

$$\begin{pmatrix} \tilde{x} \\ \tilde{y} \end{pmatrix} \rightarrow \begin{pmatrix} \alpha_a & -\beta_a \\ \beta_a & \alpha_a \end{pmatrix} \begin{pmatrix} \tilde{x} \\ \tilde{y} \end{pmatrix} + \begin{pmatrix} \tilde{f}(\tilde{x}, \tilde{y}) \\ \tilde{g}(\tilde{x}, \tilde{y}) \end{pmatrix}, \quad (3.5.17)$$

where,

$$\begin{cases} \tilde{f}(\tilde{x}, \tilde{y}) = \frac{1}{\Theta_{12}} (\Theta_{13}u^2 + \Theta_{14}uv + \Theta_{15}v^2 + \Theta_{16}u^3 + \Theta_{17}u^2v + \Theta_{18}uv^2 + \Theta_{19}v^3) \\ \quad + \frac{1}{\Theta_{12}} O(|u|, |v|)^4, \\ \tilde{g}(\tilde{x}, \tilde{y}) = \left( \frac{\Theta_{13}(\alpha_a - \Theta_{11})}{\beta_a \Theta_{12}} - \frac{\Theta_{23}}{\beta_a} \right) u^2 + \left( \frac{\Theta_{14}(\alpha_a - \Theta_{11})}{\beta_a \Theta_{12}} - \frac{\Theta_{24}}{\beta_a} \right) uv + \Theta_{27}u^2v + \Theta_{28} \\ \quad uv^2 + \left( \frac{\Theta_{15}(\alpha_a - \Theta_{11})}{\beta_a \Theta_{12}} - \frac{\Theta_{25}}{\beta_a} \right) uv^2 + \left( \frac{\Theta_{13}(\alpha_a - \Theta_{11})}{\beta_a \Theta_{16}} - \frac{\Theta_{23}}{\beta_a} \right) u^3 + \Theta_{29}v^3 + O((|u|, |v|)^4) \end{cases} \quad (3.5.18)$$

$u = a_{12}\tilde{x}$  and  $v = (\alpha_a - \varrho_{11})u - \beta_a v$ . Next, the nonzero real number that follows is defined:

$$\mathcal{L} = \left( \left[ -Re \left( \frac{(1 - 2\xi_1)\xi_2^2}{1 - \xi_1} \mathcal{C}_{20}\mathcal{C}_{11} \right) - \frac{1}{2}|\mathcal{C}_{11}|^2 - |\mathcal{C}_{02}|^2 + Re(\xi_2\mathcal{C}_{21}) \right] \right)_{\tilde{\gamma}=0},$$

where

$$\begin{aligned}
\mathcal{C}_{20} &= \frac{1}{8} \left[ \tilde{f}_{\tilde{x}\tilde{x}} + 2\tilde{g}_{\tilde{x}\tilde{y}} - \tilde{f}_{\tilde{y}\tilde{y}} + i \left( \tilde{g}_{\tilde{x}\tilde{x}} - 2\tilde{f}_{\tilde{x}\tilde{y}} - \tilde{g}_{\tilde{y}\tilde{y}} \right) \right], \\
\mathcal{C}_{11} &= \frac{1}{4} \left[ \tilde{f}_{\tilde{x}\tilde{x}} + i \left( \tilde{g}_{\tilde{x}\tilde{x}} + \tilde{g}_{\tilde{y}\tilde{y}} \right) + \tilde{f}_{\tilde{y}\tilde{y}} \right], \\
\mathcal{C}_{02} &= \frac{1}{8} \left[ \tilde{f}_{\tilde{x}\tilde{x}} - 2\tilde{g}_{\tilde{x}\tilde{y}} - \tilde{f}_{\tilde{y}\tilde{y}} + i \left( \tilde{g}_{\tilde{x}\tilde{x}} + 2\tilde{f}_{\tilde{x}\tilde{y}} - \tilde{g}_{\tilde{y}\tilde{y}} \right) \right], \\
\mathcal{C}_{21} &= \frac{1}{16} \left[ \tilde{g}_{\tilde{x}\tilde{x}\tilde{y}} + \tilde{g}_{\tilde{y}\tilde{y}\tilde{y}} + \tilde{f}_{\tilde{x}\tilde{x}\tilde{x}} + \tilde{f}_{\tilde{x}\tilde{y}\tilde{y}} + i \left( \tilde{g}_{\tilde{x}\tilde{x}\tilde{x}} + \tilde{g}_{\tilde{x}\tilde{y}\tilde{y}} - \tilde{f}_{\tilde{x}\tilde{x}\tilde{y}} - \tilde{f}_{\tilde{y}\tilde{y}\tilde{y}} \right) \right].
\end{aligned}$$

By analyzing these facts, we can derive the following result:

**Theorem 3.5.3.** *Assuming that  $L$  is not equal to zero, the system (3.1.5) undergoes Hopf bifurcation at the unique positive fixed point  $(\hat{x}, \hat{y})$  when the parameter  $\tilde{\gamma}$  changes within a narrow range of the parameter  $\gamma_2$ . Moreover, if  $\tilde{\gamma}$  is greater than  $\gamma_2$ , an attracting invariant closed curve bifurcates from the fixed point when  $L$  is less than zero, while a repelling invariant closed curve bifurcates when  $L$  is greater than zero.*

## 3.6 Numerical simulations

The Neimark-Sacker bifurcation and period-doubling bifurcation of systems (3.1.4) and (3.1.5) will be discussed numerically in this section. The importance of using numerical simulations of the bifurcation in the prey-predator model in our research must be understood before we discuss them. Using numerical simulations, we can study how the system changes under multiple conditions using a realistic and practical approach. Through numerical simulation, we can confirm different dynamic behaviors, including bifurcation, chaos, and periodicity. By employing numerical methods, we can gain deep insights into the behavior of these systems under varying parameters and initial conditions, which is critical for both theoretical understanding and practical applications. Numerical simulations in the context of the prey-predator model enable us to investigate how slight changes to the initial conditions or system parameters may significantly impact the populations of prey and predator species. Based on this, we may identify possible actions to decrease the adverse effects of environmental variations and develop accurate predictions about the behavior of natural ecosystems. We shall first provide the following numerical example to verify that Hopf bifurcation occurs in the system (3.1.4).

**Example 7.** *In this example, we will discuss the Hopf bifurcation of the system (3.1.4) at the positive fixed point. The Hopf bifurcation is arising at different parameters. Generally, it was observed that this bifurcation is emerging if we select the parametric set below:*

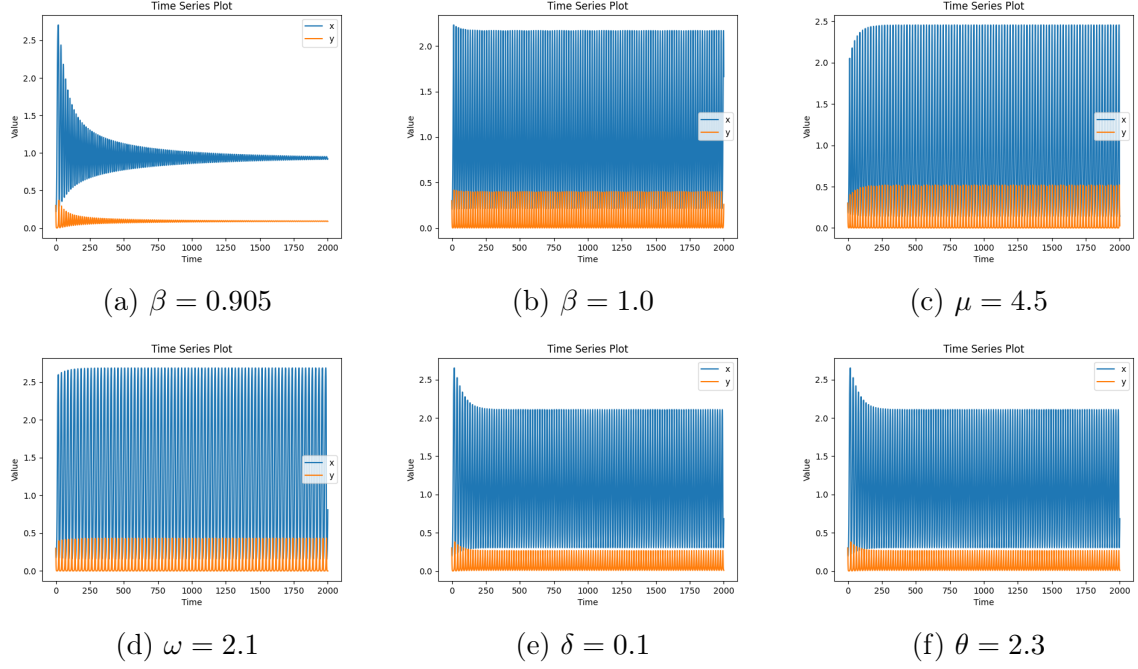


Figure 3.3: Time-series plot. The parameter values for plot (a) are:  $\gamma = 1.8, F = 0.27, \mathcal{K} = 2.91, \Lambda = 1.19, \mu = 3.81, \omega = 0.3, \zeta = 0.19, \beta = 0.905, \theta = 2.6, \delta = 0.1$ . For plot (b), the values are:  $\gamma = 1.8, F = 0.27, \mathcal{K} = 2.91, \Lambda = 1.19, \mu = 3.81, \omega = 0.3, \zeta = 0.19, \beta = 1.0, \theta = 2.6, \delta = 0.1$ . For plot (c), the parameters are:  $\gamma = 1.8, F = 0.27, \mathcal{K} = 2.91, \Lambda = 1.19, \mu = 4.5, \omega = 0.3, \zeta = 0.19, \beta = 0.9, \theta = 2.6, \delta = 0.1$ . For plot (d), we have:  $\gamma = 1.8, F = 0.27, \mathcal{K} = 2.91, \Lambda = 1.19, \mu = 3.81, \omega = 2.1, \zeta = 0.19, \beta = 0.9, \theta = 2.6, \delta = 0.1$ . For plot (e), we choose:  $\gamma = 1.8, F = 0.27, \mathcal{K} = 2.91, \Lambda = 1.19, \mu = 3.81, \omega = 0.3, \zeta = 0.19, \beta = 0.9, \theta = 2.6, \delta = 0.1$ , and for plot (f), we fix:  $\gamma = 1.8, F = 0.27, \mathcal{K} = 2.91, \Lambda = 1.19, \mu = 3.81, \omega = 0.3, \zeta = 0.19, \beta = 0.9, \theta = 2.3, \delta = 0.1$ .

$$\mathcal{S} = \{\gamma = 1.8, F = 0.27, \mathcal{K} = 2.91, \Lambda = 1.19, \mu = 3.81, \omega = 0.3, \zeta = 0.19, \beta = 0.9, \theta = 2.6, \delta = 0.1\}. \quad (3.6.1)$$

In this case, the initial population was assumed to be  $(x_0, y_0) = (0.3, 0.3)$ . For the above parameter set, the positive fixed point becomes  $(0.957564676866582, 0.10990382742646633)$ . To confirm the mathematical bifurcation conditions, we will vary one parameter and fix the rest of the parameters as given in the above set. That particular parameter will be considered a bifurcation parameter. We first determine the fixed point using the approximate value of a selected bifurcation parameter. Next, we compute the specific bifurcation parameter value using this approximate fixed point, and we use mathematical conditions to confirm the existence of the Hopf bifurcation. It is essential to mention that the reason for the minor difference between the graphical outcome and the calculated bifurcation parameter's value is that the fixed point was calculated using an approximation. However, the exact value of the bifurcation parameter can reduce the difference between the math-

emational and visual variations. Also, pre-defined libraries in MATCONT can be used to determine the exact value of bifurcation parameters. First, we will choose  $\beta \in [0.8, 1.0]$  and fix the rest of the parameters as given in the above set. At  $\beta = 0.8049166431618142$ , the forward bifurcation occurs. For this particular value of  $\beta$ , the Jacobian matrix becomes:

$$\mathbf{M}_\beta = \begin{pmatrix} 0.286837 & -3.03241 \\ 0.0639366 & -0.286837 \end{pmatrix}. \quad (3.6.2)$$

The roots of (3.6.2) are pure imaginary numbers  $\{0.334076i, -0.334076i\}$ . Hence, it confirms the occurrence of Hopf bifurcation in (3.1.4) for parameter  $\beta$ . Similarly, if we vary  $\mu \in [3.3, 4]$ , for  $\mu = 3.3948506261293243$ , we have:

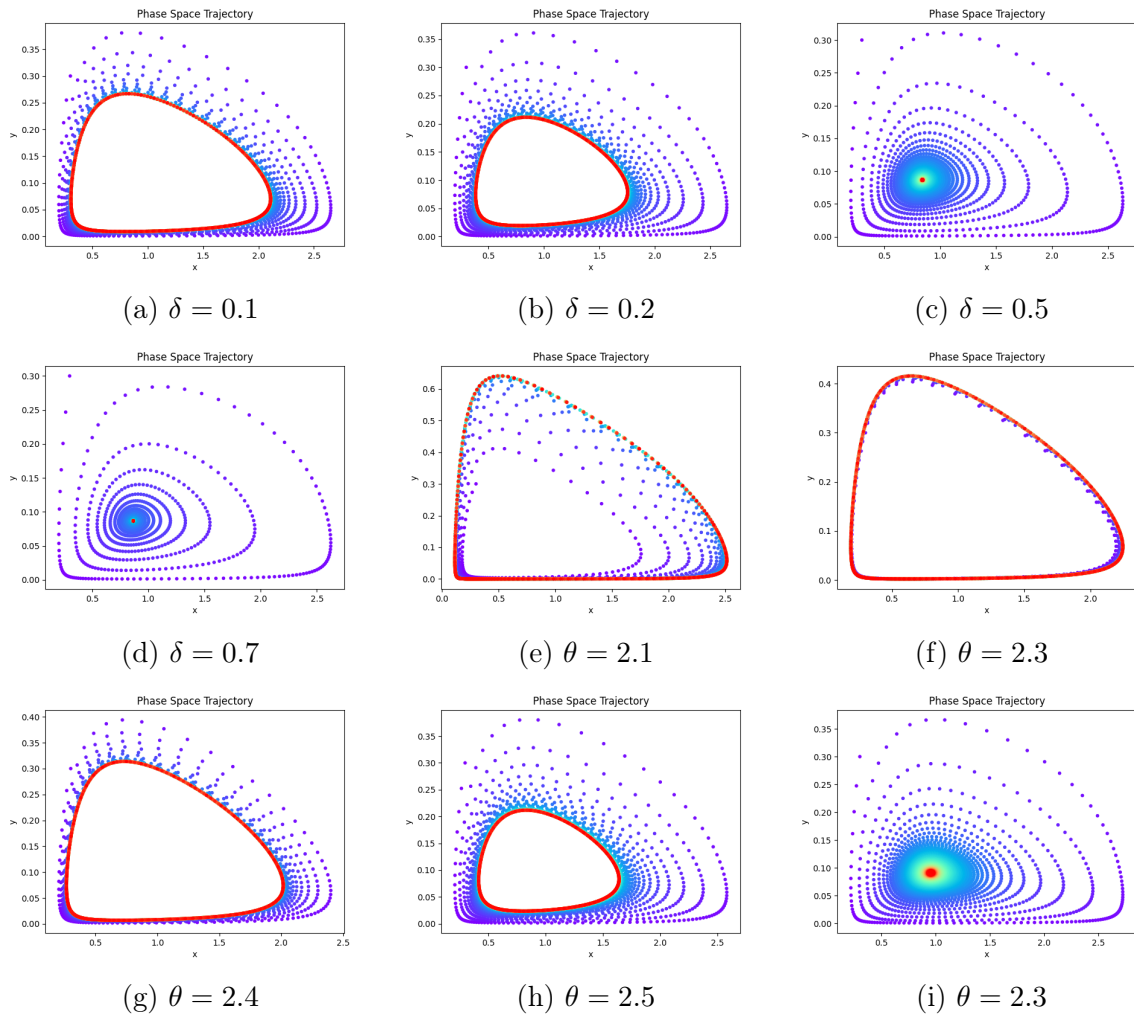


Figure 3.4: Phase plots display bifurcation plots for various parameter values, including  $\delta$  and  $\theta$ . They confirm the occurrence of backward Hopf bifurcation in the system (3.1.4). Each sub-figure represents a specific value of the bifurcation parameter for which the plot is displayed. The remaining parameter values are chosen from the set  $\mathcal{S}$  by selecting that specific bifurcation value.

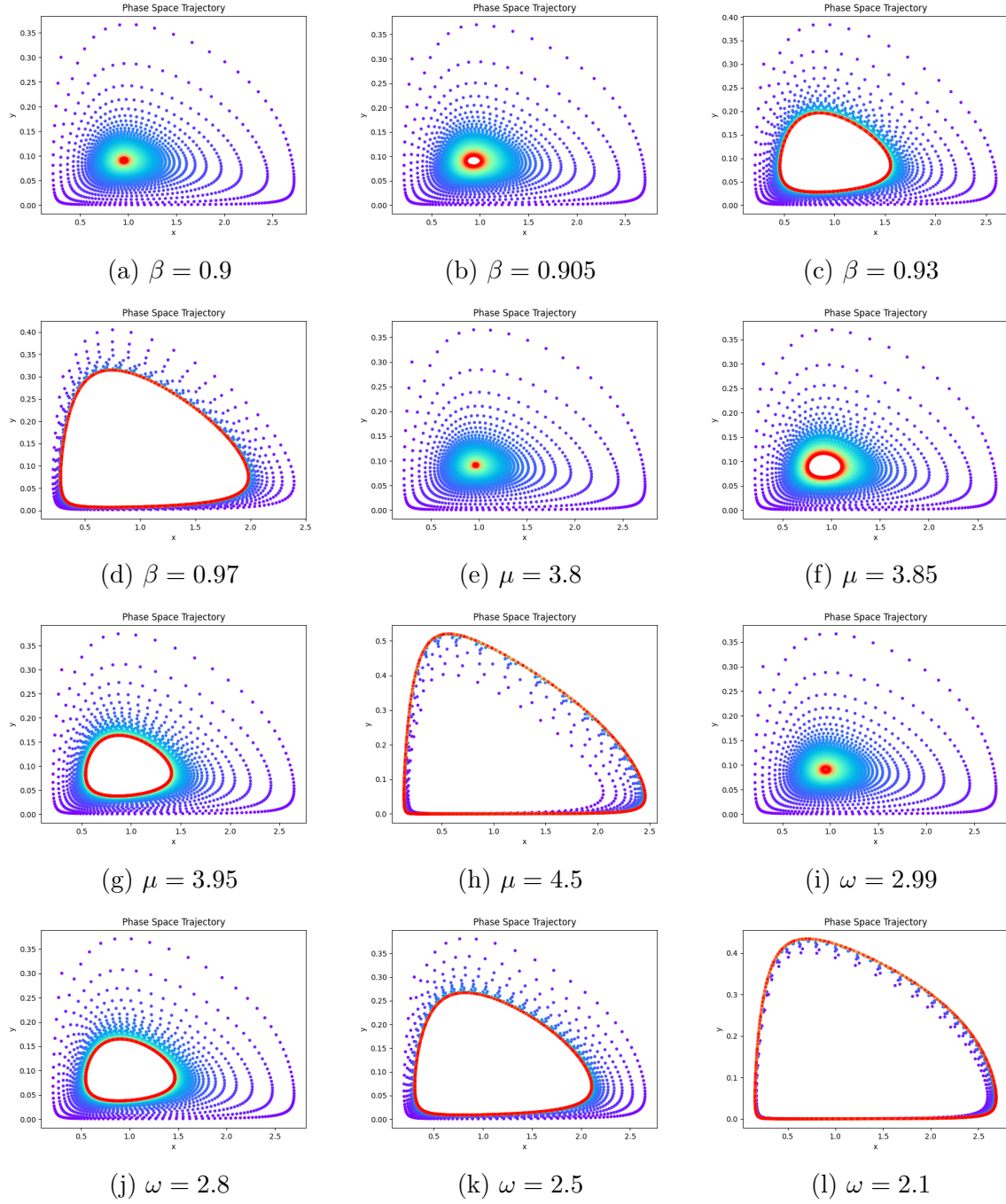


Figure 3.5: **Phase plots:** These diagrams show bifurcation plots for various parameter values, including  $\beta$ ,  $\mu$ , and  $\omega$ . The phase charts confirm the occurrence of forward Hopf bifurcation in the system (3.1.4). Each sub-figure indicates the specific value of the bifurcation parameter for which the plot is displayed. The remaining parameter values are chosen from the set  $\mathcal{S}$  by selecting that specific bifurcation value.

$$\mathbf{M}_\mu = \begin{pmatrix} 0.295492 & -2.7163 \\ 0.0636996 & -0.295492 \end{pmatrix}. \quad (3.6.3)$$

With latent roots:  $\{0.292766i, -0.292766i\}$ . For parameter  $\mu$ , the bifurcation can be noticed in a forward direction. Similarly, at  $\omega = 0.4396567623749219$ , the backward Hopf bifurcation can be observed when  $\omega \in [0, 0.5]$ . At  $\omega = 0.4396567623749219$ , we have: The phase space trajectories are given in figure 3.5. From these trajectories, it can be noticed that the bifurcation is going in the reverse direction.

$$\mathbf{M}_\omega = \begin{pmatrix} 0.271967 & -2.74244 \\ 0.0848718 & -0.271967 \end{pmatrix}, \quad (3.6.4)$$

with  $\{0.398484i, -0.398484i\}$  as eigenvalues. Now, to observe the bifurcation in  $\delta$ , we choose  $\delta \in [0, 1.5]$ . At  $\delta = 1.3549443154920353$ , the system bifurcates. Hence, we have

$$\mathbf{M}_\delta = \begin{pmatrix} 0.286837 & -3.03241 \\ 0.0714893 & -0.286837 \end{pmatrix}, \quad (3.6.5)$$

with  $\lambda_{1,2} = \{0.366756i, -0.366756i\}$ . Finally, at  $\theta = 2.875846366959323$ , the system also bifurcates in the range  $[2.5, 3]$ . Thus, for these values, the Jacobian matrix is:

$$\mathbf{M}_\theta = \begin{pmatrix} 0.286837 & -3.03241 \\ 0.0714893 & -0.286837 \end{pmatrix}, \quad (3.6.6)$$

with  $\{0.366756i, -0.366756i\}$  as the eigenvalues. The direction of the bifurcation can be seen from the plots in Figures 3.5 and 3.4. Whereas the time-series plots in Figure 3.3 confirm the existence of bifurcation in the system (3.1.4). It can be observed from the analysis that the system can experience a Hopf bifurcation when particular parameters vary, which can result in the system moving from a stable equilibrium to an oscillation of its limit cycles. Eventually, this may lead to changes in the two species populations, which could collapse the total ecosystem. It is crucial to understand how to prevent Hopf bifurcations and to put these strategies into practice with management plans to protect and sustain ecological systems.

**Example 8.** For this example, we consider the case where a Neimark-Sacker bifurcation occurs in the system (3.1.5). We took  $\gamma$  as a bifurcation parameter to study Hopf bifurcation and fixed the other parameters to specific numerical values. If the parametric set below exists,



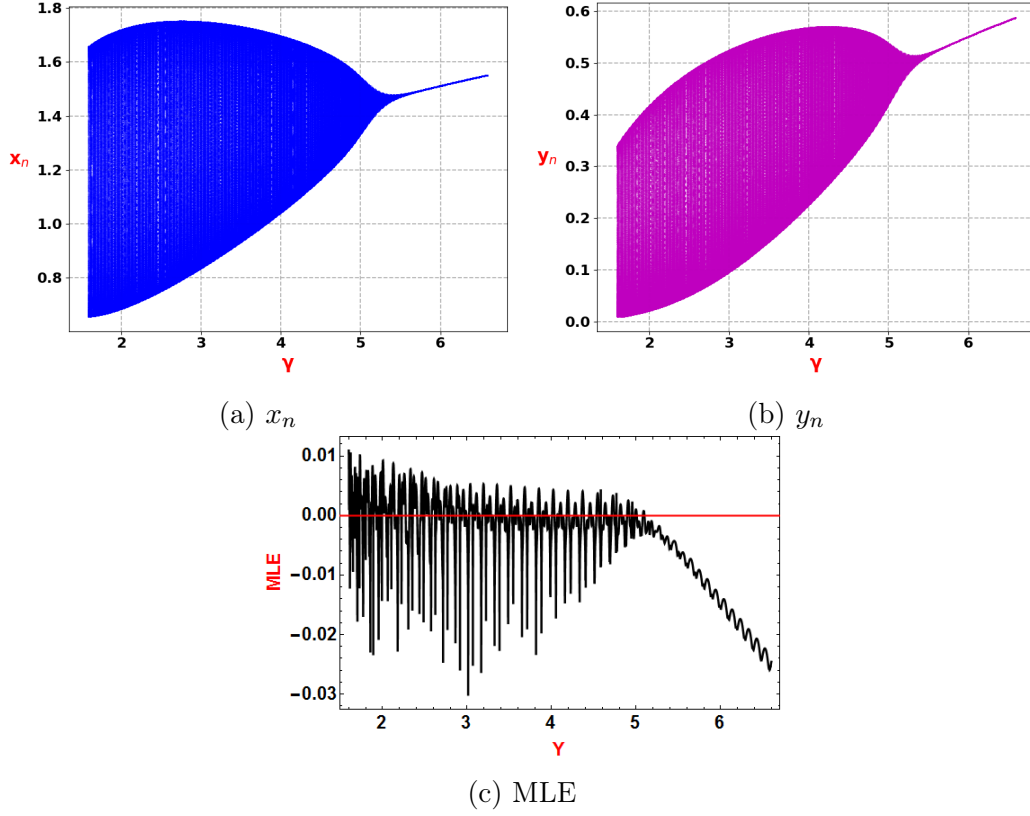


Figure 3.6: Diagrams of bifurcations and MLE for system (3.1.5).

$$\mathcal{S}_\gamma = \{F = 0.32, \mathcal{K} = 2.22, \Lambda = 2.60, \mu = 2.82, \omega = 1.67, \zeta = 0.11, \beta = 2.02, \theta = 2.15, \delta = 1.01\},$$

with a population of  $(x_0, y_0) = (0.5564, 0.5676)$  as the initial value, then the system (3.1.5) encounters a Hopf bifurcation when  $\gamma \in [1.6, 6.6]$ . According to our findings, the system (3.1.5) loses stability around  $\gamma = 5.102$ . The fix parameter set  $\mathcal{S}_\gamma$  with  $\gamma = 5.102$  we have  $(\hat{x}, \hat{y}) = (1.4442371857229968, 0.48685467919366576)$  as the numerical value of positive fixed point. The system (3.1.5) is as follows at these values:

$$\begin{cases} x_{n+1} = x_n \exp \left[ \frac{5.102}{1+0.32y_n} \left( 1 - \frac{x_n}{2.22} \right) \frac{x_n}{x_n+2.60} - \frac{2.82y_n}{x+1.67} - 0.11 \right], \\ y_{n+1} = y_n \exp \left[ \frac{(2.82)(2.02)x_n}{x_n+1.67} - 2.15 - 1.01y_n \right]. \end{cases} \quad (3.6.7)$$

For these parameter values, the resulting Jacobian matrix is as follows:

$$\begin{pmatrix} \hat{x} \left( \frac{\gamma(\kappa\Lambda - \hat{x}(2\Lambda + \hat{x}))}{(\Lambda + \hat{x})^2(F\hat{y}\kappa + \kappa)} + \frac{\mu\hat{y}}{(\omega + \hat{x})^2} \right) + 1 & \hat{x} \left( \frac{\gamma F \hat{x}(\hat{x} - \kappa)}{\kappa(\Lambda + \hat{x})(F\hat{y} + 1)^2} - \frac{\mu}{\omega + \hat{x}} \right) \\ \frac{\beta\mu\omega\hat{y}}{(\omega + \hat{x})^2} & 1 - \delta\hat{y} \end{pmatrix} = \begin{pmatrix} 0.53306 & -1.52805 \\ 0.477543 & 0.508277 \end{pmatrix}. \quad (3.6.8)$$

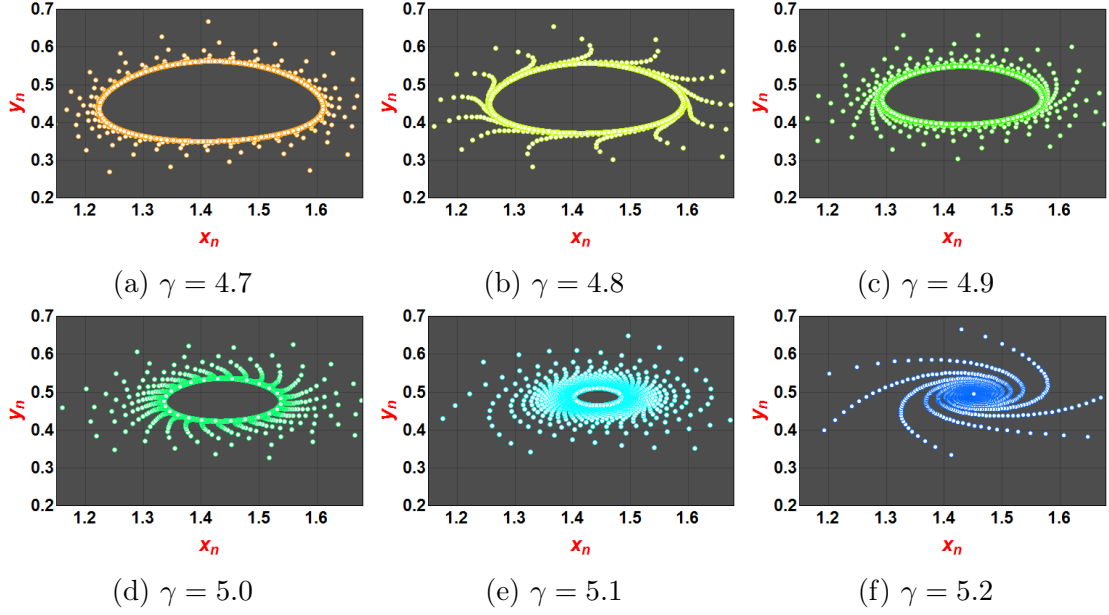


Figure 3.7: Phase plots for different  $\gamma$  values.

The set of the latent roots of the (3.6.8) is:

$$\Delta_{1,2} = \{0.520668 + 0.854141i, 0.520668 - 0.854141i\},$$

with  $|\Delta_{1,2}| = 1$ . Figures 3.7c and 3.7 represent the graphical results.

**Example 9.** This example demonstrates the simultaneous occurrence of a flip and Hopf bifurcation in the system (3.1.5). To achieve this, we select  $\gamma$  as the bifurcation parameter. The remaining factors are limited to the specified numerical values listed below:

$$\mathcal{Q}_\gamma = \{F = 0.11, \mathcal{K} = 2.30, \Lambda = 0.59, \mu = 2.92, \omega = 1.19, \zeta = 0.11, \beta = 0.99, \theta = 0.99, \delta = 1.04\}.$$

The initial conditions are assumed to be  $(1.7529, 1.3376)$ . When  $\gamma$  is equal to 1.412, the backward Hopf bifurcation occurs, and when  $\gamma$  is equal to 5.53741, the forward flip bifurcation occurs. As a result, the region  $[1, 1.412]$  experiences a Hopf bifurcation, but the region  $[5.53741, 5.96]$  undergoes a flip bifurcation, which results in chaos. For  $\gamma = 1.412$  with  $\mathcal{Q}_\gamma$  the Jacobian matrix calculated at  $(\hat{x}, \hat{y}) = (0.9510575193694013, 0.2827817773733809)$  is provided below:

$$\Omega_{Hopf}(\hat{x}, \hat{y}) = \begin{pmatrix} 1.01162 & -1.34735 \\ 0.212207 & 0.705907 \end{pmatrix}. \quad (3.6.9)$$

The set of the latent roots of (3.6.9) is:

$$\bar{\Delta}_{1,2} = \{0.858761 + 0.5124i, 0.858761 - 0.5124i\},$$

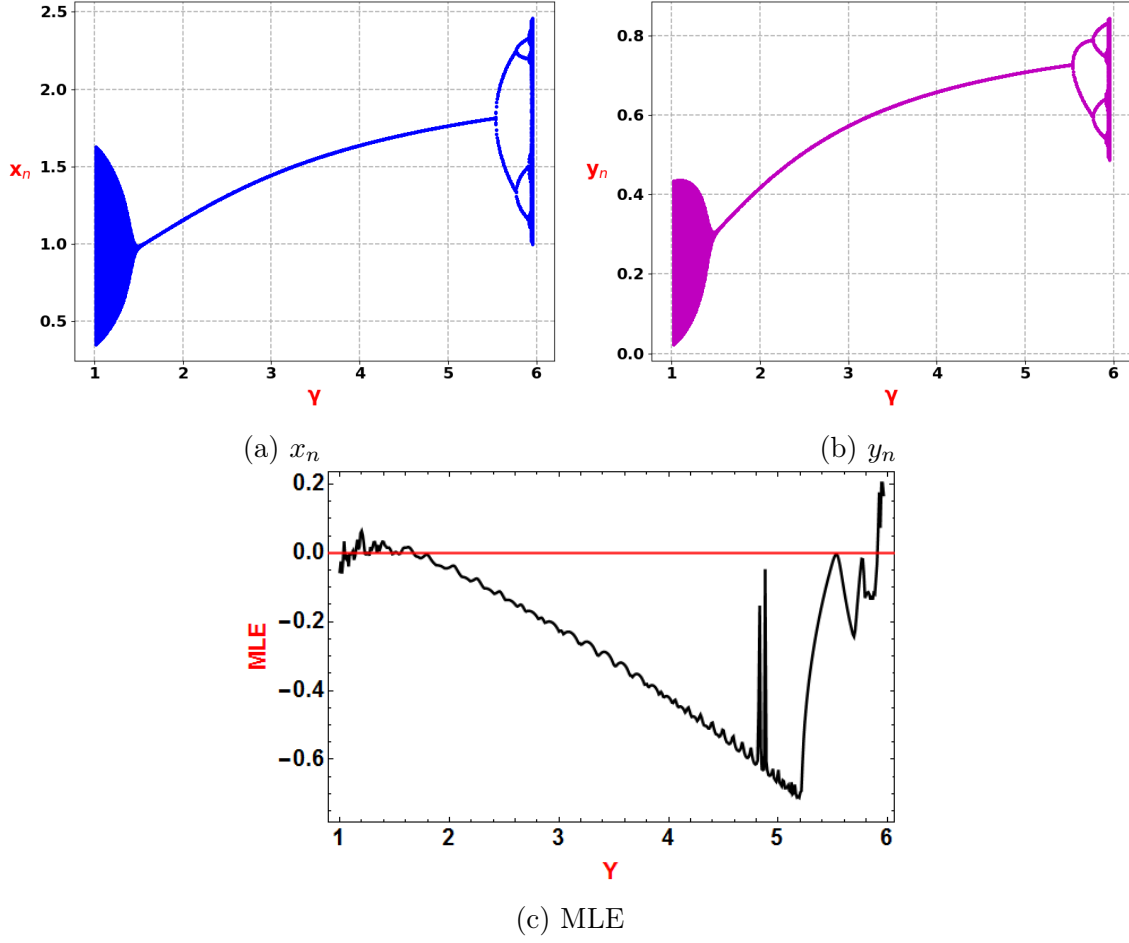


Figure 3.8: Diagrams of bifurcations and MLE for system (3.1.5).

with  $|\bar{\Delta}_1| = 1$  and  $\bar{\Delta}_1 < 1$ . The graphical results in Figure 3.8 also confirm the occurrence of flip bifurcation in the system (4.1.5). Whereas, for  $\gamma = 5.53741$  with  $\mathcal{Q}_\gamma$ , the Jacobian matrix evaluated at  $(\hat{x}, \hat{y}) = (1.8147585333311815, 0.7268576579192267)$  is given below:

$$\Omega_{Flip}(\hat{x}, \hat{y}) = \begin{pmatrix} -1.42619 & -1.91447 \\ 0.276946 & 0.244068 \end{pmatrix}. \quad (3.6.10)$$

The associated eigenvalues are:

$$\{-1, -0.182116\}.$$

Therefore, both types of bifurcation arise since the eigenvalues criterion is met, which confirms their occurrence. The outcomes are represented graphically in Figures 3.8, 3.9, and 3.10.

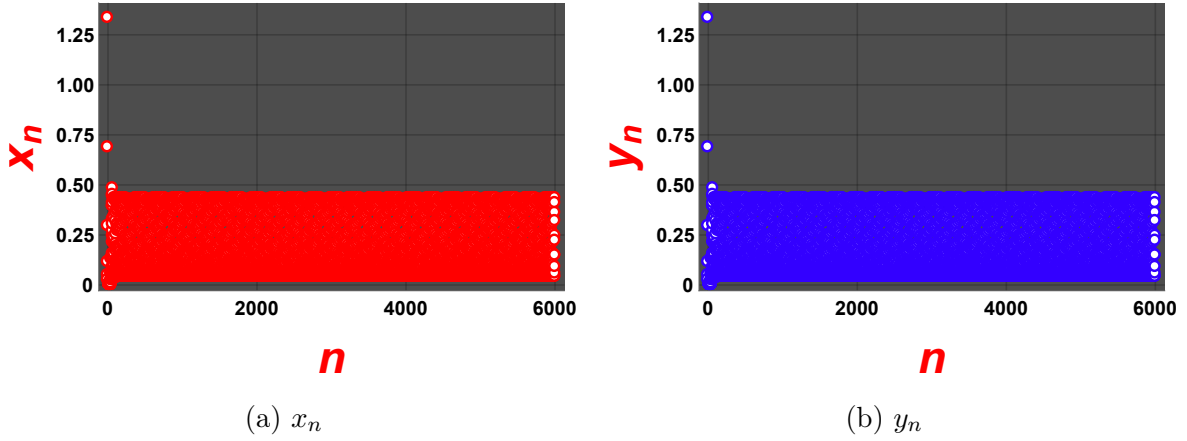


Figure 3.9: Bifurcation plots for (3.1.5).

### 3.6.1 Bi-parameter plots

The bi-parameter plots are essential for exploring the model's behavior and providing insights into the system's dynamics. Studying two-parameter Lyapunov exponent and two-parameter period-doubling bifurcation plots can be highly stimulating because they help us comprehend the behavior of complicated systems, like chaotic and periodic patterns. We may learn more about the underlying dynamics and even make predictions about future behavior by examining how these systems behave when their parameters are changed. To this end, we have carefully selected two parameters, namely, the growth rate of the prey  $\gamma$  and the carrying capacity  $\mathcal{K}$ , to discuss and analyze the dynamics in a two-dimensional parameter space. In the literature, two types of techniques have been used to characterize the parameter-space dynamics of dynamical systems: the Lyapunov exponents between the parameters and the isoperiodic diagrams. By constructing the Lyapunov exponent between these parameters, we can better understand how stable the periodic behavior of the system is embedded in the chaotic region. Ultimately, this information will help us judge the bi-stability of the system. In our analysis, we will use the Lyapunov exponent to confirm the periodic and chaotic dynamics of the system. Specifically, we compute the Lyapunov exponent  $\lambda_{1,2}$  of our model using the following system of equations:

$$\lambda_{1,2} = \lim_{n \rightarrow \infty} \frac{1}{n} \ln |\alpha_q|, q = 1, 2.$$

Here,  $\alpha_q$ ,  $q = 1, 2$  are the two eigenvalues of the product matrix  $\alpha = \prod_{p=1}^n \xi_p$ , and  $\xi_p$  is the Jacobian matrix of the system calculated at the point  $(x_p, y_p)$  at the  $p$ -th iteration. These two exponents can be rearranged such that  $\lambda_1 \geq \lambda_2$ . If the Lyapunov exponent is positive, the system is chaotic. In contrast, a negative Lyapunov exponent suggests that the system is periodic, and if the Lyapunov exponent is equal to zero, the system manifests quasi-periodic behavior. We vary the parameter space  $(\gamma \times \mathcal{K})$  to construct the

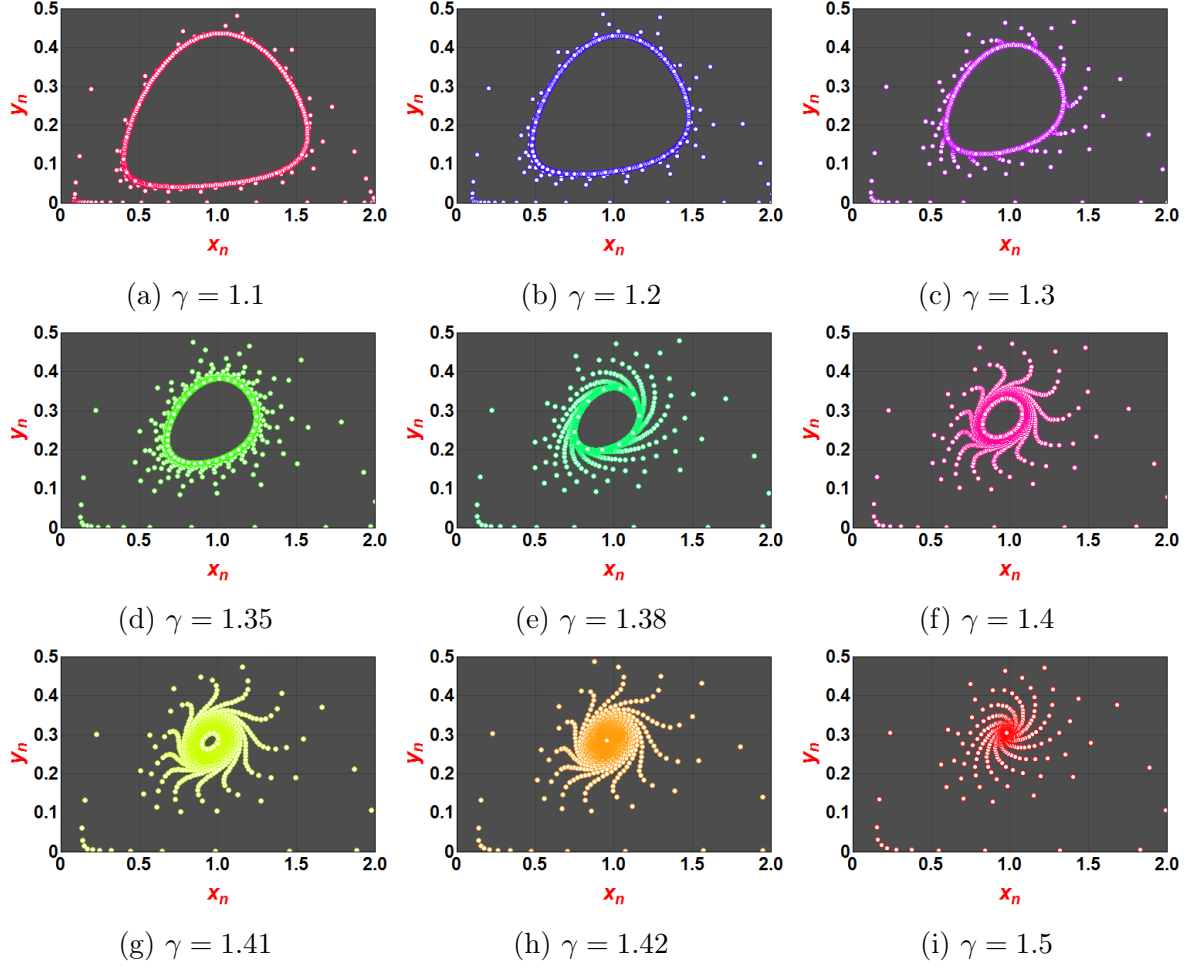


Figure 3.10: Phase plots for different  $\gamma$  values.

Lyapunov exponent while fixing the other parameters. This approach will enable us to gain valuable insights into the system's behavior and understand how it evolves.

In Figure 3.11(a), we can see the graphical representation of the Lyapunov exponent, which indicates the complex dynamics of the model (3.1.5). To generate these plots, we chose  $F = 0.82$ ,  $\Lambda = 0.16$ ,  $\mu = 0.95$ ,  $\omega = 2.54$ ,  $\zeta = 0.04$ ,  $\beta = 4.31$ ,  $\theta = 1.0$ , and  $\delta = 4.81$ , with  $(2.0, 2.8)$  as the system's initial values. The plots confirm the model's chaotic and periodic regimes. Moving on to Plot 3.11 (b), we observe the period-doubling bifurcation phenomenon of the model in the rectangular space  $[2.3, 2.9] \times [0.01, 13]$ . Figure 3.11 (a) further confirms the occurrence of period-doubling bifurcation, with the Lyapunov exponent values labeled in the color bar with different colors indicating the additional weight of the Lyapunov exponent.

From our analysis, we found that the increase in the intrinsic growth rate of the prey population with less carrying capacity leads to chaos in the system. Looking at Figure 3.11, we concluded that when there is less growth of the prey, the system is less chaotic

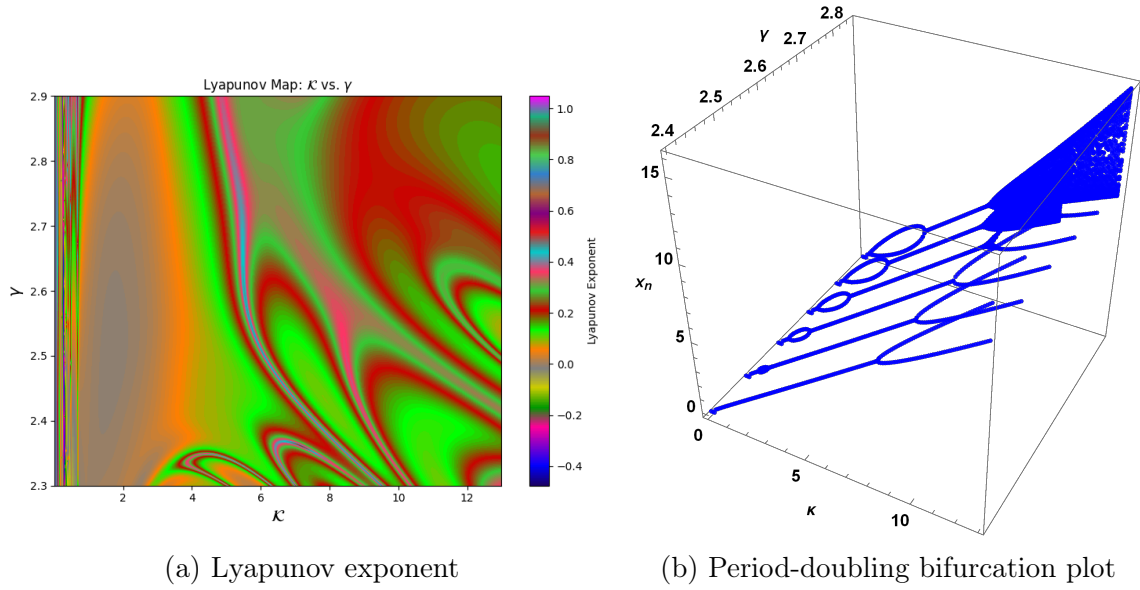


Figure 3.11: The Lyapunov exponent and the two-parameter bifurcation diagrams for the system (3.1.5).

at the fixed carrying capacity. However, if the growth rate increases, then the chaoticness of the system rises at the same carrying capacity, which is also biologically accurate.

To mitigate the chaos, various approaches can be adopted, such as introducing predators in the population to maintain the prey population, prey harvesting, migration of prey species, etc. In the next section, we will present a technique for adopting these approaches through a controlled parameter.

### 3.7 Chaos control

The idea of chaos control is to suppress or eliminate any chaotic aspects while keeping the system operational as desired. Several chaos control strategies have been developed to maintain stability in chaotic systems. Managing population dynamics and other complex systems where chaos can lead to unpredictable behavior is made easier with the help of these strategies. This section emphasizes the benefits of using chaotic control techniques over traditional management methods and the importance of doing so in our prey-predator context. By stabilizing the system and preventing bifurcation, these strategies can substantially impact conservation and population management activities.

Some authors confirm the existence of chaos in a system using the Lyapunov exponent [111]. However, some use mathematical techniques to prove that chaos exists in a system, [112]. According to some authors, period-doubling bifurcation confirms chaos in the system. Using the arguments in [111], in this article, we also use the Lyapunov exponent

in Section 3.6.1 that shows there is chaos in the system

So, different control techniques are used to delay or eliminate the chaotic dynamics of any population model. Recently, some used methods can be seen in the articles ([113], [114], [115], and [116]). We used a simple hybrid control feedback technique here. This control strategy stabilizes the system and avoids bifurcation by combining parameter perturbation and feedback control. The comparable controlled system is presented below:

$$\begin{cases} x_{n+1} = \Psi_1 x_n \exp \left[ \frac{\gamma}{1+F y_n} \left( 1 - \frac{x_n}{\mathcal{K}} \right) \frac{x_n}{x_n + \Lambda} - \frac{\mu y_n}{x_n + \omega} - \zeta \right] + (1 - \Psi_1) x_n, \\ y_{n+1} = \Psi_1 y_n \exp \left[ \frac{\mu \beta x_n}{x_n + \omega} - \theta - \delta y_n \right] + (1 - \Psi_1) y_n. \end{cases} \quad (3.7.1)$$

where  $\Psi \in (0, 1)$  is the controlled parameter, and in (3.7.1), feedback control and parameter perturbation are combined in the controlled approach. Selecting an appropriate controlled parameter,  $\Psi_1$ , allows us to prevent, delay, or enhance chaos in the controlled system. The controlled system's Jacobian matrix  $\mathcal{C}_{control}$ , which was evaluated at  $(\hat{x}, \hat{y})$ , is presented below:

$$\mathcal{C}_{control} = \begin{pmatrix} \hat{x} \left( \frac{\gamma(\mathcal{K}\Lambda - \hat{x}(2\Lambda + \hat{x}))}{(\Lambda + \hat{x})^2(F\hat{y}\kappa + \mathcal{K})} + \frac{\mu\hat{y}}{(\omega + \hat{x})^2} \right) \Psi_1 + 1 & \hat{x} \left( \frac{\gamma F \hat{x}(\hat{x} - \mathcal{K})}{\mathcal{K}(\Lambda + \hat{x})(F\hat{y} + 1)^2} - \frac{\mu}{\omega + \hat{x}} \right) \Psi_1 \\ \frac{\beta\mu\omega\hat{y}\Psi_1}{(\omega + \hat{x})^2} & 1 - \delta\hat{y}\Psi_1 \end{pmatrix}.$$

To get the stability of the model, we have to modify the control parameter  $\Psi_1$  values so that the eigenvalues of the matrix  $\mathcal{C}_{control}$  lie within an open unit disc. The main goal of controlling chaotic dynamics in biological systems is to prevent excess resources or the extinction of entire species. This can be performed in prey-predator models by stabilizing populations at a sustainable level, a handling purpose that has biological validity. Furthermore, the controlled system can study how various control measures affect the dynamics of prey-predator relationships. For instance, you can examine the efficacy of different management techniques, such as eliminating predators or providing more resources for prey, by changing the value of  $\Psi_1$ .

## 3.8 Conclusion

The prey and predator populations are taken into account in this model. In our model's assumptions, prey increases exponentially without predators but declines due to perdition. On the other hand, the predator population grows as it eats the prey population

while decreasing in the absence of prey. A set of coupled differential equations that describe the seasonal changes of the two populations governs the model. The chosen values of the critical parameters significantly impact how the model behaves. These additional details are: Important novel insights about the behavior of ecological systems have been gained from examining the two-dimensional prey-predator model. The stability analysis of the fixed points in both the discrete and continuous forms of the model has led to a deeper understanding of the system's dynamics.

Additionally, multi-parameter bifurcations were investigated, including a bifurcation between two parameters that had never been observed before for this model. By studying the Lyapunov exponents, we better understand the complex behavior and sensitivity of the initial conditions. The study has analyzed the forward and backward Hopf, Neimark-Sacker, and period-doubling bifurcations with various parameters. A greater comprehension of the system's dynamics has resulted from the stability analysis of the fixed points in both the discrete and continuous forms of the model. The investigation of the periodic solutions also included a previously unidentified behavior of the model.

Based on bi-parameter analysis, we discovered that the system becomes chaotic when the intrinsic growth rate of the prey population increases relative to its carrying capacity. We deduced from the graphical analysis that the system is less chaotic when the prey grows slower at the fixed carrying capacity. On the other hand, the system becomes more disorganized at the same carrying capacity if the growth rate increases. The bifurcations in the system cause significant fluctuations in predator and prey species, so these results have significant consequences for controlling ecological systems. A simple control method is also suggested in the article for managing the chaos in the system. Given how sensitive environmental systems are to even the most minor changes in their parameters, this method is quite helpful in preserving their stability.

Controlling the bifurcation may significantly affect how ecological systems are maintained, especially in population conservation and sustainability management activities. The high population density of the prey population during periods when the Allee and fear effects are weak might also result in an unstable prey-predator system. These findings have significant consequences for ecological modeling, enabling us to manage and protect natural ecosystems with knowledge, especially in the context of changing environmental conditions and upcoming dangers.



## Chapter 4

# Fixed points stability, multi-parameter bifurcation analysis, and chaos control of a prey-predator model incorporating the Allee effect and fear effect

### 4.1 Introduction

This chapter has been published, and its published version can be obtained from the reference [117]. Ecologists have been very interested in how predators and prey interact for a long time. They often use a well-known model called the Lotka-Volterra model to understand these interactions. Ecologists can better understand how these complicated relationships perform within the natural world by including the fear and Allee effects in studying predator-prey interactions along with the Lotka-Volterra model. According to current research, the fear and Allee effects have been found to have a major impact on population dynamics. The fear effect, first proposed by [87], refers to the phenomenon where prey exhibits increased vigilance and decreased activity when predators are present. By engaging in this behavior, there is a chance that fewer prey-predator contacts will occur, which will eventually result in reduced predator attacks. On the other hand, the Allee effect, first proposed by [4], refers to the concept that there is a population density below which a species cannot survive due to lower reproductive success or higher mortality. Allee studied population fluctuations and discovered the Allee effect, which is when the birth rate decreases while the death rate increases if the population density is too low. Recent studies have highlighted the importance of incorporating these additional factors into prey-predator models. Prey-predator models may produce more accurate and realis-

tic forecasts of population dynamics by including these extra variables. However, ongoing research is still into how these elements affect the model's stability and bifurcation. The stability and bifurcation of a prey-predator model that includes both the fear effect and the Allee effect will be investigated in this chapter. We will investigate the effects of these extra variables on the prey-predator system's dynamics using a mathematical approach. One can find many works to study such effects in the literature, including some interesting results discussed here.

Huang et al. [89] studied the Allee effect, a fear effect, and prey refuge on a prey-predator model. They proved the complexity of the model by increasing the Allee effect, or prey refuge. Additionally, they demonstrated that the Allee or fear effect can reduce the predator density at positive fixed points but does not affect the prey density. Lai et al. [90] examined fear and the additive Allee effect to analyze the dynamic behavior of a prey-predator model. By adding the fear impact on the prey species, they discovered that the density of predator species decreased with increasing fear effect strength. The final prey density is unaffected by the fear effect, though. Xie [91] examined the impact of Allee and the fear effect on a prey-predator model with a Holling type-II functional response. In addition to observing that the system encounters Hopf bifurcation, the author also deduced the requirements for the stability of fixed points. The fear effect was also found to boost the stability of the positive fixed point of the system by rejecting periodic solutions, and the Allee effect also significantly impacted the persistence of the predator species. Li et al. [92] studied the dynamical analysis of a prey-predator model under the influence of the fear effect, weak Allee effect, and delay. They established the stability requirements and demonstrated the model's potential to bifurcate. They increase the realism of the model by including the gestation delay. Their research indicates that the Allee effect and the delay weaken the model; however, the fear effect can encourage stable coexistence.

Many environmental factors might cause the Allee effect, including the inability to mate at low densities, genetic inbreeding, social favoritism of reproduction, low mate success rates, declining inbreeding rates, etc. Recently, there has been a surge in interest among scientists in researching the effects of including the Allee effect in prey-predator dynamics. By comparing the dynamical features of the logistic prey growth term in the ratio-dependent prey-predator model with and without the Allee effect, the authors [34] demonstrated that the Allee effect might be used to eliminate the oscillation behavior of species densities. Furthermore, the causes of various bifurcation behaviors were deduced and quantitatively confirmed using parametric diagrams and phase plots. The authors [93] examined the same discrete-time model and demonstrated how changing the integral step size might lead to period doubling and an invariant circle to produce chaotic orbits. Liange et al. [94] work on a Leslie-type model with a ratio-dependent type interaction

term and state-impulsive feedback control. They use the geometry theory of differential equations to determine the conditions for existence, uniqueness, and orbital asymptotic stability of the periodic solution of order 1. The authors [95] demonstrated the limit cycle dynamics of a prey-predator model of the Leslie type with fear and the Allee effect. They demonstrated that the system exhibited saddle-node bifurcation through numerical examples and validated their theoretical findings. [96], these authors examined the intricate dynamics of a Leslie-Gower prey-predator model that is ratio-dependent and includes the Allee and fear effects. The Allee effect and the fear effect are considered in the model, which can have significant implications for population growth. Here, we elaborate on the mathematical model and the presumptions made. From the article by [56], we have the following model:

$$\begin{cases} \frac{dx}{dt} = \alpha x \left(1 - \frac{x}{K}\right) - \frac{\beta xy}{x+\mathcal{L}}, \\ \frac{dy}{dt} = \gamma y + \frac{\xi \beta xy}{x+\mathcal{L}} - \theta y^2. \end{cases} \quad (4.1.1)$$

First, introduce the fear effect in the model (4.1.1). The fear effect, also known as predator avoidance behavior, is presented in prey-predator models to more accurately reflect the behavior of animals in the wild. In nature, prey animals often exhibit behaviors that help them avoid or escape predators, such as running or hiding. Such behaviors may significantly affect the dynamics of both prey and predator populations. By considering the impact of fear in a prey-predator model, scientists can better understand how these behaviors influence the populations of different species and how they interact with one another. To introduce the fear effect, we have to add the term  $\frac{1}{1+Fy}$  in the model (4.1.1), which represents the fear effect with parameter  $F$  as a level of fear. Thus, by adding the fear effect, the model (4.1.1) becomes:

$$\begin{cases} \frac{dx}{dt} = \frac{\alpha x}{1+Fy} \left(1 - \frac{x}{K}\right) - \frac{\beta xy}{x+\mathcal{L}}, \\ \frac{dy}{dt} = \gamma y + \frac{\xi \beta xy}{x+\mathcal{L}} - \theta y^2. \end{cases} \quad (4.1.2)$$

The model will now include the Allee effect (4.1.2). The Allee effect is a term used in population ecology to describe a phenomenon where the growth rate of the population decreases as the population density becomes too low. For this, let  $\mathcal{U}(A, x)$  be the fertility of a species with  $x$  adults in an isolated patch. Fertility increases with population density, the description of which is:

$$\mathcal{U}(A, x) = \frac{\alpha x}{x + A}, \quad (4.1.3)$$

where  $\alpha$  denotes the inherent growth rates of the prey population and  $x$  is the prey population density at time  $t$ ,  $A > 0$  represents the level of Allee, which can determine how much of an impact Allee has on the prey.  $\mathcal{U}(A, x)$  satisfied  $\lim_{A \rightarrow +\infty} \mathcal{U}(A, x) = 0$ ,

$\lim_{x \rightarrow 0} \mathcal{U}(A, x) = 0$ ,  $\lim_{A \rightarrow 0} \mathcal{U}(A, x) = \alpha$ ,  $\lim_{x \rightarrow +\infty} \mathcal{U}(A, x) = \alpha$ ,  $\frac{\partial \mathcal{U}(A, x)}{\partial A} < 0$ . More details regarding the Allee effect are in the article by [99]. Thus, the model (4.1.2) with the Allee effect becomes:

$$\begin{cases} \frac{dx}{dt} = \frac{\alpha x}{1+Fx} \left(1 - \frac{x}{K}\right) \frac{x}{x+A} - \frac{\beta xy}{x+\mathcal{L}}, \\ \frac{dy}{dt} = \gamma y + \frac{\xi \beta xy}{x+\mathcal{L}} - \theta y^2. \end{cases} \quad (4.1.4)$$

Thus, our desired model is a system (4.1.4). Here,  $x$  and  $y$  reflect the densities of prey and predator populations, respectively;  $\alpha$  and  $\beta$  indicate the inherent growth rates of the relevant prey and predator, and  $\gamma$  indicates the growth rate of the predator as a result of substitute resources. Moreover,  $\theta$  indicates a conflict between individuals of predator species when overcrowding is occurring (i.e., crowding effect);  $\mathcal{L}$  stands for the half-saturation constant;  $\xi$  shows the predator conversion rate; and  $K$  indicates the prey's carrying capacity in a specific ecosystem. The fear effect in the model (4.1.4) can be analyzed from the plot 4.1.

The discretization of the continuous-time model is crucial from a biological perspective because it permits the simulation of predator-prey dynamics over discrete time scales, allowing for easier comparison with actual population data and more efficient incorporation of time-sensitive ecological components. Therefore, we intend to discuss the dynamics of the model (4.1.4) in both discrete and continuous form. For this purpose, we use the piece-wise constant argument to convert the above system (4.1.4) into discrete format as follows:

$$\begin{cases} x_{n+1} = x_n \exp \left[ \frac{\alpha}{1+Fx_n} \left(1 - \frac{x_n}{K}\right) \frac{x_n}{x_n+A} - \frac{\beta y_n}{x_n+\mathcal{L}} \right], \\ y_{n+1} = y_n \exp \left[ \gamma + \frac{\xi \beta x_n}{x_n+\mathcal{L}} - \theta y_n \right]. \end{cases} \quad (4.1.5)$$

Here, we make the following assumptions: All the biological parameters are positive, while the populations of both prey and predators must remain non-negative. We will enforce this constraint in the initial conditions and throughout the simulation. The prey population exhibits logistic growth, wherein it experiences an exponential increase proportionate to its present size but eventually levels off as it nears the carrying capacity  $K$  of the ecosystem. The model contains intra and inter-species interactions, representing the complicated relationship between prey and predator populations through conflicts caused by overcrowding and dynamics between predators and prey. Resources other than prey can cause the predator population to increase. This shows the ability of predators to find additional food sources during periods of low prey populations. The prey population growth should saturate as it approaches the carrying capacity  $K$ . The

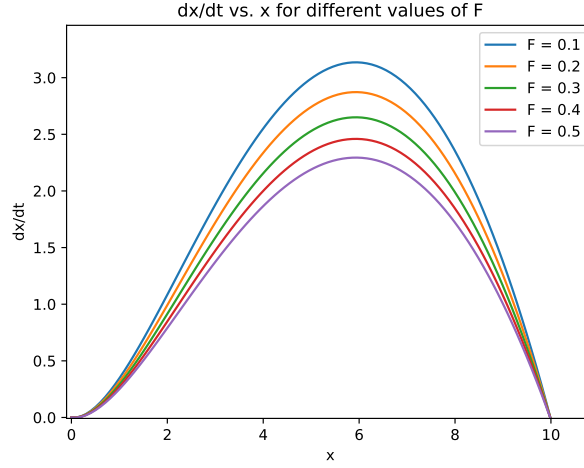


Figure 4.1: Fear effect for  $\alpha = 2.65$ ,  $K = 10$ ,  $A = 5$ ,  $\beta = 0.02$ ,  $\mathcal{L} = 0.3$ , and  $y = 1$ .

chapter is vital because we present a detailed mathematical model incorporating the fear and Allee effects. It will help us better understand the complex relationships between prey populations and predators. Here, we present an in-depth study of multi-parameter bifurcations. The findings have important implications for ecological system management and preservation. Detailed numerical examples are included, and mathematical proofs are used to support our theoretical conclusions. This study will contribute to the growing body of literature on the effects of additional factors on prey-predator dynamics and provide valuable insights for those working in ecology and preservation. Now, we will discuss the critical results related to the fixed points of systems (4.1.4) and (4.1.5).

## 4.2 Positivity and uniform boundedness of the solutions

**Theorem 4.2.1.** *Let  $(x(0), y(0)) > 0$ , then the solution of the system (4.1.4) uniquely exists and is positive for all  $t \geq 0$ .*

*Proof.* Since the right-hand side of the system (4.1.4) is continuous and locally Lipschitzian in  $\mathbb{R}_+^2$ , the solution of the system (4.1.4) exists uniquely in  $[0, \mathcal{I})$  where  $0 < \mathcal{I} \leq \infty$ . Thus, we have:

$$\begin{cases} x(t) = x(0) \exp \left[ \int_0^t \left\{ \frac{\alpha}{1+Fy(\xi)} \left( 1 - \frac{x(\xi)}{K} \right) \frac{x(\xi)}{x(\xi)+A} - \frac{\beta y(\xi)}{x(\xi)+\mathcal{L}} \right\} d\xi \right] > 0, \\ y(t) = y(0) \exp \left[ \int_0^t \left\{ \gamma + \frac{\xi \beta x(\xi)}{x(\xi)+\mathcal{L}} - \theta y(\xi) \right\} d\xi \right] > 0. \end{cases} \quad (4.2.1)$$

□

**Theorem 4.2.2.** *The prey population of the system (4.1.4) is uniformly bounded in  $\mathbb{R}$ .*

*Proof.* From the first differential equation of (4.1.4), we have:

$$\begin{aligned}\frac{dx}{dt} &\leq \alpha x \left(1 - \frac{x}{K}\right), \\ \implies \lim_{t \rightarrow \infty} \sup x(t) &\leq K.\end{aligned}$$

□

Now, we will show that every solution of the system (4.1.5) is bounded.

**Lemma 4.2.3.** ([74]) *Suppose that  $s_t$  satisfies  $s_0 > 0$  and  $s_{t+1} \leq s_t \exp[c(1 - ds_t)]$  for  $t \in [0, \infty]$ , where  $d > 0$  is a constant. Then  $\lim_{t \rightarrow \infty} \sup s_t \leq \frac{1}{cd} \exp(c - 1)$ .*

**Lemma 4.2.4.** *Every positive solution  $(x_n, y_n)$  of the system (4.1.5) is uniformly bounded.*

*Proof.* Let  $(x_n, y_n)$  be the positive solution of (4.1.5) with starting population  $(x_0, y_0) > 0$ . Then we have:

$$x_{n+1} \leq x_n \exp \left[ \alpha \left(1 - \frac{x_n}{K}\right) \right], \quad (4.2.2)$$

for all  $n = 0, 1, 2, \dots$ . From Lemma 4.2.3, we have

$$\lim_{n \rightarrow \infty} \sup x_n \leq \frac{K}{\alpha} \exp(\alpha - 1) := \Pi_1.$$

Similarly, we have

$$\begin{aligned}y_{n+1} &\leq y_n \exp [\gamma + \xi \beta x_n - \theta y_n] \\ &\leq y_n \exp [\gamma + \xi \beta \Pi_1 - \theta y_n] \\ &= y_n \exp (\gamma + \xi \beta \Pi_1) \left[ 1 - \frac{\theta}{\gamma + \xi \beta \Pi_1} y_n \right].\end{aligned} \quad (4.2.3)$$

From Lemma 4.2.3, we have

$$\lim_{n \rightarrow \infty} \sup y_n \leq \frac{1}{\theta} \exp(\gamma + \xi \beta \Pi_1 - 1) := \Pi_2.$$

Thus, it shows that  $\lim_{n \rightarrow \infty} \sup (x_n, y_n) \leq \Pi$ , where  $\Pi = \max[\Pi_1, \Pi_2]$ . Hence, the proof is completed. □

### 4.3 Stability of the fixed points

The fixed point  $(\bar{x}, \bar{y})$  of the model (4.1.4) can be obtained by solving the equations that follow:

$$\begin{cases} 0 = \frac{\alpha\bar{x}}{1+F\bar{y}} \left(1 - \frac{\bar{x}}{K}\right) \frac{\bar{x}}{x_n+A} - \frac{\beta\bar{x}\bar{y}}{\bar{x}+\mathcal{L}}, \\ 0 = \gamma\bar{y} + \frac{\xi\beta\bar{x}\bar{y}}{\bar{x}+\mathcal{L}} - \theta\bar{y}^2. \end{cases}$$

These equations yield the following fixed points:  $E_{Trivial} = (0, 0)$ ,  $E_{Prey} = (K, 0)$ ,  $E_{Predator} = (0, \frac{\gamma}{\theta})$ , and  $E_{Positive} = (\bar{x}, \bar{y})$ .

**Lemma 4.3.1.** *The fixed point  $E_{Trivial}(0, 0)$  of system (4.1.4) is unstable.*

*Proof.* The variational matrix  $\Pi_{Trivial}$  of system (4.1.4) at  $E_{Trivial}(0, 0)$  is given below:

$$\Pi_{Trivial}(0, 0) = \begin{pmatrix} 0 & 0 \\ 0 & \gamma \end{pmatrix}. \quad (4.3.1)$$

The latent roots of (4.3.1) are:  $\Theta_{\{a,b\}} = \{0, \gamma\}$ . Thus  $E_{Trivial}(0, 0)$  is unstable.  $\square$

**Lemma 4.3.2.** *The fixed point  $E_{Prey} = (K, 0)$  of (4.1.4) is a saddle point.*

*Proof.* The variational matrix  $\Pi_{Prey}$  of system (4.1.4) at  $E_{Prey} = (K, 0)$  is given below:

$$\Pi_{Prey}(K, 0) = \begin{pmatrix} -\frac{\alpha K}{A+K} & -\frac{\beta K}{\mathcal{L}+K} \\ 0 & \gamma + \frac{\beta K \xi}{\mathcal{L}+K} \end{pmatrix}. \quad (4.3.2)$$

From (4.3.2) we have latent roots:

$$\Theta_{\{a,b\}} = \left\{ -\frac{\alpha K}{A+K}, \frac{\beta K \xi + \gamma K + \gamma \mathcal{L}}{K + \mathcal{L}} \right\}.$$

Now, it is easy to see that  $E_{Prey} = (K, 0)$  is always a saddle point.  $\square$

**Lemma 4.3.3.** *The fixed point  $E_{Predator} = (0, \frac{\gamma}{\theta})$  is a sink.*

*Proof.* At  $E_{Predator} = (0, \frac{\gamma}{\theta})$ , we have the following variational matrix:

$$\Pi_{Predator}\left(0, \frac{\gamma}{\theta}\right) = \begin{pmatrix} -\frac{\beta\gamma}{\mathcal{L}\theta} & 0 \\ \frac{\beta\gamma\xi}{\mathcal{L}\theta} & -\gamma \end{pmatrix}. \quad (4.3.3)$$

The eigenvalues are  $\{-\gamma, -\frac{\beta\gamma}{\theta\mathcal{L}}\}$ . Using stability criteria, we can see that  $E_{Predator} = (0, \frac{\gamma}{\theta})$  is always a sink.  $\square$

At  $(\bar{x}, \bar{y})$ , the Jacobian matrix of the system (4.1.4) is obtained by

$$J(\bar{x}, \bar{y}) = \begin{pmatrix} \nu_{11} & \bar{x} \left( \frac{\alpha F \bar{x} (\bar{x} - K)}{K(A + \bar{x})(F\bar{y} + 1)^2} - \frac{\beta}{\mathcal{L} + \bar{x}} \right) \\ \frac{\mathcal{L}\beta\xi\bar{y}}{(\mathcal{L} + \bar{x})^2} & \gamma - 2\theta\bar{y} + \frac{\beta\xi\bar{x}}{\mathcal{L} + \bar{x}} \end{pmatrix},$$

where

$$\nu_{11} = \frac{\alpha\bar{x}(2AK + \bar{x}(-3A + K - 2\bar{x}))}{(A + \bar{x})^2(F\bar{y}K + K)} - \frac{\mathcal{L}\beta\bar{y}}{(\mathcal{L} + \bar{x})^2}.$$

The characteristic function is:

$$\Omega(\Theta) = \Theta^2 + (\Omega_{Tr})\Theta + \Omega_{Det},$$

where,

$$\begin{aligned} \Omega_{Tr} &= \left( \frac{\mathcal{L}\beta\bar{y}}{(\mathcal{L} + \bar{x})^2} - \frac{\alpha\bar{x}(2AK + \bar{x}(-3A + K - 2\bar{x}))}{(A + \bar{x})^2(F\bar{y}K + K)} \right) \\ &\quad - \left( \gamma - 2\theta\bar{y} + \frac{\beta\xi\bar{x}}{\mathcal{L} + \bar{x}} \right), \end{aligned} \quad (4.3.4)$$

and

$$\begin{aligned} \Omega_{Det} &= \left( \frac{\alpha\bar{x}(2AK + \bar{x}(-3A + K - 2\bar{x}))}{(A + \bar{x})^2(F\bar{y}K + K)} - \frac{\mathcal{L}\beta\bar{y}}{(\mathcal{L} + \bar{x})^2} \right) \\ &\quad \left( \gamma - 2\theta\bar{y} + \frac{\beta\xi\bar{x}}{\mathcal{L} + \bar{x}} \right) \\ &\quad - \left( \bar{x} \left( \frac{\alpha F \bar{x} (\bar{x} - K)}{K(A + \bar{x})(F\bar{y} + 1)^2} - \frac{\beta}{\mathcal{L} + \bar{x}} \right) \right) \left( \frac{\mathcal{L}\beta\xi\bar{y}}{(\mathcal{L} + \bar{x})^2} \right). \end{aligned}$$

**Theorem 4.3.4.**  $E_{Positive} = (\bar{x}, \bar{y})$  is locally asymptotically stable if  $\Omega_{Tr} > 0$  and  $\Omega_{Det} > 0$ .

We will discuss the stability of the fixed points in the system (4.1.5). By resolving the following equations, the fixed points of the model (4.1.5) can be determined:

$$\begin{cases} \bar{x} = \bar{x} \exp \left[ \frac{\alpha}{1+F\bar{y}} \left( 1 - \frac{\bar{x}}{K} \right) \frac{\bar{x}}{\bar{x}+A} - \frac{\beta\bar{y}}{\bar{x}+\mathcal{L}} \right], \\ \bar{y} = \bar{y} \exp \left[ \gamma + \frac{\xi\beta\bar{x}}{\bar{x}+\mathcal{L}} - \theta\bar{y} \right]. \end{cases}$$

These equations yield the following fixed point:

$$E_{Trivial}^* = (0, 0), E_{Prey}^* = (K, 0), E_{Predator}^* = \left( 0, \frac{\gamma}{\theta} \right), \text{ and } E_{Positive}^* = (\bar{x}, \bar{y}).$$

**Lemma 4.3.5.** The fixed point  $E_{Trivial}^*(0, 0)$  of system (4.1.5) is unstable.



*Proof.* The variational matrix  $\Pi_{Trivial}^*$  of system (4.1.5) at  $E_{Trivial}^*(0,0)$  is given below:

$$\Pi_{Trivial}^*(0,0) = \begin{pmatrix} 1 & 0 \\ 0 & e^\gamma \end{pmatrix}. \quad (4.3.5)$$

The latent roots of (4.3.5) are:  $\Theta_{\{a,b\}}^* = \{1, e^\gamma\}$ . Using the Jury stability criterion, it is easy to see that  $E_{Trivial}^*(0,0)$  is unstable.  $\square$

**Lemma 4.3.6.** *The fixed point  $E_{Prey}^* = (K, 0)$  of (4.1.5) is a*

- (I) *source if  $\alpha > \frac{2A+2K}{K}$ ,*
- (II) *saddle point if  $0 < \alpha < \frac{2A+2K}{K}$ .*

*Proof.* The variational matrix  $\Pi_{Prey}^*$  of system (4.1.5) at  $E_{Prey}^* = (K, 0)$  is given below:

$$\Pi_{Prey}^*(K,0) = \begin{pmatrix} 1 - \frac{\alpha K}{A+K} & -\frac{\beta K}{\mathcal{L}+K} \\ 0 & e^{\gamma + \frac{\beta K \xi}{\mathcal{L}+K}} \end{pmatrix}. \quad (4.3.6)$$

From (4.3.6) we have latent roots:  $\Theta_{\{a,b\}}^* = \left\{ e^{\gamma + \frac{\beta K \xi}{\mathcal{L}+K}}, \frac{A+K-\alpha K}{A+K} \right\}$ . Using Jury conditions, it is easy to see that  $E_{Prey}^* = (K, 0)$  is a source if  $\alpha > \frac{2A+2K}{K}$ , saddle point if  $0 < \alpha < \frac{2A+2K}{K}$ . The topological classification of  $E_{Prey}^* = (K, 0)$  is given in Figure 4.2.  $\square$

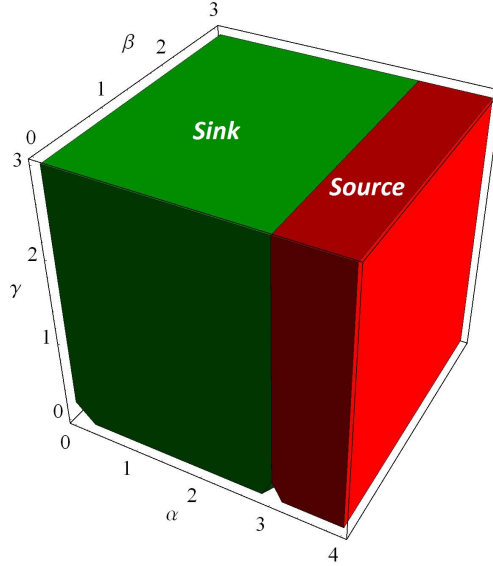


Figure 4.2: Topological classification of  $E_{Prey}^* = (K, 0)$ .

**Lemma 4.3.7.** *The fixed point  $E_{Predator}^* = (0, \frac{\gamma}{\theta})$  is a*

- (I) *sink if  $0 < \gamma < 2$ ,*

(II) saddle if  $\gamma > 2$ ,

(III) non-hyperbolic if  $\gamma = 2$ .

*Proof.* At  $E_{Predator}^* = (0, \frac{\gamma}{\theta})$  we have the following variational matrix:

$$\Pi_{Predator}^* \left(0, \frac{\gamma}{\theta}\right)^* = \begin{pmatrix} e^{-\frac{\beta\gamma}{A\theta}} & 0 \\ \frac{\beta\gamma\xi}{\mathcal{L}\theta} & 1 - \gamma \end{pmatrix}. \quad (4.3.7)$$

For (4.3.7), the subsequent is our latent roots for characteristic function:

$$\Theta_{\{a,b\}}^* = \left\{1 - \gamma, e^{-\frac{\beta\gamma}{A\theta}}\right\}.$$

Using Jury stability criteria, we can see that  $E_{Predator}^* = (0, \frac{\gamma}{\theta})$  is a sink if  $0 < \gamma < 2$ , saddle point if  $\gamma > 2$ , and non-hyperbolic if  $\gamma = 2$ . Figure 4.3 displays the topological classification of  $E_{Predator}^* = (0, \frac{\gamma}{\theta})$ .  $\square$

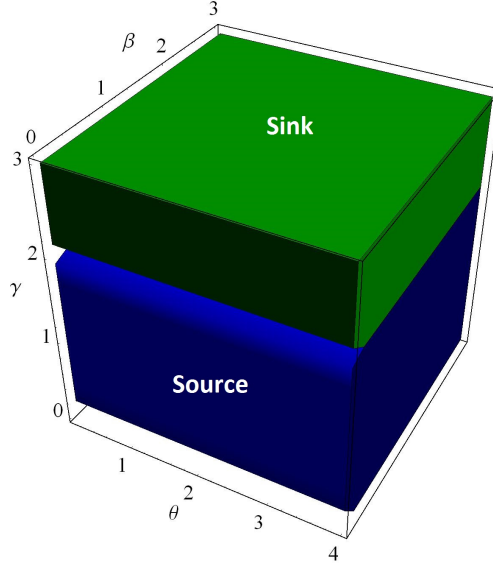


Figure 4.3: Topological classification of  $E_{Predator}^* = (0, \frac{\gamma}{\theta})$ .

At  $(\bar{x}, \bar{y})$  the Jacobian matrix of the system (4.1.5) is obtained by

$$J(\bar{x}, \bar{y}) = \begin{pmatrix} \tau_{11} & \bar{x} \left( \frac{\alpha F \bar{x} (\bar{x} - K)}{K(A + \bar{x})(F\bar{y} + 1)^2} - \frac{\beta}{\mathcal{L} + \bar{x}} \right) \\ \frac{\mathcal{L}\beta\xi\bar{y}}{(\mathcal{L} + \bar{x})^2} & 1 - \theta\bar{y} \end{pmatrix},$$

where

$$\tau_{11} = \bar{x} \left( \frac{\alpha(AK - \bar{x}(2A + \bar{x}))}{(A + \bar{x})^2(F\bar{y}K + K)} + \frac{\beta\bar{y}}{(\mathcal{L} + \bar{x})^2} \right) + 1.$$

The characteristic function is:

$$\Omega(\Theta) = \Theta^2 - (\Omega_{Tr})\Theta + \Omega_{Det},$$

where,

$$\begin{aligned}\Omega_{Tr} &= \frac{\alpha\bar{x}(AK - \bar{x}(\bar{x} + 2A))}{(\bar{x} + A)^2(KF\bar{y} + K)} + \bar{y}\left(\frac{\beta\bar{x}}{(\bar{x} + \mathcal{L})^2} - \theta\right) + 2, \\ \text{and} \\ \Omega_{Det} &= \left(\bar{x}\left(\frac{\alpha(AK - \bar{x}(2A + \bar{x}))}{(A + \bar{x})^2(F\bar{y}K + K)} + \frac{\beta\bar{y}}{(\mathcal{L} + \bar{x})^2}\right) + 1\right)(1 \\ &\quad - \theta\bar{y}) - \left(\bar{x}\left(\frac{\alpha F\bar{x}(\bar{x} - K)}{K(A + \bar{x})(F\bar{y} + 1)^2} - \frac{\beta}{\mathcal{L} + \bar{x}}\right)\right)\left(\frac{\mathcal{L}\beta\xi\bar{y}}{(\mathcal{L} + \bar{x})^2}\right).\end{aligned}$$

The stability conditions can now be calculated using the Routh-Hurwitz criterion. Thus, we have the following theorem:

**Theorem 4.3.8.** *The fixed point  $(\bar{x}, \bar{y})$  of system (4.1.5) is a*

- Ca :** *Source iff  $|\Omega_{Det}| > 1$ , and  $|\Omega_{Tr}| < |1 + \Omega_{Det}|$ ,*
- Cb :** *Saddle point iff  $(\Omega_{Tr})^2 > 4(\Omega_{Det})$ , and  $|\Omega_{Tr}| > |1 + \Omega_{Det}|$ ,*
- Cc :** *Non-hyperbolic point iff  $|\Omega_{Tr}| = |1 + \Omega_{Det}|$ , or  $\Omega_{Det} = 1$ , and  $\Omega_{Tr} \leq 2$ .*
- Cd :** *If condition Cc does not hold then  $(\bar{x}, \bar{y})$  is a sink iff  $|\Omega_{Tr}| < 1 + \Omega_{Det} < 2$ .*

## 4.4 Bifurcation analysis

Tracing the bifurcation in all parameters of a prey-predator model is essential because it allows scientists to understand how small changes in specific parameters can significantly change the system's overall behavior. Bifurcations occur when a slight change in a parameter causes the system to transition from one stable state to another. These transitions can be used to identify critical thresholds, or "tipping points," beyond which the system can no longer return to its original state. In the context of a prey-predator model, bifurcations can reveal how changes in the environment, such as changes in the prey or predator populations, can affect the system's dynamics. For example, a slight increase in the predator population may cause a bifurcation in the prey population, leading to a significant decline in prey animals. This information can be used to develop conservation strategies that target specific parameters and preserve the balance of the ecosystem. In addition, by identifying bifurcations in all parameters, scientists can understand how different parts of a system are interconnected and how they interact. This can help identify potential sources of instability in the system and inform management decisions that aim

to maintain the stability of the ecosystem. In this chapter, we will also examine the bifurcation at different parameters. For simplicity, we will present theoretical calculations by choosing one bifurcation parameter. Similarly, one can also find the theoretical results for other parameters.

For Hopf bifurcation, we observed the limit cycles of both discrete and continuous models. It has been noted that Hopf bifurcation produces adjacent invariant circles. Alternatively, some isolated orbits with periodic behavior can be found along with trajectories that densely cover the consistent circle ([98]). If a stable, closed, constant curve exists, the bifurcation can be supercritical; otherwise, it can be sub-critical. A slight modification in a parametric factor during flip bifurcation leads the system to adopt a new behavior with twice the period of the initial system. We have only noticed the flip bifurcation in the system (4.1.5). For interested readers to study further results on Hopf and flip bifurcations, relevant papers include those by [118], [100], [101], [102], [19], [103], [111], [112], [113], and [114]. Some recent work related to advances in the related bifurcations and their application areas is provided by [115] and [116]. We have the following criteria for these two types of bifurcation: The variational matrix of (4.1.5) at  $(\bar{x}, \bar{y})$  is:

$$J(\bar{x}, \bar{y}) = \begin{pmatrix} \tau_{11} & \bar{x} \left( \frac{\alpha F \bar{x} (\bar{x} - K)}{K(A + \bar{x})(F\bar{y} + 1)^2} - \frac{\beta}{\mathcal{L} + \bar{x}} \right) \\ \frac{\mathcal{L}\beta\xi\bar{y}}{(\mathcal{L} + \bar{x})^2} & 1 - \theta\bar{y} \end{pmatrix},$$

where

$$\tau_{11} = \bar{x} \left( \frac{\alpha(AK - \bar{x}(2A + \bar{x}))}{(A + \bar{x})^2(F\bar{y}K + K)} + \frac{\beta\bar{y}}{(\mathcal{L} + \bar{x})^2} \right) + 1.$$

The characteristic function is:

$$\Omega(\Gamma) = \Gamma^2 - (\Omega_{Tr})\Gamma + \Omega_{Det}, \quad (4.4.1)$$

where,

$$\begin{aligned} \Omega_{Tr} &= \frac{\alpha\bar{x}(AK - \bar{x}(\bar{x} + 2A))}{(\bar{x} + A)^2(KF\bar{y} + K)} + \bar{y} \left( \frac{\beta\bar{x}}{(\bar{x} + \mathcal{L})^2} - \theta \right) + 2, \\ \text{and} \\ \Omega_{Det} &= \left( \bar{x} \left( \frac{\alpha(AK - \bar{x}(2A + \bar{x}))}{(A + \bar{x})^2(F\bar{y}K + K)} + \frac{\beta\bar{y}}{(\mathcal{L} + \bar{x})^2} \right) + 1 \right) (1 \\ &\quad - \theta\bar{y}) - \left( \bar{x} \left( \frac{\alpha F \bar{x} (\bar{x} - K)}{K(A + \bar{x})(F\bar{y} + 1)^2} - \frac{\beta}{\mathcal{L} + \bar{x}} \right) \right) \left( \frac{\mathcal{L}\beta\xi\bar{y}}{(\mathcal{L} + \bar{x})^2} \right). \end{aligned}$$

Let  $(\Omega_{Tr})^2 > 4\Omega_{Det}$ , and  $(\Omega_{Tr}) + \Omega_{Det} = -1$ , then it follows that:

$$\begin{aligned}
\alpha &= \left[ K (\bar{x} + A)^2 (F\bar{y} + 1)^2 (\bar{y}(\bar{x}(2\bar{x}(\theta\bar{x} - \beta + 3\theta\mathcal{L}) + \mathcal{L}(6\theta\mathcal{L} - \beta(\beta\xi + 2))) + 2\theta\mathcal{L}^3) + \right. \\
&\quad \left. \beta\theta\bar{x}\bar{y}^2 (\bar{x} + \mathcal{L}) - 4(\bar{x} + \mathcal{L})^3 \right) \left] \left[ \frac{1}{\tilde{P}} \right], \text{ where} \\
\tilde{P} &= \bar{x}(\bar{x} + \mathcal{L}) \left( \bar{y} \left( \bar{x} \left( \bar{x} \left( \bar{x}(\theta - 2F) - F(4(A + \mathcal{L}) + \beta\xi\mathcal{L}) + 2\theta(A + \mathcal{L})) + A(-K(\theta \right. \right. \right. \\
&\quad \left. \left. \left. - 2F) - \mathcal{L}F(\beta\xi + 8) + 4\theta\mathcal{L}) + \mathcal{L}(\beta K\xi F + \mathcal{L}(\theta - 2F)) \right) + A\mathcal{L}(KF(\beta\xi + 4) - 2\theta K \right. \right. \\
&\quad \left. \left. + 2\mathcal{L}(\theta - 2F)) \right) - AK\mathcal{L}^2(\theta - 2F) \right) + \theta F\bar{y}^2 (\bar{x} + \mathcal{L})^2 (2A\bar{x} + \bar{x}^2 - AK) \\
&\quad \left. - 2(\bar{x} + \mathcal{L})^2 (2A\bar{x} + \bar{x}^2 - AK) \right).
\end{aligned}$$

For the above value of  $\alpha$ , the roots of (4.4.1) are  $\Gamma_1 = -1$  and  $\Gamma_2 \neq 1$ . Now for the above value of  $\alpha$ , consider the following set:

$$\begin{aligned}
F_{B1} &= \left\{ (\alpha, F, K, \beta, A, \gamma, \xi, \mathcal{L}, \theta) \in \mathbb{R}_+^9 : (\Omega_{Tr})^2 > \right. \\
&\quad \left. 4\Omega_{Det}, (\Omega_{Tr}) + \Omega_{Det} = -1, \text{ and } |\Gamma_2| \neq 1 \right\}.
\end{aligned}$$

When the parameters vary in the small neighborhood of the set  $F_{B1}$ , then the flip bifurcation occurs in the system (4.1.5) at  $(\bar{x}, \bar{y})$ . Considering the arbitrary parameters  $(\alpha = \alpha_1, F, K, \beta, A, \gamma, \xi, \mathcal{L}, \theta) \in F_{B1}$ , then in terms of these parameters, the system (4.1.5) can be written as:

$$\begin{cases} x_{n+1} \rightarrow x_n \exp \left[ \frac{\alpha_1}{1+F y_n} \left( 1 - \frac{x_n}{K} \right) \frac{x_n}{x_n+A} - \frac{\beta y_n}{x_n+\mathcal{L}} \right], \\ y_{n+1} \rightarrow y_n \exp \left[ \gamma + \frac{\xi \beta x_n}{x_n+\mathcal{L}} - \theta y_n \right]. \end{cases} \quad (4.4.2)$$

Consider the perturbation of (4.4.2) as below:

$$\begin{cases} x_{n+1} \rightarrow x_n \exp \left[ \frac{\alpha_1 + \bar{\alpha}}{1+F y_n} \left( 1 - \frac{x_n}{K} \right) \frac{x_n}{x_n+A} - \frac{\beta y_n}{x_n+\mathcal{L}} \right], \\ y_{n+1} \rightarrow y_n \exp \left[ \gamma + \frac{\xi \beta x_n}{x_n+\mathcal{L}} - \theta y_n \right]. \end{cases} \quad (4.4.3)$$

Let  $u = x - \bar{x}$  and  $v = y - \bar{y}$ . The transformation of the positive fixed point of (4.4.3) to

its origin gives us the following system:

$$\begin{cases} u \rightarrow \varrho_{11}u + \varrho_{12}v + \varrho_{13}u^2 + \varrho_{14}uv + \varrho_{15}v^2 + \varrho_{16}u^3 + \varrho_{17}u^2v + \varrho_{18}uv^2 + \varrho_{19}v^3 + \varsigma_{11}\bar{\alpha}u \\ + \varsigma_{12}\bar{\alpha}v + \varsigma_{13}\bar{\alpha}^2 + \varsigma_{14}uv\bar{\alpha} + \varsigma_{15}u^2\bar{\alpha} + \varsigma_{16}v^2\bar{\alpha} + \varsigma_{17}u\bar{\alpha}^2 + \varsigma_{18}v\bar{\alpha}^2 + \varsigma_{19}\bar{\alpha}^3 + O(u, v, \bar{\alpha})^4, \\ v \rightarrow \varrho_{21}u + \varrho_{22}v + \varrho_{23}u^2 + \varrho_{24}uv + \varrho_{25}v^2 + \varrho_{26}u^3 + \varrho_{27}u^2v + \varrho_{28}uv^2 + \varrho_{29}v^3 \\ + O(u, v, \bar{\alpha})^4, \end{cases} \quad (4.4.4)$$

where

$$\left\{ \begin{aligned} \varrho_{11} &= \bar{x} \left( \frac{\alpha_1(AK - \bar{x}(\bar{x} + 2A))}{(\bar{x} + A)^2(KF\bar{y} + K)} + \frac{\beta\bar{y}}{(\bar{x} + \mathcal{L})^2} \right) + 1, \varrho_{12} = \bar{x} \left( \frac{\alpha_1 F \bar{x}(\bar{x} - K)}{K(\bar{x} + A)(F\bar{y} + 1)^2} - \frac{\beta}{\bar{x} + \mathcal{L}} \right), \\ \varrho_{13} &= \frac{\alpha_1(AK - \bar{x}(\bar{x} + 2A))}{(\bar{x} + A)^2(KF\bar{y} + K)} + \frac{1}{2}\bar{x} \left( -\frac{2\alpha_1 A(A + K)}{(\bar{x} + A)^3(KF\bar{y} + K)} + \left( \frac{\alpha_1(AK - \bar{x}(\bar{x} + 2A))}{(\bar{x} + A)^2(KF\bar{y} + K)} \right. \right. \\ &\quad \left. \left. + \frac{\beta\bar{y}}{(\bar{x} + \mathcal{L})^2} \right)^2 - \frac{2\beta\bar{y}}{(\bar{x} + \mathcal{L})^3} \right) + \frac{\beta\bar{y}}{(\bar{x} + \mathcal{L})^2}, \varrho_{14} = \frac{\alpha_1 F \bar{x}(\bar{x} - K)}{K(\bar{x} + A)(F\bar{y} + 1)^2} \\ &\quad + \bar{x} \left( \frac{\alpha_1 F(2A\bar{x} + \bar{x}^2 - AK)}{K(\bar{x} + A)^2(F\bar{y} + 1)^2} + \left( \frac{\alpha_1 F \bar{x}(\bar{x} - K)}{K(\bar{x} + A)(F\bar{y} + 1)^2} - \frac{\beta}{\bar{x} + \mathcal{L}} \right) \left( \frac{\alpha_1(AK - \bar{x}(\bar{x} + 2A))}{(\bar{x} + A)^2(KF\bar{y} + K)} \right. \right. \\ &\quad \left. \left. + \frac{\beta\bar{y}}{(\bar{x} + \mathcal{L})^2} \right) + \frac{\beta}{(\bar{x} + \mathcal{L})^2} \right) - \frac{\beta}{\bar{x} + \mathcal{L}}, \varrho_{15} = \frac{1}{2}\bar{x} \left( \frac{2\alpha_1 F^2 \bar{x}(1 - \frac{\bar{x}}{K})}{(\bar{x} + A)(F\bar{y} + 1)^3} + \right. \\ &\quad \left( \frac{\alpha_1 F \bar{x}(K - \bar{x})}{K(\bar{x} + A)(F\bar{y} + 1)^2} + \frac{\beta}{\bar{x} + \mathcal{L}} \right)^2 \Bigg), \varrho_{16} = \frac{1}{6} \left( -\frac{6\alpha_1 A(A + K)}{(\bar{x} + A)^3(KF\bar{y} + K)} + \right. \\ &\quad \left. 3 \left( \frac{\alpha_1(AK - \bar{x}(\bar{x} + 2A))}{(\bar{x} + A)^2(KF\bar{y} + K)} + \frac{\beta\bar{y}}{(\bar{x} + \mathcal{L})^2} \right)^2 + 4\bar{x} \left( -\frac{\alpha_1 A(A + K)}{(\bar{x} + A)^3(KF\bar{y} + K)} - \frac{\beta\bar{y}}{(\bar{x} + \mathcal{L})^3} \right) \right. \\ &\quad \left( \frac{\alpha_1(AK - \bar{x}(\bar{x} + 2A))}{(\bar{x} + A)^2(KF\bar{y} + K)} + \frac{\beta\bar{y}}{(\bar{x} + \mathcal{L})^2} \right) + \bar{x} \left( -\frac{2\alpha_1 A(A + K)}{(\bar{x} + A)^3(KF\bar{y} + K)} + \right. \\ &\quad \left( \frac{\alpha_1(AK - \bar{x}(\bar{x} + 2A))}{(\bar{x} + A)^2(KF\bar{y} + K)} + \frac{\beta\bar{y}}{(\bar{x} + \mathcal{L})^2} \right)^2 - \frac{2\beta\bar{y}}{(\bar{x} + \mathcal{L})^3} \Bigg) \left( \frac{\alpha_1(AK - \bar{x}(\bar{x} + 2A))}{(\bar{x} + A)^2(KF\bar{y} + K)} \right. \\ &\quad \left. + \frac{\beta\bar{y}}{(\bar{x} + \mathcal{L})^2} \right) + 6\bar{x} \left( \frac{\alpha_1 A(A + K)}{(\bar{x} + A)^4(KF\bar{y} + K)} + \frac{\beta\bar{y}}{(\bar{x} + \mathcal{L})^4} \right) - \frac{6\beta\bar{y}}{(\bar{x} + \mathcal{L})^3} \Bigg), \\ \varrho_{17} &= \left( \frac{\alpha_1(-2A\bar{x} - \bar{x}^2 + AK)}{K(\bar{x} + A)^2(F\bar{y} + 1)} + \frac{\beta\bar{y}}{(\bar{x} + \mathcal{L})^2} \right) \left( \frac{\alpha_1 F \bar{x}(\bar{x} - K)}{K(\bar{x} + A)(F\bar{y} + 1)^2} - \frac{\beta}{\bar{x} + \mathcal{L}} \right) \\ &\quad + \left( \frac{\beta}{(\bar{x} + \mathcal{L})^2} - \frac{\alpha_1 F(-2A\bar{x} - \bar{x}^2 + AK)}{K(\bar{x} + A)^2(F\bar{y} + 1)^2} \right) + \frac{1}{2}\bar{x} \left( \left( 2 \left( \frac{\alpha_1(-2A\bar{x} - \bar{x}^2 + AK)}{K(\bar{x} + A)^2(F\bar{y} + 1)} \right. \right. \right. \end{aligned} \right.$$

$$\begin{aligned}
& + \frac{\beta \bar{y}}{(\bar{x} + \mathcal{L})^2} \left( \left( \frac{\beta}{(\bar{x} + \mathcal{L})^2} - \frac{\alpha_1 F(-2A\bar{x} - \bar{x}^2 + AK)}{K(\bar{x} + A)^2(F\bar{y} + 1)^2} \right) + 2 \left( \frac{\alpha_1 A F(A + K)}{K(\bar{x} + A)^3(F\bar{y} + 1)^2} - \right. \right. \\
& \left. \left. \frac{\beta}{(\bar{x} + \mathcal{L})^3} \right) \right) + \left( \frac{\alpha_1 F \bar{x}(\bar{x} - K)}{K(\bar{x} + A)(F\bar{y} + 1)^2} - \frac{\beta}{\bar{x} + \mathcal{L}} \right) \left( \left( \frac{\alpha_1(-2A\bar{x} - \bar{x}^2 + AK)}{K(\bar{x} + A)^2(F\bar{y} + 1)} + \frac{\beta \bar{y}}{(\bar{x} + \mathcal{L})^2} \right)^2 \right. \\
& \left. + 2 \left( -\frac{\alpha_1 A(A + K)}{K(\bar{x} + A)^3(F\bar{y} + 1)} - \frac{\beta \bar{y}}{(\bar{x} + \mathcal{L})^3} \right) \right), \varrho_{18} = \frac{1}{2} \left( \frac{2\alpha_1 F^2 \bar{x}(1 - \frac{\bar{x}}{K})}{(\bar{x} + A)(F\bar{y} + 1)^3} + \left( \frac{\alpha_1 F \bar{x}(\bar{x} - K)}{K(\bar{x} + A)(F\bar{y} + 1)^2} \right. \right. \\
& \left. \left. - \frac{\beta}{\bar{x} + \mathcal{L}} \right)^2 \right) + \bar{x} \left( \frac{\alpha_1 F^2(-2A\bar{x} - \bar{x}^2 + AK)}{K(\bar{x} + A)^2(F\bar{y} + 1)^3} + \frac{1}{2} \left( \frac{\alpha_1(-2A\bar{x} - \bar{x}^2 + AK)}{K(\bar{x} + A)^2(F\bar{y} + 1)} + \frac{\beta \bar{y}}{(\bar{x} + \mathcal{L})^2} \right) \right. \\
& \left( \frac{2\alpha_1 F^2 \bar{x}(1 - \frac{\bar{x}}{K})}{(\bar{x} + A)(F\bar{y} + 1)^3} + \left( \frac{\alpha_1 F \bar{x}(\bar{x} - K)}{K(\bar{x} + A)(F\bar{y} + 1)^2} - \frac{\beta}{\bar{x} + \mathcal{L}} \right)^2 \right) + \left( \frac{\alpha_1 F \bar{x}(\bar{x} - K)}{K(\bar{x} + A)(F\bar{y} + 1)^2} - \frac{\beta}{\bar{x} + \mathcal{L}} \right) \\
& \left( \frac{\beta}{(\bar{x} + \mathcal{L})^2} - \frac{\alpha_1 F(-2A\bar{x} - \bar{x}^2 + AK)}{K(\bar{x} + A)^2(F\bar{y} + 1)^2} \right) \Bigg), \varrho_{19} = \left( -\frac{\bar{x}}{6K^3(\bar{x} + A)^3(\bar{x} + \mathcal{L})^3(F\bar{y} + 1)^6} \right) \\
& \left( 4\alpha_1 K F^2 \bar{x}(\bar{x} + A)(K - \bar{x})(\bar{x} + \mathcal{L})^2(F\bar{y} + 1) \left( \beta K(\bar{x} + A)(F\bar{y} + 1)^2 \right. \right. \\
& \left. \left. + \alpha_1 F \bar{x}(K - \bar{x})(\bar{x} + \mathcal{L}) \right) + \left( \beta K(\bar{x} + A)(F\bar{y} + 1)^2 + \alpha_1 F \bar{x}(K - \bar{x})(\bar{x} + \mathcal{L}) \right) \right. \\
& \left( \left( \beta K(\bar{x} + A)(F\bar{y} + 1)^2 + \alpha_1 F \bar{x}(K - \bar{x})(\bar{x} + \mathcal{L}) \right)^2 + 2\alpha_1 K F^2 \bar{x}(\bar{x} + A)(K - \bar{x}) \right. \\
& \left. (\bar{x} + \mathcal{L})^2(F\bar{y} + 1) \right) + 6\alpha_1 K^2 F^3 \bar{x}(\bar{x} + A)^2(K - \bar{x})(\bar{x} + \mathcal{L})^3(F\bar{y} + 1)^2 \Bigg), \\
& \stackrel{S_{11}}{=} \frac{\bar{x}((\bar{x} + A)(1 - \frac{\bar{x}}{K}) - \frac{\bar{x}(\bar{x} + 2A)}{K} + \bar{x}(\bar{x} + A)(1 - \frac{\bar{x}}{K}) \left( \frac{\alpha_1(AK - \bar{x}(\bar{x} + 2A))}{(\bar{x} + A)^2(KF\bar{y} + K)} + \frac{\beta \bar{y}}{(\bar{x} + \mathcal{L})^2} \right) + A)}{(\bar{x} + A)^2(F\bar{y} + 1)}, \\
& \stackrel{S_{12}}{=} \frac{\bar{x}^2(\bar{x} - K) \left( \frac{K(\bar{x} + A)(F\bar{y} + 1)(F\bar{x} + \beta F\bar{y} + \beta + \mathcal{L}F)}{\bar{x} + \mathcal{L}} + \alpha_1 F \bar{x}(K - \bar{x}) \right)}{K^2(\bar{x} + A)^2(F\bar{y} + 1)^3}, \\
& \stackrel{S_{13}}{=} \frac{\bar{x}^3(K - \bar{x})^2}{2K^2(\bar{x} + A)^2(F\bar{y} + 1)^2}, \quad S_{14} = \left( -\frac{1}{K^3(\bar{x} + A)^4(\bar{x} + \mathcal{L})^3(F\bar{y} + 1)^4} \right) \left( \bar{x} \left( K(\bar{x} + A)^2(K - \bar{x}) \right. \right. \\
& (\bar{x} + \mathcal{L})^2(F\bar{y} + 1) \left( \beta K(\bar{x} + A)(F\bar{y} + 1)^2 + \alpha_1 F \bar{x}(K - \bar{x})(\bar{x} + \mathcal{L}) \right) + K(\bar{x} + A) \\
& (\bar{x} + \mathcal{L})^2(F\bar{y} + 1)(AK - \bar{x}(\bar{x} + 2A)) \left( \beta K(\bar{x} + A)(F\bar{y} + 1)^2 + \alpha_1 F \bar{x}(K - \bar{x}) \right. \\
& (\bar{x} + \mathcal{L}) \Big) - K \bar{x}(\bar{x} + A)(K - \bar{x})(\bar{x} + \mathcal{L})(F\bar{y} + 1) \left( \beta K(\bar{x} + A)^2(F\bar{y} + 1)^2 + \right. \\
& \alpha_1 F(\bar{x} + \mathcal{L})^2(2A\bar{x} + \bar{x}^2 - AK) \Big) + \bar{x}(K - \bar{x}) \left( K(\bar{x} + A)(F\bar{y} + 1) \left( F\bar{x} + \beta F\bar{y} \right. \right. \\
& \left. \left. + \beta + \mathcal{L}F \right) + \alpha_1 F \bar{x}(K - \bar{x})(\bar{x} + \mathcal{L}) \right) \left( \beta K \bar{y}(\bar{x} + A)^2(F\bar{y} + 1) - \alpha_1(\bar{x} + \mathcal{L})^2 \right. \\
& \left. (2A\bar{x} + \bar{x}^2 - AK) \right) + K^2 F(\bar{x} + A)^2(\bar{x} + \mathcal{L})^3(F\bar{y} + 1)^2(AK - \bar{x}(\bar{x} + 2A)) \\
& \left. \left. + F(\bar{x} + A)^3(K - \bar{x})(\bar{x} + \mathcal{L})^3(KF\bar{y} + K)^2 \right) \right), \quad S_{15} = \frac{-2A\bar{x} - \bar{x}^2 + AK}{K(\bar{x} + A)^2(F\bar{y} + 1)} \\
& + \frac{1}{2} \bar{x} \left( \left( \frac{2(-2A\bar{x} - \bar{x}^2 + AK) \left( \frac{\alpha_1(-2A\bar{x} - \bar{x}^2 + AK)}{K(\bar{x} + A)^2(F\bar{y} + 1)} + \frac{\beta \bar{y}}{(\bar{x} + \mathcal{L})^2} \right)}{K(\bar{x} + A)^2(F\bar{y} + 1)} - \frac{2A(A + K)}{K(\bar{x} + A)^3(F\bar{y} + 1)} \right) + \right. \\
& \left. \frac{\bar{x}(1 - \frac{\bar{x}}{K}) \left( \left( \frac{\alpha_1(-2A\bar{x} - \bar{x}^2 + AK)}{K(\bar{x} + A)^2(F\bar{y} + 1)} + \frac{\beta \bar{y}}{(\bar{x} + \mathcal{L})^2} \right)^2 + 2 \left( -\frac{\alpha_1 A(A + K)}{K(\bar{x} + A)^3(F\bar{y} + 1)} - \frac{\beta \bar{y}}{(\bar{x} + \mathcal{L})^3} \right) \right)}{(\bar{x} + A)(F\bar{y} + 1)} \right) +
\end{aligned}$$

$$\left\{ \begin{aligned}
& \frac{\bar{x}\left(1-\frac{\bar{x}}{K}\right)\left(\frac{\alpha_1(-2A\bar{x}-\bar{x}^2+AK)}{K(\bar{x}+A)^2(F\bar{y}+1)}+\frac{\beta\bar{y}}{(\bar{x}+\mathcal{L})^2}\right)}{(\bar{x}+A)(F\bar{y}+1)}, \varsigma_{16} = \left(\frac{1}{2K^3(\bar{x}+A)^3(\bar{x}+\mathcal{L})^2(F\bar{y}+1)^5}\right) \left(\bar{x}^2(K-\bar{x}) \right. \\
& \left(2KF(\bar{x}+A)(\bar{x}+\mathcal{L})(F\bar{y}+1)(\beta K(\bar{x}+A)(F\bar{y}+1)^2+\alpha_1 F\bar{x}(K-\bar{x})(\bar{x}+\mathcal{L})) \right. \\
& \left. +(\beta K(\bar{x}+A)(F\bar{y}+1)^2+\alpha_1 F\bar{x}(K-\bar{x})(\bar{x}+\mathcal{L}))^2+2\alpha_1 KF^2\bar{x}(\bar{x}+A) \right. \\
& \left. (K-\bar{x})(\bar{x}+\mathcal{L})^2(F\bar{y}+1)+2K^2F^2(\bar{x}+A)^2(\bar{x}+\mathcal{L})^2(F\bar{y}+1)^2\right) \Bigg), \\
\varsigma_{17} &= \left(\frac{1}{2(\bar{x}+A)^4(\bar{x}+\mathcal{L})^2(KF\bar{y}+K)^3}\right) \left(\bar{x}^2(K-\bar{x}) \left(\bar{x}(K-\bar{x}) \left(\beta K\bar{y}(\bar{x}+A)^2(F\bar{y}+1) \right. \right. \right. \\
& \left. \left. -\alpha_1(\bar{x}+\mathcal{L})^2(2A\bar{x}+\bar{x}^2-AK)\right) +K(\bar{x}+A)^2(K-\bar{x})(\bar{x}+\mathcal{L})^2(F\bar{y}+1) \right. \\
& \left. \left. +2K(\bar{x}+A)(\bar{x}+\mathcal{L})^2(F\bar{y}+1)(AK-\bar{x}(\bar{x}+2A))\right)\right), \\
\varsigma_{18} &= -\frac{\bar{x}^3(K-\bar{x})^2(K(\bar{x}+A)(F\bar{y}+1)(2F\bar{x}+\beta F\bar{y}+\beta+2\mathcal{L}F)+\alpha_1 F\bar{x}(K-\bar{x})(\bar{x}+\mathcal{L}))}{2K^3(\bar{x}+A)^3(\bar{x}+\mathcal{L})(F\bar{y}+1)^4}, \\
\varsigma_{19} &= \frac{\bar{x}^4\left(1-\frac{\bar{x}}{K}\right)^3}{6(\bar{x}+A)^3(F\bar{y}+1)^3}, \varrho_{21} = \frac{\beta\xi\mathcal{L}\bar{y}}{(\bar{x}+\mathcal{L})^2}, \varrho_{22} = 1-\theta\bar{y}, \varrho_{23} = \frac{\beta\xi\mathcal{L}\bar{y}(\mathcal{L}(\beta\xi-2)-2\bar{x})}{2(\bar{x}+\mathcal{L})^4}, \\
\varrho_{24} &= \frac{\beta\xi\mathcal{L}(1-\theta\bar{y})}{(\bar{x}+\mathcal{L})^2}, \varrho_{25} = \frac{1}{2}\theta(\theta\bar{y}-2), \varrho_{26} = \frac{\beta\xi\mathcal{L}\bar{y}(6\bar{x}(\bar{x}+\mathcal{L}(2-\beta\xi))+\mathcal{L}^2(\beta\xi(\beta\xi-6)+6))}{6(\bar{x}+\mathcal{L})^6}, \\
\varrho_{27} &= -\frac{\beta\xi\mathcal{L}(\theta\bar{y}-1)(\mathcal{L}(\beta\xi-2)-2\bar{x})}{2(\bar{x}+\mathcal{L})^4}, \varrho_{28} = \frac{\beta\theta\xi\mathcal{L}(\theta\bar{y}-2)}{2(\bar{x}+\mathcal{L})^2}, \varrho_{29} = \frac{1}{2}\theta(\theta\bar{y}-2).
\end{aligned} \right.$$

If  $T = \begin{pmatrix} \varrho_{12} & \varrho_{12} \\ -1-\varrho_{11} & \Gamma_2-\varrho_{11} \end{pmatrix}$  be a non-singular matrix, then consider the following translation:

$$\begin{pmatrix} u \\ v \end{pmatrix} = T \begin{pmatrix} \tilde{x} \\ \tilde{y} \end{pmatrix}. \quad (4.4.5)$$

Taking  $T^{-1}$  on both sides of (4.4.5), we get

$$\begin{pmatrix} \tilde{x} \\ \tilde{y} \end{pmatrix} \rightarrow \begin{pmatrix} -1 & 0 \\ 0 & \Gamma_2 \end{pmatrix} \begin{pmatrix} \tilde{x} \\ \tilde{y} \end{pmatrix} + \begin{pmatrix} f(u, v, \bar{\alpha}) \\ g(u, v, \bar{\alpha}) \end{pmatrix}, \quad (4.4.6)$$

$$\begin{aligned}
f(u, v, \bar{\alpha}) &= \frac{(\Gamma_2 - \varrho_{11}) \varsigma_{19} \bar{\alpha}^3}{\varrho_{12} (\Gamma_2 + 1)} + \frac{(\Gamma_2 - \varrho_{11}) \varsigma_{17} \bar{\alpha}^2 u}{\varrho_{12} (\Gamma_2 + 1)} + \frac{(\Gamma_2 - \varrho_{11}) \varsigma_{18} \bar{\alpha}^2 v}{\varrho_{12} (\Gamma_2 + 1)} \\
&+ \frac{(\Gamma_2 - \varrho_{11}) \varsigma_{13} \bar{\alpha}^2}{\varrho_{12} (\Gamma_2 + 1)} + \frac{(\Gamma_2 - \varrho_{11}) \varsigma_{15} \bar{\alpha} u^2}{\varrho_{12} (\Gamma_2 + 1)} + \frac{(\Gamma_2 - \varrho_{11}) \varsigma_{14} \bar{\alpha} v u}{\varrho_{12} (\Gamma_2 + 1)} \\
&+ \frac{(\Gamma_2 - \varrho_{11}) \varsigma_{11} i \bar{\alpha}}{\varrho_{12} (\Gamma_2 + 1)} + \frac{(\Gamma_2 - \varrho_{11}) \varsigma_{16} \bar{\alpha} v^2}{\varrho_{12} (\Gamma_2 + 1)} + \frac{(\Gamma_2 - \varrho_{11}) \varsigma_{12} v \bar{\alpha}}{\varrho_{12} (\Gamma_2 + 1)} \\
&+ \left( \frac{(\Gamma_2 - \varrho_{11}) \varrho_{16}}{\varrho_{12} (\Gamma_2 + 1)} - \frac{\varrho_{26}}{\Gamma_2 + 1} \right) u^3 + \left( \frac{(\Gamma_2 - \varrho_{11}) \varrho_{17}}{\varrho_{12} (\Gamma_2 + 1)} - \frac{\varrho_{27}}{\Gamma_2 + 1} \right) \\
&(v u^2) + \left( \frac{(\Gamma_2 - \varrho_{11}) \varrho_{13}}{\varrho_{12} (\Gamma_2 + 1)} - \frac{\varrho_{23}}{\Gamma_2 + 1} \right) u^2 + \left( \frac{(\Gamma_2 - \varrho_{11}) \varrho_{18}}{\varrho_{12} (\Gamma_2 + 1)} - \frac{\varrho_{28}}{\Gamma_2 + 1} \right)
\end{aligned}$$



$$\begin{aligned}
& v^2 u + \left( \frac{(\Gamma_2 - \varrho_{11}) \varrho_{14}}{\varrho_{12} (\Gamma_2 + 1)} - \frac{\varrho_{24}}{\Gamma_2 + 1} \right) uv + \left( \frac{(\Gamma_2 - \varrho_{11}) \varrho_{19}}{\varrho_{12} (\Gamma_2 + 1)} - \frac{\varrho_{29}}{\Gamma_2 + 1} \right) v^3 \\
& + \left( \frac{(\Gamma_2 - \varrho_{11}) \varrho_{15}}{\varrho_{12} (\Gamma_2 + 1)} - \frac{\varrho_{25}}{\Gamma_2 + 1} \right) v^2, \\
g(u, v, \bar{\alpha}) = & \frac{(1 + \varrho_{11}) \varsigma_{19} \bar{\alpha}^3}{\varrho_{12} (\Gamma_2 + 1)} + \frac{(1 + \varrho_{11}) \varsigma_{17} \bar{\alpha}^2 u}{\varrho_{12} (\Gamma_2 + 1)} + \frac{(1 + \varrho_{11}) \varsigma_{18} \bar{\alpha}^2 v}{\varrho_{12} (\Gamma_2 + 1)} \\
& + \frac{(1 + \varrho_{11}) \varsigma_{13} \bar{\alpha}^2}{\varrho_{12} (\Gamma_2 + 1)} + \frac{(1 + \varrho_{11}) \varsigma_{15} \bar{\alpha} u^2}{\varrho_{12} (\Gamma_2 + 1)} + \frac{(1 + \varrho_{11}) \varsigma_{14} \bar{\alpha} v u}{\varrho_{12} (\Gamma_2 + 1)} \\
& + \frac{(1 + \varrho_{11}) \varsigma_{11} u \bar{\alpha}}{\varrho_{12} (\Gamma_2 + 1)} + \frac{(1 + \varrho_{11}) \varsigma_{16} \bar{\alpha} v^2}{\varrho_{12} (\Gamma_2 + 1)} + \frac{(1 + \varrho_{11}) \varsigma_{12} v \bar{\alpha}}{\varrho_{12} (\Gamma_2 + 1)} \\
& + \left( \frac{(1 + \varrho_{11}) \varrho_{16}}{\varrho_{12} (\Gamma_2 + 1)} + \frac{\varrho_{26}}{\Gamma_2 + 1} \right) u^3 + \left( \frac{(1 + \varrho_{11}) \varrho_{17}}{\varrho_{12} (\Gamma_2 + 1)} + \frac{\varrho_{27}}{\Gamma_2 + 1} \right) v u^2 \\
& + \left( \frac{(1 + \varrho_{11}) \varrho_{13}}{\varrho_{12} (\Gamma_2 + 1)} + \frac{\varrho_{23}}{\Gamma_2 + 1} \right) u^2 + \left( \frac{(1 + \varrho_{11}) \varrho_{18}}{\varrho_{12} (\Gamma_2 + 1)} + \frac{\varrho_{28}}{\Gamma_2 + 1} \right) v^2 u \\
& + \left( \frac{(1 + \varrho_{11}) \varrho_{14}}{\varrho_{12} (\Gamma_2 + 1)} + \frac{\varrho_{24}}{\Gamma_2 + 1} \right) uv + \left( \frac{(1 + \varrho_{11}) \varrho_{19}}{\varrho_{12} (\Gamma_2 + 1)} + \frac{\varrho_{29}}{\Gamma_2 + 1} \right) v^3 \\
& + \left( \frac{(1 + \varrho_{11}) \varrho_{15}}{\varrho_{12} (\Gamma_2 + 1)} + \frac{\varrho_{25}}{\Gamma_2 + 1} \right) v^2.
\end{aligned}$$

If we consider  $W^c(0, 0, 0)$  to be the center manifold of (4.4.6) computed at  $(0, 0)$  in a restricted neighborhood of  $\bar{\alpha} = 0$ , we can approximate  $W^c(0, 0, 0)$  as follows:

$$W^c(0, 0, 0) = \{(\tilde{x}, \tilde{y}, \bar{\alpha}) \in R^3 : \tilde{y} = \omega_1 \tilde{x}^2 + \omega_2 \tilde{x} \bar{\alpha} + \omega_3 \bar{\alpha}^2 + O((|\tilde{x}| + |\bar{\alpha}|)^3)\},$$

where,

$$\begin{aligned}
\omega_1 &= - \left[ \frac{1}{\varrho_{12} (\Gamma_2^2 - 1)} \right] \left[ \varrho_{11}^3 \varrho_{15} - \varrho_{11}^2 \varrho_{12} \varrho_{14} + \varrho_{11}^2 \varrho_{12} \varrho_{25} + \varrho_{11} \varrho_{12}^2 \varrho_{13} - \varrho_{11} \varrho_{12}^2 \varrho_{24} \right] \\
&- \left[ \frac{1}{\varrho_{12} (\Gamma_2^2 - 1)} \right] \left[ \varrho_{12}^3 \varrho_{23} + 3 \varrho_{11}^2 \varrho_{15} - 2 \varrho_{11} \varrho_{12} \varrho_{14} + 2 \varrho_{11} \varrho_{12} \varrho_{25} + \varrho_{12}^2 \varrho_{13} - \varrho_{12}^2 \varrho_{24} \right] \\
&- \frac{3 \varrho_{15} \varrho_{11} - \varrho_{12} \varrho_{14} + \varrho_{25} \varrho_{12} + \varrho_{15}}{\varrho_{12} (\Gamma_2^2 - 1)}, \\
\omega_2 &= \frac{(1 + \varrho_{11}) (\varsigma_{12} \varrho_{11} - \varsigma_{11} \varrho_{12} + \varsigma_{12})}{\varrho_{12} (\Gamma_2^2 - 1)}, \\
\omega_3 &= \frac{(1 + \varrho_{11}) \varsigma_{13}}{\varrho_{12} (\Gamma_2 + 1) (-\Gamma_2 + 1)}.
\end{aligned}$$

Consequently, the map that is only applicable to the center manifold  $W^c(0, 0, 0)$  is provided by:

$$F : \quad \tilde{x} \rightarrow -\tilde{x} + \chi_1 \tilde{x}^2 + \chi_2 \tilde{x} \bar{\alpha} + \chi_3 \tilde{x}^2 \bar{\alpha} + \chi_4 \tilde{x} \bar{\alpha}^2 + \chi_5 \tilde{x}^3 + O((|\tilde{x}|, |\bar{\alpha}|)^4),$$

where,

$$\begin{aligned}
\chi_1 &= \left( -\frac{(-\Gamma_2 + \varrho_{11}) \varrho_{13}}{\varrho_{12} (\Gamma_2 + 1)} - \frac{\varrho_{23}}{\Gamma_2 + 1} \right) \varrho_{12}^2 + \left( -\frac{(-\Gamma_2 + \varrho_{11}) \varrho_{14}}{\varrho_{12} (\Gamma_2 + 1)} - \frac{\varrho_{24}}{\Gamma_2 + 1} \right) \\
&\quad (-1 - \varrho_{11}) \varrho_{12} + \left( -\frac{(-\Gamma_2 + \varrho_{11}) \varrho_{15}}{\varrho_{12} (\Gamma_2 + 1)} - \frac{\varrho_{25}}{\Gamma_2 + 1} \right) (-1 - \varrho_{11})^2, \\
\chi_2 &= -\frac{(-\Gamma_2 + \varrho_{11}) \varsigma_{11}}{\Gamma_2 + 1} - \frac{(-\Gamma_2 + \varrho_{11}) \varsigma_{12} (-1 - \varrho_{11})}{\varrho_{12} (\Gamma_2 + 1)}, \\
\chi_3 &= -\frac{(-\Gamma_2 + \varrho_{11}) \varrho_{12} \varsigma_{15}}{\Gamma_2 + 1} - \frac{(-\Gamma_2 + \varrho_{11}) \varsigma_{14} (-1 - \varrho_{11})}{\Gamma_2 + 1} - \frac{(-\Gamma_2 + \varrho_{11}) \varsigma_{11} \omega_1}{\Gamma_2 + 1} \\
&\quad - \frac{(-\Gamma_2 + \varrho_{11}) \varsigma_{16} (-1 - \varrho_{11})^2}{\varrho_{12} (\Gamma_2 + 1)} - \frac{(-\Gamma_2 + \varrho_{11}) \varsigma_{12} (\Gamma_2 - \varrho_{11}) \omega_1}{\varrho_{12} (\Gamma_2 + 1)} \\
&\quad + 2 \left( -\frac{(-\Gamma_2 + \varrho_{11}) \varrho_{13}}{\varrho_{12} (\Gamma_2 + 1)} - \frac{\varrho_{23}}{\Gamma_2 + 1} \right) \varrho_{12}^2 \omega_2 + \left( -\frac{(-\Gamma_2 + \varrho_{11}) \varrho_{14}}{\varrho_{12} (\Gamma_2 + 1)} - \frac{\varrho_{24}}{\Gamma_2 + 1} \right) \\
&\quad (-1 - \varrho_{11}) \varrho_{12} \omega_2 + \left( -\frac{(-\Gamma_2 + \varrho_{11}) \varrho_{14}}{\varrho_{12} (\Gamma_2 + 1)} - \frac{\varrho_{24}}{\Gamma_2 + 1} \right) (\Gamma_2 - \varrho_{11}) \\
&\quad \omega_2 \varrho_{12} + 2 \left( -\frac{(-\Gamma_2 + \varrho_{11}) \varrho_{15}}{\varrho_{12} (\Gamma_2 + 1)} - \frac{\varrho_{25}}{\Gamma_2 + 1} \right) (-1 - \varrho_{11}) (\Gamma_2 - \varrho_{11}) \omega_2, \\
\chi_4 &= -\frac{(-\Gamma_2 + \varrho_{11}) \varsigma_{17}}{\Gamma_2 + 1} - \frac{(-\Gamma_2 + \varrho_{11}) \varsigma_{18} (-1 - \varrho_{11})}{\varrho_{12} (\Gamma_2 + 1)} - \frac{(-\Gamma_2 + \varrho_{11}) \varsigma_{11} \omega_2}{\Gamma_2 + 1} \\
&\quad - \frac{(-\Gamma_2 + \varrho_{11}) \varsigma_{12} (\Gamma_2 - \varrho_{11}) \omega_2}{\varrho_{12} (\Gamma_2 + 1)} + 2 \left( -\frac{(-\Gamma_2 + \varrho_{11}) \varrho_{13}}{\varrho_{12} (\Gamma_2 + 1)} - \frac{\varrho_{23}}{\Gamma_2 + 1} \right) \varrho_{12}^2 \omega_3 \\
&\quad + \left( -\frac{(-\Gamma_2 + \varrho_{11}) \varrho_{14}}{\varrho_{12} (\Gamma_2 + 1)} - \frac{\varrho_{24}}{\Gamma_2 + 1} \right) (-1 - \varrho_{11}) \varrho_{12} \omega_3 \\
&\quad + \left( -\frac{(-\Gamma_2 + \varrho_{11}) \varrho_{14}}{\varrho_{12} (\Gamma_2 + 1)} - \frac{\varrho_{24}}{\Gamma_2 + 1} \right) (\Gamma_2 - \varrho_{11}) \omega_3 \varrho_{12} \\
&\quad + 2 \left( -\frac{(-\Gamma_2 + \varrho_{11}) \varrho_{15}}{\varrho_{12} (\Gamma_2 + 1)} - \frac{\varrho_{25}}{\Gamma_2 + 1} \right) (-1 - \varrho_{11}) (\Gamma_2 - \varrho_{11}) \omega_3, \\
\chi_5 &= -\frac{(-\Gamma_2 + \varrho_{11}) \varsigma_{19}}{\varrho_{12} (\Gamma_2 + 1)} - \frac{(-\Gamma_2 + \varrho_{11}) \varsigma_{11} \omega_3}{\Gamma_2 + 1} - \frac{(-\Gamma_2 + \varrho_{11}) \varsigma_{12} (\Gamma_2 - \varrho_{11}) \omega_3}{\varrho_{12} (\Gamma_2 + 1)}.
\end{aligned}$$

Now, we define the following two discriminatory quantities:

$$\Phi_1 = \left( \frac{\partial^2 F}{\partial \tilde{x} \partial \bar{\alpha}} + \frac{1}{2} \frac{\partial F}{\partial \bar{\alpha}} \frac{\partial^2 F}{\partial \tilde{x}^2} \right)_{(0,0)} = \chi_2,$$

$$\Phi_2 = \left( \frac{1}{6} \frac{\partial^3 F}{\partial \tilde{x}^3} + \left( \frac{1}{2} \frac{\partial^2 F}{\partial \tilde{x}^2} \right)^2 \right)_{(0,0)} = \chi_5 + \chi_1^2.$$

The following theorem is the result of the above discussion:

**Theorem 4.4.1.** *If  $\Phi_1 \neq 0$ , then the system (4.1.5) experiences flip bifurcation at the specific fixed point  $(\bar{x}, \bar{y})$  if  $\Phi_2 \neq 0$  when the parameter varies in the neighborhood of  $\bar{\alpha}$ .*

Additionally, the period-two orbits that split off from  $(\bar{x}, \bar{y})$  are stable if  $\Phi_2 > 0$ ; however, they are unstable if  $\Phi_2 < 0$ .

#### 4.4.1 Hopf bifurcation

The Hopf bifurcation in the continuous-time system (4.1.4) will be studied first. The presence of center points in the corresponding linear system is a requirement for the Hopf bifurcation of a two-dimensional continuous-time nonlinear system. The latent roots of the fixed point of a two-dimensional model are:

$$\Theta_{1,2} = \frac{1}{2} \left[ \mathcal{A} \pm \sqrt{\mathcal{A} - 4\mathcal{B}} \right].$$

When  $\mathcal{A} = 0$  and  $\mathcal{B} > 0$ , the latent roots  $\Theta_{1,2} = \sqrt{-\mathcal{B}}$  are pure imaginary numbers, and the fixed point is the center point. At  $(\bar{x}, \bar{y})$ , the Jacobian matrix of the system (4.1.4) is obtained by where,

$$J(\bar{x}, \bar{y}) = \begin{pmatrix} \nu_{11} & \bar{x} \left( \frac{\alpha F \bar{x} (\bar{x} - K)}{K(A + \bar{x})(F\bar{y} + 1)^2} - \frac{\beta}{\mathcal{L} + \bar{x}} \right) \\ \frac{\mathcal{L}\beta\xi\bar{y}}{(\mathcal{L} + \bar{x})^2} & \gamma - 2\theta\bar{y} + \frac{\beta\xi\bar{x}}{\mathcal{L} + \bar{x}} \end{pmatrix},$$

where

$$\nu_{11} = \frac{\alpha\bar{x}(2AK + \bar{x}(-3A + K - 2\bar{x}))}{(A + \bar{x})^2(F\bar{y}K + K)} - \frac{\mathcal{L}\beta\bar{y}}{(\mathcal{L} + \bar{x})^2}.$$

The characteristic function is:

$$\Omega(\Theta) = \Theta^2 - \mathcal{A}\Theta + \mathcal{B}, \quad (4.4.7)$$

where,

$$\begin{aligned} \mathcal{A} &= \left( \frac{\mathcal{L}\beta\bar{y}}{(\mathcal{L} + \bar{x})^2} - \frac{\alpha\bar{x}(2AK + \bar{x}(-3A + K - 2\bar{x}))}{(A + \bar{x})^2(F\bar{y}K + K)} \right) - \left( \gamma - 2\theta\bar{y} + \frac{\beta\xi\bar{x}}{\mathcal{L} + \bar{x}} \right), \\ \text{and} \\ \mathcal{B} &= \left( \frac{\alpha\bar{x}(2AK + \bar{x}(-3A + K - 2\bar{x}))}{(A + \bar{x})^2(F\bar{y}K + K)} - \frac{\mathcal{L}\beta\bar{y}}{(\mathcal{L} + \bar{x})^2} \right) \left( \gamma - 2\theta\bar{y} + \frac{\beta\xi\bar{x}}{\mathcal{L} + \bar{x}} \right) \\ &\quad - \left( \bar{x} \left( \frac{\alpha F \bar{x} (\bar{x} - K)}{K(A + \bar{x})(F\bar{y} + 1)^2} - \frac{\beta}{\mathcal{L} + \bar{x}} \right) \right) \left( \frac{\mathcal{L}\beta\xi\bar{y}}{(\mathcal{L} + \bar{x})^2} \right). \end{aligned}$$

Therefore, we have the following theorem to discuss the Hopf bifurcation of the system (4.1.4).

**Theorem 4.4.2.** *The positive fixed point  $(\bar{x}, \bar{y})$  of (4.1.4) undergoes Hopf bifurcation*

when

$$\alpha = \frac{(\bar{x} + A)^2 (KF\bar{y} + K) \left( \frac{\beta\mathcal{L}\bar{y}}{(\bar{x}+\mathcal{L})^2} - \frac{\beta\xi\bar{x}}{\bar{x}+\mathcal{L}} + 2\theta\bar{y} - \gamma \right)}{\bar{x}(\bar{x}(-2\bar{x} - 3A + K) + 2AK)},$$

and

$$\begin{aligned} 0 < & \left( \frac{\alpha\bar{x}(2AK + \bar{x}(-3A + K - 2\bar{x}))}{(A + \bar{x})^2(F\bar{y}K + K)} - \frac{\mathcal{L}\beta\bar{y}}{(\mathcal{L} + \bar{x})^2} \right) \left( \gamma - 2\theta\bar{y} + \frac{\beta\xi\bar{x}}{\mathcal{L} + \bar{x}} \right) \\ & - \left( \bar{x} \left( \frac{\alpha F\bar{x}(\bar{x} - K)}{K(A + \bar{x})(F\bar{y} + 1)^2} - \frac{\beta}{\mathcal{L} + \bar{x}} \right) \right) \left( \frac{\mathcal{L}\beta\xi\bar{y}}{(\mathcal{L} + \bar{x})^2} \right). \end{aligned}$$

We have the following discussion for the rest of the fixed points of the system (4.1.4). There is no Hopf bifurcation at the system (4.1.4) boundary and trivial fixed points. The variational matrix of system (4.1.4) with the characteristic function at  $(0, 0)$  is given below:

$$\begin{pmatrix} 0 & 0 \\ 0 & \gamma \end{pmatrix}. \quad (4.4.8)$$

$$\mathcal{P}(\lambda) = \lambda^2 - \gamma\lambda.$$

Comparing the above equation with (4.4.7), we have  $\mathcal{B} = 0$ , therefore no Hopf bifurcation. Similarly, the variational matrix of system (4.1.4) at  $(K, 0)$  is given below:

$$\begin{pmatrix} -\frac{\alpha K}{A+K} & -\frac{\beta K}{\mathcal{L}+K} \\ 0 & \gamma + \frac{\beta K \xi}{\mathcal{L}+K} \end{pmatrix}. \quad (4.4.9)$$

The characteristic equation is:

$$\begin{aligned} \mathcal{P}(\lambda) = & -\frac{\alpha\gamma K}{A+K} + \frac{\alpha K\lambda}{A+K} - \frac{\gamma K\lambda}{A+K} - \frac{A\gamma\lambda}{A+K} + \frac{K\lambda^2}{A+K} + \frac{A\lambda^2}{A+K} \\ & - \frac{\alpha\beta K^2\xi}{(A+K)(K+\mathcal{L})} - \frac{\beta K^2\lambda\xi}{(A+K)(K+\mathcal{L})} - \frac{A\beta K\lambda\xi}{(A+K)(K+\mathcal{L})}. \end{aligned}$$

Here,  $\mathcal{B} = -\frac{\alpha\gamma K}{A+K} - \frac{\alpha\beta K^2\xi}{(A+K)(K+\mathcal{L})} < 0$ . One of the conditions of Hopf bifurcation fails, therefore there is no Hopf bifurcation at  $(K, 0)$ . At  $(0, \frac{\gamma}{\theta})$ , we have the following variational matrix:

$$\begin{pmatrix} -\frac{\beta\gamma}{\mathcal{L}\theta} & 0 \\ \frac{\beta\gamma\xi}{\mathcal{L}\theta} & -\gamma \end{pmatrix}. \quad (4.4.10)$$

The characteristic function is:

$$\mathcal{P}(\lambda) = \gamma\lambda + \lambda^2 + \frac{\beta\gamma^2}{\theta\mathcal{L}} + \frac{\beta\gamma\lambda}{\theta\mathcal{L}}.$$

Here  $\mathcal{A} = \gamma + \frac{\beta\gamma}{\theta\mathcal{L}} \neq 0$ . As a result, one of the conditions of Hopf bifurcation is violated. Therefore, there is no Hopf bifurcation. We now study the Neimark-Sacker bifurcation of the system (4.1.5) at the specific positive fixed point  $(\bar{x}, \bar{y})$  using the bifurcation theory and  $\alpha$  as a bifurcation parameter. We derived the essential conditions for the system (4.1.5) to have a non-hyperbolic fixed point with two complex conjugate eigenvalues of modulus one. Assume the parameter set  $\Psi_{NS} = \{(\alpha, F, K, \beta, A, \gamma, \xi, \mathcal{L}, \theta) : \Omega_{Tr}^2 - 4\Omega_{Det} < 0 \text{ and } \Omega_{Det} = 1 \text{ for equation (4.4.1)}\}$ . The positive fixed point of the system (4.1.5) experiences Neimark-Sacker bifurcation for  $\alpha = \alpha_2$  when the parameters vary in the small range around  $\Psi_{NS}$ . In this case, we investigate the system (4.1.5) with these parameters, which are defined by the following map:

$$\begin{cases} x_{n+1} \rightarrow x_n \exp \left[ \frac{\alpha_2}{1+Fy_n} \left( 1 - \frac{x_n}{K} \right) \frac{x_n}{x_n+A} - \frac{\beta y_n}{x_n+\mathcal{L}} \right], \\ y_{n+1} \rightarrow y_n \exp \left[ \gamma + \frac{\xi\beta x_n}{x_n+\mathcal{L}} - \theta y_n \right]. \end{cases} \quad (4.4.11)$$

The following map can be used to represent a map (4.4.11) perturbation when  $\bar{\alpha}$  is used as the bifurcation parameter:

$$\begin{cases} x_{n+1} \rightarrow x_n \exp \left[ \frac{\alpha_2 + \bar{\alpha}}{1+Fy_n} \left( 1 - \frac{x_n}{K} \right) \frac{x_n}{x_n+A} - \frac{\beta y_n}{x_n+\mathcal{L}} \right], \\ y_{n+1} \rightarrow y_n \exp \left[ \gamma + \frac{\xi\beta x_n}{x_n+\mathcal{L}} - \theta y_n \right]. \end{cases} \quad (4.4.12)$$

where  $|\bar{\alpha}| \ll 1$ , is taken as small perturbation parameter. The characteristic function  $\Omega(\Theta)$  of (4.4.12) at  $(\bar{x}, \bar{y})$  with  $\Omega(\Theta) = 0$  has two complex conjugate roots with modulus one when

$$\begin{aligned} \alpha_2 &= \left[ K\bar{y}(\bar{x}+A)^2(F\bar{y}+1)^2 \left( \bar{x} \left( \beta\theta\bar{y}(\bar{x}+\mathcal{L}) + \bar{x}(\theta\bar{x} - \beta + 3\theta\mathcal{L}) + \mathcal{L}(3\theta\mathcal{L} \right. \right. \right. \\ &\quad \left. \left. \left. - \beta(\beta\xi + 1)) \right) + \theta\mathcal{L}^3 \right) \right] \left[ \frac{1}{\hat{P}} \right], \text{ where} \\ \hat{P} &= \bar{x}(\bar{x}+\mathcal{L}) \left( \bar{y} \left( \bar{x} \left( \bar{x} \left( \bar{x}(\theta - F) - F(2(A+\mathcal{L}) + \beta\xi\mathcal{L}) + 2\theta(A+\mathcal{L}) \right) \right. \right. \right. \\ &\quad \left. \left. \left. + A(K(F-\theta) - \mathcal{L}F(\beta\xi + 4) + 4\theta\mathcal{L}) + \mathcal{L}(\beta K\xi F + \mathcal{L}(\theta - F)) \right) + A\mathcal{L}(KF(\beta\xi + \right. \right. \right. \\ &\quad \left. \left. \left. 2) - 2\theta K + 2\mathcal{L}(\theta - F)) \right) + AK\mathcal{L}^2(F - \theta) \right) + \theta F\bar{y}^2(\bar{x}+\mathcal{L})^2(2A\bar{x} + \bar{x}^2 - AK) \right. \\ &\quad \left. - (\bar{x}+\mathcal{L})^2(2A\bar{x} + \bar{x}^2 - AK) \right). \end{aligned}$$

Taking  $u = x - \bar{x}$  and  $v = y - \bar{y}$ , where  $(\bar{x}, \bar{y})$  is the positive fixed point of the system (4.4.12), or equivalently positive fixed point of (4.1.5). Transforming the fixed point  $(\bar{x}, \bar{y})$  to origin  $(0, 0)$ , we get the underlying map:

$$\begin{cases} u \rightarrow \varrho_{11}u + \varrho_{12}v + \varrho_{13}u^2 + \varrho_{14}uv + \varrho_{15}v^2 + \varrho_{16}u^3 + \\ \varrho_{17}u^2v + \varrho_{18}uv^2 + \varrho_{19}v^3 + O(|u|, |v|)^4, \\ v \rightarrow \varrho_{21}u + \varrho_{22}v + \varrho_{23}u^2 + \varrho_{24}uv + \varrho_{25}v^2 + \varrho_{26}u^3 \\ + \varrho_{27}u^2v + \varrho_{28}uv^2 + \varrho_{29}v^3 + O(|u|, |v|)^4. \end{cases} \quad (4.4.13)$$

The coefficients  $\varrho_{11}, \varrho_{12}, \varrho_{13}, \varrho_{14}, \varrho_{15}, \varrho_{16}, \varrho_{17}, \varrho_{18}, \varrho_{19}, \varrho_{21}, \varrho_{22}, \varrho_{23}, \varrho_{24}, \varrho_{25}, \varrho_{26}, \varrho_{18}$ , and  $\varrho_{29}$  are given above can be calculated by replacing  $\alpha_1$  by  $\alpha_2 + \bar{\alpha}$ . The characteristic function of (4.4.12) at the fixed point  $(0, 0)$  can be expressed as follows:

$$\Omega(\Theta) = \Theta^2 - (\Omega_{Tr}(\bar{\alpha}))\Theta + \Omega_{Det}(\bar{\alpha}), \quad (4.4.14)$$

where,

$$\begin{aligned} \Omega_{Tr} &= \frac{(\bar{\alpha} + \alpha_2) \bar{x} (AK - \bar{x}(\bar{x} + 2A))}{(\bar{x} + A)^2 (KF\bar{y} + K)} + \bar{y} \left( \frac{\beta \bar{x}}{(\bar{x} + \mathcal{L})^2} - \theta \right) + 2, \text{ and} \\ \Omega_{Det} &= \left( \bar{x} \left( \frac{(\bar{\alpha} + \alpha_2) (AK - \bar{x}(2A + \bar{x}))}{(A + \bar{x})^2 (F\bar{y}K + K)} + \frac{\beta \bar{y}}{(\mathcal{L} + \bar{x})^2} \right) + 1 \right) (1 - \theta \bar{y}) - \\ &\quad \left( \bar{x} \left( \frac{(\bar{\alpha} + \alpha_2) F \bar{x} (\bar{x} - K)}{K (A + \bar{x}) (F\bar{y} + 1)^2} - \frac{\beta}{\mathcal{L} + \bar{x}} \right) \right) \left( \frac{\mathcal{L} \beta \xi \bar{y}}{(\mathcal{L} + \bar{x})^2} \right). \end{aligned}$$

As  $(\alpha_2, F, K, \beta, A, \gamma, \xi, \mathcal{L}, \theta) \in \Psi_{NS}$ , the roots of (4.4.14) are conjugate complex numbers  $\Theta_1, \Theta_2$  with  $|\Theta_1| = |\Theta_2| = 1$ . Thus, it is obvious that:  $\Theta_1, \Theta_2 = \frac{\Omega_{Tr}}{2} \pm \frac{i}{2} \sqrt{4\Omega_{Det} - \Omega_{Tr}^2}$ . We have  $|\Theta_1| = |\Theta_2| = \sqrt{\Omega_{Det}}$ , with  $\left( \frac{d|\Theta_{1,2}|}{d\bar{\alpha}} \right)_{\bar{\alpha}=0} \neq 0$ . Moreover, we assume that  $\Omega_{Tr}(0) = \frac{(\bar{\alpha} + \alpha_2) \bar{x} (AK - \bar{x}(\bar{x} + 2A))}{(\bar{x} + A)^2 (KF\bar{y} + K)} + \bar{y} \left( \frac{\beta \bar{x}}{(\bar{x} + \mathcal{L})^2} - \theta \right) + 2 \neq 0, -1$ . Further,  $(\alpha_2, F, K, \beta, A, \gamma, \xi, \mathcal{L}, \theta) \in \Psi_{NS}$  implies that  $-2 < \Omega_{Tr}(0) < 2$ . Thus,  $\Omega_{Tr}(0) \neq \pm 2, 0, -1$  gives  $\Theta_1^r, \Theta_2^r \neq 1$  for all  $r = 1, 2, 3, 4$  at  $\bar{\alpha} = 0$ . Therefore, when  $\bar{\alpha} = 0$  and the following criteria are met, the roots of (4.4.14) do not occur at the point where the unit circle and coordinate axes intersect. Now transforming the fixed point  $(\bar{x}, \bar{y})$  of (4.4.12) to the origin, we get the normal form of (4.4.12) as:

$$\begin{pmatrix} \tilde{x} \\ \tilde{y} \end{pmatrix} \rightarrow \begin{pmatrix} \varrho_{11} & \varrho_{12} \\ \varrho_{21} & \varrho_{22} \end{pmatrix} \begin{pmatrix} \tilde{x} \\ \tilde{y} \end{pmatrix} + \begin{pmatrix} \tilde{f}(\tilde{x}, \tilde{y}) \\ \tilde{g}(\tilde{x}, \tilde{y}) \end{pmatrix}, \quad (4.4.15)$$

where,

$$\begin{cases} \tilde{f}(\tilde{x}, \tilde{y}) = \frac{1}{\varrho_{12}} \left( \varrho_{13}u^2 + \varrho_{14}uv + \varrho_{15}v^2 + \varrho_{16}u^3 + \varrho_{17}u^2v + \varrho_{18}uv^2 + \varrho_{19}v^3 \right) \\ + \frac{1}{\varrho_{12}} O(|u|, |v|)^4, \\ \tilde{g}(\tilde{x}, \tilde{y}) = \left( \frac{\varrho_{13}(\alpha_a - \varrho_{11})}{\beta_a \varrho_{12}} - \frac{\varrho_{23}}{\beta_a} \right) u^2 + \left( \frac{\varrho_{14}(\alpha_a - \varrho_{11})}{\beta_a \varrho_{12}} - \frac{\varrho_{24}}{\beta_a} \right) uv + \varrho_{27}u^2v \\ + \varrho_{28}uv^2 \left( \frac{\varrho_{15}(\alpha_a - \varrho_{11})}{\beta_a \varrho_{12}} - \frac{\varrho_{25}}{\beta_a} \right) uv^2 + \left( \frac{\varrho_{13}(\alpha_a - \varrho_{11})}{\beta_a \varrho_{16}} - \frac{\varrho_{23}}{\beta_a} \right) u^3 + \varrho_{29}v^3 + O((|u|, |v|)^4). \end{cases} \quad (4.4.16)$$

$u = a_{12}\tilde{x}$  and  $v = (\alpha_a - \varrho_{11})u - \beta_a v$ . The following nonzero real number is defined next:

$$L = \left\{ \left( \left[ -Re \left( \frac{(1 - 2\Gamma_1)\Gamma_2^2}{1 - \Gamma_1} \zeta_{20}\zeta_{11} \right) - \frac{1}{2}|\zeta_{11}|^2 - |\zeta_{02}|^2 + Re(\Gamma_2\zeta_{21}) \right] \right) \right\}_{\bar{\alpha}=0}, \quad (4.4.17)$$

where

$$\begin{aligned} \zeta_{20} &= \frac{1}{8} \left[ \tilde{f}_{\tilde{x}\tilde{x}} + 2\tilde{g}_{\tilde{x}\tilde{y}} - \tilde{f}_{\tilde{y}\tilde{y}} + i \left( \tilde{g}_{\tilde{x}\tilde{x}} - 2\tilde{f}_{\tilde{x}\tilde{y}} - \tilde{g}_{\tilde{y}\tilde{y}} \right) \right], \\ \zeta_{11} &= \frac{1}{4} \left[ \tilde{f}_{\tilde{x}\tilde{x}} + i \left( \tilde{g}_{\tilde{x}\tilde{x}} + \tilde{g}_{\tilde{y}\tilde{y}} \right) + \tilde{f}_{\tilde{y}\tilde{y}} \right], \\ \zeta_{02} &= \frac{1}{8} \left[ \tilde{f}_{\tilde{x}\tilde{x}} - 2\tilde{g}_{\tilde{x}\tilde{y}} - \tilde{f}_{\tilde{y}\tilde{y}} + i \left( \tilde{g}_{\tilde{x}\tilde{x}} + 2\tilde{f}_{\tilde{x}\tilde{y}} - \tilde{g}_{\tilde{y}\tilde{y}} \right) \right], \\ \zeta_{21} &= \frac{1}{16} \left[ \tilde{g}_{\tilde{x}\tilde{x}\tilde{y}} + \tilde{g}_{\tilde{y}\tilde{y}\tilde{y}} + \tilde{f}_{\tilde{x}\tilde{x}\tilde{x}} + \tilde{f}_{\tilde{x}\tilde{y}\tilde{y}} + i \left( \tilde{g}_{\tilde{x}\tilde{x}\tilde{x}} + \tilde{g}_{\tilde{x}\tilde{y}\tilde{y}} - \tilde{f}_{\tilde{x}\tilde{x}\tilde{y}} - \tilde{f}_{\tilde{y}\tilde{y}\tilde{y}} \right) \right]. \end{aligned}$$

Analyzing these facts we can write the following result.

**Theorem 4.4.3.** *When the parameter  $\alpha$  changes within a narrow neighborhood of the parameter  $\alpha = \alpha_2$ , then the system (4.1.5) experiences Hopf bifurcation at the positive fixed point  $(\bar{x}, \bar{y})$ . This is assuming that  $L \neq 0$  holds. Additionally, for  $\alpha > \alpha_2$ , an attracting invariant closed curve bifurcates from the fixed point if  $L < 0$ , and for  $\alpha > \alpha_2$ , a repelling invariant closed curve bifurcates if  $L > 0$ .*

## 4.5 Numerical simulations

In this section, we will discuss the numerical values of parameters where the systems (4.1.4) and (4.1.5) undergo bifurcation. The biological significance of the parameters, which reflect essential ecosystem components, is used to drive parameter selection in simulations. This method makes individual parameter impacts visible, facilitating comprehensive ecological analysis. The biological motivation for tracing bifurcation in these parameters, such as  $\alpha$ ,  $\beta$ ,  $\gamma$ ,  $\theta$ ,  $\mathcal{L}$ ,  $\xi$ ,  $F$ ,  $A$ , and  $K$ , is to understand how particular ecological conditions affect predator-prey dynamics. This knowledge is essential for en-

vironmental management and conservation initiatives because it informs choices about resource availability, interactions between species, and population limits, ultimately assisting in the sustainable management of ecosystems.

**Example 10.** *In this example, we will discuss the Hopf bifurcation of the system (4.1.4) at the positive fixed point. If we choose the following parametric set:*

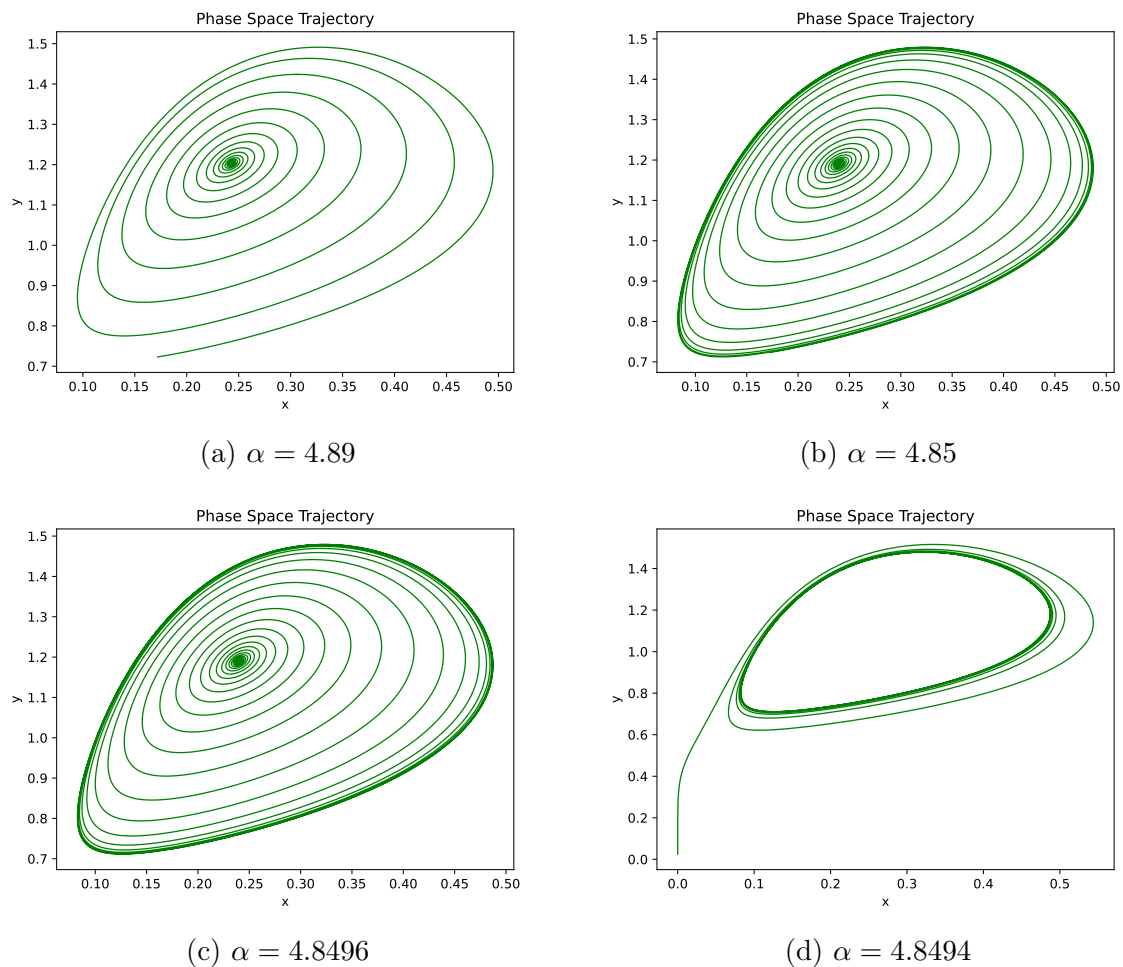


Figure 4.4: Phase plots for different values of  $\alpha$  indicate backward Hopf bifurcation in (4.1.4).

$$F = 0.79, \beta = 2.04, \mathcal{L} = 0.81, \gamma = 0.01, \xi = 1.0, K = 1.39, \theta = 0.4, A = 0.11,$$

and  $(x_0, y_0) = (0.172, 0.723)$ . Then, Hopf bifurcation arises at the positive fixed point. In particular, the Hopf bifurcation appears at the parameter  $\alpha$  when  $\alpha \in [4.8494, 4.89]$ . The phase space trajectories are given in figure 4.4. From these trajectories, it can be noticed that the bifurcation is going in the reverse direction. This implies that when the biological



parameters have values:

$$F = 0.79, \beta = 2.04, \mathcal{L} = 0.81, \gamma = 0.01, \xi = 1.0, K = 1.39, \theta = 0.4, A = 0.11,$$

and the population of the species starts initially from  $(x_0, y_0) = (0.172, 0.723)$ , then the inherent growth rate of the prey  $\alpha$  must be greater than 4.89. The low inherent rate for the above fixed biological constraints causes the Hopf bifurcation in the system (4.4.3). This means that perdition may cause the extinction of the prey population. Similarly, Hopf bifurcation in the model (4.4.3) can also be observed regarding other parameters.

**Example 11.** This example deals with Hopf bifurcation in the system (4.1.5). In this system, the Hopf bifurcation occurs at seven different parameters. By varying one parameter and fixing the rest of the parameters, we will discuss the Hopf bifurcation in the system (4.1.5). Here, we will present the approximate value of the bifurcation parameters up to a few decimal places. So, the determinants of the complex eigenvalues calculated for the particular parameter set with the bifurcation value are approximately equal to one. First, we will discuss the bifurcation in the parameter  $\alpha$ . If we have the following parametric set:

$$\Phi_\alpha = \{F = 0.3, K = 7, A = 0.1, \beta = 1.803, \mathcal{L} = 0.5, \gamma = 1.65, \xi = 0.19, \text{ and } \theta = 0.8\},$$

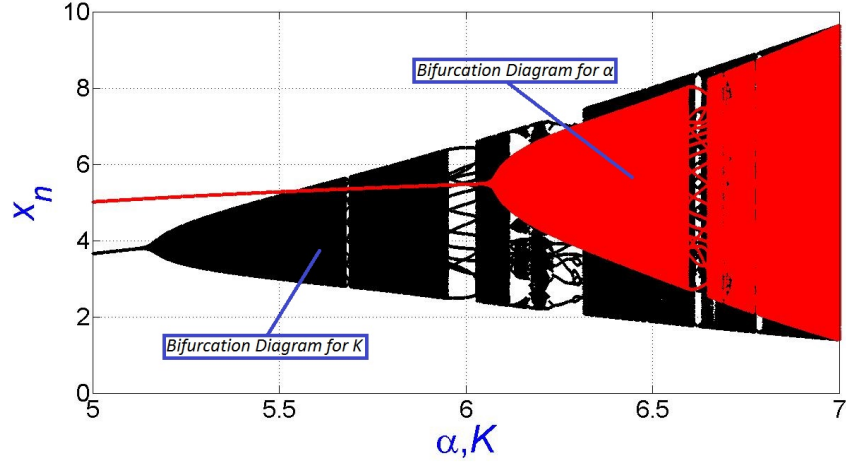
with a starting population of  $(x_0, y_0) = (2.4569, 2.4676)$ , then the system (4.1.5) undergoes Hopf bifurcation when  $\alpha \in [5, 7]$ . We observed that at  $\alpha = 6.079$ , the system (4.1.5) loses its stability. For the above set  $\Phi_\alpha$  and with  $\alpha = 6.079$ , we have  $(5.497336772510419, 2.4550122786982076)$  as a positive fixed point. The system (4.1.5) at these values is:

$$\begin{cases} x_{n+1} = x_n \exp \left[ \frac{6.079}{1+0.3y_n} \left( 1 - \frac{x_n}{7} \right) \frac{x_n}{x_n+0.1} - \frac{1.803y_n}{x_n+0.5} \right], \\ y_{n+1} = y_n \exp \left[ 1.65 + \frac{(0.19)(1.803)x_n}{x_n+0.5} - 0.8y_n \right]. \end{cases} \quad (4.5.1)$$

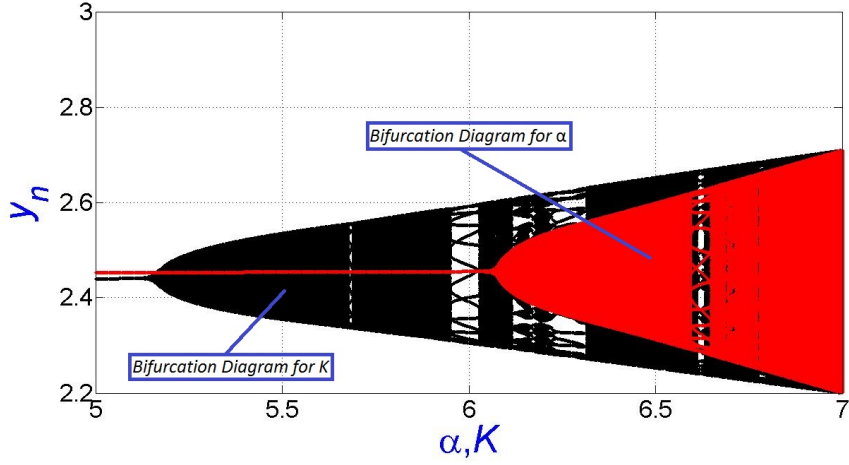
The Jacobian matrix of (4.5.1) with characteristic function is:

$$\Sigma_\alpha(5.497336772510419, 2.4550122786982076) = \begin{pmatrix} -1.0104 & -2.35364 \\ 0.0116911 & -0.96401 \end{pmatrix},$$

$$\Omega(\xi)_\alpha = 1.0015508976493441 + 1.9744085042670956\xi + \xi^2. \quad (4.5.2)$$



(a) Plots for  $x_n$



(b) Plots for  $y_n$

Figure 4.5: Hopf bifurcation diagrams in the range  $[5, 7]$ .

The roots of (4.5.2) are:

$$\xi_{1,2} = \{-0.9872042521335478 \pm 0.16425182561782i\},$$

with  $|\xi_{1,2}| = 1$ . Thus, the parameters of system (4.5.1),  $(\alpha, F, K, A, \beta, \mathcal{L}, \gamma, \xi, \theta) \in \Phi_{NS}$ . Now we will choose  $K$  as a bifurcation parameter and fix  $\alpha = 7$ . The set  $\Phi_\alpha$  becomes

$$\begin{aligned} \Phi_K = \{ & \alpha = 7, F = 0.3, A = 0.1, \beta = 1.803, \mathcal{L} = 0.5, \\ & \gamma = 1.65, \xi = 0.19, \text{ and } \theta = 0.8 \}. \end{aligned}$$

The starting population for the remaining discussion remains the same. The exact value of  $K$  at which the system (4.1.5) loses its stability is  $K = 5.163$ . For this value of  $K$  with

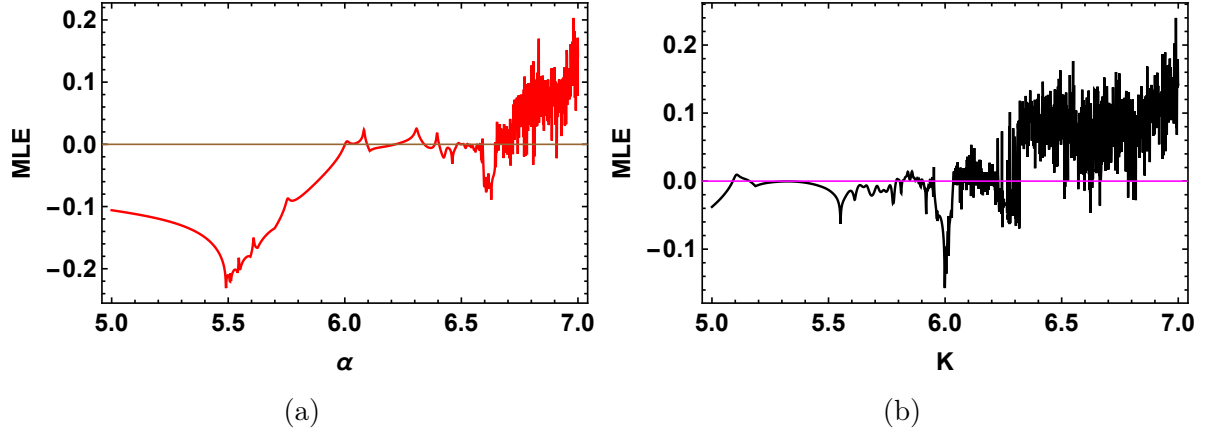


Figure 4.6: MLE plots for  $\alpha$  and  $K$

set  $\Phi_K$ , we have the following characteristic function of Jacobian matrix:

$$\Sigma_K(3.8302944548361992, 2.4412686914477018) = \begin{pmatrix} -0.996442 & -2.26904 \\ 0.0222998 & -0.953015 \end{pmatrix}.$$

$$\Omega(\xi)_K = 1.0002229376224936 + 1.9494567409504375\xi + \xi^2. \quad (4.5.3)$$

The solution set of equation (4.5.3) is

$$\xi_{1,2} = \{0.9747283704752188 \pm 0.22389180738298195i\},$$

with  $|\xi_{1,2}| = 1$ . Therefore, the Hopf bifurcation is emerging in the system (4.1.5) for the parameter set  $\Phi_K$  with  $K = 5.163$ . If we select  $F$  as a bifurcation parameter and fix the rest of the parameters, then we have the following set of parameters:

$$\Phi_F = \{\alpha = 7, K = 7, A = 0.1, \beta = 1.803, \mathcal{L} = 0.5, \gamma = 1.65, \xi = 0.19, \text{ and } \theta = 0.8\}.$$

At  $F = 0.4075$ , the system (4.1.5) bifurcates when  $F \in [0.25, 0.7]$ . This time, the backward bifurcation occurs. For  $F = 0.4075$  with set  $\Phi_F$ , we have:

$$\Sigma_F(5.496510505123591, 2.4550073595158697) = \begin{pmatrix} -1.00879 & -2.47917 \\ 0.0116943 & -0.964006 \end{pmatrix}.$$

$$\Omega(\xi)_F = 1.0014701485844997 + 1.9727943289584056\xi + \xi^2. \quad (4.5.4)$$

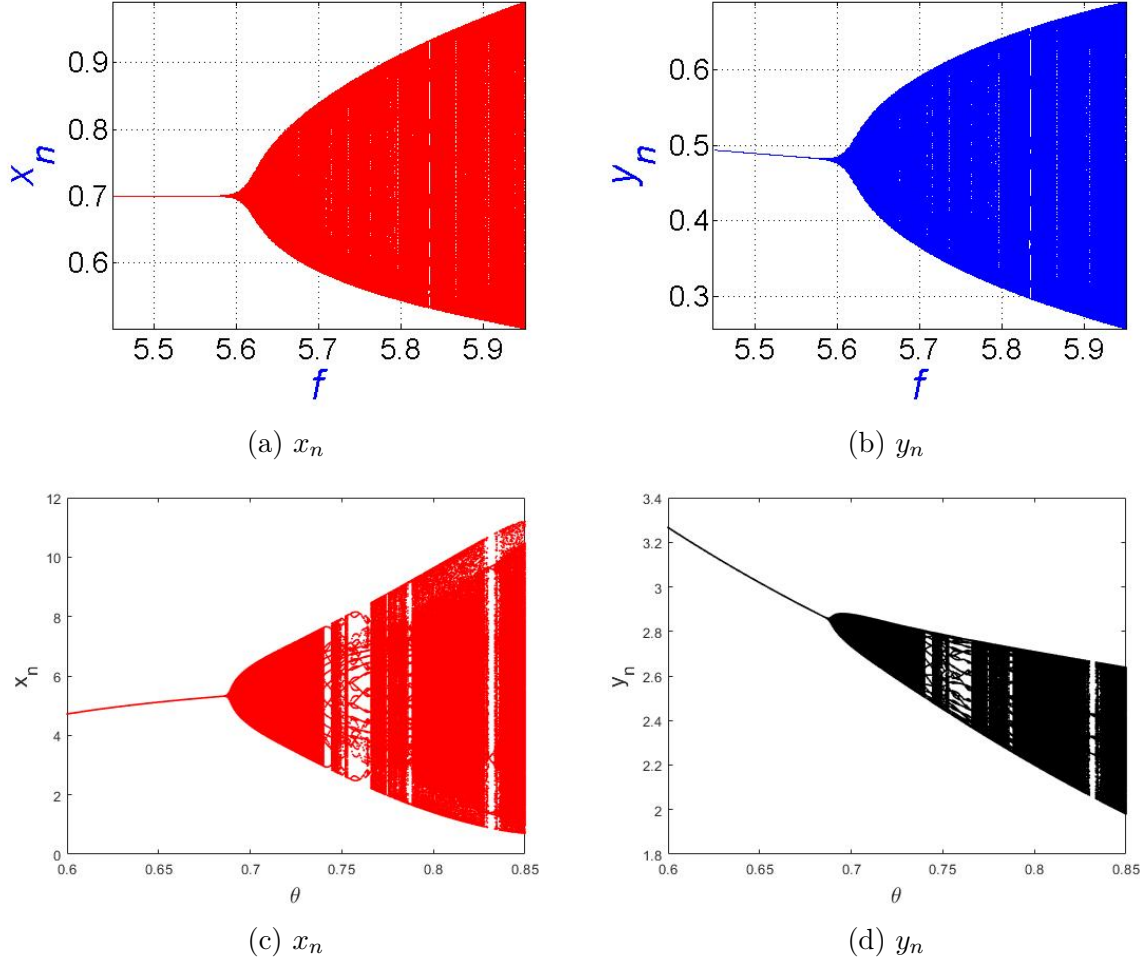


Figure 4.7: One parameter bifurcation diagrams when  $F \in [0.25, 0.7]$ , and  $\theta \in [0.6, 0.85]$ .

The roots of the equation (4.5.4) are

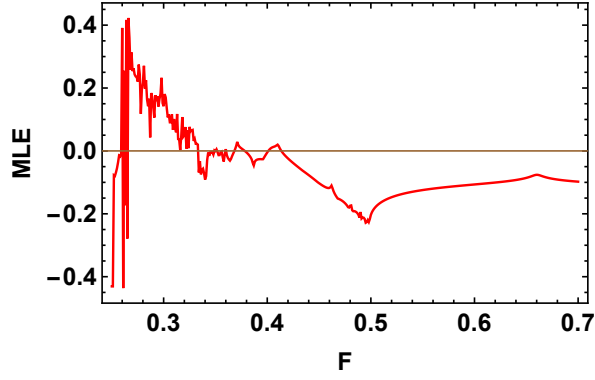
$$\xi_{1,2} = \{0.9863971644792028 \pm 0.16879212805071303i\},$$

with  $|\xi_{1,2}| = 1$ . Now we choose  $\theta$  as a bifurcation parameter and the other parametric set as follows:

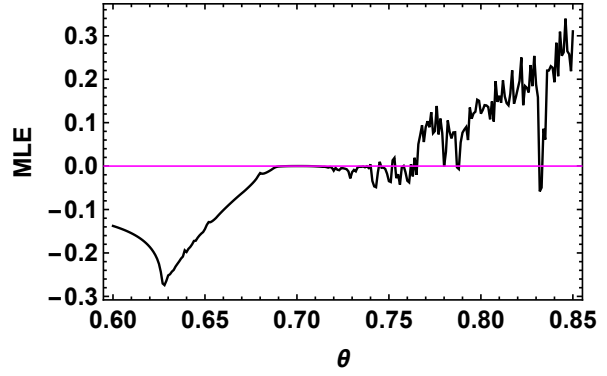
$$\Phi_\theta = \{\alpha = 7, K = 7, A = 0.1, \beta = 1.803, \mathcal{L} = 0.5, \gamma = 1.65, \xi = 0.19, \text{ and } F = 0.3\}.$$

The bifurcation happens at  $\theta = 0.6889$  when  $\theta \in [0.6, 0.85]$ . Thus, we have:

$$\Sigma_\theta(5.336360119474886, 2.849792546261007) = \begin{pmatrix} -1.00278 & -2.40835 \\ 0.0143301 & -0.963222 \end{pmatrix}.$$

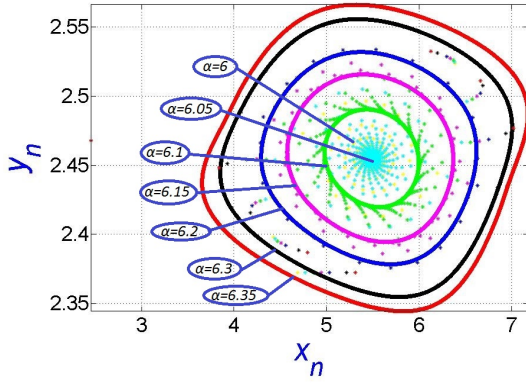


(a) MLE plot for  $F$ .

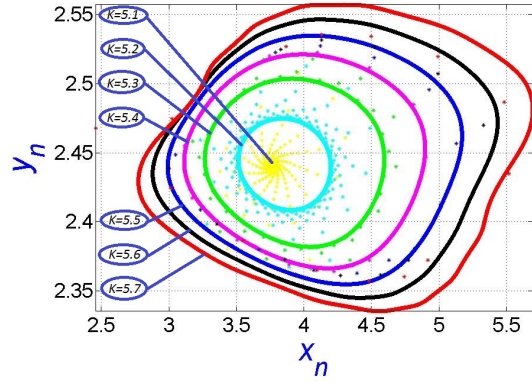


(b) MLE plot for  $\theta$ .

Figure 4.8: MLE plots for  $F$  and  $\theta$

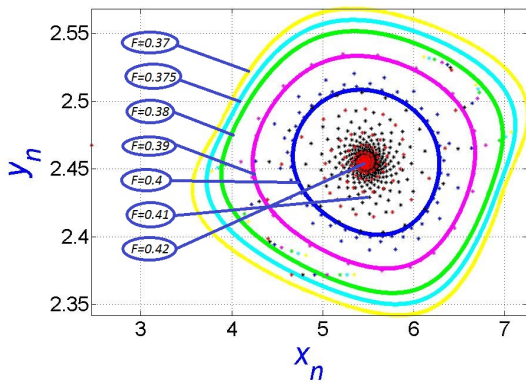


(a) Phase plots for  $\alpha$ .

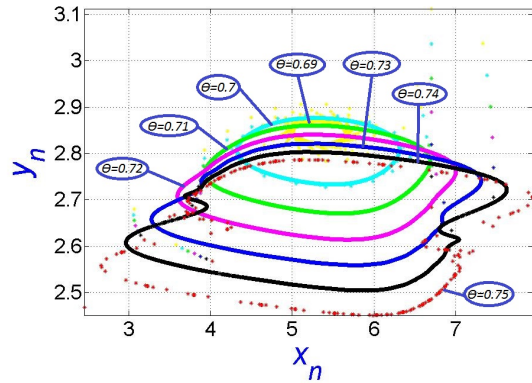


(b) Phase plots for  $K$ .

Figure 4.9: Phase plots confirm the existence of Hopf bifurcation when  $\alpha$  and  $K$  are chosen as bifurcation parameters.

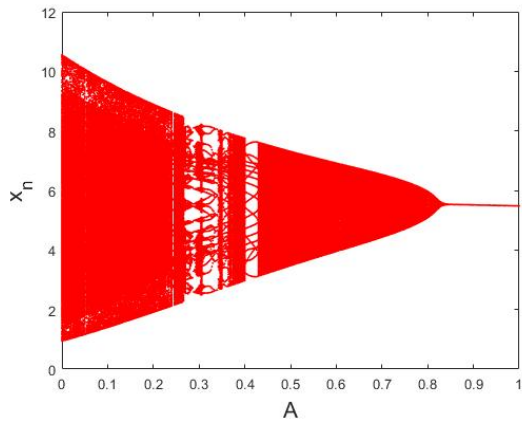


(a) Phase plots for  $F$ .

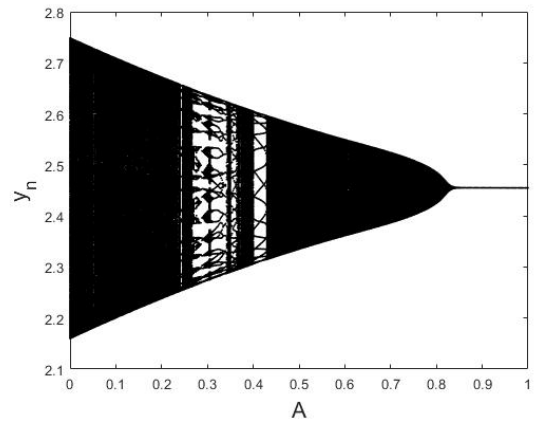


(b) Phase plots for  $\theta$ .

Figure 4.10: Phase plots confirm the existence of Hopf bifurcation when  $F$  and  $\theta$  are chosen as bifurcation parameters.

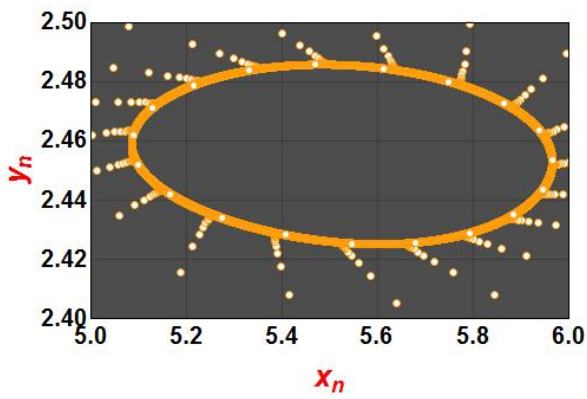


(a) Bifurcation plot for  $x_n$

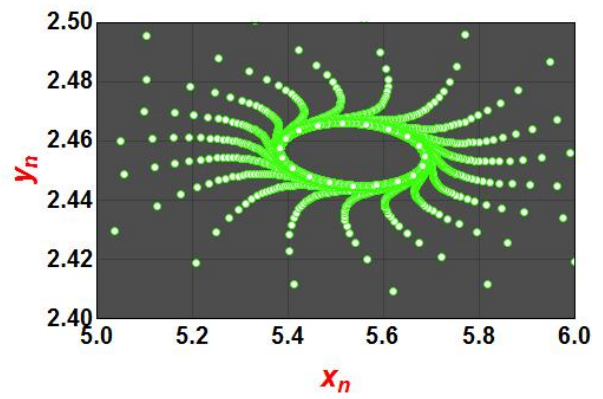


(b) Bifurcation plot for  $y_n$

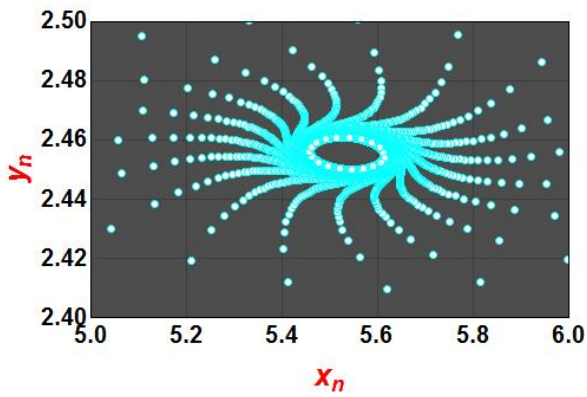
Figure 4.11: Bifurcation plots for parameter  $A$ .



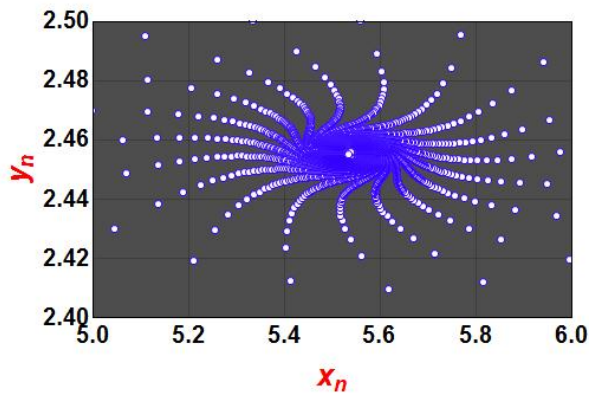
(a)  $A = 0.8$



(b)  $A = 0.82$



(c)  $A = 0.822$



(d)  $A = 0.823$

Figure 4.12: Phase plots for different values of  $A$ .

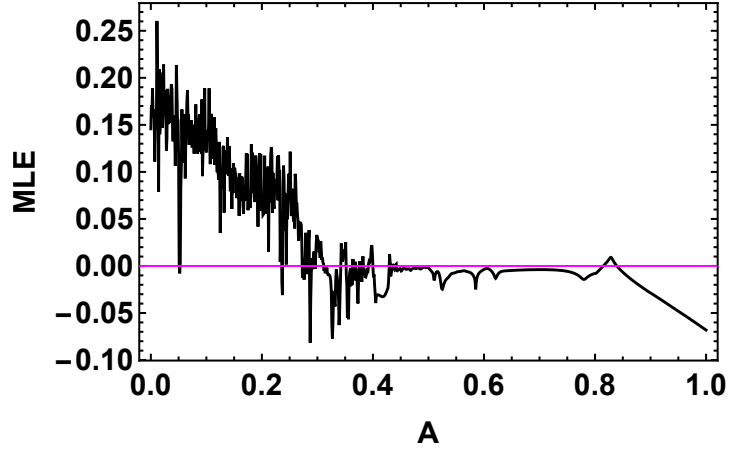


Figure 4.13: MLE plot for  $A$ .

$$\Omega(\xi)_\theta = 1.000407683946828 + 1.9659980100331875\xi + \xi^2. \quad (4.5.5)$$

The latent roots of (4.5.5) are:  $\xi_{1,2} = \{0.9829990050165938 \pm 0.18471773083062384i\}$ , with  $|\xi_{1,2}| = 1$ . If we vary  $A \in [0, 1]$  and fix rest of the parameters as:

$$\Phi_A = \{\alpha = 7, K = 7, d = 0.8, \beta = 1.803, \mathcal{L} = 0.5, \gamma = 1.65, \xi = 0.19, \text{ and } F = 0.3\}.$$

Then the system (4.1.5) undergoes Hopf bifurcation at  $A = 0.822$ . We have the Jacobian matrix

$$\Sigma_A(5.537771976635198, 2.455251364530071) = \begin{pmatrix} -1.0095 & -2.35511 \\ 0.0115362 & -0.964201 \end{pmatrix}.$$

$$\Omega(\xi)_A = 1.00053304716 + 1.97370429736\xi + \xi^2. \quad (4.5.6)$$

The latent roots of (4.5.6) are:

$$\xi_{1,2} = \{0.9868521486819868 \pm 0.16326629721089742i\},$$

with absolute value  $|\xi_{1,2}| = 1$ . The details about the figures used in this example are as follows: The bifurcation plots between the parameters  $\alpha$  and  $K$  are given in figure 4.5, whereas the corresponding maximum Lyapunov exponents are given in figure 4.6. Figure 4.7 represents the bifurcation plots for parameters  $F$  and  $\theta$ , respectively. Figures 4.9 and 4.10 show the phase plots of different parameters. Figure 4.8 represents the maximum Lyapunov exponents of  $F$  and  $\theta$ . Last but not least, the phase portraits and the bifurcation plots of parameter  $A$  are given in figure 4.12 and 4.11. The MLE plot for  $A$  is given in figure 4.13.



Hence, in this example, we studied the Hopf bifurcation in different system parameters (4.1.5). We noticed that the bifurcation is reversed in fear and the Allee effect parameters. In all other parameters, the focus of bifurcation is forward. We also constructed MLE graphs and phase plots to confirm the direction of bifurcations. Thus, we conclude that the backward bifurcation of the Allee and fear effects demonstrates that the model is stabilized by an increase in the fear effect when the crowding effect is present. Likewise, the model is stabilized by a more significant Allee effect. While the reduction of these two effects leads to an increase in growth rate and system bifurcates because of overcrowding, the increase in the Allee and fear effects should only occur to a certain extent to ensure that the excess on both impacts controls the crowding effect. In the following example, we will study flip bifurcation in a system (4.1.5). We also observed that the flip bifurcation is occurring for different parameters. Thus, we have the following example:

**Example 12.** If we have  $\alpha = 7$ ,  $F = 0.2$ ,  $K = 1.6$ ,  $A = 0.1$ ,  $\beta = 1.1$ ,  $\mathcal{L} = 1.2$ ,  $\gamma = 0.5$ ,  $\xi = 0.1$ , and  $\theta = 0.2$  with a starting population of  $(x_0, y_0) = (1.06, 2.758)$ , then the system (4.1.5) undergoes flip bifurcation. The bifurcation occurs at the eight parameters  $\alpha, \gamma, K, \mathcal{L}, \beta, \xi, A, F$ . The parametric variation for bifurcation is:  $\alpha \in [6, 8.1]$ ,  $\gamma \in [0.4, 0.65]$ ,  $K \in [1, 3]$ ,  $\mathcal{L} \in [0.8, 1.7]$ ,  $\beta \in [0.8, 1.7]$ ,  $\xi \in [0, 0.3]$ ,  $A \in [0, 0.3]$ ,  $F \in [0.1, 0.3]$ . First, we will discuss the bifurcation in the parameter  $\alpha$ . If we have the following particular parametric set:

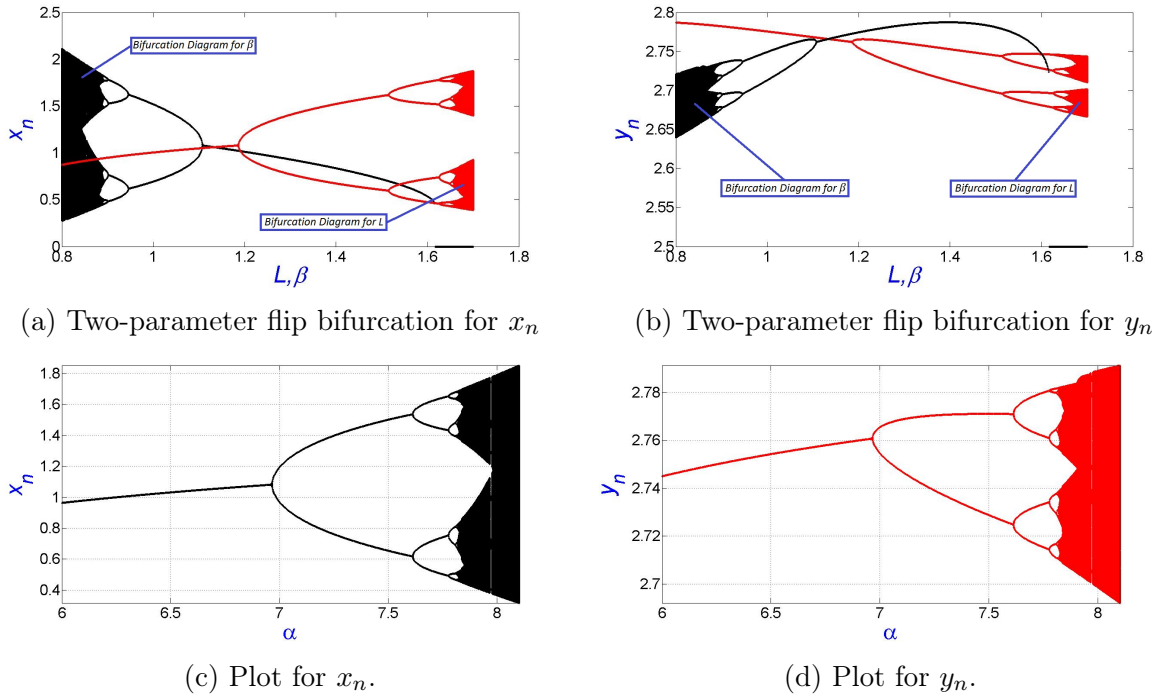


Figure 4.14: Plots for  $\alpha$ ,  $L$ , and  $\beta$ .



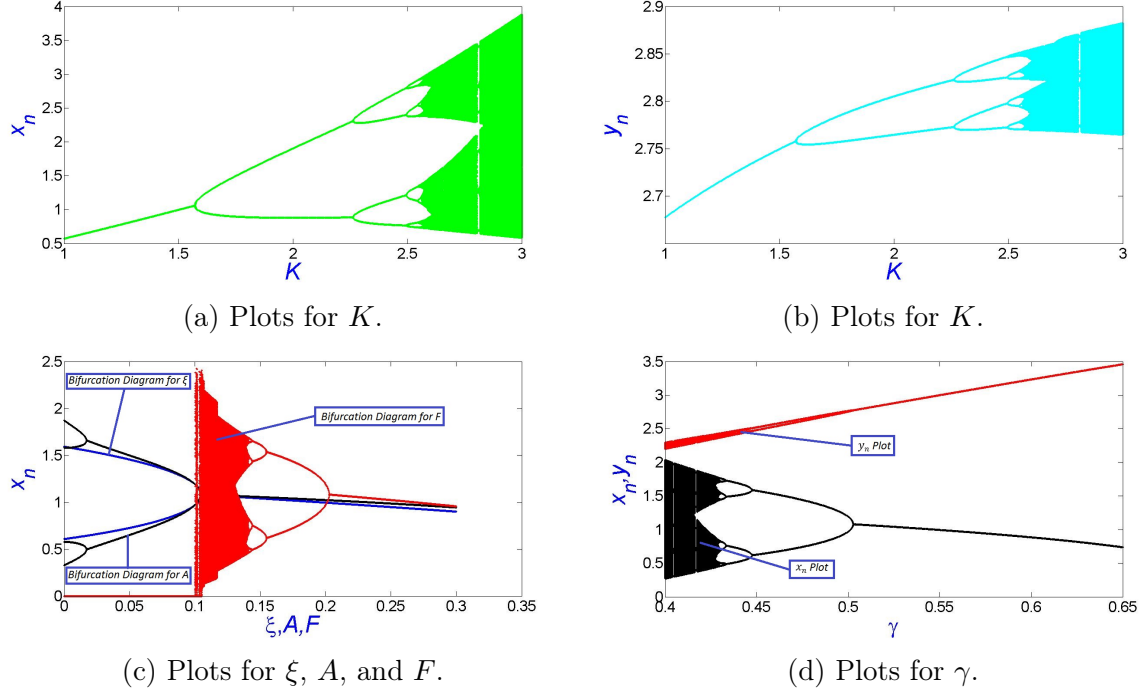


Figure 4.15: Bifurcation plot

$$\Phi_\alpha = \{\alpha = 6.967, F = 0.2, K = 1.6, A = 0.1, \beta = 1.1, \\ \mathcal{L} = 1.2, \gamma = 0.5, \xi = 0.1, \text{ and } \theta = 0.2\}.$$

For these parametric values, the fixed point is  $(1.0817209568081427, 2.7607446473545734)$ . The system (4.1.5) becomes:

$$\begin{cases} x_{n+1} = x_n \exp \left[ \frac{6.967}{1+0.2y_n} \left( 1 - \frac{x_n}{1.6} \right) \frac{x_n}{x_n+0.1} - \frac{1.1y_n}{x_n+1.2} \right], \\ y_{n+1} = y_n \exp \left[ 0.5 + \frac{(0.1)(1.1)x_n}{x_n+1.2} - 0.2y_n \right]. \end{cases} \quad (4.5.7)$$

The variational matrix of (4.5.7) with characteristic function at the positive fixed point is:

$$\mathcal{V}_\alpha(1.0817209568081427, 2.7607446473545734) = \begin{pmatrix} -1.03425 & -0.707 \\ 0.0699963 & 0.447851 \end{pmatrix},$$

$$\Omega(\xi) = -0.413701515606289 + 0.5863964973072586\xi + \xi^2. \quad (4.5.8)$$

The roots of (4.5.8) are:  $\xi_{1,2} = \{-1, 0.413673\}$ , with  $|\xi_1| = 1$ . Similarly, the particular

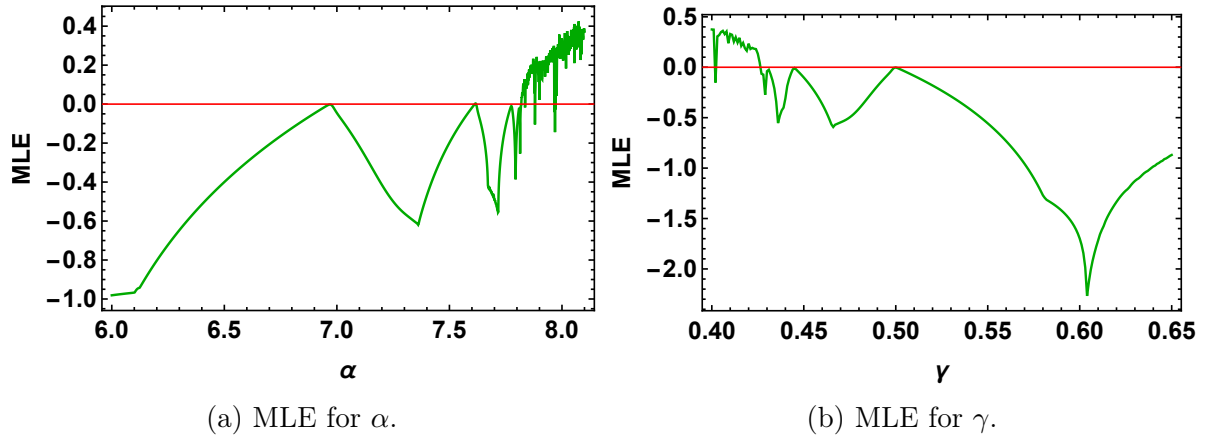


Figure 4.16: MLE plots for  $\alpha$  and  $\gamma$ .

value of bifurcation in the parameter  $\gamma = 0.4998$ . Thus the parametric set for  $\gamma$  is

$$\begin{aligned}\Phi_\gamma &= \{\alpha = 7, F = 0.2, K = 1.6, A = 0.1, \beta = 1.1, \mathcal{L} \\ &= 1.2, \gamma = 0.5, \xi = 0.1, \text{ and } \theta = 0.2\}.\end{aligned}$$

The Jacobian matrix with a characteristic function is:

$$\mathcal{V}_\gamma(1.0852402020919543, 2.760190097480421) \quad (4.5.9)$$

$$= \begin{pmatrix} -1.05801 & -0.708183 \\ 0.0697669 & 0.447962 \end{pmatrix}, \quad (4.5.10)$$

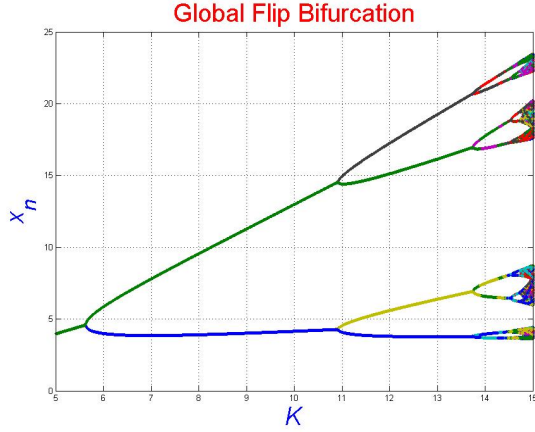
$$\Omega(\xi) = -0.4245387770435508 + 0.6100441404859769\xi + \xi^2. \quad (4.5.11)$$

The roots of (4.5.11) are:  $\xi_{1,2} = \{-1, 0.414406\}$ . Similarly, for other bifurcation parameters, we have the following parametric sets that satisfy the period-doubling bifurcation conditions:

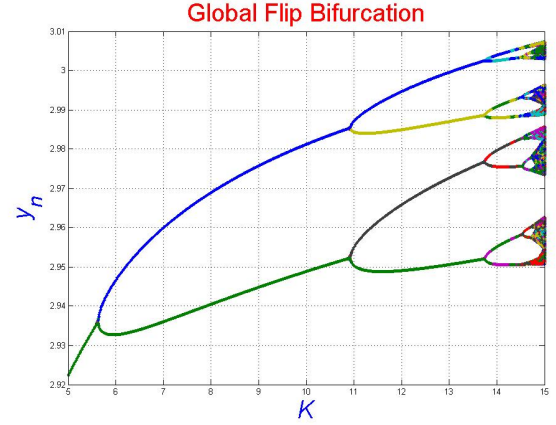
$$\begin{aligned}\Phi_\beta &= \{\alpha = 7, F = 0.2, K = 1.6, A = 0.1, \beta = 1.108, \mathcal{L} = 1.2, \gamma = 0.5, \xi = 0.1, \theta = 0.2\}. \\ \Phi_{\mathcal{L}} &= \{\alpha = 7, F = 0.2, K = 1.6, A = 0.1, \beta = 1.1, \mathcal{L} = 1.185, \gamma = 0.5, \xi = 0.1, \theta = 0.2\}. \\ \Phi_\xi &= \{\alpha = 7, F = 0.2, K = 1.6, A = 0.1, \beta = 1.1, \mathcal{L} = 1.2, \gamma = 0.5, \xi = 0.1001, \theta = 0.2\}. \\ \Phi_A &= \{\alpha = 7, F = 0.2, K = 1.6, A = 0.1018, \beta = 1.1, \mathcal{L} = 1.2, \gamma = 0.5, \xi = 0.1, \theta = 0.2\}. \\ \Phi_F &= \{\alpha = 7, F = 0.2001, K = 1.6, A = 0.1, \beta = 1.1, \mathcal{L} = 1.2, \gamma = 0.5, \xi = 0.1, \theta = 0.2\}. \\ \Phi_K &= \{\alpha = 7, F = 0.2, K = 1.572, A = 0.1, \beta = 1.1, \mathcal{L} = 1.2, \gamma = 0.5, \xi = 0.1, \theta = 0.2\}.\end{aligned}$$

The bifurcation plots and MLE plots of different parameters are given in figures 4.14, 4.15, and 4.16.

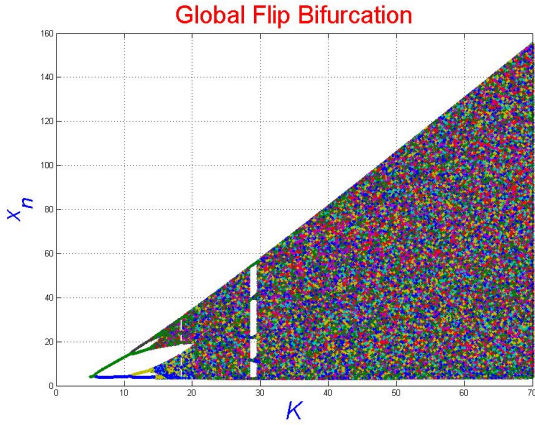
**Example 13.** Setting  $\alpha = 4.9$ ,  $F = 0.2$ ,  $A = 0.1$ ,  $\beta = 1.1$ ,  $\mathcal{L} = 1.2$ ,  $\gamma = 0.5$ ,  $\xi = 0.1$ , and  $\theta = 0.2$  and  $K \in [5, \infty)$  with a starting population of  $(x_0 = 1.06, y_0 = 2.758)$ , then the system (4.1.5) undergoes flip bifurcation. We numerically found that for all values of  $K > 0.7434403908774643$ , system (4.1.5) bifurcates as shown in Figure. The value for different parameters at which the bifurcation emerges is  $K = 0.7434403908774643$ . For these parametric values, the fixed point becomes  $(0.70106954954813, 2.7028270098498623)$ . The Jacobian matrix of (4.1.5) with characteristic function at the positive fixed point is:



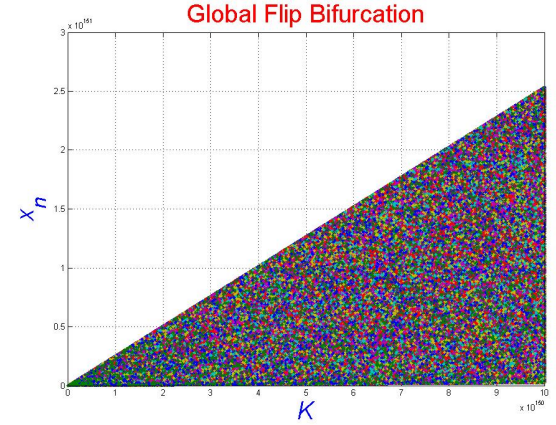
(a)  $5 \leq K \leq 15$



(b)  $5 \leq K \leq 15$



(c)  $5 \leq K \leq 70$



(d)  $5 \leq K \leq 100^{160}$

Figure 4.17: Bifurcation diagrams for different ranges of the bifurcation parameter  $K$ .

$$\begin{aligned} & \Sigma(1.1844506342089802, 2.192273174477881) \\ &= \begin{pmatrix} -1.02842 & -0.420093 \\ 0.098718 & 0.459435 \end{pmatrix}, \end{aligned}$$

$$\Omega(\xi) = -0.431019 + 0.568981\xi + \xi^2. \quad (4.5.12)$$

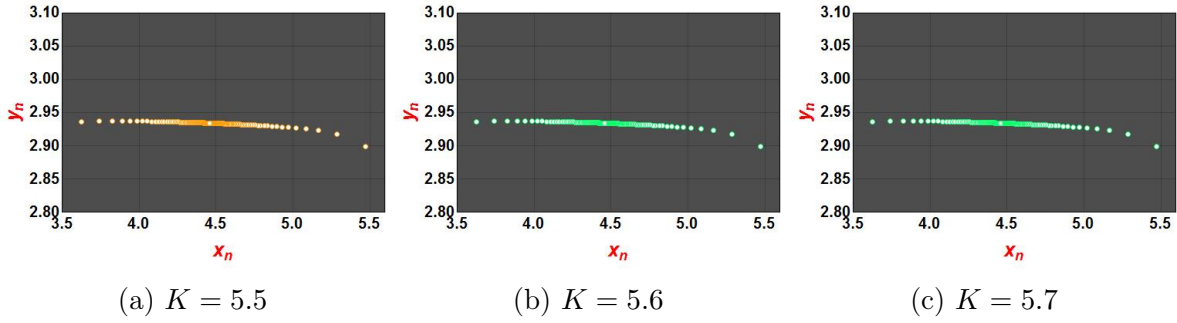


Figure 4.18: Phase plots.

The roots of (4.5.12) are:

$$\xi_{1,2} = \{-1, 0.431019\},$$

with  $|\xi_{1,2}| = 1$ . Thus, the parameters of system (4.1.5)  $(\alpha, F, K, A, \beta, \mathcal{L}, \gamma, \xi, \theta) \in \Phi_{FB}$ . The bifurcation plots are given in figure 5.5, whereas the phase plots are given in figure 4.18. The bifurcation plot (d) of figure 5.5 represents the bifurcation behavior that persists for very high values of the bifurcation parameter  $K$ . One can also get the same bifurcation behavior of the prey population for greater values of  $K$ .

## 4.6 Chaos control

In this section, we will study the chaos in the system (4.1.5). We will use the two-parameter Lyapunov exponent plots to confirm the chaos in the model. Different colours in the colour bar in the plots indicate different values of the Lyapunov exponent. Colours corresponding to positive values in Figures 4.20 mean chaos in the system. Figure 4.20 clearly shows various chaotic and periodic windows that appear for different parameter values. To clearly identify the periodic regime due to Arnold's tongues, we have drawn periodic plots ???. So, these figures confirm the presence of chaos and complex periods in the system. Apart from this, the chaos in the system can be confirmed by many mathematical methods, as recently [147] confirmed the chaos in their model with Marto's sense [[148] and [149]]. But here, we leave it as a future research motivation to confirm the chaos in the system using mathematical methods. Various methods are used to control the chaos found in any model. A detailed comparison of the more common of these methods is given in reference [20]. We used a hybrid control feedback technique to control the chaos in the prey-predator system in our work. This control strategy stabilizes the system and avoids bifurcation by combining parameter perturbation and feedback control. The comparable controlled system is presented below if system (4.1.5)

experiences Hopf and flip bifurcation at the positive fixed point  $(\bar{x}, \bar{y})$ :

$$\begin{cases} x_{n+1} = \mathcal{P}_1 x_n \exp \left[ \frac{\alpha}{1+Fy_n} \left( 1 - \frac{x_n}{K} \right) \frac{x_n}{x_n+A} - \frac{\beta y_n}{x_n+\mathcal{L}} \right] \\ + (1 - \mathcal{P}_1)x_n, \\ y_{n+1} = \mathcal{P}_1 y_n \exp \left[ \gamma + \frac{\xi \beta x_n}{x_n+\mathcal{L}} - \theta y_n \right] + (1 - \mathcal{P}_1)y_n. \end{cases} \quad (4.6.1)$$

where the controlled parameter is  $\mathcal{P}_1 \in (0, 1)$  and in (4.6.1), the controlled approach combines parameter perturbation and feedback control. We can prevent, postpone, or promote chaos in the controlled system by choosing a suitable regulated parameter, denoted as  $\mathcal{P}_1$ . The controlled system's variational matrix  $\mathcal{V}_{Control}$ , which was evaluated at  $(\bar{x}, \bar{y})$ , is presented below:

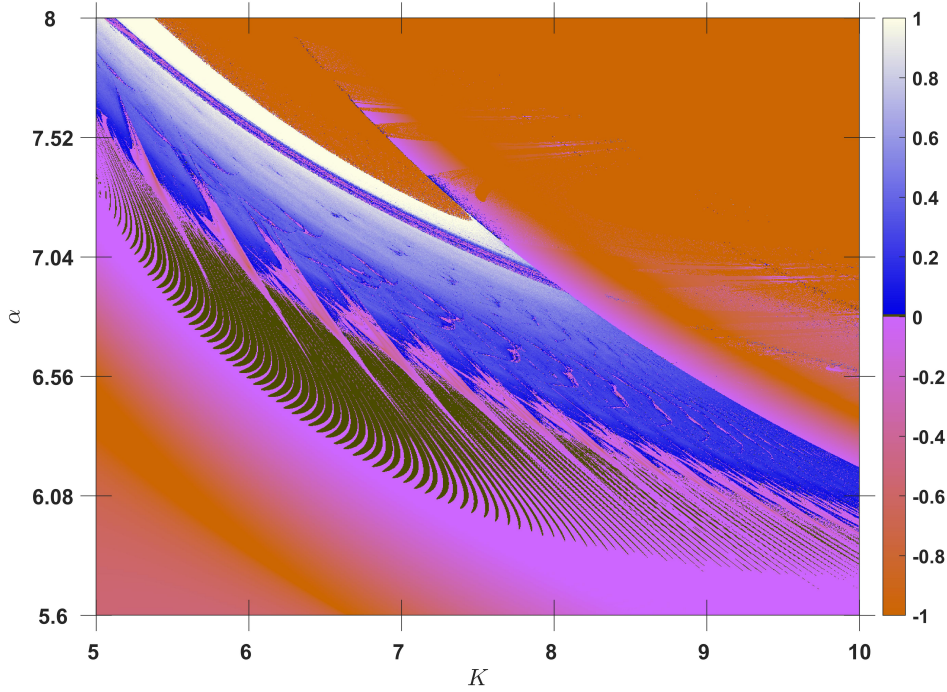


Figure 4.19: Lyapunov exponent plot in the parameter space  $(K, \alpha) \in [5, 10] \times [5.6, 8]$ , when  $F = 0.3, \beta = 1.803, \gamma = 1.65, \xi = 0.19, \theta = 0.8, \mathcal{L} = 0.5$ , and  $A = 0.1$ , with initial conditions  $(x_0, y_0) = (2.4569, 2.4676)$ . In the color bars of the plots, the Lyapunov exponent is depicted by various colors. Positive values in the system are represented by colors that indicate chaos, whereas negative values are represented by colors that indicate stability.

$$\mathcal{V}_{Control} = \begin{pmatrix} \omega_{11} & \bar{x} \left( \frac{\alpha F \bar{x} (\bar{x} - K)}{K(A + \bar{x})(F\bar{y} + 1)^2} - \frac{\beta}{\mathcal{L} + \bar{x}} \right) \mathcal{P}_1 \\ \frac{\mathcal{L} \beta \xi \bar{y} \mathcal{P}_1}{(\mathcal{L} + \bar{x})^2} & 1 - \theta \bar{y} \mathcal{P}_1 \end{pmatrix},$$

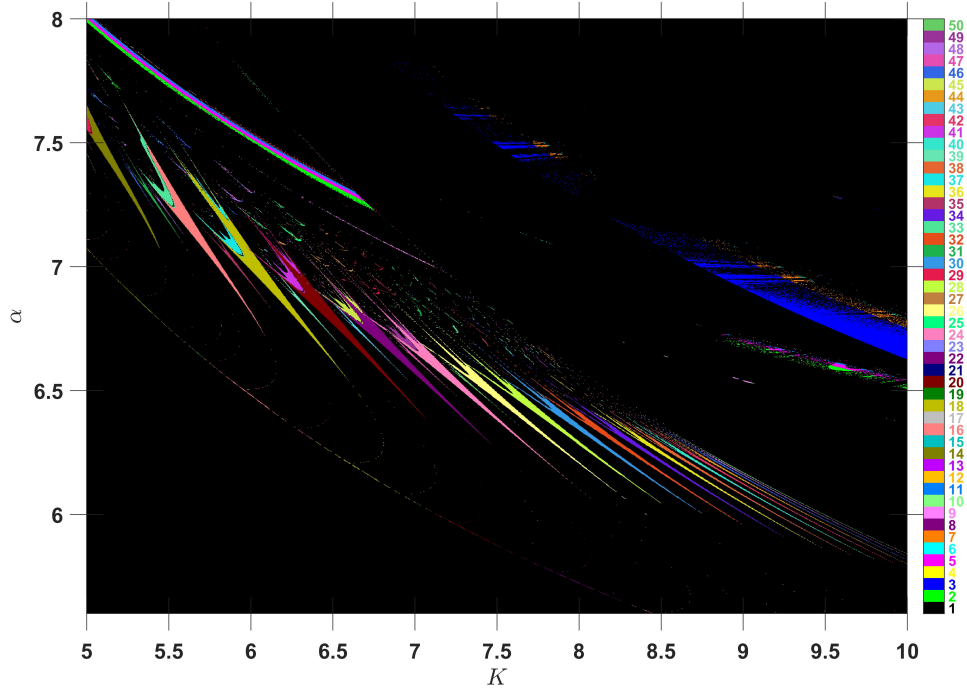


Figure 4.20: Isoperiodic diagrams related to the Plot 4.19 in the parameter space  $(K, \alpha) \in [5, 10] \times [5.6, 8]$ , when  $F = 0.3, \beta = 1.803, \gamma = 1.65, \xi = 0.19, \theta = 0.8, \mathcal{L} = 0.5$ , and  $A = 0.1$ , with initial conditions  $(x_0, y_0) = (2.4569, 2.4676)$ . In the plots' colour bars, boxes of different colours represent different periods, with period numbers labeled in each box.

where

$$\omega_{11} = \bar{x} \left( \frac{\alpha (AK - \bar{x} (2A + \bar{x}))}{(A + \bar{x})^2 (F\bar{y}K + K)} + \frac{\beta\bar{y}}{(\mathcal{L} + \bar{x})^2} \right) \mathcal{P}_1 + 1.$$

If the roots of the characteristic function of  $\mathcal{V}_{Control}$  exist in an open unit disc, the fixed point  $(\bar{x}, \bar{y})$  of the controlled system (4.6.1) is locally asymptotically stable. The primary motivation for controlling chaotic dynamics in biological systems is to avoid the extinction of species or over-exploitation of resources. In the context of prey-predator models, this can be achieved by stabilizing the populations at a sustainable level, which can be interpreted as a biologically meaningful control objective. In addition, the controlled system can be used to investigate the effects of different types of control interventions on prey-predator dynamics. For example, by varying the value of  $\mathcal{P}_1$ , you can investigate the effectiveness of different management strategies, such as predator removal or introducing additional resources for prey. Controlling chaos in the parameters of a prey-predator model has important biological implications. In a stable ecosystem, the population growth rates of prey and predators ( $\alpha$  and  $\beta$ ) should be balanced. However, if the growth rate of either species increases too much, it can lead to the over-exploitation of resources and, eventually, the collapse of the entire ecosystem. One can stabilize the ecosystem



and prevent its failure by controlling the growth rates of prey and predators. Therefore, chaos in the intrinsic growth rate of prey and predators must be maintained. If predators can access alternative food sources, they may not depend solely on the prey population for survival. This can lead to unpredictable fluctuations in predator population size. By controlling the growth rate of predators due to alternative resources  $\gamma$ , one can ensure that the predator population does not exceed a sustainable level. Intra-specific competition  $\theta$  among predators can lead to overcrowding and depletion of resources, which can cause the predator population to decline. By controlling the strength of intra-specific competition among predators, one can ensure that the predator population remains sustainable. The conversion rate  $\xi$  determines how much prey biomass is converted into predator biomass. If the conversion rate is too high, it can lead to overexploitation of prey and, eventually, the collapse of the ecosystem. By controlling the conversion rate, one can maintain a sustainable balance between the numbers of prey and predators. The carrying capacity  $K$  is the maximum number of individuals a particular habitat can support. By controlling the carrying capacity of prey, one can ensure that the prey population does not exceed the habitat's carrying capacity, which can lead to the depletion of resources and the eventual collapse of the ecosystem. It is crucial to remember that our control technique has some limitations. While it offers a way to keep the system from bifurcating and stabilizing it, it might not work in all situations or for all parameter ranges. The prey-predator model's specific properties and the control parameters' values determine how well the control approach works. Therefore, an in-depth understanding of the system's dynamics and careful selection of control situations are required.

## 4.7 Conclusion

In this chapter, we consider two populations: the prey and the predator. In the absence of predators, the prey population increases exponentially; nevertheless, predation causes the population to decline. On the other hand, the predator population grows as it feeds on the prey population but declines in the absence of prey. The model is governed by a collection of coupled differential equations describing the dynamics of the two populations over time. The model's behavior is highly sensitive to the parameters' values. Here's what each parameter represents:  $\alpha$ : the intrinsic growth rate of the prey population in the absence of predators. This parameter determines how fast the prey population grows when no predators are around.  $\beta$ : the predation rate. This parameter determines how fast the predator population grows as it feeds on the prey population.  $\gamma$ : the growth rate of the predator population in the absence of prey. This parameter represents alternative food sources available to the predator and how fast the predator population grows when it doesn't have prey to feed on.  $\theta$ : the death rate of the predator population due to

overcrowding. This parameter represents intra-species competition among predators for resources and how fast the predator population declines when it becomes too large.  $F$ : is the fear effect of the prey population.  $K$ : the carrying capacity of the prey population in a particular habitat. This parameter represents the maximum number of prey that the habitat can support.  $\mathcal{L}$ : the half saturation constant. This parameter represents the prey density at which the predating rate is half its maximum value.  $\xi$ : the conversion rate for a predator. This parameter represents how efficiently the predator population converts prey into new predators. By varying these parameters, we simulated different scenarios and observed how the two populations interacted with each other over time. For example, increasing the perdition rate  $\beta$  can lead to a decline in the prey population, which in turn causes a decline in the predator population. On the other hand, increasing the intrinsic growth rate of the prey population  $\alpha$  can increase both populations. Still, the system can become unstable and lead to population crashes.

Moreover, the analysis of the two-dimensional prey-predator model has provided crucial insights into the behavior of ecological systems. The stability analysis of the fixed points in both the discrete and continuous forms of the model has led to a deeper understanding of the system's dynamics. Additionally, multi-parameter bifurcations were investigated. The study has analyzed the forward and backward Hopf and flip bifurcations that happen in various parameters. These findings have significant implications for managing ecological systems, given that these bifurcations can lead to drastic changes in the quantity of predator and prey species. Moreover, the study proposes a simple control technique to manage the bifurcation in the system. This technique could be highly beneficial in maintaining the stability of ecological systems, which are often highly sensitive to small changes in their parameters. Especially in the context of population management and conservation initiatives, the ability to control the bifurcation may substantially impact the management of natural systems. Additionally, the mathematical proof that only the positive fixed point in the continuous-time model experiences Hopf bifurcation offers a critical insight into the system's dynamics. The backward Hopf and flip bifurcation in the fear and Allee effects indicate that when the fear effect and Allee effect are low, the predator population can easily catch the prey, increasing the predator population size. When the predator population increases, the prey population may also decline. If the Allee effect causes the prey population to fall below its minimum threshold, the prey species may finally become extinct. The high population density of the prey population during periods when the Allee and fear effects are weak might also result in an unstable prey-predator system. The high population density of the prey population due to the crowding effect can lead to increased competition for resources and mating partners, which can cause the prey population to decline rapidly. Additionally, the high population density of the predator population can cause over-exploitation of the prey population,



leading to a decline in the prey population. Suppose the prey population falls below its minimum threshold due to the Allee effect. In that case, it can lead to the extinction of the prey population, causing the predator population to decline due to a lack of food resources. However, suppose the predator population size is not reduced enough. In that case, it can lead to over-exploitation of the prey population, causing it to decline rapidly and collapse the entire system. Therefore, in our case, the low values of fear and the Allee effect could lead to instability in the system due to the crowding effect, which can cause the prey population to decline rapidly, leading to the collapse of the entire system. However, the increase in the Allee and fear must be to a certain extent to stabilize the population.

# Chapter 5

## Fixed points stability, bifurcation analysis, and chaos control of an epidemic model with vaccination and vital dynamics

### 5.1 Introduction

Epidemiology, the study of the spread and control of infectious diseases, plays a crucial role in understanding and preventing the spread of disease. One important aspect of epidemiology is the development and use of mathematical models to predict and control the spread of disease. In this chapter, we will explore a specific type of mathematical model known as a discrete-time epidemic model with vaccination and vital dynamics. Mathematical models have been used for many years to determine the rate of population growth, control diseases, determine the consistency of chemical reactions, determine economic stability, formulate game theory, and so on. Mathematical differential models are used if the population is continuous, while mathematical difference models are used for seasonal populations. Recently, [126] discussed the dynamic aspects of the 3D chemical model and proved that the model is globally stable. Khan [115] controlled the chaos of the 4D chemical model. Difference models have been popular for many years due to their excellent numerical and computational results, which is why many mathematicians are working on difference models. Abbasi and Din [20] discretized the continuous model using piecewise constant arguments. They studied the model's behavior with the crowding effect and discussed the stability of equilibrium and bifurcation. Additionally, they analyze various chaos control strategies and conclude that a simple feedback control approach

with just one control parameter is more effective than other comparable control theory techniques. Din *et al.* [127] discretized a chemical model using a nonstandard scheme and investigated the qualitative analysis of it. Khan [128] discretized the predator-prey model and analyzed the effect of Holling type-II on it. Moreover, the author also introduced the new controlled strategy by modifying the hybrid control strategy and proved that the newly introduced technique is more effective and feasible.

Additionally, the behavior of a population in response to an infection is studied using mathematical models. The models are used to comprehend the disease's behavior. In the literature, various discrete and continuous-time mathematical models that have been developed and examined for multiple diseases include [129] and [130]. Numerous studies have been conducted on the traditional SIR model of disease transmission. In line with other models, overlapping disease populations are studied using continuous-time SIR models, whereas seasonal disease populations are studied using discrete-time SIR population models. Discrete-time disease models have attracted increased interest because of their detailed dynamics and attractive numerical outcomes. A discrete SIRS epidemic system was examined by Xiang *et al.* [131] to better understand how vaccination affected it. Franoosh and Parsamanesh [132] dynamically analyzed a discrete SIS system with bi-linear incidence. The authors investigate the model's bifurcation and equilibrium stability. Additionally, both susceptible individuals and recent immigrants are included in the vaccine program. Different epidemic models are discretized by Liu *et al.* [133] utilizing backward and forward Euler methods. Using these discretization techniques, they looked into the stability behavior of endemic equilibrium. They concluded that the backward Euler method is best for endemic equilibrium's overall stability, whereas the forward Euler method makes models more dynamically rich than continuous models. In their analysis of a SIRS epidemic model with a non-linear incidence, Hu *et al.* [134] demonstrate the conditions for the local stability of the boundary and positive equilibrium. A disease model for Babesiosis disease transmission in bovine and tick populations is discretized by Aranda *et al.* [135]. They demonstrated persistence, local equilibrium stability, and the behavior of border equilibrium points globally. The comparison principle is used by Ma *et al.* [136] to examine the overall behavior of the positive steady-state of a discrete SIR model. Using an unconventional finite difference approach, Cui and Zhang [137] discretized a SIR model and derived adequate requirements for its global stability. Mickens [138] uses unconventional discretization for numerical approaches to ensure that the solutions to difference equations are positive. Vecchio and Izzo [139] discretized an epidemic model using implicit and explicit Euler methods and showed attractive results for the solution's positivity, boundedness, and global stability. Van den Driessche and Yakubu [140] investigate a few discrete epidemic models developed for SEIR diseases, animal anthrax, and human cholera. They demonstrated these models' worldwide sta-

bility and endurance. The most well-known types of epidemic models among them are SIS (susceptible-infected-susceptible) models. Vaccinating the infected population is essential to managing and eradicating the infected population. To do this, it is conceivable to incorporate a compartment for vaccinated individuals into the SIS model and obtain SIVS individuals [141] and [142].

Recently, mathematicians have used several SIR models to control the coronavirus epidemic. Liu and Li [143] derive an epidemic model with a discrete state structure and prove its global stability and persistence. They apply their results to the COVID-19 pandemic. Alqahtani [144] took the SIR model for coronavirus disease and proved that hospital resources, such as hospital beds, should be increased to diagnose the disease in any society better. Lin *et al.* [145] proposed the SEIR model for the Corona epidemic and proved that we could control the outbreak through social isolation strategies and government initiatives. Wells *et al.* [146] and Gnostic *et al.* [147] proved that we can stop the spread of COVID-19 globally by imposing travel restrictions and closing borders. Khan *et al.* [148] discretized a diabetic compartmental model disclosed to COVID-19 and proved that the quarantined compartment must not be kept empty to stabilize the system. Motivated by the above literature, we consider the discrete-time SIS epidemic model in this chapter from [149]. The model we will discuss includes vaccination, an important intervention strategy for controlling the spread of disease, and vital dynamics, which consider births and deaths in the population. This model will be used to simulate the spread of a disease in a population and to evaluate the effectiveness of different vaccination strategies. The results of this chapter will provide valuable insights into the dynamics of disease spread and the impact of interventions such as vaccination on the control of epidemics. Overall, we aim to contribute to understanding the spread of infectious diseases and developing effective intervention strategies through mathematical modeling. Mainly, we investigate the local stability of equilibria, global stability, bifurcation theory with numerical examples, and chaos control. Moreover, the model is discretized using Euler's method, and the stability of the equilibria is analyzed. Finally, we conclude the results. The three-dimensional Lotka-Volterra predator-prey system is given below:

$$\begin{cases} I_{t+1} = \frac{bS_t I_t}{N_t} + [1 - (a + c)]I_t, \\ S_{t+1} = (1 - q)aN_t - \frac{bS_t I_t}{N_t} + [1 - (a + p)]S_t + cI_t + dV_t, \\ V_{t+1} = qaN_t + pS_t + [1 - (a + d)]V_t. \end{cases} \quad (5.1.1)$$

Here,  $a$  and  $N$  are positive, while  $c, p, d, b$  and  $q$  are non-negative. Natural death rates are represented by the parameter  $a$ , contact rates by  $b$ , cure rates by  $c$ , immunity loss rates by  $d$ , and vaccination rates for newcomers and susceptible individuals by  $q$  and  $p$ , respectively. The model's flow diagram and transmissions between its sub-population

and their respective transmission rates are depicted in the diagram 5.1. The susceptible individuals become infected at the standard incidence rate of  $\frac{bS_t I_t}{N_t}$ . Moreover,  $N_{t+1} = N_t$ .

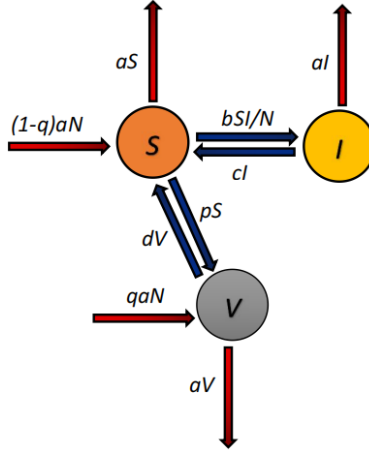


Figure 5.1: The model's flowchart and transmission rates.

Let  $V_t = N - S_t - I_t$ , the above system (5.1.1) becomes:

$$\begin{cases} I_{t+1} = \frac{bS_t I_t}{N} + [1 - (a + c)]I_t, \\ S_{t+1} = [(1 - q)a + d]N - \frac{bS_t I_t}{N} + [1 - (a + p + d)]S_t + (c - d)I_t. \end{cases} \quad (5.1.2)$$

The necessary conditions for the non-negativity of the solution of the system (5.1.2) are given below:

$$a + p + d + b < 1, a + c < 1. \quad (5.1.3)$$

The criteria we present here serve as the natural prerequisites for the system (5.1.2). While these criteria are sufficient, they are not necessary for the solutions to be non-negativity. We introduce a novel approach where less than one susceptible person every unit of time dies, acquires an infection, or receives vaccinations. Similarly, according to the second criterion, less than one sick individual dies or recovers for every unit of time. This unique method adds a fresh perspective to our understanding of disease dynamics and control methods. This chapter is innovative and essential since it uses two separate models to represent the same population and takes the novel method of employing fixed point techniques to prove the global stability of the system (5.1.2). To the best of our knowledge, no earlier studies have investigated this nature. We thoroughly examine the system's global stability in the model (5.1.2). This lets us know how the system reacts to parameter changes and the circumstances necessary for long-term illness control. This approach improves our comprehension of the underlying dynamics and makes it possible to pinpoint important variables and preventative measures for developing infectious illnesses. In the second model (5.2.7), we will explore the bifurcation behavior of the

system. We will examine the system's behavior during bifurcation in the second model (5.2.7). Understanding how small parameter changes can result in qualitative shifts in the system dynamics is possible through bifurcation analysis. We highlight the complex interaction between several parameters and their bearing on the system's behavior by analyzing one parametric bifurcation and a codimension-two bifurcation. By providing a deeper insight into the underlying mechanisms influencing disease patterns, this chapter will help develop specific treatment methods.

## 5.2 Stability of the fixed points

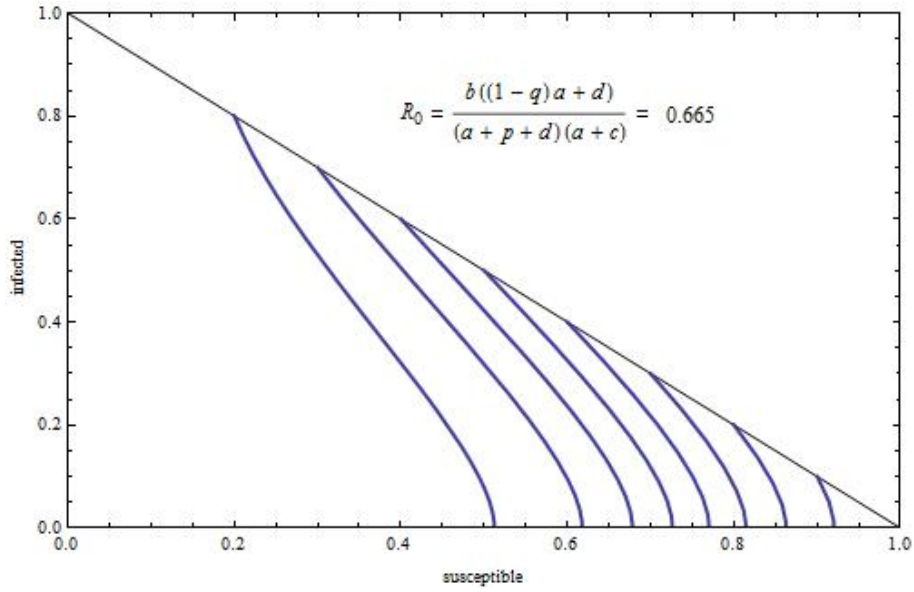


Figure 5.2: Basic reproduction number for  $a = 0.9, b = 1.9, c = 0.6, d = 0.3, p = 0.4$  and  $q = 0.4$ .

The equilibria of the system (5.1.2) are solutions of the following system:

$$\begin{cases} 0 = \frac{bS_t I_t}{N_t} + [1 - (a + c)]I_t, \\ 0 = [(1 - q)a + d]N - \frac{bS_t I_t}{N} + [1 - (a + p + d)]S_t + (c - d)I_t, \end{cases} \quad (5.2.1)$$

Solving the above equations we get

$E^0 = \left(0, \frac{[(1-q)a+d]N}{a+p+d}\right)$ , and  $E^*(I^*, S^*) = \left(\frac{[(1-q)a+d]bN - (a+p+d)(a+c)N}{b(a+d)}, \frac{(a+c)N}{b}\right)$ . The fixed point  $E^*(I^*, S^*)$  is positive when  $[(1 - q)a + d]bN - (a + p + d)(a + c)N > 0$  iff  $R_0 = \frac{b[(1-q)a+d]}{(a+p+d)(a+c)} > 1$ . Here  $R_0$  is the basic reproduction number of system (5.1.2), see [150]. Figure 5.2 shows the plot for the basic reproduction number  $R_0$ .

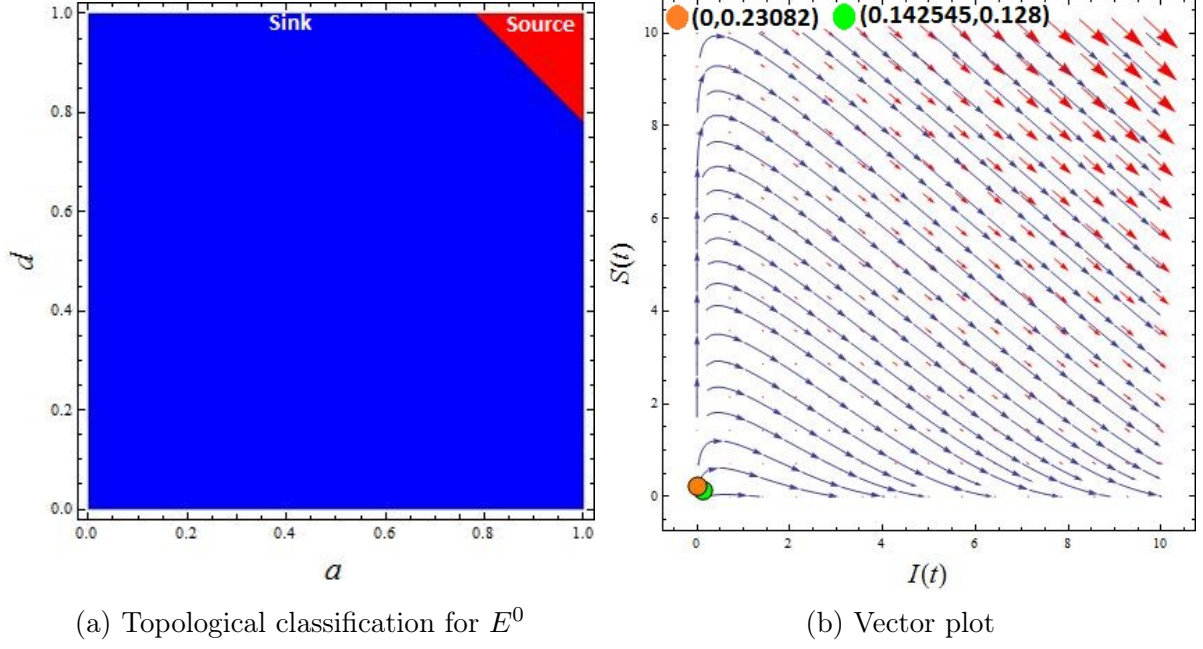


Figure 5.3: Plots of system (5.1.2) for  $b = 1.2, c = 0.18, p = 0.22, q = 0.4, N = 0.32, h = 0.35, a \in (0, 1)$ , and  $d \in (0, 1)$ .

The variational matrix  $V_{E^0}$  of (5.1.2) calculated at  $E^0 = \left(0, \frac{[(1-q)a+d]N}{a+p+d}\right)$  is given as:

$$V_{E^0} = \begin{pmatrix} 1 - a - c + \frac{b(a+d-aq)}{a+d+p} & 0 \\ c - d - \frac{b(a+d-aq)}{a+d+p} & 1 - a - d - p \end{pmatrix},$$

Characteristic polynomial of  $V_{E^0}$  is:

$$P(\lambda) = \lambda^2 - \text{Tr}(V_{E^0})\lambda + \text{Det}(V_{E^0}),$$

where

$$\text{Tr}(V_{E^0}) = 2 - 2a - c - d - p + \frac{b(a+d-aq)}{a+d+p},$$

and

$$\begin{aligned} \text{Det}(V_{E^0}) &= \frac{(-1 + a + d + p)(a^2 + (-1 - b + c)d + (-1 + c)p)}{a + d + p} \\ &+ \frac{(-1 + a + d + p)(a(-1 + c + d + p + b(-1 + q)))}{a + d + p}. \end{aligned}$$

The eigenvalues of  $V_{E^0}$  are  $\lambda_1 = 1 - a - d - p$  and  $\lambda_2 = 1 - a - c + \frac{b(a+d-aq)}{a+d+p}$ . By our assumptions  $a + p + d + b < 1$  and  $a + c < 1$ , one can see that  $|\lambda_1| < 1$ , but  $|\lambda_2| < 1$  iff  $R_0 < 1$ . The following lemma for the local stability of  $V_{E^0}$  can therefore be written as:

**Lemma 5.2.1.** *Assume that the condition (5.1.3) holds then the steady-state  $E^0$  of the*

system (5.1.2) is a

- (I) sink if  $|1 - a - c + \frac{b(a+d-aq)}{a+d+p}| < 1$  i.e.  $R_0 < 1$  or  $a + c - 2 < \frac{b(a+d-aq)}{a+d+p} < a + c$ ;  
 (II) saddle point if  $|1 - a - c + \frac{b(a+d-aq)}{a+d+p}| > 1$ .

The topological classification and vector plot for the fixed point  $E^0$  are given in figure 5.3. From figure 5.3, we see that if condition (5.1.3) fails, then the system (5.1.2) at  $E^0$  goes towards instability.

Variational matrix  $V_{E^*}$  of (5.1.2) at  $E^* = \left( \frac{[(1-q)a+d]bN-(a+p+d)(a+c)N}{b(a+d)}, \frac{(a+c)N}{b} \right)$  is given by:

$$V_{E^*} = \begin{pmatrix} 1 & -\frac{a^2-bd+c(d+p)+a(c+d+p+b(-1+q))}{a+d} \\ -a-d & \frac{d-bd+(c-d)(d+p)+a(1+c-d+b(-1+q))}{a+d} \end{pmatrix},$$

The characteristic polynomial of variational matrix  $V_{E^*}$  is:

$$P(\lambda) = \lambda^2 - Tr(V_{E^*})\lambda + Det(V_{E^*}),$$

where

$$Tr(V_{E^*}) = 1 + \frac{d - bd + (c - d)(d + p) + a(1 + c - d + b(-1 + q))}{a + d},$$

and

$$\begin{aligned} Det(V_{E^*}) &= -\frac{1}{a+d} [a^3 - d - b(-1+d)d + (c(-1+d) + d)(d+p) \\ &+ a(-1+d(1+d+p) + c(-1+2d+p) + b(1+d(-2+q) - q)) \\ &+ a^2(c+2d+p+b(-1+q))]. \end{aligned}$$

The eigenvalues of  $V_{E^*}$  are

$$\begin{aligned} \lambda_1 &= \frac{1}{2(a+d)} (2a - ab + ac - d^2 + cp - d(-2 + a + b - c + p) + abq) + \\ &\frac{1}{2(a+d)} \left( \sqrt{4(a+d)(\mu_1) + (\mu_2)^2} \right), \\ \lambda_2 &= -\frac{1}{2(a+d)} (-2a + ab - ac + d^2 - cp + d(-2 + a + b - c + p) - ab) \\ &- \frac{1}{2(a+d)} \left( \sqrt{4(a+d)(\mu_1) + (\mu_2)^2} \right), \text{ where} \\ \mu_1 &= a^3 - d - b(-1+d)d + (c(-1+d) + d)(d+p) + a(-1+d(1+d+p) \\ &+ c(-1+2d+p) + b(1+d(-2+q) - q)) + a^2(c+2d+p+b(-1+q)), \text{ and} \\ \mu_2 &= d^2 - cp + d(-2 + b - c + p) + a(-2 + b - c + d - bq). \end{aligned}$$



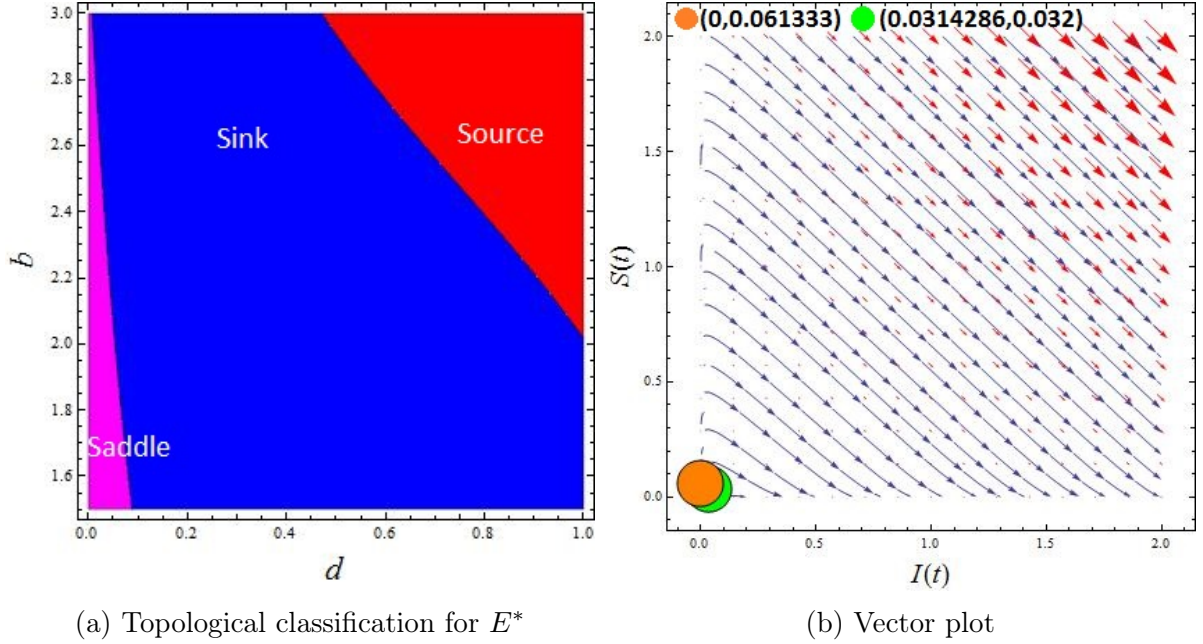


Figure 5.4: Plots of system (5.1.2) for  $a = 0.2, c = 0.6, p = 0.5, q = 0.4, N = 0.1, h = 0.5, d \in (0, 1)$ , and  $b \in (1.5, 3)$ .

We use the following lemma to study the local stability of the model (5.1.2) at  $E^*$ .

**Lemma 5.2.2.** *Let  $\mu_3 = -d - bd(d - 1) + ((d - 1)c + d)(d + p)$ ,  $\mu_4 = -1 + d(1 + p + d) + c(-1 + 2d + p) + b(1 + d(-2 + q) - q)$ ,  $\mu_5 = c + 2d + p + b(-1 + q)$  and  $\mu_6 = d - bd + (c - d)(d + p) + a(1 - d + c + b(q - 1))$ , then*

$$\begin{aligned} \text{Tr}(V_{E^*}) &= 1 + \frac{\mu_6}{a + d}, \text{ and} \\ \text{Det}(V_{E^*}) &= -\frac{1}{a + d} (\mu_3 + a^3 + a^2(\mu_5) + a(\mu_4)). \end{aligned}$$

We have these conditions for the positive fixed point

(I) The unique positive fixed point  $E^*$  is source iff

$$\left| -\frac{1}{a + d} (\mu_3 + a^3 + a^2(\mu_5) + a(\mu_4)) \right| > 1,$$

and

$$\left| 1 + \frac{\mu_6}{a + d} \right| < \left| 1 - \frac{1}{a + d} (\mu_3 + a^3 + a^2(\mu_5) + a(\mu_4)) \right|.$$

(II) The unique positive fixed point  $E^*$  is the saddle point iff

$$\left( 1 + \frac{\mu_6}{a + d} \right)^2 > 4 \left( -\frac{1}{a + d} (\mu_3 + a^3 + a^2(\mu_5) + a(\mu_4)) \right),$$

and

$$\left| 1 + \frac{\mu_6}{a+d} \right| > \left| 1 - \frac{1}{a+d} (\mu_3 + a^3 + a^2(\mu_5) + a(\mu_4)) \right|.$$

(III) The unique positive fixed point  $E^*$  is a non-hyperbolic point iff

$$\left| 1 + \frac{\mu_6}{a+d} \right| = \left| 1 - \frac{1}{a+d} (\mu_3 + a^3 + a^2(\mu_5) + a(\mu_4)) \right|, \quad (5.2.2)$$

or

$$-\frac{1}{a+d} (\mu_3 + a^3 + a^2(\mu_5) + a(\mu_4)) = 1 \text{ and } \left| 1 + \frac{\mu_6}{a+d} \right| \leq 2. \quad (5.2.3)$$

We will demonstrate the necessary and sufficient criteria for the source of  $E^*$  in the subsequent theorem.

**Theorem 5.2.3.** *If neither (5.2.2) nor (5.2.3) holds, then the interior fixed point  $E^* = \left( \frac{[(1-q)a+d]bN - (a+p+d)(a+c)N}{b(a+d)}, \frac{(a+c)N}{b} \right)$  is sink iff*

$$\left| 1 + \frac{\mu_6}{a+d} \right| < 1 - \frac{1}{a+d} (\mu_3 + a(\mu_4) + a^2(\mu_5) + a^3) < 2.$$

The topological classification and vector plot for a fixed point  $E^*$  are given in the figure 5.4.

### 5.2.1 Global stability of the positive fixed point

We shall first demonstrate that the system (5.1.2)'s overall population is bounded, resulting in the following theorem:

**Theorem 5.2.4.** *The total population of the system (5.1.2) is bounded.*

*Proof.*

$$\begin{aligned} I_{t+1} + S_{t+1} &= \frac{bS_t I_t}{N_t} + [1 - (a+c)]I_t \\ &+ [(1-q)a+d]N - \frac{bS_t I_t}{N} + [1 - (a+p+d)]S_t + (c-d)I_t \\ &= (1-a)I_t + [(1-q)a+d]N - [1 - (a+p+d)]S_t + (c-d)I_t \\ &\leq (1-a)I_t + [a+d]N - [1-a]S_t \\ P_{t+1} &\leq (1-a)P_t + [(1-q)a+d]N \\ P_t &\leq \frac{N(1 - (1-a)^t)(-1+a)(-d-a+qa)}{(1-a)a} + (1-a)^{t-1}C_1 \end{aligned}$$

Applying  $\lim_{t \rightarrow \infty}$ , we get

$$P_t \leq \frac{N(a + d - qa)}{a}.$$

□

For the global consistency of  $E^* = \left( \frac{[(1-q)a+d]bN-(a+p+d)(a+c)N}{b(a+d)}, \frac{(a+c)N}{b} \right)$  we will use the following theorems (see [19]):

**Theorem 5.2.5.** *Let  $(\chi, d)$  be a metric space,  $g : \chi^n \rightarrow \chi$  and  $f : \mathbb{R}_+^3 \rightarrow \mathbb{R}_+$  such that:*

(i)  *$f$  is an  $n$  dimensional  $(c)$ -comparison function;*

(ii)  *$\forall y_0, \dots, y_{n-1}, y_n \in \chi$  we have*

$$d(g(y_0, \dots, y_{n-1}), g(y_1, \dots, y_n)) \leq f(d(y_0, y_1), \dots, d(y_{n-1}, y_n));$$

(iii)  *$\forall \mathbb{R}$  we have*

$$f(m, 0, \dots, 0) + f(0, m, 0, \dots, 0) + \dots + f(0, \dots, 0, m) \leq f(m, \dots, m).$$

*Then:*

(a) *the operator  $B_g : \chi^n \rightarrow \chi^n$  is a Picard operator;*

(b) *we have the estimation*

$$d(y_k, y^*) \leq n \cdot \sum_{i=0}^{\infty} \phi^{[\frac{k}{n}]}(d_0) \cdot \frac{\alpha^{[\frac{k}{n}]}}{1 - \alpha},$$

*where  $(y_k)_{k \in \mathbb{N}}$  is any solution of (1),  $d_0 = \max_{i=0, k-1} d(y_i, y_{i+1})$  and  $\phi : \mathbb{R}_+ \rightarrow \mathbb{R}_+$*

$$\phi(m) = \psi(m, \dots, m).$$

**Theorem 5.2.6.** *Let  $(\chi, d)$  be a metric space,  $g : \chi^n \rightarrow \chi$  such that:*

(i) *there exist  $p_i \in \mathbb{R}_+$ ,  $i = \overline{1, k}$ , with  $\alpha = \sum_{i=1}^n p_i < 1$  such that*

$$d(g(\bar{x}, \bar{y})) \leq \sum_{i=1}^n p_i d(x_i, y_i),$$

*for all  $\bar{x} = (x_1, \dots, x_n), \bar{y} = (y_1, \dots, y_n) \in \chi^n$ . Then:*

(a) *the operator  $B_g : \chi^n \rightarrow \chi^n$  is a Picard operator;*

(b) *we have the estimation*

$$d(y_k, y^*) \leq n \cdot d_0 \cdot \frac{\alpha^{[\frac{k}{n}]}}{1 - \alpha},$$

*where  $(y_k)_{k \in \mathbb{N}}$  is any solution of (1),  $d_0 = \max_{i=0, k-1} d(y_i, y_{i+1})$ .*

(c) operator  $g$  is continuous in  $(y^*, \dots, y^*) \in \chi^n$

Using Theorem 5.2.5 and Theorem 5.2.6 we can easily find the global consistency of the system (5.1.2) which is given in the theorem below:

**Theorem 5.2.7.** *Let  $I_t \in (0, M_1]$ ,  $S_t \in (0, M_2]$ . If  $|\frac{bM_1}{N}| < 1$  and condition (5.1.3) holds, then the unique positive steady-state  $R^* = (I^*, S^*)$  of the system (5.1.2) is globally asymptotically stable. We have the following estimation:*

$$\delta(R_t, R^*) \leq \frac{\alpha^n}{1 - \alpha} \cdot \max \{ \delta(R_0 - R_1), \dots, \delta(R_{n-1} - R_n) \},$$

where  $\alpha = |\frac{bM_1}{N}| + |1 - (a + c)| + |1 - (a + p + d)| + |c - d|$  and  $\delta$  is the metric on the space  $Y = (0, M_1] \times (0, M_2]$  defined by

$$\delta(R_1, R_2) = \max \{ |I_1 - I_2|, |S_1 - S_2| \}$$

$$\forall R_1 = (I_1, S_1), R_2 = (I_2, S_2) \in Y.$$

*Proof.* The system (5.1.2) can also be written as:

$$\begin{cases} f_1(I_t, S_t) = \frac{bS_t I_t}{N} + [1 - (a + c)]I_t, \\ f_2(I_t, S_t) = [(1 - q)a + d]N - \frac{bS_t I_t}{N} + [1 - (a + p + d)]S_t + (c - d)I_t. \end{cases} \quad (5.2.4)$$

Let  $Y = (0, M_1] \times (0, M_2]$ . Then it is obvious that the metric space  $(Y, \delta)$  is complete.

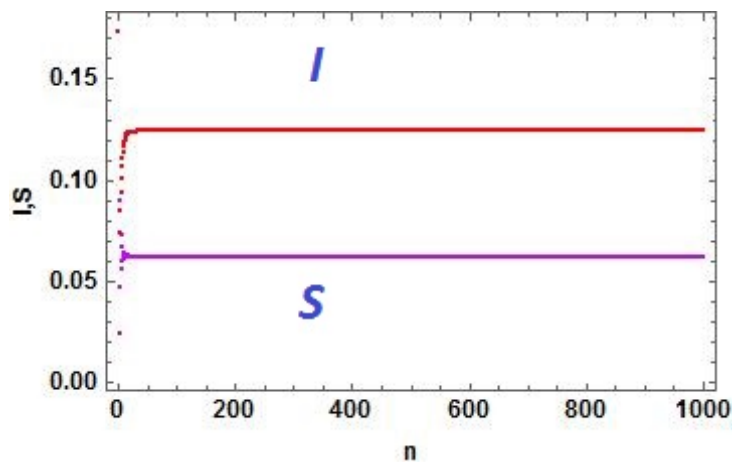


Figure 5.5: Stability diagrams

Let  $f = (f_1, f_2) : Y^{n+1} \rightarrow Y$ .

$$\begin{aligned}
|f_1(I, S) - f_1(I^*, S^*)| &= \left| \frac{bS_t I_t}{N_t} + [1 - (a + c)]I_t - \left[ \frac{bS_t^* I_t^*}{N_t^*} + [1 - (a + c)]I_t^* \right] \right| \\
&= \left| \frac{b}{N} (S_t I_t - S_t^* I_t^*) + [1 - (a + c)] (I_t - I_t^*) \right| \\
&\leq \left| \frac{b}{N} \right| |(S_t I_t - S_t^* I_t^*)| + |[1 - (a + c)]| |(I_t - I_t^*)| \\
&\leq \left| \frac{bM_1}{N} \right| |(S_t - S_t^*)| + |[1 - (a + c)]| |(I_t - I_t^*)|,
\end{aligned}$$

It can be seen from condition (5.1.3) that  $|1 - (a + c)| < 1$ .

$$\begin{aligned}
|f_2(I, S) - f_2(I^*, S^*)| &= \left| [(1 - q)a + d]N - \frac{bS_t I_t}{N} + [1 - (a + p + d)]S_t + (c - d)I_t \right. \\
&\quad \left. - \left[ [(1 - q)a + d]N - \frac{bS_t^* I_t^*}{N} + [1 - (a + p + d)]S_t^* + (c - d)I_t^* \right] \right| \\
&\leq \left| \frac{bM_1}{N} \right| |S_t - S_t^*| + |1 - (a + p + d)| |S_t - S_t^*| + \\
&\quad |c - d| |I_t - I_t^*|.
\end{aligned}$$

Condition (5.1.3) shows that  $|1 - (a + p + d)| < 1$  and  $|c - d| < 1$ .  
and we have

$$\delta(f(R_0, \dots, R_n), f(R_0^*, \dots, R_n^*)) \leq \frac{bM_1}{N} \max\{\delta(R_0, R_0^*), \delta(R_n, R_n^*)\}.$$

For this case, we consider the function  $\psi : \mathbb{R}_+^2 \rightarrow \mathbb{R}_+$

$$\psi(s_0, s_1) = \max\{\delta(R_0, R_0^*), \delta(R_n, R_n^*)\}$$

which is a (c)-comparison function in two dimensions. Thus, there exists an operator  $A_f : X^2 \rightarrow X^2$  that is a Picard operator, and therefore the given system is globally asymptotically stable for the positive fixed point. The global stability of the model (5.1.2) can be seen from figure 5.5.  $\square$

Discretizing a continuous-time model is essential because it allows for using digital computers for simulations and analysis, implementing digital control techniques, and applying stability analysis techniques specific to discrete-time systems. It also simplifies applying numerical methods and algorithms to the system. Discretizing also aids in decreasing system complexity and improving its accessibility. Furthermore, discretizing allows for incorporating discrete-time measurements, such as those taken at fixed intervals, into the

model. As a result, the model may be more accurate and realistic. It is crucial to discretize continuous-time models using Euler's forward scheme because it is a simple and valuable technique that, for small time steps, yields an accurate approximation of the continuous-time model. Additionally, because it is a stable approach, the solution of the discrete-time system won't gradually become unbounded. It can also be combined with other discretization techniques to increase the model's accuracy and discretize numerous continuous-time models, including linear and nonlinear systems. It is also frequently applied in various academic disciplines, including physics, engineering, and computer science. It can be used to discretize continuous-time models for real-time applications, like control systems, where the time step needs to be tiny to ensure accurate and responsive control. Due to the advantages of Euler's method, we also discretized the SIV model discussed above with this method. The above-mentioned model has also been written in the literature as a continuous-time model. The following system of ordinary differential equations can be used to express the model shown in figure 5.1 as a continuous-time model (see [152] and [153]):

$$\begin{cases} \frac{dI}{dt} = \frac{bSI}{N} - (a + c)I, \\ \frac{dS}{dt} = (1 - q)aN - \frac{bSI}{N} - (a + p)S + cI + dV, \\ \frac{dV}{dt} = qaN + pS - (a + d)V. \end{cases} \quad (5.2.5)$$

All the parameters are positive and have the same biological meanings as given in the model (5.1.1). The population size is constant since  $\frac{dN}{dt} = 0$ . Similar to model (5.1.2), by replacing the variable  $V$  with  $V = N - S - I$  and leaving out the variable  $V$ , we obtain the following two-dimensional system:

$$\begin{cases} \frac{dI}{dt} = \frac{bSI}{N} - (a + c)I, \\ \frac{dS}{dt} = [(1 - q)a + d]N - \frac{bSI}{N} - (a + p + d)S + (c - d)I, \end{cases} \quad (5.2.6)$$

Using forward Euler scheme the system (5.2.6) can be discretized as follows:

$$\begin{cases} I_{t+1} = I_t + h(\frac{bS_t I_t}{N} - (a + c)I_t), \\ S_{t+1} = S_t + h([(1 - q)a + d]N - \frac{bS_t I_t}{N} - (a + p + d)S_t + (c - d)I_t), \end{cases} \quad (5.2.7)$$

where  $h \in [0, 1]$  is the step size. The fixed points and the basic reproduction number of the systems (5.2.7) and (5.1.2) are the same. The fixed points of (5.2.7) can be calculated by solving the following system of equations:

$$\begin{cases} I = I + h\left(\frac{bSI}{N} - (a+c)I\right), \\ S = S + h\left([(1-q)a+d]N - \frac{bS_t I_t}{N} - (a+p+d)S + (c-d)I\right). \end{cases}$$

Solving above system, we get:

$E^0 = \left(0, \frac{[(1-q)a+d]N}{a+p+d}\right)$ , and  $E^* = \left(\frac{[(1-q)a+d]bN - (a+p+d)(a+c)N}{b(a+d)}, \frac{(a+c)N}{b}\right)$  as the fixed points of (5.2.7). The stability analysis of the fixed points  $E^0$  and  $E^*$  are given below:

**Theorem 5.2.8.** *For the boundary fixed point  $E^0 = \left(0, \frac{[(1-q)a+d]N}{a+p+d}\right)$  of the system (5.2.7), the following conditions hold:*

- (I) *The fixed point  $E^0$  of system (5.2.7) is sink when  $1 - \frac{2}{(a+c)h} < R_0 < 1$ .*
- (II) *The fixed point  $E^0$  of system (5.2.7) is saddle when  $1 < R_0 < 1 - \frac{2}{(a+c)h}$ .*

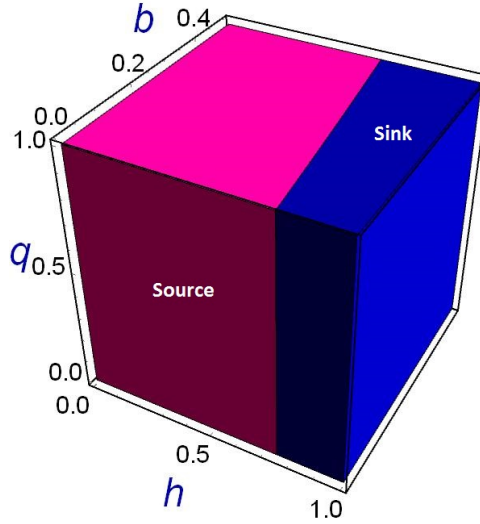


Figure 5.6: Plots of  $E^0$  for  $a = 0.4, c = 0.4, p = 0.2, N = 0.1, d = 0.1, h \in (0, 1), b \in (0.4, 0.9)$  and  $q \in (0, 1)$ .

*Proof.* The Jacobian matrix of the system (5.2.7) at  $E^0 = \left(0, \frac{[(1-q)a+d]N}{a+p+d}\right)$  is given by

$$V_{E^0} = \begin{pmatrix} 1 + h\left(-a - c + \frac{b(a+d-aq)}{a+d+p}\right) & 0 \\ h\left(c - d - \frac{b(a+d-aq)}{a+d+p}\right) & 1 - h(a + d + p) \end{pmatrix},$$

$$V_{E^0} = \begin{pmatrix} 1 + h(-a - c + R_0(a + c)) & 0 \\ h(c - d - R_0(a + c)) & 1 - h(a + d + p) \end{pmatrix}. \quad (5.2.8)$$

The matrix (5.2.8) have the following characteristic polynomial:

$$P(\lambda) = \lambda^2 - A_1\lambda + A_2,$$

where

$$A_1 = -2 + h(2a + c + d + p) - (a + c)hR_0,$$

and

$$A_2 = -(-1 + h(a + d + p))(1 - (a + c)h + (a + c)hR_0).$$

The eigenvalues are:

$$\lambda_1 = 1 - h(a + d + p), \text{ and } \lambda_2 = 1 + (a + c)h(-1 + R_0).$$

The topological classification for  $E^0$  of system (5.2.7) is given in figure 5.6.  $\square$

For the stability analysis of the positive fixed point of the system (5.2.7), we have the following calculation: The Variational matrix of the system (5.2.7) at  $E^*$  is given by

$$\begin{aligned} V_{E^*} &= \begin{pmatrix} 1 & -\frac{h(a^2 - bd + c(d+p) + a(c+d+p+b(-1+q)))}{a+d} \\ -(a+d)h & 1 - \frac{h(bd - (c-d)(d+p) + a(b-c+d-bq))}{a+d} \end{pmatrix}, \\ &= \begin{pmatrix} 1 & \frac{(a+c)h(a+d+p)(-1+bR_0)}{a+d} \\ -(a+d)h & 1 - \frac{h(a+d+p)(c-d+(a+c)R_0)}{a+d} \end{pmatrix}. \end{aligned}$$

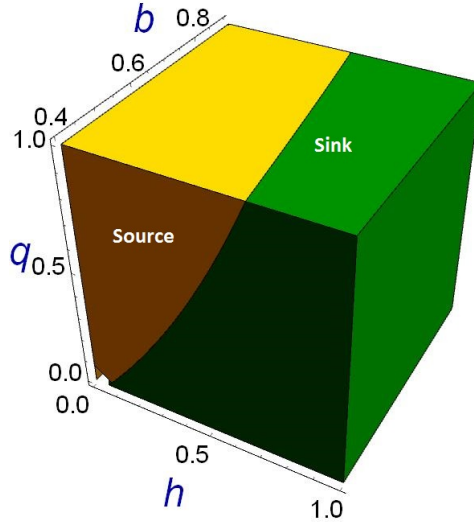


Figure 5.7: Plot of  $E^*$  for  $a = 0.4, c = 0.4, p = 0.2, N = 0.1, d = 0.1, h \in (0, 1), b \in (0.4, 0.9)$  and  $q \in (0, 1)$ .



The characteristic polynomial of  $V_{E^*}$  is

$$P(\lambda) = (\lambda)^2 - B_1\lambda + B_2, \quad (5.2.9)$$

where

$$Tr = B_1 = 2 - \frac{h(a+d+p)(c-d+(a+c)R_0)}{a+d},$$

and

$$\begin{aligned} Det = B_2 = & -\frac{(a+d)(-1+(a+c)h)(1+(a+d)h) + h(c-d+(a+c)(a+d)h)p}{a+d} \\ & - \frac{(a+c)h(-1+b(a+d)h)(a+d+p)R_0}{a+d}. \end{aligned}$$

**Theorem 5.2.9.** *Let  $E^* = \left( \frac{[(1-q)a+d]bN-(a+p+d)(a+c)N}{b(a+d)}, \frac{(a+c)N}{b} \right)$  is the positive fixed point of the system (5.2.7), then the following conditions hold:*

(I) *Fixed point  $E^*$  of the model (5.2.7) is source iff*

$$|B_2| > 1, \text{ and } |B_1| < |1 + B_2|.$$

(II) *Fixed point  $E^*$  of the model (5.2.7) is saddle point iff*

$$(B_1)^2 > 4B_2, \text{ and } |B_1| > |1 + B_2|.$$

(III) *Fixed point  $E^*$  of the model (5.2.7) is non-hyperbolic point iff*

$$|B_1| = |1 + B_2|, \text{ and} \quad (5.2.10)$$

$$B_2 = 1, \text{ or } |B_1| \leq 2. \quad (5.2.11)$$

(IV) *If neither (5.2.10) nor (5.2.11) holds, then the unique positive fixed point of system (5.2.7) is sink iff*

$$|B_1| < 1 + B_2 < 2.$$

Figure 5.7 represents the topological classification of the positive fixed point of the system (5.2.7).

### 5.3 Bifurcation analysis

An essential tool in the study of dynamic systems is bifurcation analysis. It enables us to comprehend how minor changes in system parameters can result in significant changes in the system's behavior. By examining these changes, we can gain insight

into the underlying mechanisms of the system and make predictions about how it will respond to certain situations. The flip and Hopf bifurcations are two significant types of bifurcations. A flip bifurcation occurs when a stable equilibrium state loses stability and is replaced by two new stable equilibrium states. This bifurcation is often encountered in systems with symmetry breaking, such as in the formation of fluid patterns and the dynamics of populations. However, if a stable equilibrium state loses stability and is replaced by a stable limit cycle, this is known as a Hopf bifurcation. This bifurcation frequently occurs in oscillatory systems, such as the dynamics of chemical reactions and the regulation of mechanical systems. Thus, bifurcation analysis is a potent technique that enables us to comprehend dynamic systems' behavior and predict how they will act in various scenarios. Understanding the flip and Hopf bifurcations is crucial in physics, chemistry, engineering, biology, and many other fields where dynamic systems are studied. In this section, we also discuss the bifurcation behavior of the system (5.2.7) at  $(I^*, S^*) = \left( \frac{[(1-q)a+d]bN-(a+p+d)(a+c)N}{b(a+d)}, \frac{(a+c)N}{b} \right)$ .

### 5.3.1 Period-doubling bifurcation

Initially, we discuss the period-doubling bifurcation of the system (5.2.7) at  $(I^*, S^*)$ . Where  $(I^*, S^*)$  is the fixed point of system (5.2.7). The Jacobian matrix of system (5.2.7) at  $(I^*, S^*)$  is given below:

$$J(I^*, S^*) = \begin{pmatrix} \frac{N-N(a+c)h+bhS^*}{N} & \frac{bhI^*}{N} \\ h(c-d-\frac{bS^*}{N}) & 1-h(a+d+p)-\frac{bhI^*}{N} \end{pmatrix}, \quad (5.3.1)$$

The characteristic polynomial of (5.3.1) is:

$$P(\Omega) = \Omega^2 - (2 - \theta_1 h)\Omega + (1 - \theta_1 h + \theta_2 h^2), \quad (5.3.2)$$

where,  $\theta_1 = 2a + c + d + p + \frac{bI^*}{N} - \frac{bS^*}{N}$  and  $\theta_2 = (a + c)(a + d + p) + \frac{b(a+d)I^*}{N} - \frac{b(a+d+p)S^*}{N}$ . Assume that

$$(2 - \theta_1 h)^2 > 4(1 - \theta_1 h + \theta_2 h^2). \quad (5.3.3)$$

Then the condition  $P(-1) = 0 = 1 + (2 - (\theta_1)h) + 1 - (\theta_1)h + (\theta_2)h^2$ , implies that

$$h = \frac{\theta_1 - \sqrt{\theta_1^2 - 4\theta_2}}{\theta_2}. \quad (5.3.4)$$

The root of the equation (5.3.2) for  $P(\Omega) = 0$  are:

$$\Omega_1 = -1 \text{ and } \Omega_2 = \frac{\theta_1 \left( -\theta_1 + \sqrt{\theta_1^2 - 4\theta_2} \right) + 3\theta_2}{\theta_2},$$

with

$$\left| \frac{\theta_1 \left( -\theta_1 + \sqrt{\theta_1^2 - 4\theta_2} \right) + 3\theta_2}{\theta_2} \right| \neq 1. \quad (5.3.5)$$

Let  $\Phi_{FB} = \{(a, c, d, p, q, N, b, h) \in \mathbb{R}_+ : (5.3.3), (5.3.4) \text{ and } (5.3.5) \text{ are satisfied}\}$ . It is examined that when the parametric values change in a small neighborhood of  $\Phi_{FB}$ , then the flip bifurcation emerges for system (5.2.7) at  $(I^*, S^*)$ . Consider the arbitrary parameters  $(a, c, d, p, q, N, b, \tilde{h}) \in \Phi_{FB}$ , then the map (5.2.7) can be written as:

$$\begin{cases} I \rightarrow I + \tilde{h} \left( \frac{bSI}{N} - (a + c)I \right), \\ S \rightarrow S + \tilde{h} \left( [(1 - q)a + d]N - \frac{bSI}{N} - (a + p + d)S_t + (c - d)I \right), \end{cases} \quad (5.3.6)$$

Consider  $h^*$  be a limited perturbation parameter, then the perturbation of (5.3.6) is:

$$\begin{cases} I \rightarrow I + \left( \tilde{h} + h^* \right) \left( \frac{bSI}{N} - (a + c)I \right), \\ S \rightarrow S + \left( \tilde{h} + h^* \right) \left( [(1 - q)a + d]N - \frac{bSI}{N} - (a + p + d)S_t + (c - d)I \right), \end{cases} \quad (5.3.7)$$

where  $|h^*| < 1$ .

Let  $U = I - I^*$  and  $V = S - S^*$ , then the system (5.3.7) can be written as:

$$\begin{pmatrix} U \\ V \end{pmatrix} \rightarrow \begin{pmatrix} f_1(U, V, h^*) \\ g_1(U, V, h^*) \end{pmatrix}, \quad (5.3.8)$$

where

$$\begin{aligned} f_1(U, V, h^*) &= \left( 1 + \tilde{h} \left( \frac{bS^*}{N} - a - c \right) \right) U + \frac{\tilde{h}bI^*}{N} V + \left( \frac{bI^*S^*}{N} - (a + c)I^* \right) h^* \\ &+ \frac{\tilde{h}b}{N} UV + \left( \frac{bS^*}{N} - a - c \right) h^* U + \frac{bI^*}{N} h^* V + \frac{b}{N} h^* UV \\ &+ O(|U|, |V|, |h^*|)^4, \\ g_1(U, V, h^*) &= \tilde{h} \left( -\frac{bS^*}{N} + c - d \right) U + \left( 1 + \tilde{h} \left( -\frac{bI^*}{N} - a - p - d \right) \right) V \\ &+ \left[ ((1 - q)a + d)N - \frac{bI^*S^*}{N} - (a + p + d)S^* + (c - d)I^* \right] h^* \\ &- \frac{\tilde{h}b}{N} UV + \left( -\frac{bS^*}{N} + c - d \right) h^* U + \left( -\frac{bI^*}{N} - a - p - d \right) h^* V \\ &- \frac{b}{N} h^* UV + O(|U|, |V|, |h^*|)^4. \end{aligned}$$

Consider the translation that follows:

$$\begin{pmatrix} U \\ V \end{pmatrix} = T \begin{pmatrix} \tilde{I} \\ \tilde{S} \end{pmatrix},$$

where

$$T = \begin{pmatrix} \frac{\tilde{h}bI^*}{N} & \frac{\tilde{h}bI^*}{N} \\ -1 - \left(1 + h\left(\frac{bS^*}{N} - a - c\right)\right) & \Omega_2 - \left(1 + h\left(\frac{bS^*}{N} - a - c\right)\right) \end{pmatrix}.$$

Taking  $T^{-1}$  on both sides of (5.3.8), we get

$$\begin{pmatrix} \tilde{I} \\ \tilde{S} \end{pmatrix} \rightarrow \begin{pmatrix} -1 & 0 \\ 0 & \Omega_2 \end{pmatrix} \begin{pmatrix} \tilde{I} \\ \tilde{S} \end{pmatrix} + \begin{pmatrix} f_2(U, V, h^*) \\ g_2(U, V, h^*) \end{pmatrix}, \quad (5.3.9)$$

where

$$\begin{aligned} f_2(U, V, h^*) &= \frac{1}{\Omega_2 + 1} \left[ \left( -\frac{(-\Omega_2 + a_{11})a_{16}}{a_{12}} - a_{26} \right) h^*UV \right] \\ &+ \frac{1}{\Omega_2 + 1} \left[ \left( -\frac{(-\Omega_2 + a_{11})a_{14}}{a_{12}} - a_{24} \right) h^*U \right] \\ &+ \frac{1}{\Omega_2 + 1} \left[ \left( -\frac{(-\Omega_2 + a_{11})a_{15}}{a_{12}} - a_{25} \right) Vh^* \right] \\ &+ \frac{1}{\Omega_2 + 1} \left[ \left( -\frac{(-\Omega_2 + a_{11})a_{13}}{a_{12}} - a_{23} \right) UV \right], \\ g_2(U, V, h^*) &= \frac{1}{\Omega_2 + 1} \left[ \left( \frac{(1 + a_{11})a_{16}}{a_{12}} + a_{26} \right) h^*UV \right] \\ &+ \frac{1}{\Omega_2 + 1} \left[ \left( \frac{(1 + a_{11})a_{14}}{a_{12}} + a_{24} \right) h^*U \right] \\ &+ \frac{1}{\Omega_2 + 1} \left[ \left( \frac{(1 + a_{11})a_{15}}{a_{12}} + a_{25} \right) Vh^* \right] \\ &+ \frac{1}{\Omega_2 + 1} \left[ \left( \frac{(1 + a_{11})a_{13}}{a_{12}} + a_{23} \right) UV \right], \end{aligned}$$

$$\begin{aligned} a_{11} &= \left( 1 + h \left( \frac{bS^*}{N} - a - c \right) \right), a_{12} = \frac{\tilde{h}bI^*}{N}, a_{13} = \frac{\tilde{h}b}{N}, a_{14} = \left( \frac{bS^*}{N} - a - c \right), \\ a_{15} &= \frac{bI^*}{N}, a_{16} = \frac{b}{N}, a_{23} = \frac{\tilde{h}b}{N}, a_{24} = \left( -\frac{bS^*}{N} + c - d \right), \end{aligned}$$

$$a_{25} = \left( -\frac{bI^*}{N} - a - p - d \right), a_{26} = \frac{b}{N}.$$

Now, applying the center manifold theorem to (5.3.9) at  $(0, 0)$  in the limited neighborhood of  $h^* = 0$ . Then  $W^c(0, 0, 0)$  can be approximately calculated as:

$$W^c(0, 0, 0) = \{(U, V, h^*) \in \mathbb{R}^3 : m_1 U^2 + m_2 U h^* m_3 h^{*2} + O(|U| + |h^*|)^3\},$$

where

$$\begin{aligned} m_1 &= \frac{a_{12}(-1 - a_{11})}{1 - \Omega_2} \left( \frac{(1 + a_{11})a_{13}}{a_{12}(\Omega_2 + 1)} + \frac{a_{23}}{\Omega_2 + 1} \right), m_3 = 0, \\ m_2 &= \frac{1}{1 - \Omega_2} \left( \left( \frac{(1 + a_{11})a_{14}}{a_{12}(\Omega_2 + 1)} + \frac{a_{24}}{\Omega_2 + 1} \right) a_{12} \right. \\ &\quad \left. + \frac{1}{\Omega_2 + 1} \left( \frac{(1 + a_{11})a_{15}}{a_{12}(\Omega_2 + 1)} + \frac{a_{25}}{\Omega_2 + 1} \right) (-1 - a_{11}) \right). \end{aligned}$$

Thus, the map restricted to center manifold  $W^c(0, 0, 0)$  is given by

$$f : \tilde{I} \rightarrow -\tilde{I} + \xi_1 \tilde{I}^2 + \xi_2 \tilde{I} h^* + \xi_3 \tilde{I}^2 h^* + \xi_4 \tilde{I} h^{*2} + \xi_5 \tilde{I}^3 + O(|\tilde{I}| + |h^*|)^4),$$

where

$$\begin{aligned} \xi_1 &= \frac{1}{(\Omega_2 + 1)} \left( -\frac{(-\Omega_2 + a_{11})a_{13}}{a_{12}} - a_{23} \right) a_{12} (-1 - a_{11}), \\ \xi_2 &= \frac{1}{(\Omega_2 + 1)} \left\{ \left( -\frac{(-\Omega_2 + a_{11})a_{14}}{a_{12}} - a_{24} \right) a_{12} \right\} \\ &\quad + \frac{1}{(\Omega_2 + 1)} \left\{ \left( -\frac{(-\Omega_2 + a_{11})a_{15}}{a_{12}} - a_{25} \right) (-1 - a_{11}) \right\}, \\ \xi_3 &= \left( -\frac{(-\Omega_2 + a_{11})a_{16}}{a_{12}(\Omega_2 + 1)} - \frac{a_{26}}{\Omega_2 + 1} \right) a_{12} (-1 - a_{11}) \\ &\quad + \left( -\frac{(-\Omega_2 + a_{11})a_{14}}{a_{12}(\Omega_2 + 1)} - \frac{a_{24}}{\Omega_2 + 1} \right) a_{12} m_1 \\ &\quad + \left( -\frac{(-\Omega_2 + a_{11})a_{15}}{a_{12}(\Omega_2 + 1)} - \frac{a_{25}}{\Omega_2 + 1} \right) (\Omega_2 - a_{11}) m_1 \\ &\quad + \left( -\frac{(-\Omega_2 + a_{11})a_{13}}{a_{12}(\Omega_2 + 1)} - \frac{a_{23}}{\Omega_2 + 1} \right) a_{12} (\Omega_2 - a_{11}) m_2 \\ &\quad + \left( -\frac{(-\Omega_2 + a_{11})a_{13}}{a_{12}(\Omega_2 + 1)} - \frac{a_{23}}{\Omega_2 + 1} \right) a_{12} m_2 (-1 - a_{11}), \end{aligned}$$

$$\begin{aligned}
\xi_4 &= \frac{1}{(\Omega_2 + 1)} \left\{ \left( -\frac{(-\Omega_2 + a_{11}) a_{14}}{a_{12}} - a_{24} \right) a_{12} m_2 \right\} \\
&+ \frac{1}{(\Omega_2 + 1)} \left\{ \left( -\frac{(-\Omega_2 + a_{11}) a_{15}}{a_{12}} - a_{25} \right) (\Omega_2 - a_{11}) m_2 \right\} \\
&+ \frac{1}{\Omega_2 + 1} \left\{ \left( -\frac{(-\Omega_2 + a_{11}) a_{13}}{a_{12}} - a_{23} \right) a_{12} (\Omega_2 - a_{11}) m_3 \right\} \\
&+ \frac{1}{(\Omega_2 + 1)} \left\{ \left( -\frac{(-\Omega_2 + a_{11}) a_{13}}{a_{12}} - a_{23} \right) \right\} \\
&\quad a_{12} m_3 (-1 - a_{11}), \\
\xi_5 &= \frac{1}{(\Omega_2 + 1)} \left\{ \left( -\frac{(-\Omega_2 + a_{11}) a_{14}}{a_{12}} - a_{24} \right) a_{12} m_3 \right\} \\
&+ \frac{1}{(\Omega_2 + 1)} \left\{ \left( -\frac{(-\Omega_2 + a_{11}) a_{15}}{a_{12}} - a_{25} \right) (\Omega_2 - a_{11}) m_3 \right\}.
\end{aligned}$$

According to Flip bifurcation, the nonzero real numbers  $\gamma_1$  and  $\gamma_2$  are defined as follows:

$$\begin{aligned}
\gamma_1 &= \left( \frac{\partial^2 f}{\partial \tilde{I} \partial h^*} + \frac{1}{2} \frac{\partial f}{\partial h^*} \frac{\partial^2 f}{\partial \tilde{I}^2} \right) \Big|_{(0,0)}, \\
\gamma_2 &= \left( \frac{1}{2} \frac{\partial^3 f}{\partial \tilde{I}^3} + \left( \frac{1}{2} \frac{\partial^2 f}{\partial \tilde{I}^2} \right)^2 \right) \Big|_{(0,0)}.
\end{aligned}$$

We have found the non-zero real numbers below:

$$\begin{aligned}
\gamma_1 &= \frac{1}{\Omega_2 + 1} \left( -\frac{(-\Omega_2 + a_{11}) a_{14}}{a_{12}} - a_{24} \right) a_{12} \\
&+ \frac{1}{\Omega_2 + 1} \left( -\frac{(-\Omega_2 + a_{11}) a_{15}}{a_{12}} - a_{25} \right) (-1 - a_{11}) \neq 0, \\
\gamma_2 &= \xi_1^2 + \xi_5 \neq 0.
\end{aligned}$$

From the above calculation, we conclude the following result about the flip bifurcation of the system (5.2.7).

**Theorem 5.3.1.** *If  $\gamma_2 \neq 0$ , and the bifurcation parameter  $h^*$  alters in the limited neighborhood of  $\tilde{h}$ , then the system (5.1.2) passes through flip bifurcation at the unique positive steady-state  $\left( \frac{[(1-q)a+d]bN-(a+p+d)(a+c)N}{b(a+d)}, \frac{(a+c)N}{b} \right)$ . Also, the period-two orbits that bifurcate from fixed point  $\left( \frac{[(1-q)a+d]bN-(a+p+d)(a+c)N}{b(a+d)}, \frac{(a+c)N}{b} \right)$  are stable (resp., unstable) if  $\gamma_2 > 0$  (resp.,  $\gamma_2 < 0$ ).*

### 5.3.2 Neimark-Sacker bifurcation

Now we discuss the Neimark-Sacker bifurcation of system (5.2.7) at the fixed point  $\left(\frac{[(1-q)a+d]bN-(a+p+d)(a+c)N}{b(a+d)}, \frac{(a+c)N}{b}\right)$ . Let  $h$  be the bifurcation parameter.

$$P(\Omega) = \Omega^2 + (2 - \theta_1 h)\Omega + (1 - \theta_1 h + \theta_2 h^2) = 0,$$

has both complex conjugate roots with a modulus equal to one if the following conditions are satisfied:

$$\theta_1^2 < 4|\theta_2|, \text{ and } h \approx 0 \text{ or } h = \frac{\theta_1}{\theta_2},$$

where,  $\theta_1 = 2a + c + d + p + \frac{bI^*}{N} - \frac{bS^*}{N}$  and  $\theta_2 = (a + c)(a + d + p) + \frac{b(a+d)I^*}{N} - \frac{b(a+d+p)S^*}{N}$ . Consider that

$$\phi_{NS} = \left\{ (a, c, d, p, q, N, b, h) : h \approx 0 (\text{or } h = \frac{\theta_1}{\theta_2}), \theta_1^2 < 4|\theta_2| \right\}.$$

Whenever the bifurcation parameter  $h$  varies in the limited neighborhood of  $\phi_{NS}$ , then  $E^* = \left(\frac{[(1-q)a+d]bN-(a+p+d)(a+c)N}{b(a+d)}, \frac{(a+c)N}{b}\right)$  undergoes Hopf bifurcation. Consider the system (5.2.7) with arbitrary parameters  $(a, c, d, p, q, N, b, h)$ , described by the following map:

$$\begin{cases} I \rightarrow I + \tilde{h}(\frac{bSI}{N} - (a + c)I), \\ S \rightarrow S + \tilde{h}([(1 - q)a + d]N - \frac{bSI}{N} - (a + p + d)S_t + (c - d)I). \end{cases} \quad (5.3.10)$$

Let  $\tilde{h}$  be a bifurcation parameter and consider perturbation of (5.3.10) as given below:

$$\begin{cases} I \rightarrow I + (\tilde{h} + h_1) \left( \frac{bSI}{N} - (a + c)I \right), \\ S \rightarrow S + (\tilde{h} + h_1) \left( [(1 - q)a + d]N - \frac{bSI}{N} - (a + p + d)S_t + (c - d)I \right). \end{cases} \quad (5.3.11)$$

where  $|h_1| \ll 1$  is limited perturbation parameter. Consider the transformations  $U = I - I^*$  and  $V = S - S^*$ . Transforming the fixed point  $E^*(I^*, S^*)$  of system (5.3.11) to the point  $(0, 0)$  we have

$$\begin{pmatrix} \tilde{U} \\ \tilde{V} \end{pmatrix} \rightarrow \begin{pmatrix} f_3(U, V) \\ g_3(U, V) \end{pmatrix}, \quad (5.3.12)$$

where

$$\begin{aligned} f_3(U, V) &= \left(1 + \tilde{h} \left(\frac{bS^*}{N} - a - c\right)\right) U + \frac{\tilde{h}bI^*}{N} V + \frac{\tilde{h}b}{N} UV + O(|U|, |V|)^4, \\ g_3(U, V) &= \tilde{h} \left(-\frac{bS^*}{N} + c - d\right) U + \left(1 + \tilde{h} \left(-\frac{bI^*}{N} - a - p - d\right)\right) V \\ &\quad - \frac{\tilde{h}b}{N} UV + O(|U|, |V|)^4. \end{aligned}$$

The characteristic equation of system (5.3.11) at  $E^*(I^*, S^*)$  is given below:

$$P(\Omega) = \Omega^2 - (2 - \theta_1(\tilde{h} + h_1))\Omega + (1 - \theta_1(\tilde{h} + h_1) + \theta_2(\tilde{h} + h_1)^2), \quad (5.3.13)$$

where,  $\theta_1 = 2a + c + d + p + \frac{bI^*}{N} - \frac{bS^*}{N}$  and  $\theta_2 = (a + c)(a + d + p) + \frac{b(a+d)I^*}{N} - \frac{b(a+d+p)S^*}{N}$ . The root of the equation (5.3.13) for  $P(\Omega) = 0$  are complex conjugate numbers  $\Omega_1$  and  $\Omega_2$  with  $|\Omega_1| = 1 = |\Omega_2|$ . Then it follows that:

$$\Omega_1, \Omega_2 = \frac{1}{2} \left( 2 - (\tilde{h} + h_1)\theta_1 \pm \iota(\tilde{h} + h_1)\sqrt{\theta_1^2 - 4\theta_2} \right). \quad (5.3.14)$$

Then we get

$$\left( \frac{d|\Omega_1|}{dh_1} \right)_{h_1=0} = \left( \frac{d|\Omega_2|}{dh_1} \right)_{h_1=0} = \frac{1}{2} \left( -\theta_1 \pm \iota\sqrt{\theta_1^2 - 4\theta_2} \right). \quad (5.3.15)$$

Let  $Tr(h_1) = 2 - \theta_1(\tilde{h} + h_1)$ . Then  $Tr(0) = 2 - \theta_1(\tilde{h}) \neq 0, -1$ . Moreover,  $(a, c, d, p, q, N, b, h) \in \phi_{NS}$  implies that  $-2 < Tr(0) < 2$ . Thus,  $Tr(0) \neq \pm 2, 0, 1$  gives  $\Omega_1^2, \Omega_2^2 \neq 1 \forall n = 1, 2, 3, 4$  at  $h_1 = 0$ . Thus, the roots of (5.3.13) lie outside the area where the coordinate axes and the unit circle intersect when  $h_1 = 0$  and if  $Tr(0) \neq 0, 1$ . To discuss the normal form of system (5.3.12) at  $h_1 = 0$ , we take  $\xi_a = \frac{2 - \theta_1\tilde{h}}{2}$  and  $\eta_a = \frac{1 - \theta_1(\tilde{h}) + \theta_2(\tilde{h})^2}{2}$ . Consider the translation given below

$$\begin{pmatrix} U \\ V \end{pmatrix} \rightarrow \begin{pmatrix} a_{12} & 0 \\ \xi_a - a_{11} & \eta_a \end{pmatrix} \begin{pmatrix} \tilde{I} \\ \tilde{S} \end{pmatrix}. \quad (5.3.16)$$

Using translation (5.3.16), the map (5.3.12) can be written as:

$$\begin{pmatrix} \tilde{I} \\ \tilde{S} \end{pmatrix} \rightarrow \begin{pmatrix} \xi_a & -\eta_a \\ \eta_a & \xi_a \end{pmatrix} \begin{pmatrix} U \\ V \end{pmatrix} + \begin{pmatrix} \bar{f}(U, V) \\ \bar{g}(U, V) \end{pmatrix}, \quad (5.3.17)$$



where

$$\bar{f}(U, V) = \frac{f_3(U, V)}{a_{12}}, \bar{g}(U, V) = \left( \frac{\xi_a - a_{11}}{\eta_a a_{11}} \right) f_3(U, V) - \frac{g_3(U, V)}{\eta_a}, U = a_{12} \tilde{I}, \text{ and } V = (\xi_a - a_{11}) \tilde{I} - \eta_a \tilde{S}.$$

The following first Lyapunov exponent is defined next:

$$L = -Re \left[ \frac{(1 - 2\bar{\Omega})\bar{\Omega}^2}{1 - \bar{\Omega}} \Theta_{11} \Theta_{20} \right] - \frac{1}{2} \|\Theta_{02}\|^2 - \|\Theta_{02}\|^2 + Re(\bar{\Omega} \Theta_{21}), \quad (5.3.18)$$

where

$$\begin{aligned} \Theta_{20} &= \frac{1}{8} [\bar{f}_{\tilde{I}\tilde{I}} - \bar{f}_{\tilde{S}\tilde{S}} + 2\bar{g}_{\tilde{I}\tilde{S}}] + \iota [\bar{g}_{\tilde{I}\tilde{I}} + \bar{g}_{\tilde{S}\tilde{S}} - 2\bar{f}_{\tilde{I}\tilde{S}}], \\ \Theta_{11} &= \frac{1}{4} [\bar{f}_{\tilde{I}\tilde{I}} + \bar{f}_{\tilde{S}\tilde{S}} + \iota [\bar{g}_{\tilde{I}\tilde{I}} + \bar{g}_{\tilde{S}\tilde{S}}]], \\ \Theta_{02} &= \frac{1}{8} [\bar{f}_{\tilde{I}\tilde{I}} - \bar{f}_{\tilde{S}\tilde{S}} + 2\bar{g}_{\tilde{I}\tilde{S}}] + \iota [\bar{g}_{\tilde{I}\tilde{I}} + \bar{g}_{\tilde{S}\tilde{S}} + 2\bar{f}_{\tilde{I}\tilde{S}}], \\ \Theta_{21} &= \frac{1}{8} [\bar{f}_{\tilde{I}\tilde{I}\tilde{I}} + \bar{f}_{\tilde{S}\tilde{S}\tilde{S}} + \bar{g}_{\tilde{I}\tilde{I}\tilde{S}} + \bar{g}_{\tilde{S}\tilde{S}\tilde{S}} + \iota (\bar{g}_{\tilde{I}\tilde{I}\tilde{I}} + \bar{g}_{\tilde{I}\tilde{S}\tilde{S}} - \bar{f}_{\tilde{I}\tilde{I}\tilde{S}} - \bar{f}_{\tilde{I}\tilde{I}\tilde{I}})]. \end{aligned}$$

Analyzing the aforementioned calculation and Hopf bifurcation conditions discussed in [145], we have the following theorem:

**Theorem 5.3.2.** *When the parameter  $\tilde{h}$  changes within a narrow neighborhood of  $h_1$ , the system (5.3.11) experiences Hopf bifurcation at the unique positive fixed point  $E^*$ . This assumes that at the system (5.3.11), the condition  $L \neq 0$  holds. Additionally, for  $\tilde{h} > h_1$ , an attracting invariant closed curve bifurcates from the fixed point if  $L < 0$ , and for  $\tilde{h} < h_1$ , a repelling invariant closed curve bifurcates if  $L > 0$ .*

### 5.3.3 Codimension-two bifurcation analysis

This section will discuss different cases of non-hyperbolic conditions for co-dimension two bifurcation analysis [16]. Codimension-two bifurcation refers to the study of changes in the qualitative behavior of a system when two or more parameters are varied simultaneously. In this kind of analysis, the system is often described by a collection of differential or difference equations, and the bifurcations happen when specific critical values of the parameters are reached. These bifurcations can cause chaos in the system, periodic orbits, or the presence or disappearance of equilibrium solutions. Limit cycles, tori, and strange attractors are examples of the complex dynamic structures to which co-dimension two bifurcations are frequently connected. They are crucial for understanding the behavior of various biological and dynamic systems and are researched using analytical and numerical methods. We will use eigenvalues to analyze this bifurcation, leaving the nor-

mal form for further analysis. For this we have variational matrix of system (5.2.7) at  $E^*(I^*, S^*) = \left( \frac{[(1-q)a+d]bN-(a+p+d)(a+c)N}{b(a+d)}, \frac{(a+c)N}{b} \right)$ :

$$V_{E^*} = \begin{pmatrix} 1 & -\frac{h(a^2-bd+c(d+p)+a(c+d+p+b(-1+q)))}{a+d} \\ -(a+d)h & 1 - \frac{h(bd-(c-d)(d+p)+a(b-c+d-bq))}{a+d} \end{pmatrix}.$$

The characteristic polynomial of  $V_{E^*}$  is

$$P(\mu) = (\mu)^2 - \Theta_1(I^*, S^*)\mu + \Theta_2(I^*, S^*), \quad (5.3.19)$$

where

$$\begin{aligned} \Theta_1(I^*, S^*) &= 2 - \frac{h(a(b(-q) + b - c + d) + bd - (c - d)(d + p))}{a + d}, \text{ and} \\ \Theta_2(I^*, S^*) &= \frac{a^3(-h^2) - a^2h^2(b(q - 1) + c + 2d + p) - ah(bdh(q - 2))}{a + d} \\ &+ \frac{-bq + b + hp(c + d) + dh(2c + d) - c + d + a + bdh(dh - 1)}{a + d} \\ &+ \frac{-h(d + p)(c(dh - 1) + d) + d}{a + d}. \end{aligned}$$

The roots of equation (5.3.19) are

$$\mu_1 = \frac{-\Theta_1(I^*, S^*) + \sqrt{\Theta_1(I^*, S^*)^2 - 4\Theta_2(I^*, S^*)}}{2},$$

and

$$\mu_2 = \frac{-\Theta_1(I^*, S^*) - \sqrt{\Theta_1(I^*, S^*)^2 - 4\Theta_2(I^*, S^*)}}{2}.$$

Now we discuss the criteria of co-dimension two bifurcations in terms of eigenvalues. The system (5.2.7) exhibits different resonance behavior at the fixed point  $E^*(I^*, S^*)$  according to the following conditions:

- C1** The system (5.2.7) exhibits 1:1 resonance behavior at  $E^*(I^*, S^*)$ , if  $\Theta_1(I^*, S^*) = -2$  and  $\Theta_2(I^*, S^*) = 1$ , with  $\mu_1 = \mu_2 = 1$ ,
- C2** The system (5.2.7) exhibits 1:2 resonance behavior at  $E^*(I^*, S^*)$ , if  $\Theta_1(I^*, S^*) = 2$  and  $\Theta_2(I^*, S^*) = 1$ , with  $\mu_1 = \mu_2 = -1$ ,
- C3** The system (5.2.7) exhibits 1:3 resonance behavior at  $E^*(I^*, S^*)$ , if  $\Theta_1(I^*, S^*) = 1$  and  $\Theta_2(I^*, S^*) = 1$ , with  $\mu_1, 2 = \frac{-1 \pm \sqrt{3}i}{2}$ .

- C4** The system (5.2.7) exhibits 1:4 resonance behavior at  $E^*(I^*, S^*)$ , if  $\Theta_1(I^*, S^*) = 0$  and  $\Theta_2(I^*, S^*) = 1$ , with  $\mu_1, 2 = \pm \nu$ .

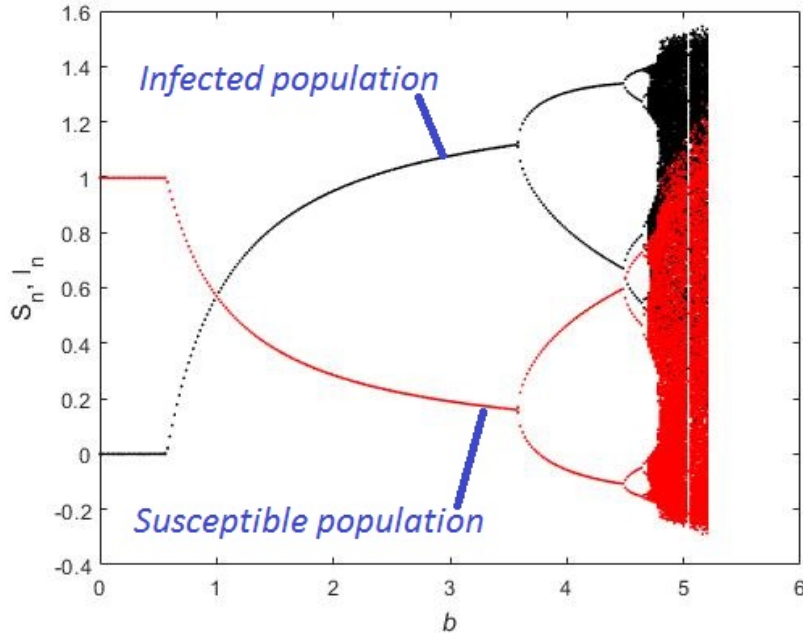
Codimension-two bifurcations can significantly influence the dynamics of a susceptible, infected, and vaccinated (SIV) model. A codimension-two bifurcation in an SIV model may cause the unexpected emergence of a new stable equilibrium state or the loss of stability in an existing equilibrium state. This could lead to a sudden change in the number of infected individuals or the rate of disease spread. Furthermore, the co-dimension of two bifurcations may result in the creation of novel periodic or chaotic dynamics, making it more challenging to predict the progression of a disease. In general, developing successful vaccination treatments and correctly predicting and containing the spread of infectious diseases depend on having a thorough grasp of the effects of co-dimension two bifurcations on an SIV model.

## 5.4 Numerical simulations

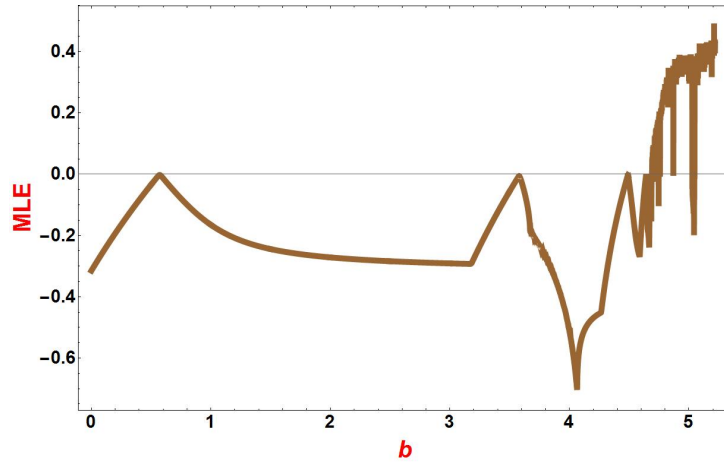
The behavior of dynamic systems can be studied using computer algorithms through numerical simulation of dynamic systems. It is crucial to use SIV models because they enable us to examine the dynamics of infectious diseases and estimate the number of infected individuals over time, which can be used to comprehend the spread of the disease and the efficacy of various interventions. Numerical simulations are a crucial part of our research because they offer a realistic and dynamic examination of the behaviour of the second model. Simulations have significant advantages in presenting complicated and real-world disease dynamics, while theoretical analysis provides essential insights. Through simulations, we may track the evolution of the system under different parameter configurations, test the validity of theoretical conclusions, measure the success of interventions, and explore complicated aspects that may be difficult to analyze. Our study, a collaborative effort between researchers and policymakers, provides an in-depth understanding of the dynamics of infectious diseases, enabling us to create successful plans for disease control and prevention. We do this by combining theoretical analysis with numerical simulations.

**Example 14.** *This example will confirm the chaos in the system (5.2.7). The cure rate  $b$  causes the chaotic behaviour in the model due to flip bifurcation. The bifurcation in the cure rate parameter  $b$  holds important biological implications. It may reflect shifts between endemic and epidemic conditions and impact public health strategies and policies. The dynamics of infectious diseases and the efficacy of vaccination as a preventative intervention are greatly improved by research on these bifurcations. In this context, we consider the parameters  $a = 0.1, c = 0.2, d = 0.2, p = 0.1, q = 0.9, N = 1.9, h = 0.9$ , and*

the variable  $b \in (0, 10]$ . We also consider the initial conditions  $(I_0, S_0) = (0.5, 0.8)$ , which are crucial in causing our interesting investigation to motivate this interesting structure further. To verify the theoretical results of the flip bifurcation phenomenon, we shall establish the above parametric values as constants, namely:  $a = 0.1, c = 0.2, d = 0.2, p = 0.1, q = 0.9, N = 1.9, h = 0.9$ , and  $b = 0.5714285714285715$ . The variational matrix can



(a)



(b)

Figure 5.8: Diagrams showing the bifurcations and MLE for system (5.2.7).

be obtained by using these fixed parametric values, and it is shown below for analysis:

$$\mathcal{V} = \begin{pmatrix} 1 & 4.163336342344337^{-17} \\ -0.27 & 0.64 \end{pmatrix}. \quad (5.4.1)$$

The characteristic function is:

$$Ch(\Theta) = \Theta^2 - 1.64\Theta + 0.64.$$

The characteristic functions connected to the roots of the aforementioned variational matrix are examined, and we find that they produce a set of  $\{1, 0.64\}$ . This outcome shows that the criteria required for the flip bifurcation phenomenon have been satisfied. By doing this research, we validate the theoretical hypotheses and establish a solid foundation for investigating the flip bifurcation in the studied system. The effects of this phenomenon are clearly shown in the bifurcation plots presented in Figure 5.8. These graphs give an in-depth visual representation of how the system (5.2.7) goes through significant changes and transformations. They present an extensive, straightforward overview of the system's behavior and growth.

**Example 15.** This example shows how the step size causes chaos in the system (5.2.7). It enables us to investigate how modifications to the step size  $h$  may impact the stability and dynamics of the disease system. Let we have the parametric values:

$$a = 0.59, c = 0.45, d = 0.7, p = 0.19, q = 0.8, N = 9.5, b = 5.4 \text{ and } h \in (0, 1)$$

with initial conditions  $(I_0, S_0) = (1.8472, 1.71243)$ , then at  $h = 0.7671363091831889$  the system (5.2.7) undergoes flip bifurcation. The positive fixed point of the system (5.2.7) is stable for  $0 \leq h < 0.7671363091831889$ . For the parametric set:

$$h = 0.7671363091831889, a = 0.59, c = 0.45, d = 0.7, p = 0.19, q = 0.8, N = 9.5, \text{ and } b = 5.4$$

the positive steady-state of the model (5.2.7) can be calculated as  $(3.92492, 1.82963)$ . This positive fixed-point loses its stability at  $h = 0.7671363091831889$ ; as a result, the system undergoes a flip bifurcation. Thus,  $E^*$  for system (5.2.7) loses its stability at  $h = 0.7671363091831889$  and  $(0, 0.7)$  is the non-chaotic region. The system (5.2.7) at the parametric values  $a = 0.59, c = 0.45, d = 0.7, p = 0.19, q = 0.8, N = 9.5, b = 5.4$  and  $h = 0.7671363091831889$  is given as:

$$\begin{cases} I_{t+1} = I_t + 0.7671363091831889 \left( \frac{5.3S_t I_t}{1.5} - (0.455)I_t \right), \\ S_{t+1} = S_t + 0.7671363091831889 \left( [0.226]1.5 - \frac{5.3S_t I_t}{1.5} - (0.545)S_t + (0.1)I_t \right), \end{cases} \quad (5.4.2)$$

The Jacobian matrix of (5.4.2) is:

$$J_* = \begin{pmatrix} 1 & 1.7114870525807886 \\ -0.9896058388463137 & -1.8468487901719075 \end{pmatrix}, \quad (5.4.3)$$

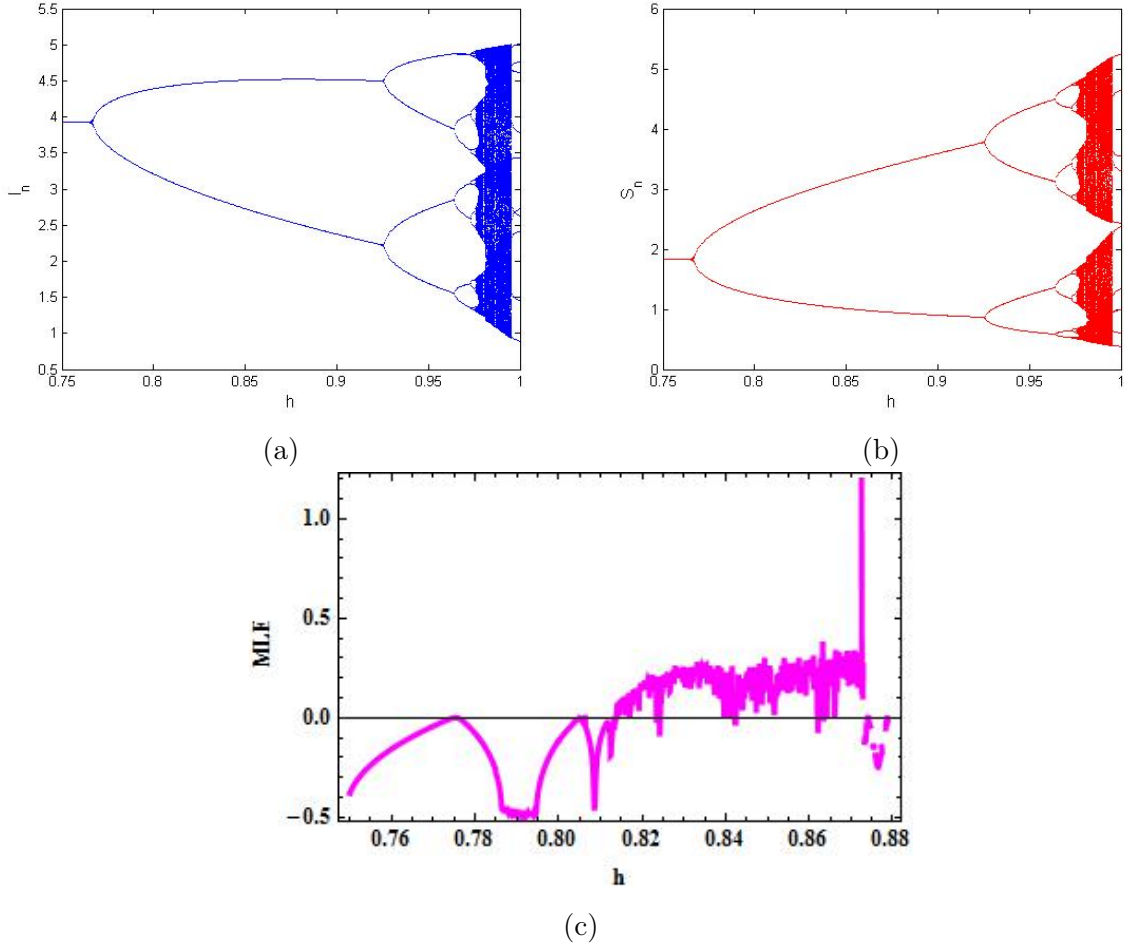


Figure 5.9: Diagrams of bifurcations and MLE for system (5.2.7).

The characteristic polynomial of (5.4.3) is given by

$$P(\lambda) = \lambda^2 + 0.846849\lambda - 0.153151, \quad (5.4.4)$$

Furthermore, the roots of (5.4.4) are calculated as:

$$\lambda_1 = -1 \text{ and } \lambda_2 = 0.153151.$$

Thus, the parameters  $(a, c, d, p, q, N, b, h) = (0.59, 0.45, 0.7, 0.19, 0.8, 9.5, 5.4, 0.691527) \in \Phi_{FB}$ . The bifurcation diagrams are depicted in figure 5.9, and the phase plots are given in figure 5.10.

**Example 16.** If  $a = 0.01, c = 0.001, d = 0.4, p = 0.01, q = 0.01, N = 20.4, b = 0.45$  and  $h \in (0, 1)$  with initial conditions  $(I_0, S_0) = (1.8472, 1.71243)$ , then at  $h = 0.0000001$  the system (5.2.7) undergoes Hopf bifurcation. For  $h = 0.0000001$  and other parametric values given above, the positive fixed point of the system (5.2.7) can be cal-

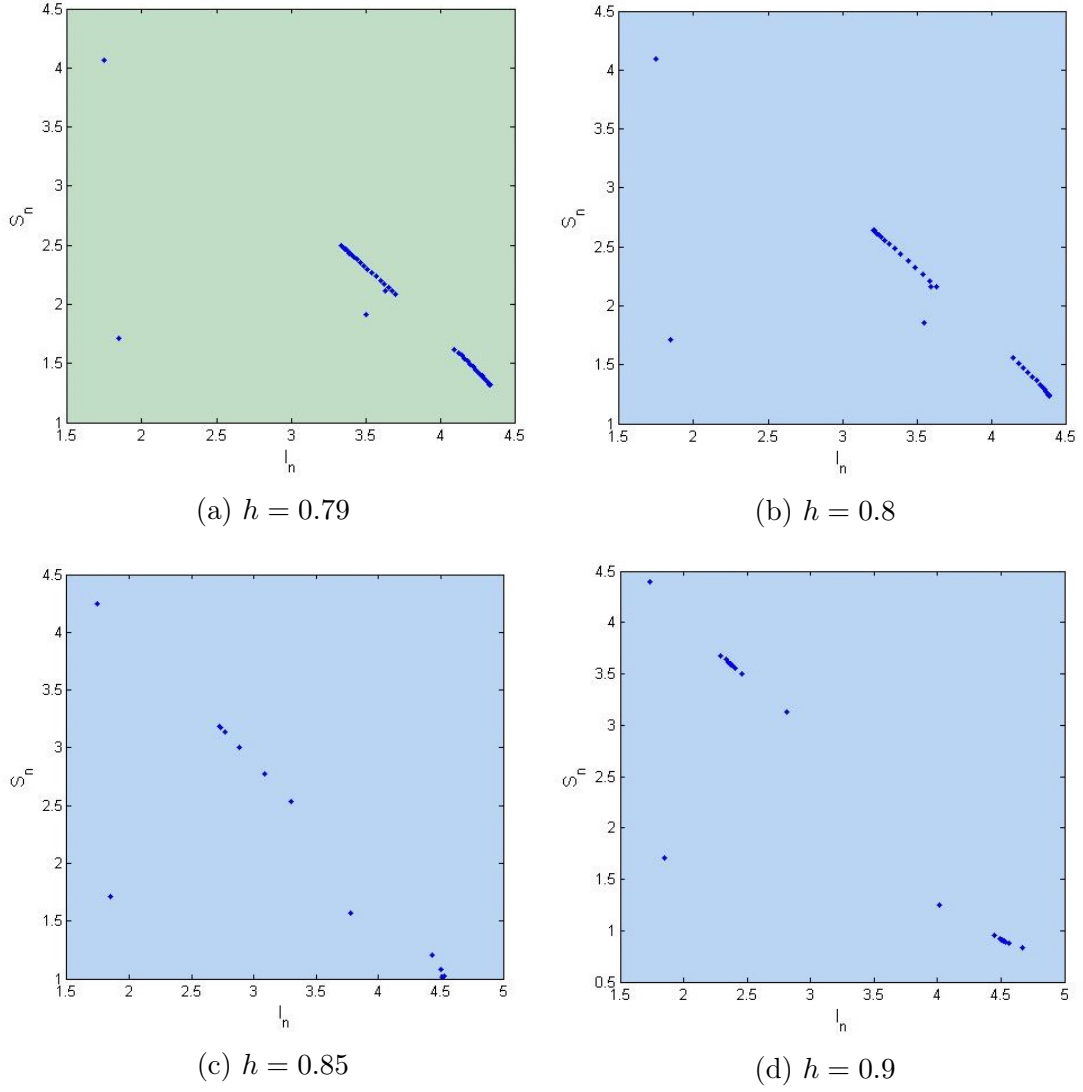


Figure 5.10: Phase plots for different values of  $h$ .

culated as  $(19.8842, 0.498666667)$ . This positive fixed point loses its stability at  $h = 0.0000001$ ; as a result, the system undergoes Hopf bifurcation. Thus,  $E^*$  for system (5.2.7) loses its stability at  $h = 0.0000001$ . The system (5.2.7) at the parametric values  $a = 0.01, c = 0.001, d = 0.4, p = 0.01, q = 0.01, N = 20.4, b = 0.45$  and  $h = 0.0000001$  is given as:

$$\begin{cases} I_{t+1} = I_t + 1. \times 10^{-7}(-0.011I_t + 0.0220588I_tS_t), \\ S_{t+1} = S_t + 1. \times 10^{-7}(8.36196 - 0.399I_t - 0.42S_t - 0.0220588I_tS_t), \end{cases} \quad (5.4.5)$$

The Jacobian matrix of (5.4.5) is:

$$J_{**} = \begin{pmatrix} 1 & 4.3862195121951216 \times 10^{-8} \\ -4.1 \times 10^{-8} & 1 \end{pmatrix}, \quad (5.4.6)$$

The characteristic polynomial of (5.4.6) is given by

$$P(\lambda) = \lambda^2 - 1.99999999141378049\lambda - 0.99999999141378066, \quad (5.4.7)$$

Furthermore, the roots of (5.4.7) are calculated as  $\lambda_1 = 0.9999999570689024 + 1.28496 \times$

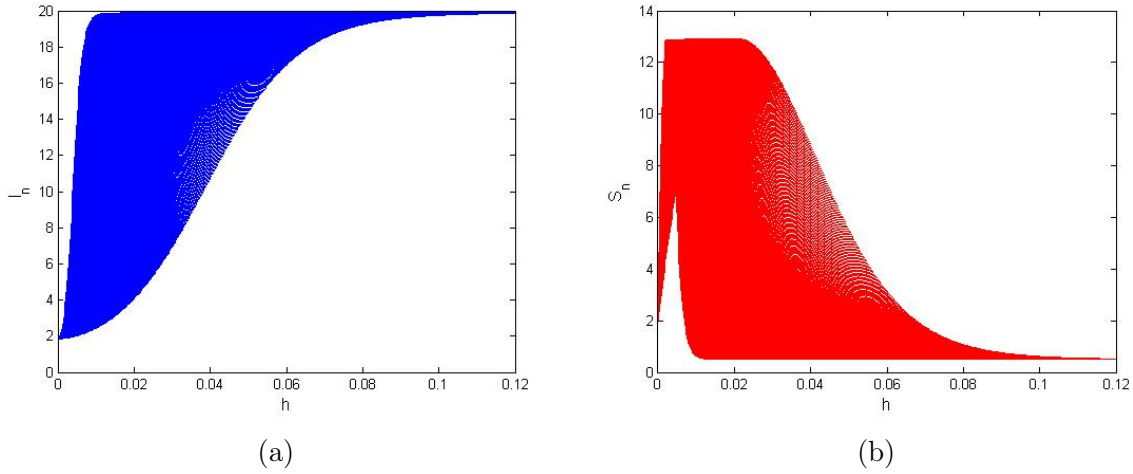


Figure 5.11: Bifurcation diagrams for system (5.2.7).

$10^{-8}\iota$  and  $\lambda_2 = 0.9999999570689024 - 1.28496 \times 10^{-8}\iota$  with  $|\lambda_{12}| = 1$ . Thus, the given parameters in the system  $(a, c, d_*, p, q, N, b, h) = (0.01, 0.001, 0.4, 0.01, 0.01, 20.4, 0.45, 0.0000001) \in \phi_{NS}$  The phase portraits, diagrams of bifurcations and MLE of system (5.4.5) are plotted in figure 5.11:

**Example 17.** Here, we present an example of codimension-2 bifurcation behavior of system (5.2.7) at  $E^*(I^*, S^*)$ . Let we have the parametric values as:  $a = 0.02, d = 0.4, p = 0.01, q = 0.1, N = 20.4, h = 0.0000001$  and  $b, c$  are free. Then the system (5.2.7) exhibits 1:1 resonance behavior at  $E^*(I^*, S^*)$ . Particularly, if  $a = 0.02, c = 0.1, d = 0.4, p = 0.01, q = 0.1, N = 20.4, b = 0.45$  and  $h = 0.0000001$ . Then the characteristic function of system (5.2.7) at  $E^*(I^*, S^*)$  is

$$C(\mu) = \mu^2 - 2\mu + 0.9999999,$$

with eigenvalues  $\mu_{1,2} = 1$ . Hence, the condition of 1:1 resonance behavior in terms of eigenvalues is satisfied.



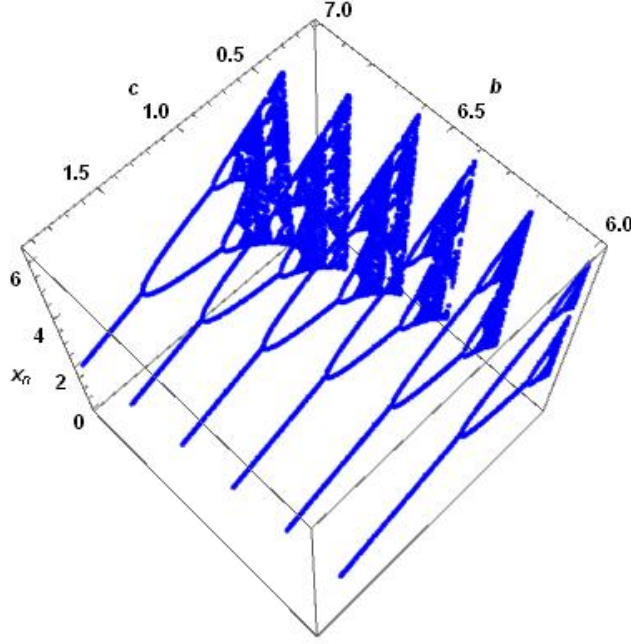


Figure 5.12: Plot of model (5.2.7) with  $a = 0.59$ ,  $N = 9.5$ ,  $d = 0.7$ ,  $p = 0.19$ ,  $q = 0.8$ ,  $h = 0.8$ , and  $(b, c) \in [6, 7] \times [0.1, 4]$ . We consider  $(I_0, S_0) = (1.8472, 1.71243)$  an initial conditions.

## 5.5 Chaos control

Chaos control is a technique for controlling chaotic systems and making them predictable. This can be achieved by introducing a small perturbation into the system at a particular time and location, which can predictably alter the system's behavior. The significance of chaos control rests in its ability to stabilize chaotic systems, which are otherwise unpredictable and challenging. By controlling chaos, we can make the system more predictable and stable, which can be helpful in a wide range of applications such as secure communication, robotic control, and power systems. Additionally, chaos control can regulate chaotic systems, which is beneficial for distributed network control or oscillator synchronization. Thus, chaos control stabilizes chaotic systems and makes them predictable. It is essential because it allows us to control and manipulate chaotic systems, which can have many uses in different fields. We use the hybrid technique given in [75] to manage the chaos in the system (5.2.7). The flip bifurcation, Hopf bifurcation, and chaos that result from flip bifurcation are all controlled using this control approach by various researchers (see [19]). The system (5.2.7) is obtained by applying the modified hybrid approach as follows:

$$\begin{cases} I_{t+1} = \zeta^3 \left[ I_t + h \left( \frac{bS_t I_t}{N_t} - (a+c)I_t \right) \right] + [1 - \zeta^3] I_t, \\ S_{t+1} = \zeta^3 \left[ S_t + h \left( [(1-q)a + d]N - \frac{bS_t I_t}{N} - (a+p+d)S_t + (c-d)I_t \right) \right] \\ + [1 - \zeta^3] S_t, \end{cases} \quad (5.5.1)$$

where  $0 < \zeta < 1$  is a control parameter. The Jacobian matrix of (5.5.1) at  $(I^*, S^*)$  is

$$J = \begin{pmatrix} \frac{N - a^3 N(a+c)h + a^3 b h S^*}{N} & \frac{a^3 b h I^*}{N} \\ a^3 h \left( c - d - \frac{b S^*}{N} \right) & - \frac{N(-1 + a^3 h(a+d+p)) + a^3 b h I^*}{N} \end{pmatrix}. \quad (5.5.2)$$

The characteristic polynomial of (5.5.2) is:

$$P(\lambda) = \lambda^2 - Tr(I^*, S^*)\lambda + Det(I^*, S^*), \quad (5.5.3)$$

where

$$\begin{aligned} Tr(I^*, S^*) &= \frac{-N(-2 + a^3 h(2a + c + d + p)) + a^3 b h(-I^* + S^*)}{N}, \\ Det(I^*, S^*) &= \frac{a^3 b h(-1 + a^3(a + d)h) I^*}{N} \\ &+ \frac{(-1 + a^3 h(a + d + p))(N(-1 + a^3(a + c)h) - a^3 b h S^*)}{N}. \end{aligned}$$

The roots of (5.5.3) lie in the open disc if the following conditions are satisfied:

$$|Tr(I^*, S^*)| < 1 + Det(I^*, S^*) < 2.$$

We intend to improve the accuracy and predictability of the SIV model and to obtain insights into the dynamics of infectious diseases by applying a modified hybrid approach to control the chaos.

## 5.6 Conclusion

The stability and bifurcation analysis of the epidemic model is crucial in understanding the dynamics of disease spread and the impact of intervention measures such as vaccination. The co-dimension, two-bifurcation, and one-parameter bifurcation analysis in the discrete-time epidemic model with vaccination and vital dynamics provide a comprehensive understanding of the interplay between various factors affecting disease spread and the potential outcomes. The results of this analysis not only aid in predicting disease outbreaks and evaluating control strategies but also highlight the critical parameters

that can impact the spread of the disease. These findings are invaluable in developing effective public health policies to prevent and control the spread of infectious diseases. Ultimately, stability and bifurcation analysis are critical to ensuring public health and safety by providing a deeper understanding of the complex interactions that drive the spread of diseases. Mainly, we investigated an SIV model through a vaccination campaign. The continuous version of the model is discretized using the forward Euler approach, and the impact of the step size on the dynamics of the model is examined. Both endemic and disease-free equilibrium exist in the presented model. Under specified parametric circumstances, the stability of equilibria in discrete and continuous forms was investigated. The endemic equilibrium  $E^*$  and the disease-free equilibrium  $E^0$  were sufficiently stabilized locally according to our established conditions. The model's equilibria are demonstrated to be globally asymptotically stable using the Picard iteration theorem. It was also noted that the fundamental reproduction number  $R_0$  is crucial in deciding how dynamically the model behaves. Additionally, by selecting step size  $h$  as a bifurcation parameter, the model's period-doubling and Neimark-Sacker bifurcation were examined. We also observed that the system bifurcates if we ignore the restriction on the contact rate ( $b < 1$ ). Furthermore, by decreasing the cure rate  $c$ , the Neimark-Sacker bifurcation occurs. The modified hybrid approach is used to regulate the chaos caused by bifurcation. Finally, numerical examples were provided to validate the theoretical findings by considering phase portraits, maximal Lyapunov exponents, and bifurcation diagrams. In conclusion, our study sheds light on the dynamics of the SIV model with a vaccination program. It emphasizes the significance of considering the step size while discretizing the model. We also observed that if the contact rate is low, the disease will be controlled, and if the contact rate increases, the infected population will increase. As a result, chaos occurs in the system (5.2.7). The control parameter in the controlled system (5.5.1) indicates the safety measures that can be taken to reduce the contact rate.

# Bibliography

- [1] Lotka, A. J. (1925). Elements of physical biology. Williams & Wilkins.
- [2] Volterra, V. (1927). Variazioni e fluttuazioni del numero d'individui in specie animali conviventi (Vol. 2). Societa anonima tipografica" Leonardo da Vinci".
- [3] Holling, C. S. (1965). The functional response of predators to prey density and its role in mimicry and population regulation. The Memoirs of the Entomological Society of Canada, 97(S45), 5-60.
- [4] Allee, W. C. (1938). The social life of animals.
- [5] Allee, W. C., & Emerson, A. E. (1949). Principles of animal ecology. Saunders Associates.
- [6] Stephens, P. A., Sutherland, W. J., & Freckleton, R. P. (1999). What is the Allee effect?. Oikos, 185-190.
- [7] Wang, X., Zanette, L., & Zou, X. (2016). Modelling the fear effect in predator-prey interactions. Journal of mathematical biology, 73(5), 1179-1204.
- [8] Sih, A. (1987). Prey refuges and predator-prey stability. Theoretical Population Biology, 31(1), 1-12.
- [9] Beretta, E., & Takeuchi, Y. (1988). Global asymptotic stability of Lotka-Volterra diffusion models with continuous time delay. SIAM Journal on Applied Mathematics, 48(3), 627-651.
- [10] Zhou, C., Fujiwara, M., & Grant, W. E. (2013). Dynamics of a predator-prey interaction with seasonal reproduction and continuous predation. Ecological modelling, 268, 25-36.
- [11] Aulisa, E., & Jang, S. R. J. (2014). Continuous-time predator-prey systems with Allee effects in the prey. Mathematics and Computers in Simulation, 105, 1-16.
- [12] Jamilov, U. U., Scheutzow, M., & Vorkastner, I. (2023). A prey-predator model with three interacting species. Dynamical Systems, 38(4), 493-509.

- [13] Ginoux, J. M., Rossetto, B., & Jamet, J. L. (2005). Chaos in a three-dimensional Volterra-Gause model of predator-prey type. *International Journal of Bifurcation and Chaos*, 15(05), 1689-1708.
- [14] Elaydi, S. N. An Introduction to Difference Equations [electronic resource].
- [15] Akhmet, M., Yilmaz, E., Akhmet, M., & Yilmaz, E. (2014). Differential Equations with Piecewise Constant Argument of Generalized Type. *Neural Networks with Discontinuous/Impact Activations*, 19-65.
- [16] Kuznetsov, Y. A., Kuznetsov, I. A., & Kuznetsov, Y. (1998). Elements of applied bifurcation theory (Vol. 112, pp. xx+-591). New York: Springer.
- [17] Dubey, B., Das, B., & Hussain, J. (2001). A predator-prey interaction model with self and cross-diffusion. *Ecological Modelling*, 141(1-3), 67-76.
- [18] Liu, W. M. (1994). Criterion of Hopf bifurcations without using eigenvalues. *Journal of Mathematical Analysis and Applications*, 182(1), 250-256.
- [19] Abbasi, M. A. (2024). Fixed points stability, bifurcation analysis, and chaos control of a Lotka-Volterra model with two predators and their prey. *International Journal of Biomathematics*, 17(04), 2350032.
- [20] Abbasi, M. A., & Din, Q. (2019). Under the influence of crowding effects: Stability, bifurcation and chaos control for a discrete-time predator-prey model. *International Journal of Biomathematics*, 12(04), 1950044.
- [21] Din, Q. (2018). Controlling chaos in a discrete-time prey-predator model with Allee effects. *International Journal of Dynamics and Control*, 6(2), 858-872.
- [22] Din, Q. (2018). Qualitative analysis and chaos control in a density-dependent host-parasitoid system. *International Journal of Dynamics and Control*, 6(2), 778-798.
- [23] Din, Q., Donchev, T., & Kolev, D. (2018). Stability, bifurcation analysis and chaos control in chlorine dioxide-iodine-malonic acid reaction. *MATCH Commun. Math. Comput. Chem*, 79(3), 577-606.
- [24] Din, Q., Elsadany, A. A., & Ibrahim, S. (2018). Bifurcation analysis and chaos control in a second-order rational difference equation. *International Journal of Nonlinear Sciences and Numerical Simulation*, 19(1), 53-68.
- [25] Berryman, A. A. (1992). The origins and evolution of predator-prey theory. *Ecology*, 73(5), 1530-1535.

- [26] Dhar, J. (2004). A prey-predator model with diffusion and a supplementary resource for the prey in a two-patch environment. *Mathematical Modelling and Analysis*, 9(1), 9-24.
- [27] Dhar, J., & Jatav, K. S. (2013). Mathematical analysis of a delayed stage-structured predator-prey model with impulsive diffusion between two predators territories. *Ecological Complexity*, 16, 59-67.
- [28] Dubey, B. (2007). A prey-predator model with a reserved area. *Nonlinear Analysis: Modelling and Control*, 12(4), 479-494.
- [29] Freedman, H. I. (1980). *Deterministic mathematical models in population ecology*. (No Title).
- [30] Jeschke, J. M., Kopp, M., & Tollrian, R. (2002). Predator functional responses: discriminating between handling and digesting prey. *Ecological monographs*, 72(1), 95-112.
- [31] Kooij, R. E., & Zegeling, A. (1996). A predator-prey model with Ivlev's functional response. *Journal of Mathematical Analysis and Applications*, 198(2), 473-489.
- [32] Ma, W., & Takeuchi, Y. (1998). Stability analysis on a predator-prey system with distributed delays. *Journal of computational and applied mathematics*, 88(1), 79-94.
- [33] May, R. M. (2019). *Stability and complexity in model ecosystems*. Princeton university press.
- [34] Sen, M., Banerjee, M., & Morozov, A. (2012). Bifurcation analysis of a ratio-dependent prey-predator model with the Allee effect. *Ecological Complexity*, 11, 12-27.
- [35] Sinha, S., Misra, O. P., & Dhar, J. (2010). Modelling a predator-prey system with infected prey in polluted environment. *Applied Mathematical Modelling*, 34(7), 1861-1872.
- [36] Hadziabdic, V., Mehuljic, M., & Bektesevic, J. (2017). Lotka-volterra model with two predators and their prey. *Tem Journal*, 6(1), 2217-8309.
- [37] Sun, G. Q., Jin, Z., Liu, Q. X., & Li, L. (2008). Dynamical complexity of a spatial predator-prey model with migration. *ecological modelling*, 219(1-2), 248-255.
- [38] Sun, Gui-Quan, Zhen Jin, Li Li, Mainul Haque, and Bai-Lian Li. Spatial patterns of a predator-prey model with cross diffusion. *Nonlinear Dynamics* 69 (2012): 1631-1638.

- [39] Sun, G. Q., Zhang, J., Song, L. P., Jin, Z., & Li, B. L. (2012). Pattern formation of a spatial predator-prey system. *Applied Mathematics and Computation*, 218(22), 11151-11162.
- [40] Agarwal, R. P. (2000). *Difference equations and inequalities: theory, methods, and applications*. CRC Press.
- [41] Agarwal, R. P., & Wong, P. J. (2013). *Advanced topics in difference equations* (Vol. 404). Springer Science & Business Media.
- [42] Celik, C., & Duman, O. (2009). Allee effect in a discrete-time predator-prey system. *Chaos, Solitons & Fractals*, 40(4), 1956-1962.
- [43] Gopalsamy, K. (2013). *Stability and oscillations in delay differential equations of population dynamics* (Vol. 74). Springer Science & Business Media.
- [44] Guckenheimer, J., & Holmes, P. (2013). *Nonlinear oscillations, dynamical systems, and bifurcations of vector fields* (Vol. 42). Springer Science & Business Media.
- [45] Huo, H. F., & Li, W. T. (2004). Existence and global stability of periodic solutions of a discrete predator-prey system with delays. *Applied Mathematics and Computation*, 153(2), 337-351.
- [46] Liao, X., Zhou, S., & Ouyang, Z. (2007). On a stoichiometric two predators on one prey discrete model. *Applied mathematics letters*, 20(3), 272-278.
- [47] Liu, X. (2010). A note on the existence of periodic solutions in discrete predator-prey models. *Applied Mathematical Modelling*, 34(9), 2477-2483.
- [48] Martelli, M. (2011). *Introduction to discrete dynamical systems and chaos*. John Wiley & Sons.
- [49] Murray, J. D. (2002). *Mathematical biology: I. An introduction*. Interdisciplinary applied mathematics. Mathematical Biology, Springer, 17.
- [50] Robinson, C. (1998). *Dynamical systems: stability, symbolic dynamics, and chaos*. CRC press.
- [51] Cushing, J. M., Leverage, S., Chitnis, N., & Henson, S. M. (2004). Some discrete competition models and the competitive exclusion principle. *Journal of difference Equations and Applications*, 10(13-15), 1139-1151.
- [52] Din, Q. (2017). Complexity and chaos control in a discrete-time prey-predator model. *Communications in Nonlinear Science and Numerical Simulation*, 49, 113-134.
- [53] Din, Q. (2018). Bifurcation analysis and chaos control in discrete-time glycolysis models. *Journal of Mathematical Chemistry*, 56(3), 904-931.

- [54] Din, Q. (2017). Neimark-Sacker bifurcation and chaos control in Hassell-Varley model. *Journal of Difference Equations and Applications*, 23(4), 741-762.
- [55] Din, Q., & Saeed, U. (2017). Bifurcation analysis and chaos control in a host-parasitoid model. *Mathematical Methods in the Applied Sciences*, 40(14), 5391-5406.
- [56] Dhar, J., Singh, H., & Bhatti, H. S. (2015). Discrete-time dynamics of a system with crowding effect and predator partially dependent on prey. *Applied Mathematics and Computation*, 252, 324-335.
- [57] Mickens, R. E. (2003). A nonstandard finite-difference scheme for the Lotka-Volterra system. *Applied Numerical Mathematics*, 45(2-3), 309-314.
- [58] Tassaddiq, A., Shabbir, M. S., Din, Q., & Naaz, H. (2022). Discretization, bifurcation, and control for a class of predator-prey interactions. *Fractal and Fractional*, 6(1), 31.
- [59] Agiza, H. N., Elabbasy, E. M., El-Metwally, H., & Elsadany, A. A. (2009). Chaotic dynamics of a discrete prey-predator model with Holling type II. *Nonlinear analysis: Real world applications*, 10(1), 116-129.
- [60] Salman, S. M., Yousef, A. M., & Elsadany, A. A. (2016). Stability, bifurcation analysis and chaos control of a discrete predator-prey system with square root functional response. *Chaos, Solitons & Fractals*, 93, 20-31.
- [61] Chen, Q., Teng, Z., & Hu, Z. (2013). Bifurcation and control for a discrete-time prey-predator model with Holling-IV functional response. *International Journal of Applied Mathematics and Computer Science*, 23(2), 247-261.
- [62] Li, L., & Wang, Z. J. (2013). Global stability of periodic solutions for a discrete predator-prey system with functional response. *Nonlinear Dynamics*, 72, 507-516.
- [63] Huiwang, G., Hao, W., Wenxin, S., & Xuemei, Z. (2000). Functions used in biological models and their influences on simulations.
- [64] Sun, G. Q., Zhang, G., & Jin, Z. (2009). Dynamic behavior of a discrete modified Ricker & Beverton-Holt model. *Computers & Mathematics with Applications*, 57(8), 1400-1412.
- [65] Liu, X., & Xiao, D. (2007). Complex dynamic behaviors of a discrete-time predator-prey system. *Chaos, Solitons & Fractals*, 32(1), 80-94.
- [66] Chen, Y., & Changming, S. (2008). Stability and Hopf bifurcation analysis in a prey-predator system with stage-structure for prey and time delay. *Chaos, Solitons & Fractals*, 38(4), 1104-1114.



- [67] Gakkhar, S., & Singh, A. (2012). Complex dynamics in a prey predator system with multiple delays. *Communications in Nonlinear Science and Numerical Simulation*, 17(2), 914-929.
- [68] He, Z., & Lai, X. (2011). Bifurcation and chaotic behavior of a discrete-time predator-prey system. *Nonlinear Analysis: Real World Applications*, 12(1), 403-417.
- [69] Hu, Z., Teng, Z., & Zhang, L. (2011). Stability and bifurcation analysis of a discrete predator-prey model with nonmonotonic functional response. *Nonlinear Analysis: Real World Applications*, 12(4), 2356-2377.
- [70] Jing, Z., & Yang, J. (2006). Bifurcation and chaos in discrete-time predator-prey system. *Chaos, Solitons & Fractals*, 27(1), 259-277.
- [71] Wang, W. X., Zhang, Y. B., & Liu, C. Z. (2011). Analysis of a discrete-time predator-prey system with Allee effect. *Ecological Complexity*, 8(1), 81-85.
- [72] Zhang, C. H., Yan, X. P., & Cui, G. H. (2010). Hopf bifurcations in a predator-prey system with a discrete delay and a distributed delay. *Nonlinear Analysis: Real World Applications*, 11(5), 4141-4153.
- [73] Kelley, W. G. (2010). *The theory of differential equations*. Springer.
- [74] Yang, X. (2006). Uniform persistence and periodic solutions for a discrete predator-prey system with delays. *Journal of Mathematical Analysis and Applications*, 316(1), 161-177.
- [75] Luo, X. S., Chen, G., Wang, B. H., & Fang, J. Q. (2003). Hybrid control of period-doubling bifurcation and chaos in discrete nonlinear dynamical systems. *Chaos, Solitons & Fractals*, 18(4), 775-783.
- [76] Elmaci, D., & Kangalgil, F. (2022). Stability, Neimark-Sacker Bifurcation Analysis of a Prey-Predator Model with Strong Allee Effect and Chaos Control. *Erzincan University Journal of Science and Technology*, 15(3), 775-787.
- [77] Khaliq, A., Ibrahim, T. F., Alotaibi, A. M., Shoaib, M., & El-Moneam, M. A. (2022). Dynamical analysis of discrete-time two-predators one-prey Lotka-Volterra model. *Mathematics*, 10(21), 4015.
- [78] Yousef, F., Semmar, B., & Al Nasr, K. (2022). Incommensurate conformable-type three-dimensional Lotka-Volterra model: Discretization, stability, and bifurcation. *Arab Journal of Basic and Applied Sciences*, 29(1), 113-120.

- [79] Yildiz, S., Bilazeroglu, S., & Merdan, H. (2023). Stability and bifurcation analyses of a discrete Lotka-Volterra type predator-prey system with refuge effect. *Journal of Computational and Applied Mathematics*, 422, 114910.
- [80] Priyanka, M., Muthukumar, P., & Bhalekar, S. (2022). Stability and Bifurcation Analysis of Two-Species Prey-Predator Model Incorporating External Factors. *International Journal of Bifurcation and Chaos*, 32(11), 2250172.
- [81] Kangalgil, F., & ILHAN, F. (2022). Period-doubling bifurcation and stability in a two dimensional discrete prey-predator model with Allee effect and immigration parameter on prey. *Cumhuriyet Science Journal*, 43(1), 88-97.
- [82] Xu, M., & Guo, S. (2022). Dynamics of a delayed Lotka-Volterra model with two predators competing for one prey. *Discrete & Continuous Dynamical Systems-Series B*, 27(10).
- [83] Dumbela, P. A., & Aldila, D. (2019, December). Dynamical analysis in predator-prey-scavenger model with harvesting intervention on prey population. In *AIP Conference Proceedings* (Vol. 2192, No. 1). AIP Publishing.
- [84] Belew, B., & Melese, D. (2022). Modeling and analysis of predator-prey model with fear effect in prey and hunting cooperation among predators and harvesting. *Journal of Applied Mathematics*, 2022.
- [85] Xu, C., Yuan, S., & Zhang, T. (2016). Global dynamics of a predator-prey model with defense mechanism for prey. *Applied mathematics letters*, 62, 42-48.
- [86] Abbasi, M. A. (2024). Periodic behavior and dynamical analysis of a prey–predator model incorporating the Allee effect and fear effect. *The European Physical Journal Plus*, 139(2), 1-36.
- [87] Lima, S. L., & Dill, L. M. (1990). Behavioral decisions made under the risk of predation: a review and prospectus. *Canadian journal of zoology*, 68(4), 619-640.
- [88] Dennis, B. (1989). Allee effects: population growth, critical density, and the chance of extinction. *Natural Resource Modeling*, 3(4), 481-538.
- [89] Huang, Y., Zhu, Z., & Li, Z. (2020). Modeling the Allee effect and fear effect in predator-prey system incorporating a prey refuge. *Advances in Difference Equations*, 2020, 1-13.
- [90] Lai, L., Zhu, Z., & Chen, F. (2020). Stability and bifurcation in a predator-prey model with the additive Allee effect and the fear effect. *Mathematics*, 8(8), 1280.

- [91] Xie, B. (2021). Impact of the fear and Allee effect on a Holling type II prey-predator model. *Advances in Difference Equations*, 2021, 1-15.
- [92] Li, Y. X., Liu, H., Wei, Y. M., Ma, M., Ma, G., & Ma, J. Y. (2022). Population dynamic study of prey-predator interactions with weak allee effect, fear effect, and delay. *Journal of Mathematics*, 2022, 1-15.
- [93] Cheng, L., & Cao, H. (2016). Bifurcation analysis of a discrete-time ratio-dependent predator-prey model with Allee effect. *Communications in Nonlinear Science and Numerical Simulation*, 38, 288-302.
- [94] Liang, Z., Zeng, X., Pang, G., & Liang, Y. (2017). Periodic solution of a Leslie predator-prey system with ratio-dependent and state impulsive feedback control. *Nonlinear Dynamics*, 89, 2941-2955.
- [95] Vinoth, S., Sivasamy, R., Sathiyathan, K., Unyong, B., Rajchakit, G., Vadivel, R., & Gunasekaran, N. (2021). The dynamics of a Leslie type predator-prey model with fear and Allee effect. *Advances in Difference Equations*, 2021, 1-22.
- [96] Barreira, L., Llibre, J., & Valls, C. (2012). Bifurcation of limit cycles from a 4-dimensional center in  $\mathbb{R}^m$  in resonance 1: N. *Journal of Mathematical Analysis and Applications*, 389(2), 754-768.
- [97] Wang, S., & Yu, H. (2021). Stability and bifurcation analysis of the Bazykin's predator-prey ecosystem with Holling type II functional response. *Math. Biosci. Engin*, 18, 7877-7918.
- [98] Elaydi, S. N., & Sacker, R. J. (2010). Population models with Allee effect: a new model. *Journal of Biological Dynamics*, 4(4), 397-408.
- [99] Yan, J., Li, C., Chen, X., & Ren, L. (2016). Dynamic complexities in 2-dimensional discrete-time predator-prey systems with Allee effect in the prey. *Discrete Dynamics in Nature and Society*, 2016.
- [100] Yang, R., Nie, C., & Jin, D. (2022). Spatiotemporal dynamics induced by nonlocal competition in a diffusive predator-prey system with habitat complexity. *Nonlinear Dynamics*, 110(1), 879-900.
- [101] Yang, R., Zhao, X., & An, Y. (2022). Dynamical analysis of a delayed diffusive predator-prey model with additional food provided and anti-predator behavior. *Mathematics*, 10(3), 469.
- [102] Yang, R., Song, Q., & An, Y. (2021). Spatiotemporal dynamics in a predator-prey model with functional response increasing in both predator and prey densities. *Mathematics*, 10(1), 17.

- [103] Yang, R., Jin, D., & Wang, W. (2022). A diffusive predator-prey model with generalist predator and time delay. *Aims Math*, 7(3), 4574-4591.
- [104] Wang, F., Yang, R., Xie, Y., & Zhao, J. (2023). Hopf bifurcation in a delayed reaction diffusion predator-prey model with weak Allee effect on prey and fear effect on predator. *AIMS Mathematics*, 8(8), 17719-17743.
- [105] Umrao, A. K., & Srivastava, P. K. (2023). Bifurcation analysis of a predator-prey model with Allee effect and fear effect in prey and hunting cooperation in predator. *Differential Equations and Dynamical Systems*, 1-27.
- [106] Zhu, Z., Chen, Y., Li, Z., & Chen, F. (2023). Dynamic behaviors of a Leslie-Gower model with strong Allee effect and fear effect in prey. *Math. Biosci. Eng*, 20(6), 10977-10999.
- [107] Chen, J., Chen, Y., Zhu, Z., & Chen, F. (2023). Stability and bifurcation of a discrete predator-prey system with Allee effect and other food resource for the predators. *Journal of Applied Mathematics and Computing*, 69(1), 529-548.
- [108] Games, R., & Mawhin, J. (1977). Coincidence degree and nonlinear differential equations. *Lecture Notes in Math*, 568.
- [109] Fan, M., & Wang, K. (2002). Periodic solutions of a discrete time nonautonomous ratio-dependent predator-prey system. *Mathematical and computer modelling*, 35(9-10), 951-961.
- [110] Duque, C., & Uzcategui, J. (2017). Dynamics of a discrete predator-prey system with nonconstant death rate. *Boletín de matemáticas*, 24(1), 1-17.
- [111] Wolf, A., Swift, J. B., Swinney, H. L., & Vastano, J. A. (1985). Determining Lyapunov exponents from a time series. *Physica D: nonlinear phenomena*, 16(3), 285-317.
- [112] Jia, B., Gu, H., Li, L., & Zhao, X. (2012). Dynamics of period-doubling bifurcation to chaos in the spontaneous neural firing patterns. *Cognitive neurodynamics*, 6, 89-106.
- [113] Khan, M. S., Samreen, M., Khan, M. A., & De la Sen, M. (2022). A dynamically consistent nonstandard difference scheme for a discrete-time immunogenic tumors model. *Entropy*, 24(7), 949.
- [114] Khan, M. S., Haque, M., & Khan, M. A. Stability, bifurcations and chaos control in a discrete-time predator-prey foraging arena model. *Stacey, Stability, Bifurcations and Chaos Control in a Discrete-Time Predator-Prey Foraging Arena Model*.

- [115] Khan, M. S. (2022). Bifurcation analysis of a discrete-time four-dimensional cubic autocatalator chemical reaction model with coupling through uncatalysed reactant. *MATCH Commun. Math. Comput. Chem*, 87(2), 415-439.
- [116] Khan, M. S., Samreen, M., Ozair, M., Hussain, T., Elsayed, E. M., & Gomez-Aguilar, J. F. (2022). On the qualitative study of a two-trophic plant-herbivore model. *Journal of Mathematical Biology*, 85(4), 34.
- [117] Abbasi, M. A., & Samreen, M. (2024). Analyzing multi-parameter bifurcation on a prey-predator model with the Allee effect and fear effect. *Chaos, Solitons & Fractals*, 180, 114498.
- [118] Kelley, W. G., Peterson, A. C., (2010). *The Theory of Differential Equations: Classical and Qualitative*, Springer, New York, 2010.
- [119] Din, Q., & Zulfiqar, M. A. (2022). Qualitative behavior of a discrete predator-prey system under fear effects. *Zeitschrift fur Naturforschung A*, 77(11), 1023-1043.
- [120] Marotto, F. R. (1978). Snap-back repellers imply chaos in  $R^n$ . *Journal of mathematical analysis and applications*, 63(1), 199-223.
- [121] Marotto, F. R. (2005). On redefining a snap-back repeller. *Chaos, Solitons & Fractals*, 25(1), 25-28.
- [122] Pattanayak, D., Mishra, A., Dana, S. K., & Bairagi, N. (2021). Bistability in a tri-trophic food chain model: Basin stability perspective. *Chaos: An Interdisciplinary Journal of Nonlinear Science*, 31(7).
- [123] Garai, S., Pati, N. C., Pal, N., & Layek, G. C. (2022). Organized periodic structures and coexistence of triple attractors in a predator-prey model with fear and refuge. *Chaos, Solitons & Fractals*, 165, 112833.
- [124] Oliveira, D. F., Robnik, M., & Leonel, E. D. (2011). Shrimp-shape domains in a dissipative kicked rotator. *Chaos: An Interdisciplinary Journal of Nonlinear Science*, 21(4).
- [125] Velez, J. A., Bragard, J., Perez, L. M., Cabanas, A. M., Suarez, O. J., Laroze, D., & Mancini, H. L. (2020). Periodicity characterization of the nonlinear magnetization dynamics. *Chaos: An Interdisciplinary Journal of Nonlinear Science*, 30(9).
- [126] Din, Q. (2022). Dynamics and Hopf bifurcation of a chaotic chemical reaction model. *MATCH Commun. Math. Comput. Chem*, 88, 351-369.

- [127] Din, Q., Shabbir, M. S., & Khan, M. A. (2022). A Cubic autocatalator chemical reaction model with limit cycle analysis and consistency preserving discretization. *MATCH Commun. Math. Comput. Chem*, 87, 441-462.
- [128] Khan, M. S. (2019). Stability, bifurcation and chaos control in a discrete-time prey-predator model with Holling type-II response. *Network Biology*, 9(3), 58.
- [129] Brauer, F., Castillo-Chavez, C., & Castillo-Chavez, C. (2012). *Mathematical models in population biology and epidemiology* (Vol. 2, No. 40). New York: springer.
- [130] Allen, L. (2007). *An introduction to mathematical biology*. Upper Saddle River: Pearson/Prentice Hall
- [131] Xiang, L., Zhang, Y., & Huang, J. (2020). Stability analysis of a discrete SIRS epidemic model with vaccination. *Journal of Difference Equations and Applications*, 26(3), 309-327.
- [132] Farnoosh, R., & Parsamanesh, M. (2017). Disease extinction and persistence in a discrete-time SIS epidemic model with vaccination and varying population size. *Filomat*, 31(15), 4735-4747.
- [133] Liu, J., Peng, B., & Zhang, T. (2015). Effect of discretization on dynamical behavior of SEIR and SIR models with nonlinear incidence. *Applied Mathematics Letters*, 39, 60-66.
- [134] Hu, Z., Teng, Z., & Jiang, H. (2012). Stability analysis in a class of discrete SIRS epidemic models. *Nonlinear Analysis: Real World Applications*, 13(5), 2017-2033.
- [135] Aranda, D. F., Trejos, D. Y., & Valverde, J. C. (2017). A discrete epidemic model for bovine Babesiosis disease and tick populations. *Open Physics*, 15(1), 360-369.
- [136] Ma, X., Zhou, Y., & Cao, H. (2013). Global stability of the endemic equilibrium of a discrete SIR epidemic model. *Advances in Difference Equations*, 2013, 1-19.
- [137] Cui, Q., & Zhang, Q. (2015). Global stability of a discrete SIR epidemic model with vaccination and treatment. *Journal of Difference Equations and Applications*, 21(2), 111-117.
- [138] Mickens, R. E. (1999). Discretizations of nonlinear differential equations using explicit nonstandard methods. *Journal of Computational and Applied Mathematics*, 110(1), 181-185.
- [139] Izzo, G., & Vecchio, A. (2007). A discrete time version for models of population dynamics in the presence of an infection. *Journal of Computational and Applied Mathematics*, 210(1-2), 210-221.

- [140] Van den Driessche, P., & Yakubu, A. A. (2019). Disease extinction versus persistence in discrete-time epidemic models. *Bulletin of mathematical biology*, 81(11), 4412-4446.
- [141] Kribs-Zaleta, C. M., & Velasco-Hernandez, J. X. (2000). A simple vaccination model with multiple endemic states. *Mathematical biosciences*, 164(2), 183-201.
- [142] Yang, W., Sun, C., & Arino, J. (2010). Global analysis for a general epidemiological model with vaccination and varying population. *Journal of Mathematical Analysis and Applications*, 372(1), 208-223.
- [143] Liu, S., & Li, M. Y. (2021). Epidemic models with discrete state structures. *Physica D: Nonlinear Phenomena*, 422, 132903.
- [144] Alqahtani, R. T. (2021). Mathematical model of SIR epidemic system (COVID-19) with fractional derivative: stability and numerical analysis. *Advances in Difference Equations*, 2021(1), 2.
- [145] Lin, Q., Zhao, S., Gao, D., Lou, Y., Yang, S., Musa, S. S., ... & He, D. (2020). A conceptual model for the coronavirus disease 2019 (COVID-19) outbreak in Wuhan, China with individual reaction and governmental action. *International journal of infectious diseases*, 93, 211-216.
- [146] Wells, C. R., Sah, P., Moghadas, S. M., Pandey, A., Shoukat, A., Wang, Y., ... & Galvani, A. P. (2020). Impact of international travel and border control measures on the global spread of the novel 2019 coronavirus outbreak. *Proceedings of the National Academy of Sciences*, 117(13), 7504-7509.
- [147] Gostic, K., Gomez, A. C., Mummah, R. O., Kucharski, A. J., & Lloyd-Smith, J. O. (2020). Estimated effectiveness of symptom and risk screening to prevent the spread of COVID-19. *Elife*, 9, e55570.
- [148] Khan, M. S., Ozair, M., Hussain, T., & Gomez-Aguilar, J. F. (2021). Bifurcation analysis of a discrete-time compartmental model for hypertensive or diabetic patients exposed to COVID-19. *The European Physical Journal Plus*, 136(8), 1-26.
- [149] Parsamanesh, M., Erfanian, M., & Mehrshad, S. (2020). Stability and bifurcations in a discrete-time epidemic model with vaccination and vital dynamics. *BMC Bioinformatics*, 21, 1-15.
- [150] Hethcote, H. W. (2000). The mathematics of infectious diseases. *SIAM review*, 42(4), 599-653.
- [151] Serban, M. A. (2001). Global asymptotic stability for some difference equations via fixed point.

- [152] Parsamanesh, M., & Erfanian, M. (2018). Global dynamics of an epidemic model with standard incidence rate and vaccination strategy. *Chaos, Solitons & Fractals*, 117, 192-199.
- [153] Parsamanesh, M., & Farnoosh, R. (2018). On the global stability of the endemic state in an epidemic model with vaccination. *Mathematical Sciences*, 12, 313-320.
- [154] Parsamanesh, M., & Mehrshad, S. (2019). Stability of the equilibria in a discrete-time sivs epidemic model with standard incidence. *Filomat*, 33(8), 2393-2408.



Turnitin Originality Report

Nonlinear Mathematical Models: Theory and Methods  
From Quick Submit (Quick Submit)

by Muhammad Aqib Abbasi .



- Processed on 20-Nov-2024 09:04 PKT
- ID: 2525841005
- Word Count: 51659

Similarity Index

15%

Similarity by Source

Internet Sources:

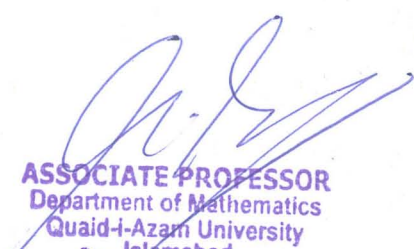
7%


Publications:

14%

Student Papers:

1%

  
ASSOCIATE PROFESSOR  
Department of Mathematics  
Quaid-i-Azam University  
Islamabad

  
Focal Person (Turnitin)  
Quaid-i-Azam University  
Islamabad

**sources:**

- 1 1% match (G. C. Layek. "An Introduction to Dynamical Systems and Chaos", Springer Science and Business Media LLC, 2024)  
G. C. Layek. "An Introduction to Dynamical Systems and Chaos". Springer Science and Business Media LLC, 2024
- 2 < 1% match (Handbook of Mathematics, 2015.)  
Handbook of Mathematics, 2015.
- 3 < 1% match (Internet from 17-May-2023)  
<https://ds.amu.edu.et/xmlui/bitstream/handle/123456789/17017/Elementary%20Differential%20Equations-Boyce.pdf?isAllowed=y&sequence=1>
- 4 < 1% match (Chirodeep Mondal, Dipak Kesh, Debasis Mukherjee. "Dynamical behavior of a discrete-time predator-prey system incorporating prey refuge and fear effect", Chinese Journal of Physics, 2024)  
Chirodeep Mondal, Dipak Kesh, Debasis Mukherjee. "Dynamical behavior of a discrete-time predator-prey system incorporating prey refuge and fear effect". Chinese Journal of Physics, 2024
- 5 < 1% match (JMR, Editor. "Journal of Mathematics Research, Vol. 2, No. 1, February 2010", Journal of Mathematics Research, 2010.)  
JMR, Editor. "Journal of Mathematics Research, Vol. 2, No. 1, February 2010", Journal of Mathematics Research, 2010.
- 6 < 1% match (publications)  
Ioannis K. Argyros. "Polynomial Operator Equations - in Abstract Spaces and Applications". CRC Press, 2020
- 7 < 1% match (Internet from 01-Nov-2022)  
[http://rdoc.univ-sba.dz/bitstream/123456789/3469/1/D3C\\_Math\\_Souna\\_fethi.pdf](http://rdoc.univ-sba.dz/bitstream/123456789/3469/1/D3C_Math_Souna_fethi.pdf)
- 8 < 1% match (Internet from 08-Oct-2022)